Mechanisms of G2 chromosomal radiosensitivity of Murine SCID cells

Thesis submitted for the degree of Doctor of Philosophy to University of St. Andrews

By

Clodagh E. Finnegan

August 2000

School of Biology, University of St. Andrews, SCOTLAND. KY16 9TS

Declaration

I, Clodagh E. Finnegan, hereby certify that this thesis, has been written by me, that it is a record of work carried out by me and that it has not been submitted in any application for a higher degree.

Date 1/8/00 Signature of candidate

I was admitted as a research student in September 1995 and as a candidate for the degree of Ph.D. in September 1995; the higher study for which this is a record was carried out in the University of St. Andrews between 1995-2000.

Date 1/8/00 Signature of candidate

I hereby certify that the candidate fulfilled the conditions of the Resolution and Regulations appropriate for her degree of Ph.D. in the University of St. Andrews and that the candidate is qualified to submit this thesis in application for that degree.

Date 8/8/00 Signature of Supervisor

Date 1/8/00 Signature of candidate

Contents

Page no

Abstract

The non-homologous end-joining (NHEJ) pathway of DNA repair has become a recent focus of attention and one of the central players of this pathway is DNA-PK_{cs} which is mutated in murine Severe Combined Immunodeficiency (SCID).

The underlying mechanisms of the variable G2 chromosomal radiosensitivity in different individuals or cell lines has been the subject of much discussion, and the use of mutant radiosensitive rodent cell lines has provided a way to begin to understand the genetics and mechanisms of chromosomal radiosensitivity. As an example of this approach SCID cells have shown an elevated G2 chromosomal response to ionising radiation (IR). This response is generally thought to be caused by the underlying double-strand break (dsb) rejoining deficiency. However, recently Bryant (1998) proposed the signal model suggesting that G2 radiosensitivity is not directly related to dsb rejoining, but is due to an enhanced conversion of dsb to chromatid breaks via a recombinational mechanism. Therefore, the aim of the work presented in this thesis was to increase our understanding of the relationship between dsb and chromatid breaks in the G2 phase of the cell cycle. The cell lines used in this research were murine fibroblastic SCID, normal CB17, $100E^{+}$ (hybrid SCID cells complemented for DNA-PK_{cs}) and $50D^{-}$ (hybrid non-complemented SCID) cells.

The kinetics of the disappearance of chromatid breaks with time in G2 SCID and CB17 (normal wildtype) cells after gamma-irradiation showed a similar rate in the two cell lines. However, there was a 1.3-1.7 fold elevated frequency of chromatid breaks in SCID relative to CB17 cells. Analysis of dsb induction in SCID and CB17 cells showed similar initial frequencies of dsb. Analysis of dsb rejoining showed a higher residual frequency of dsb in SCID compared with CB17 cells from 10 min up to 3h, which appeared to be correlated with the observed elevated frequencies of chromatid breaks.

However, further experiments involving treatment of irradiated G2 cells with the DNA synthesis inhibitor 9-β-D arabinofuranosyladenine (araA) enhanced the frequency of chromatid breaks without showing a significant effect on dsb rejoining as measured by constant field gel electrophoresis. Thus, while acknowledging the conflicting nature of these results, the araA experiments throw serious doubt upon the direct relationship between the two end-points. The reasons for these results are not at present clear and further investigation is obviously required. However, a mechanism such as that recently proposed under the signal model, where dsb are not directly involved in chromatid break formation might offer a possible explanation, namely that araA acts on the semi-final stage in the recombinational rearrangement leading to chromatid breaks.

Another factor influencing the induction of chromatid breaks was the end-structure of dsb, and this was more pronounced in SCID than normal cells, as shown by an elevated frequency of chromatid breaks in response to restriction endonucleases (RE) inducing blunt- and 3' cohesive-ends compared to those inducing 5' cohesive ends. These results suggest the molecular configuration of the dsb influences the mechanism by which dsb are converted to chromatid breaks.

Futhermore, the chromatin structure of SCID and CB17 cells was studied by flow cytometry of nucleoids under various conditions and the results revealed differences between the two lines. In addition, SCID nucleoids were in general more compact, an effect possibly correlated with an observed reduction in overall chromosome length.

Acknowledgements

I would like to express my sincere thanks to my supervisor Dr. Peter Bryant for his continual encouragement and guidance throughout the project.

I would also like to thank John, Angus and Mary for their excellent technical expertise, tremendous help and most of all good humour throughout the project. A special thank you goes to Angus who helped me with my endless experiments and to Mary for helping me feed all those hungry cells !

I would also like to thank the University of St Andrews for the award of a Maitland Ramsay scholarship which enabled me to do the project.

Finally but not least I would like to extend my thanks to my fiancé Damian who helped me keep going when I had given up hope in the USA. Also thanks to my parents and grandmother for their support and encouragement because without them I would have given up a long time ago !

I would like to dedicate this thesis to my parents and grandmother

Abbreviations

3AB -	3-aminobenzamide
AIFGE -	Asymmetric inversion field gel electrophoresis
AraA -	9-β-D-arabinofuranoslyadenine
AraC -	cytosine arabinofuranosyladenine
AraHX -	9-β-D-adeninefuranoslyhypoxanthine
AT -	Ataxia Telangiectasia disease
AT5BIVA -	SV40 virus transformed fibroblast cell lines derived from an AT heterozygous individual
ATM -	Ataxia telangiectasia mutated protein
ADA -	adenine deaminase
BALB/C	CB17 parental cells, sometimes used as controls for SCID cells
BI -	Binucleate index
BrdU -	5-bromodeoxyuridine
Bq -	Becquerel; unit of radioactivity= 1 disintegration per second
BSA -	Bovine serum albumin
CCHE -	contour clamped homogenous electrophoresis
CFGE -	constant-field gel electrophoresis
CHFGE -	continuos homogenous field gel electrophoresis
CHO -	Chinese hamster ovary cell line
DNase -	Deoxyribonuclease
dpm -	disintegrations per minute
dsb -	double-strand break
DSBR -	double-strand break repair
DNA-PK -	DNA-dependent protein kinase holoenzyme

DNA-PK$_{CS}$ - DNA-dependent protein kinase catalytic subunit

DNA-PK$_{CS}$ - DNA-dependent protein kinase gene

EB - Ethidium Bromide

EDTA - Ethylene diaminetetracetic acid

EM-9 EMS an X-ray sensitive mutation of CHO cell line

FAR - fraction of activity released

FISH - Fluorescent in situ hybridisation

FPG - Fluorescence plus Giemsa

G-light - giemsa light stained bands

Gy - Gray, unit of radiation absorbed dose= 1 joule per kilogram

γ-rays - gamma radiation

h - hour

H2A - histone 2A

H2B - histone 2B

H3 - histone 3

H4 - histone 4

^{3}H-Tdr - tritiated thymidine

HBSS - Hank's balanced salt solution

HBSS/BSA - 1% w/v bovine serum albumin in HBSS

Hepes - hypoxanthine phosphoryl transferase locus

HRR - homologous recombinational repair

Ig - immunoglobulin

IR - ionising radiation

irs - γ-ray sensitive mutant of V79 cells

ISV - inactivated sendai virus

Ki - inhibition constant

Kda - kilodalton

LET - linear energy transfer

L5178Y-R - mouse lymphoma cell line (LY-R)

L5178Y-S- radiosensitive mouse lymphoma cell line (LY-S)

MAR - matrix attachment region

min - minute

Mn - micronucleus

MW - molecular weight

Mbp - mega base pairs

MEF - mouse embryonic fibroblasts

MPF - mitosis promoting factor

NBS - Nymgen breakage syndrome

NHEJ - non-homologous end-joining

OFAGE - orthologonal field gel electrophoresis

PBS - phosphate buffered saline

PCC - premature chromosome condensation

PFGE - pulsed-field gel electrophoresis

PI-3K - phosphoinositol-3 kinase

PLD - potentially lethal damage

PMSF - Phenylmethylsulphonyl fluoride

RE - restriction endonuclease

RAG 1&2 - recombination activating genes

ROFE - rotating orthologonal gel electrophoresis

RPA - replication protein A

rpm - revolutions per minute

RSS - recognition signal sequences

SAR - scaffold attachment site

SCE - sister chromatid exchange

SCID - severe combined immunodeficiency

SLO - streptolysin-O

ssb - single-strand break

TAFE - Transverse alternating gel electrophoresis

TBE - tris borate EDTA

$t_{1/2}$ - time required for half the chromatid breaks to disappear

tk - thymidine kinase

UV - ultra violet

V-79 - Chinese hamster lung fibroblast cell line

V(D)J - variable, diversity, joining gene segments

V-C4 - X-ray sensitive mutant of V79 cells

XRCC1-9 - X-ray cross complementing 1-9 genes

XR-1 - X-ray sensitive mutant of CHO cells

XR-V9B - X-ray sensitive mutant of V79 cells

xrs - X-ray sensitive mutant of CHO cells (1-7)

$50D^{-}$ - hybrid non complemented DNA-PK $_{cs}$ cell line

$100E^{+}$ - hybrid DNA-PK $_{cs}$ complemented cell line

List of Chapters

List of Figures

Chapter Five

Chapter Six

Chapter Seven

List of Tables

Chapter One:

Chapter Two:

Chapter Three:

Chapter Four:

Chapter Five:

Chapter Six:

Chapter One
1.1: General Introduction

Chapter One:

1.1: General introduction

Much of radiation biology research in recent years has focused on DNA damage induced by ionising radiation (IR) and how the cell repairs the damage. IR causes several different types of damage but a double-strand break (dsb) is thought to be the most critical event. When a cell is exposed to IR the types of damage that are induced include single-strand breaks and double-strand breaks (dsb) in the phospho-diester backbone; base damage on one or both strands with pyrimidine bases more susceptible to damage; DNA-DNA crosslinks or DNA-protein crosslinks; sugar damage and the formation of dimers between or within two DNA strands (Tubiana *et al* 1990). For 1 Gy of low LET radiation there are thought to be some 1000 single-strand breaks induced, 40 dsb and approximately 2000 bases damaged (Blöcher 1982).

1.2: Classification of chromosomal damage

It has been postulated that a DNA dsb can lead to chromosomal damage but the exact mechanisms involved in this process are largely unknown (Bender *et al* 1974, Bryant 1984b, Natarajan and Obe 1984). Since chromosomes carry the genes for transmitting genetic material it is important to try and understand the series of events that occur after the initial ionisation leading up to the resulting chromosomal damage. There are several different types of chromosome damage depending on the cell cycle phase when the cell is exposed to radiation. The main types of damage that occur when a cell is exposed in G1, that is before DNA synthesis, are the formation of chromosome breaks and exchanges including translocations, dicentrics and rings. In G2 the damage is mainly in the form of chromatid breaks and gaps which mostly occur in only one of the chromatids. The earlier classifications of chromosomal damage (for e.g. Sax 1938, Buckton and Evans 1973) are similar today except for a few changes in the names given to particular forms of damage.

1.3: G2 chromatid radiosensitivity

Cell cycle variations in cellular and chromosomal radiosensitivities have also been demonstrated. Early experiments (e.g. Sinclair and Morton 1966, Sinclair 1968) showed that when a cell is exposed to IR the most sensitive phase of the cell cycle for cell killing is the G2/M phase. It was therefore of great interest to determine the mechanisms underlying this high G2 radiosensitivity. Since cell killing by radiation is thought to result from chromosome damage (e.g. Joshi *et al* 1982) it became important to understand the mechanisms of chromosome damage induced in G2 cells. The reason for high G2 radiosensitivity is not known but reorganisation of DNA from interphase chromatin to metaphase chromosomes may play a role and may lead to susceptibility to damaging agents (Tubiana *et al* 1990, King 1996). However there are cell cycle checkpoints during the G2 phase of the cell cycle to ensure that damage in the DNA is removed before a cell progresses to mitosis (Lehmann and Carr 1994, reviewed in Hensey *et al* 1995, Weinert 1998).

The "G2 assay" can be used to assess an individual's sensitivity to IR damage in the G2 phase of the cell cycle and it involves exposing actively growing cells to low doses of IR and sampling at short time intervals after exposure to determine the frequency of chromatid breaks and gaps in the chromosomes. An individual's response in this assay, as measured by the frequency of chromatid breaks, has been shown to vary and high G2 radiosensitivity may indicate a predisposition to cancer.

Elevated frequencies of chromatid breaks were reported in cells from individuals with various cancer prone conditions (Sanford *et al* 1989) and has been interpreted as a deficiency in DNA repair. Knight *et al* (1993) also showed that individuals with an

elevated G2 response reported having first and second degree relatives with a 3.6 and 2.2 fold higher mean frequency of cancer.

A more recent study suggested that G2 chromatid radiosensitivity may indicate the presence of low penetrance genes which may predispose some individuals to cancer (Scott *et al* 1994). Helzlsouer *et al* (1995) showed that first degree relatives of breast cancer patients gave high G2 scores indicating a familial link, providing additional evidence for the presence of cancer-predisposing genes. In an extensive familial study, Roberts *et al* (1999) demonstrated the heritability of G2 response.

Parshad *et al* (1982) investigated the response of malignant (HIT-14) and normal fibroblast cells to X-irradiation in the G2 phase of the cell cycle and they found that malignant cells were more sensitive to X-irradiation in G2 than normal cells, i.e. malignant cells produced a higher frequency of chromatid breaks and gaps than normal cells. This initiated a series of experiments which have been carried out over the past few years and are still on going. These studies have shown that skin fibroblasts derived from Ataxia Telangiectasia (AT) heterozygotes, Gardner's syndrome, Cockayne's syndrome, xeroderma pigmentosum, Bloom`s syndrome, Fanconi's anaemia, familial polyposis, retinoblastoma and Li Fraumeni patients all have elevated frequencies of chromatid breaks in G2 (Parshad *et al* 1983, 1984, 1985a, 1985b, 1993, Sanford *et al* 1987, 1989, 1993, 1996).

Sanford and Parshad (1989) reported a good discrimination between AT heterozygotes and controls using the G2 assay. AT homozygotes were 3 fold more sensitive to IR in G2 than normals and an apparently normal individual heterozygous for the AT mutation was also identified due to an elevated response to IR in G2, indicating how useful a predictive test might be (Sanford *et al* 1990). Scott *et al* (1996) also showed a two fold increased chromatid break response in G2 for AT homozygous patients compared with the average

control range using the Sanford assay. However, a percentage of patients, heterozygous for AT, were only marginally above the controls and the response of xeroderma pigmentosum, Li Fraumeni, basal cell naevus syndrome, Downs syndrome and Fanconi's anaemia were not different when compared to normal controls, which is in contrast to Sanford and Parshard's results (Scott 1996, Parshad *et al* 1983, 1984, 1985a, 1985b, 1993, Sanford *et al* 1987, 1989, 1993). Scott *et al* (1994) then devised their own "Paterson" G2 assay on peripheral blood lymphocytes which did not include centrifugation before harvesting the samples and the samples were kept on ice during harvesting and hypotonic treatment. Using this assay Scott measured the IR-induced chromatid break frequencies in peripheral blood lymphocytes of normal individuals and patients presenting with breast cancer. The study showed that 40% of the breast cancer cases had elevated radiosensitivity (i.e. in the AT- heterozygote range) whereas only 9% of controls showed such elevated radiosensitivity.

In summary the above investigations have put forward several reasons for the use of the G2 assay as a predictive test to detect an individual's sensitivity to radiation. The possible reasons for elevated G2 chromatid radiosensitivity are: (1) a deficiency in DNA repair which may be genetically determined (Sanford *et al* 1989, Parshad *et al* 1992), (2) a defect in the cell cycle checkpoint for example in AT (Scott *et al* 1981) (3) an enhanced conversion of dsb into chromatid breaks (Mozdarani *et al* 1989a, 1989b, Bryant and Slijepcevic 1993). It has been proposed that a DNA repair deficiency, evidenced by an apparent difference in "rejoining" kinetics (rate of disappearance) of G2 chromatid breaks with time, may be a predicting factor in cancer development and the genetic instabilities that arise from this may lead to tumorgenicity (reviewed in Sanford *et al* 1989). The mechanisms of conversion (3 above) are not known, however, it has been proposed that it involves cellular signalling of dsb (Bryant 1998; model discussed further below.

Assessment of G2 radiosensitivity has become important from a radioprotective point of view because a recent study has shown that patients who were repeatedly exposed to chest fluoroscopic examinations developed breast cancer (Helzlsouer *et al* 1995). These patients had an elevated G2 sensitivity which suggested there may be a link between radiation exposure, DNA repair and the development of breast cancer (Helzlsouer *et al* 1995). As this was a small study other studies are required before a definitive conclusion can be made. However, it has indicated how important and informative a predicative test might be.

1.3.1: G2 chromatid response of repair proficient and deficient mammalian mutants

Many investigations in recent years have focused on the connection between DNA dsb repair (Weaver 1996) and an elevated G2 chromosomal response to IR (Mozdarani *et al* 1989 a, 1989b, Bryant 1997). As mentioned before, dsb have been suggested as the critical events which cause cellular and chromosomal damage (Bender *et al* 1974, Natarajan and Obe 1984). Many years of research have been spent investigating the induction and repair of dsb in radiosensitive cell lines (e.g. Kemp *et al* 1986, Lehmann and Stevens 1977, Jeggo 1990). Of particular interest was a recent study by Foray *et al* (1995) who showed that AT cells actually have a faster dsb repair rate than normal cells yet there is still a 2-4 fold increased sensitivity at the chromosomal level (Mozdarani *et al* 1989a, 1989b), which questions the reasoning why or how dsb repair determines the chromosomal response of a cell line or individual. Other cell lines that have shown similar elevated G2 chromatid break response but a proficiency in repair include irs2 and VC-4 (Bryant *et al* 1993). Even after years of research, radiation biologists still have not found the underlying reason for this elevated chromosomal response and the mechanism of how a dsb is converted to chromosome damage is still not fully understood.

Recently, many rodent mutants have been identified that are defective in DNA repair (Jeggo 1990, Zdzienicka 1995 minireview) and they have been useful in trying to elucidate the unknown steps from the initial dsb to the final chromosomal response. Complementation studies of rodent DNA repair defects led to the identification of the human X-ray repair cross complementing (XRCC) genes (Thompson and Jeggo 1995) of which they are now nine known (Table 1.1 overleaf). The XRCC genes are involved in the repair of IR-caused damage including dsb, single-strand breaks (ssb) and base damage. The XRCC1 gene is involved in the repair of ssb and it activates DNA ligase I. XRCC2 has normal repair capabilities like XRCC8 but they both have chromosomal defects, and XRCC2 is thought to be involved in homologous recombination as shown by a hypersensitivity to mitomycin C (Liu *et al* 1998). The XRCC3 gene is also thought to be involved in homologous recombination (Tebbs *et al* 1995 and Liu *et al* 1998). Rodent mutants defective in XRCC4-7 genes have been shown to be defective in dsb repair and V(D)J recombination due to mutations in proteins of the non-homologous end-joining (NHEJ) pathway that involves the DNA-PK holoenzyme. Cells deficient in the XRCC8 gene, including irs2 and VC-4 cells, show normal dsb repair kinetics with radioresistant DNA synthesis and an enhanced chromosomal response to IR (Bryant *et al* 1993). UV40 cells defective for the XRCC9 gene have a broad spectrum of defects and are not similar to any other mutants. XRCC9 has been postulated to be involved in post replicative repair or cell cycle checkpoints (Liu *et al* 1997b).

Table 1.1: X-ray repair cross complementing human chromosomes groups 1-9 (XRCC1-9).

Gene	Mutant cells	Notable features	Human chromosome
XRCC1	EM-7 EM-9	defective single strand break rejoining & high spontaneous SCE frequency	19
XRCC2	Irs-1	ssb and dsb repair normal, increased spontaneous and induced chromosomal aberrations & reduced fidelity of dsb repair	7
XRCC3	Irs-1SF	defective ssb and dsb repair, reduced ssb rejoining & increased spontaneous & induced chromosomal abnormalities	14
XRCC4	XR-1	defective dsb rejoining in G1, in late S phase dsb repair normal, activates DNA ligase IV	5
XRCC5	xrs1-7 XRV15B sxi3 mouse knock out	defective dsb rejoining & VDJ recombination, altered Ku80 protein	2
XRCC6	mouse knock out	altered Ku70 protein	22
XRCC7	SCID V3 irs20 SX9	defective dsb rejoining & VDJ recombination, altered DNA-PK_{CS} protein	8
XRCC8	irs2 VC-4	repair of dsb and ssb normal but radioresistant DNA synthesis	?
XRCC9	UV40	increased spontaneous chromosomal aberrations & SCE, defective ssb rejoining	9

The identification of DNA repair deficient mutants has been useful because they can be used to study the chromosomal response of cells that are known to be defective or proficient in dsb repair. The results from these studies may be used to elucidate the pathways involved in DNA repair and identify the role each component has in dsb repair. It may also aid in the identification of the processes that are defective in the human radiosensitive cell lines and give an insight into possible genes involved in G2 radiosensitivity.

1.4: Severe combined immunodeficiency

The cell line investigated in this study was murine SCID which means severe combined immunodeficiency (Bosma *et al* 1983). The murine SCID mutation causes elevated radiosensitivity in many cell types including myeloid cells, fibroblasts, bone marrow cells and intestinal crypt cells in mice (Fulop and Philips 1990, Hendrickson *et al* 1991, Biedermann *et al* 1991) and the underlying reason has been proposed as a defect in the rejoining of dsb (Chang *et al* 1993, Nevaldine *et al* 1997). Therefore, it was of interest to study the G2 chromosomal response and dsb repair in G2 SCID fibroblasts. A previous study was carried out during this thesis work, by van Buul *et al* (1998) showing that murine SCID cells had an elevated level of chromosomal aberrations in G1 and G2 phases of the cell cycle. Other radiosensitive cells, such as AT, have been shown to have an elevated chromosomal radiosensitivity but apparently normal chromatid break and dsb repair (Liu and Bryant 1994, Foray *et al* 1995). The elevated chromatid radiosensitivity has been proposed to be the result of an enhanced conversion of dsb into chromatid breaks, rather than a deficiency in dsb repair (Mozdarani 1989a, 1989b, Liu and Bryant 1997, Bryant 1997). The G2 chromosomal response and G2 repair ability of SCID cells was studied, so that a comparison could be made with the results from other radiosensitive mutants, such as xrs5, which also have an elevated chromosomal response but apparently

normal repair in G2 (Mateos *et al* 1994). For many years the mechanisms involved in the conversion of the initial dsb into chromosome damage have been under investigation (Bryant 1997) and many questions remain unanswered today.

1.4.1: Murine severe combined immunodeficiency

SCID was first identified in humans in the 1950's (reviewed in Rosen *et al* 1984, 1995) and children homozygous for the SCID mutation usually die within three years after birth (Rosen *et al* 1995). In humans the SCID mutation can arise from autosomal recessive mutations or occur spontaneously (Rosen *et al* 1995). The murine SCID mutation was used in this study because there is only one mutation (Bosma *et al* 1983) and animal models are much easier to study as murine cells grow faster in culture. The murine SCID mutation was first identified in 1983 by Bosma *et al*. The mutation arose spontaneously whilst breeding parental CB17 mice. It was discovered incidentally because 4 out of 7 littermates lacked major serum immunoglobulin (Ig) isotypes (Bosma *et al* 1983). It was found to be a single autosomal recessive gene (Bosma *et al* 1983) and has been mapped to mouse chromosome 16 (Bosma *et al* 1989).

1.4.2: SCID immune functions and V(D)J recombination

After the SCID mouse was identified, research focused on the immunoglobulin defects and immune functions which first brought SCID to light. The general phenotype that was observed in SCID mice included very few circulating lymphocytes, the bone marrow appeared normal but all other lymphoid organs appeared very small (Custer *et al* 1985, Philips and Fulop 1989, Schuler 1990, Bosma and Carroll 1991). SCID mice were deficient in both T and B lymphocyte functions and they were highly susceptible to spontaneous T cell lymphomas (Custer *et al* 1985, Schuler 1990, Bosma and Carroll 1991).

Due to a defect in V(D)J recombination SCID mice usually had no B nor T cells, however, some B and T cells have been known to develop in mature SCID mice due to a leaky phenotype (Schuler *et al* 1986, Kim *et al* 1988, Okazaki *et al* 1988, Malynn *et al* 1988, Carroll and Bosma 1991). This was the first insight that the SCID mutation was the result of an inability to rejoin the DNA ends created during V(D)J recombination (Okazaki *et al* 1988, Weaver and Hendrickson 1989).

During V(D)J recombination the Variable (V), Diversity (D) and Joining (J) gene segments are recombined to form immunoglobulin and T cell receptors [Figure 1.1 overleaf] (reviewed in Blackwell and Alt 1989, Gellert 1992, Taccioli *et al* 1992, Lieber 1992). The process is initiated by recombination activating genes [RAG 1 and 2] (Oettinger *et al* 1990, Mombaerts *et al* 1992, Shinkai *et al* 1992, McBlane *et al* 1995, Spanopoulou *et al* 1995, Ramsden *et al* 1996) which initiate two site-specific dsb adjacent to the recombination signal sequences (RSS) and coding joint sequences. Efficient recombination requires one RSS with a 12bp spacer and another with a 23bp spacer between the heptamers and nonamers (Eastman *et al* 1996, Ramsden *et al* 1997). The products formed are signal and coding joints: signal joints are the direct ligation between the blunt ended heptamers (Hesse *et al* 1989, Schissel *et al* 1993) whereas coding joints are complex in that they require the addition or loss of nucleotides before ligation to form the new coding exon and hairpin loops are formed as an intermediate step (Blackwell and Alt 1989, Gellert 1992, Lieber 1992). The loss or addition of nucleotides at the coding ends contributes to the increased diversity within the immune system (Lieber 1992, Gerstein and Lieber 1993a, 1993b).

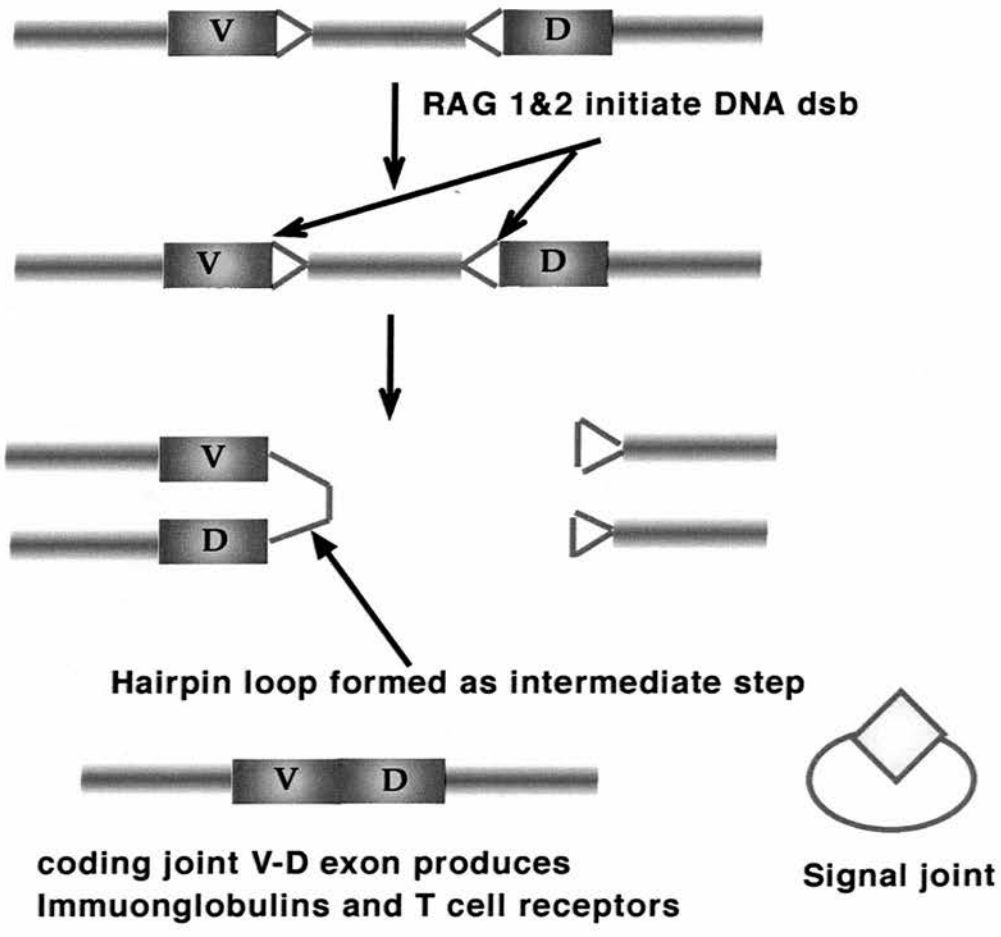

Figure 1.1: V(D)J recombination.

Modified version of Lieber et al 1997.Normally V-D or V-D-J or V-J gene segments recombine to form the Immunoglobulins and T cell receptors. In this example a V-D joint is made. RAG1&2 cut DNA at specific sites between the signal and coding joints. A hairpin loop is formed between the coding joints and it has been suggested that the DNA-PK holoenzyme combines to these DNA ends and repairs them. In SCID cells no coding joints are formed and in xrs cells no signal or coding joints are formed.

The SCID mutation causes a defect in the formation (Schuler *et al* 1991) and resolution of coding joints (Lieber *et al* 1988, Weaver and Hendrickson 1989, Blackwell and Alt 1989). The initial V(D)J recombination process is normal (Malynn *et al* 1988, Carroll and Bosma 1991) but aberrant rearrangements in the coding joints can sometimes result in the deletion of complete coding exons (Hendrickson *et al* 1988, Kim *et al* 1988, Okazaki *et al* 1988, Weaver and Hendrickson 1989). The intermediate hairpin loops formed at the coding joint ends are known to accumulate in SCID thymocytes (Roth *et al* 1992, Zhu and Roth 1996) and excessive "palindromic" nucleotide sequence insertion has been observed at the coding joint ends (Kienker *et al* 1991, Schuler *et al* 1991). The linkage between the insertion of P nucleotides and the formation of hairpin loops has been confirmed (Lewis 1994) and the longer P nucleotides may be the reason why the resolution of coding ends are defective in SCID cells. In addition to the formation of coding and signal joints two other types of joint can be formed: a hybrid joint and an open-shut joint [Figure 1.2 overleaf] (Melek *et al* 1998). Open-shut joints are formed by the rejoining of the original signal and coding ends whereas hybrid joins are formed between a signal end and a coding end that was originally flanked by the other RSS (Lewis *et al* 1991). The frequency of hybrid joins are normal in SCID and Ku80 mutant cells which may be explained by the involvement of the RAG proteins in the formation of non-standard V(D)J rearrangements (Melek *et al* 1998).

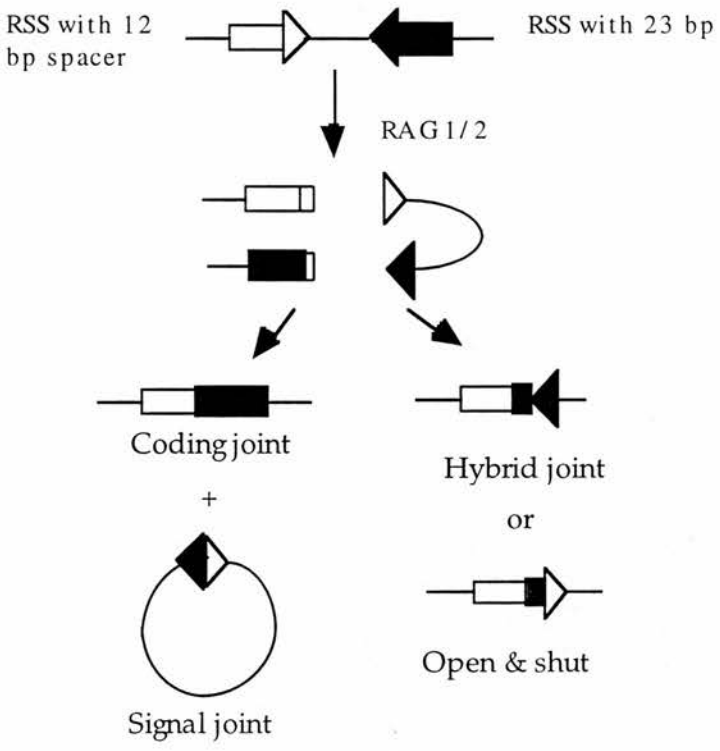

Figure 1.2. V(D)J recombination products adapted from Melek *et al* 1998. The normal products formed are coding and signal joints (shown on the left). The aberrant rearrangements that can form are shown on the right. The joining of the original signal and coding joints form open shut joints and the joining of a coding joint with a signal joint from the other segment form a hybrid joint.

1.4.3: SCID Radiosensitivity

The SCID mutation was mainly thought to affect the development of lymphoid cells due to a defective V(D)J recombination pathway, however, later studies revealed the SCID mutation was pleiotropic in nature by affecting the IR response of many cells within the body due to a defective non-homologous end joining dsb repair pathway. Fulop and Philips (1990) showed, using clonogenic assays, that SCID mice bone marrow cells were two-fold more sensitive to IR than CB17 cells. Similarly, SCID bone marrow cells restituted with normal bone marrow produced a wildtype response to IR, indicating that the radiosensitivity of SCID mice bone marrow cells was due to the SCID mutation (Fulop and Philips 1990).

The radiosensitivity studies of the SCID mouse were extended, using cell survival assays, to show that the response of bone marrow stem cells, intestinal crypt cells, epithelial skin cells and primary cultures of fibroblasts derived from a SCID mouse had an elevated response *in vivo* and *in vitro* to gamma radiation (Biedermann *et al* 1991, Hendrickson *et al* 1991). IR induces many types of damage but the exact type of damage that SCID cells were sensitive to was unknown. Therefore, chemical agents inducing, crosslinks and dsb were used to characterise the underlying cause of the radiosensitivity. UV light, mitomycin C (MMC), methylmethanesulfonate (MMS) induce ssb and crosslinks whereas bleomycin induces dsb (Biedermann *et al* 1991 and Hendrickson *et al* 1991). SCID cells had a two fold elevated sensitivity to agents inducing dsb, such as bleomycin, but there was no difference in the response of SCID and CB17 cells to the ssb and crosslinking inducing chemical agents (Biedermann *et al* 1991, Hendrickson *et al* 1991). Other investigators have shown that tumours arising in SCID mice have a two fold elevated radiosensitivity (Budach *et al* 1992). Similarly, the introduction of restriction endonucleases, RsaI and Sau3A I, by electroporation have shown that SCID cells were 3-4 fold more sensitive to

dsb than CB17 cells at the cellular end point even though the initial dsb frequency was the same in both cell lines (Chang *et al* 1993).

1.4.4: SCID repair studies

The use of chemical agents showed that dsb were thought to be the underlying cause of the radiosensitivity in SCID cells. Therefore, the induction and repair of dsb in SCID and CB17 cells was measured by neutral filter elution and asymmetric field gel electrophoresis. These studies showed similar frequencies of induced dsb in SCID and CB17 cell lines in response to IR, but there was a reduced rejoining of dsb in SCID cells (Biedermann *et al* 1991, Hendrickson *et al* 1991). The reduced ability of SCID cells to rejoin dsb was proposed to be the reason for the elevated radiosensitivity in SCID cells. Repair at the cellular level including potentially lethal damage (Biedermann *et al* 1991, Kimura *et al* 1995) and sublethal damage (Nevaldine *et al* 1997) are also reduced in SCID cells suggesting an overall defect in the repair of radiation induced DNA damage, especially dsb.

1.4.5: Complementation studies with other mammalian mutant cells

The SCID mutation, like many other rodent mutants, has elevated cellular and chromosomal radiosensitivity and a reduced ability to rejoin dsb. Therefore, it was classified as a member of the X-ray repair cross complementing (XRCC) family comprising of nine human genes which complement rodent cells defective in the repair of IR-induced damage (Thompson and Jeggo 1995, Zdzienicka 1995). The SCID mutation was complemented by the cloned human XRCC7 gene (residing on human chromosome 8) that has been confirmed using microcell mediated chromosome transfer and somatic cell hybrid studies (Komatsu *et al* 1995, Itoh *et al* 1993, Kirchgessner *et al* 1993). Studies with fragmented human chromosome 8 defined the location of the SCID mutation at 8p11.1-

q11.1 (Kurimasa *et al* 1994, Miller *et al* 1995). This was interesting because it was the first time there had been any links made between human chromosome 8 and mouse chromosome 16 (where the SCID mutation is located). Other cells complemented by the XRCC7 gene include M059J a human glioma cell line (Lees-Miller *et al* 1995), V3 and irs20 hamster cell lines (Blunt *et al* 1995, Peterson *et al* 1997) and SX9 a mouse carcinoma cell line (Lin *et al* 1997, Priestley *et al* 1998, Fukumura *et al* 1998). Complementation studies have shown that SCID cells are complemented by xrs5, xrs6, XR-V9B, XR-1, AT and NBS cells (Komatsu *et al* 1993) confirming that the SCID mutation involves a different gene but these genes may possibly be involved in a common pathway.

1.5: DNA-PK holoenzyme

Four of the XRCC genes, XRCC4-7 (see Table 1.2 and Figure 1.3), are involved in a recently discovered dsb repair pathway known as non-homologous end-joining (NHEJ). SCID cells are mutated in a gene that has been recognised as one of the central players in this process (Figure 1.3). It was initially suggested by Kirchgessner *et al* (1995) and Peterson *et al* (1995) that SCID was possibly deficient in the DNA-dependent protein kinase catalytic subunit because DNA-PK co-localised with human chromosome 8, to where the SCID mutation had been mapped (Kurisama *et al* 1994, Miller *et al* 1995). DNA-PK is a holoenzyme composed of two components DNA-PK_{CS} and Ku (Jackson 1996, Jin *et al* 1997a). Ku was first identified as an autoantigen that forms a heterodimer comprised of Ku70 and Ku80 (Reeves and Sthoeger 1989, Takiguchi *et al* 1996). Ku freely translocates along DNA in an energy independent fashion (Jin *et al* 1997a) and it binds specifically to DNA ends whether they are double stranded, single stranded or hairpin loops (Mimori and Hardin 1986, Blier *et al* 1993). Ku may bind to DNA ends in a sequence dependent manner, that may be involved in transcriptional regulation (Giffin *et al*

Table 1.2: Putative properties of XRCC4-7 genes involved in mammalian dsb repair

Gene	Mutant cells	Ku	DNA-PK$_{cs}$	DNA-PK activity	VDJ Defect	
					Coding joints	Signal joints
XRCC4	XR-1	+	+	+	-	-
XRCC5	xrs	-	+	-	-	-
	XRV15B	-	+		-	-
	sxi-3	-	+	-	-	-
	sxi-2	-	+	-	-	-
XRCC6	sxi-1	-	+	-	-	-
XRCC7	SCID	+	-	-	-	+
	V3	+	-	-	-	+
	MO59J	+	-	-	?	?

+ signifies normal activity
- signifies decreased or absent activity
Modified version from Weaver 1995.

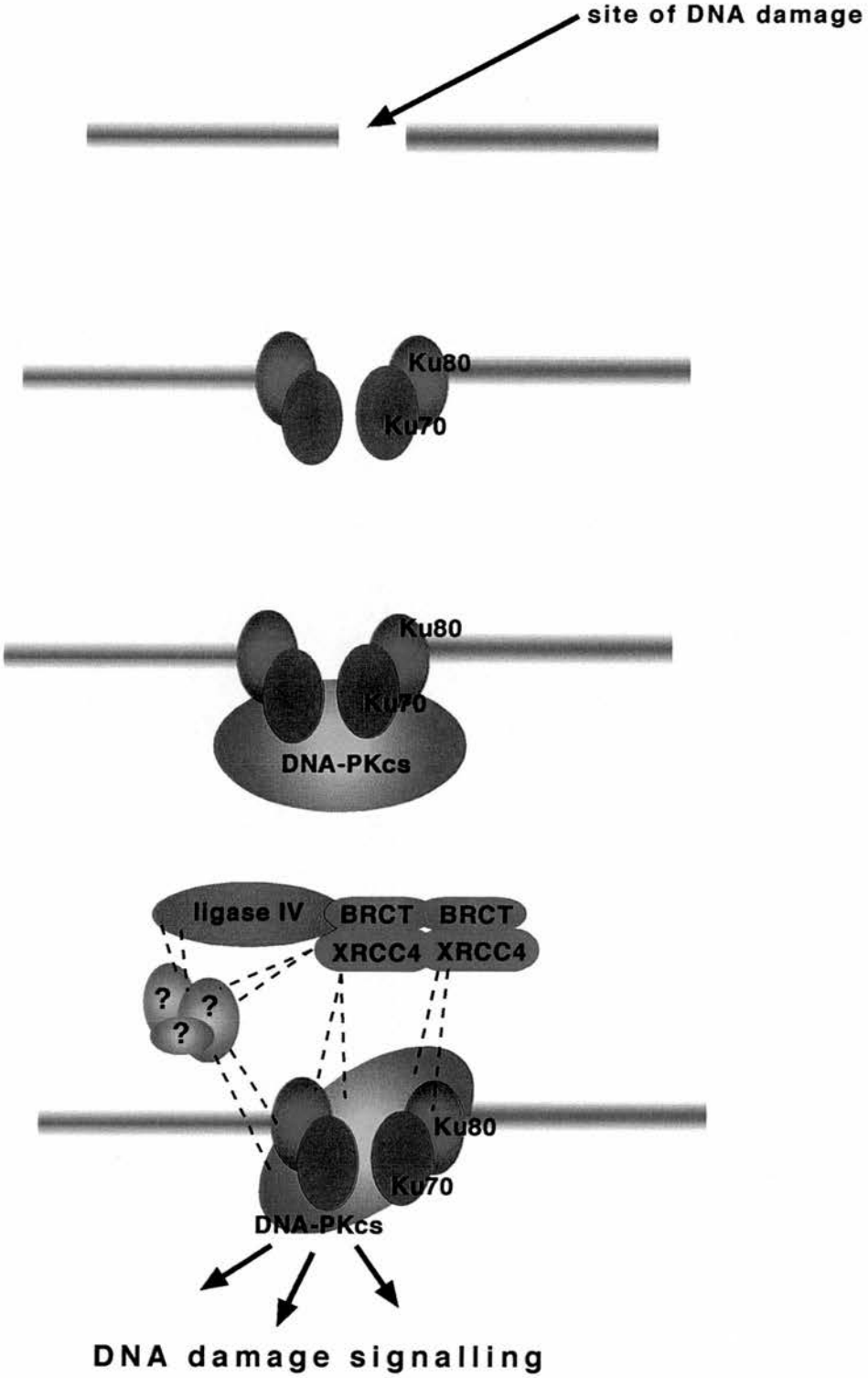

Figure 1.3: DNA-PK model. Ku binds to the DNA ends and recruits DNA-PKcs which activates the kinase activity. A DNA ligase IV-XRCC4 complex is recruited to the damaged site by either direct interactions with the DNA-PK or indirectly by other as yet unidentified components (modified version from Lieber et al 1997 and Critchlow et al 1998).

or a sequence independent manner that may involve DNA damage recognition (Jackson 1996, Jin *et al* 1997a). Ku has also been shown to self associate as tetramers in the presence of DNA ends and it forms loops in DNA (Pang *et al* 1997, Cary *et al* 1997). These studies suggest that Ku may act by tethering the broken chromosomal ends together before repair (Pang *et al* 1997, Cary *et al* 1997). The binding of Ku to the DNA ends (Rathmell and Chu 1994a) may play a role in orientation for ligation, binding or repair. More recently mouse embryonic fibroblasts deficient in Ku80 or Ku70 have confirmed the need for both factors for an interaction with DNA-PK_{cs} and Ku70 is thought to have a larger binding site for DNA than Ku80. Once Ku binds to a double-strand break (Suwa *et al* 1994) it then signals to DNA-PK_{cs} to proceed to that site (Jin and Weaver 1997b, Gu *et al* 1997). DNA-PK_{cs} activates the DNA-PK complex which recruits other repair enzymes such as ligases, nucleases and DNA polymerases, for e.g. DNA ligase IV (Figure 1.3). DNA-PK has been shown to phosphorylate downstream products involved in DNA repair such as p53 (Woo *et al* 1998), replication protein A, hsp90 (Li *et al* 1995a), transcription factors including Sp1 (Jackson *et al* 1990), Oct1, Jun (Bannister *et al* 1993) and Fos (Anderson and Leesmiller 1992, Jackson 1996, Jin *et al* 1997a, Jeggo 1997). Other possible concomitant mechanisms that DNA-PK may be involved in are: prevention of transcription from interfering with the repair process by inhibiting transcription factors, holding the ends of the chromosome in place by acting as a "scaffold" (Jackson *et al* 1995, Jeggo *et al* 1995, Roth *et al* 1995) and acting as a signalling pathway (Jackson 1996). DNA-PK autophosphorylates Ku and DNA-PK_{cs} suggesting an involvement in the regulation of association and disassociation of the DNA-PK complex, controlling the induction of the phosphorylating cascade or enabling the disassociation of the complex, allowing repair enzymes access to the damaged site (Chan and Lees-Miller 1996, Jin *et al* 1997a). Recently DNA-PK activity *in vivo* has been proposed to modulate nucleotide excision repair as DNA-PK and Ku mutants have shown sensitivity to UV light. Alternatively DNA-PK may act as a DNA damage sensor regulating DNA repair by

transcription modulation (Muller *et al* 1998). The XRCC4 35Kda gene product is a disulphide linked homodimer which can multimerise, enabling dimers to form between Ku and DNA-PK_{CS} (Figure 1.3). XRCC4 protein is thought to be involved in the assembly of DNA-PK as a stabilising factor or alignment of DNA ends (Grawunder *et al* 1998a, Leber *et al* 1998). It has also been shown to interact with DNA ligase IV, that may be required for the ligation of DNA ends (Teo and Jackson 1997, Critchlow *et al* 1997). The DNA-PK dsb repair pathway appears to be conserved through evolution as Ku70 and Ku80 homologs have been identified in yeast (Boulton and Jackson 1996). In addition to the components above the SIR proteins 2, 3 and 4, first identified as telomeric silencing proteins (Boulton and Jackson 1998) are also involved in dsb repair in yeast (Jackson 1997, Tsukamoto *et al* 1997). The search for more mammalian mutants may reveal mammalian proteins similar to the yeast SIR proteins. This illustrates how complex and diverse DNA repair is in eukaryotes. In addition, recent studies have shown that mouse embryonic stem cells defective for Ku80 possess severe growth abnormalities raising the possibility that Ku80 may also be involved in the regulation of growth (Nussenweig *et al* 1996, 1997).

1.5.1: DNA-PK activity in SCID

After the proposal that DNA-PK_{CS} was defective in SCID cells, research focused on various molecular aspects to determine the exact defect. SCID (murine) and V3 (hamster) cells do not show any detectable levels of DNA-PK activity (Blunt *et al* 1995). However, V3 cells express normal levels of Ku70 suggesting normal DNA binding activities but this is not the case for SCID cells (Boubnov and Weaver 1995). The efficiency of SCID cells to phosphorylate Ku *in vitro* was significantly depressed compared to wildtype cells, however, the levels of the Ku heterodimer were normal in both lines (Boubnov and Weaver 1995). This shows that DNA-PK_{CS} is not required for Ku to bind to DNA, but it is

required for the activation of the holoenzyme.

The protein levels of DNA-PK_{cs} are reduced but not totally ablated in SCID lymphocytes. DNA-PK has been localised to the nuclear region in SCID cells, but in CB17 cells DNA-PK was present in both the nucleus and cytosol (Danska *et al* 1996). DNA-PK activity was 20-50 fold reduced in rodent cells compared to human DNA-PK levels (Finnie *et al* 1995, Blunt *et al* 1995) but the addition of purified human DNA-PK_{cs}, by an *in vitro* assay, to V3 and SCID cells restored DNA-PK activity. The restored levels of DNA-PK activity were similar to human DNA-PK levels, suggesting that DNA-PK_{cs} is the limiting factor in rodents (Blunt *et al* 1995). xrs6 cells defective for Ku80 (Getts and Stamato 1994, Taccioli *et al* 1994b, Ross *et al* 1995) have no DNA-PK activity and reduced Ku70 levels confirming the existence of a heterodimer (Ku70-Ku80), that is required for DNA-PK activity (Finnie *et al* 1996).

1.5.2: DNA-PK is also involved in V(D)J recombination

The SCID mutation was first discovered because of the immune deficiency and this was due to an inability to resolve hairpin loops at the coding ends. V(D)J recombination and DNA repair are thought to be involved in similar pathways because mammalian mutants defective in DNA-PK are also defective in V(D)J recombination (Pergola *et al* 1993, Taccioli *et al* 1993, Jackson and Jeggo 1995, Jeggo *et al* 1995, Roth *et al* 1995, Bogue *et al* 1996, Li *et al* 1995b). Ku is thought to attach to the coding and signal ends and transmit a signal to DNA-PK_{cs} to come to the site and activate the holoenzyme to repair the DNA damage (Trolestra and Jaspers 1994, Weaver 1996, Lieber *et al* 1997). In xrs5 cells an *in vitro* assay has shown a deficiency in the formation of coding and signal joints in V(D)J recombination (Pergola *et al* 1993, Smider *et al* 1994, Taccioli *et al* 1994a, 1994b) and these cells are known to be defective in Ku80 (Getts and Stamato 1994, Taccioli *et al*

1993, Ross *et al* 1995, Singleton *et al* 1997). Ku80 is required for DNA end binding and may explain the end-joining defect in xrs6 cells (Pergola *et al* 1993, Trolestra and Jaspers 1994). In contrast, SCID cells deficient in DNA-PK_{cs} are unable to resolve the hairpin loops formed at coding ends, suggesting that DNA-PK_{cs} is required for the resolution of hairpin loops. This suggests there may be two processes, one which requires Ku for end rejoining to form signal joints and the other which requires DNA-PK holoenzyme to resolve the hairpin loops at coding ends (Grawunder *et al* 1998b). More recently, it was shown that DNA-PK can bind to DNA in the absence of Ku and vice versa. This finding may have important implications for the different pathways required for the formation of the V(D)J recombination DNA products and it may explain the different phenotypes observed with Ku80 and DNA-PK defective cells (Yaneva *et al* 1997).

1.5.3: Phosphorylation of substrates by DNA-PK

The involvement of DNA-PK in the repair of DNA damage can be investigated in SCID cells by testing whether or not SCID cells can phosphorylate DNA-PK substrates. This has been investigated for p53 and RPA which are both thought to be involved in response to IR induced damage. The results have shown that SCID cell extracts could not phosphorylate RPA *in vitro* in a kinase assay (Boubnov and Weaver 1995, Fried *et al* 1996). However, the addition of purified DNA-PK_{cs} restored the phosphorylation of RPA in SCID cell extracts, suggesting that DNA-PK is required for RPA phosphorylation (Boubnov and Weaver 1995).

p53 induction was normal in SCID mouse embryonic fibroblasts (MEFs) but it remained for a longer time period in SCID MEFs relative to CB17 MEFs and this response has been attributed to the persistence of DNA damage in SCID MEFs (Gurley *et al* 1996). A high level of apoptosis was also reported in SCID cells and the injection of damaged linear

DNA into SCID MEFs generated a p53 response similar to wildtype MEFs (Huang *et al* 1996). It was concluded that DNA-PK was not required for p53 induction (Fried *et al* 1996, Gurley *et al* 1996 and Huang *et al* 1996). However, a recent study has shown that DNA-PK is involved in the activation of p53 sequence-specific DNA binding in response to DNA damage because murine SCGRII cells and human M059J cells were used that have DNA-PK null mutations and therefore, no p53 response was induced in these cells (Woo *et al* 1998). This confirmed that DNA-PK is required for p53 induction. The previous studies reporting conflicting results, may be due to the presence of low DNA-PK levels, which are undetectable because the cells used did not have null mutations for DNA-PK (Woo *et al* 1998).

1.6: Identification of the SCID mutation

More recently, the exact DNA-PK_{CS} mutation in SCID mice has been identified, by isolating and sequencing the open reading frames from SCID and CB17 mice (Araki *et al* 1997, Blunt *et al* 1996, Danska *et al* 1996). There was 78.9% homology with human *DNA-PK_{CS}* and there were regions highly conserved between the two, suggesting that these areas may have important cellular functions. A single point mutation was identified, a transversion of a A to a T in SCID mice (Araki *et al* 1997, Blunt *et al* 1996, Danska *et al* 1996), that caused an ochre stop codon which removed 83 aa from the C terminus. The transversion created a restriction enzyme recognition site (AluI) which was a good indication that it occurred in SCID mice only as the same RE site was not present in CB17 mice (Araki *et al* 1997). The substitution occurred in the phosphatidylinositol 3-kinase domain showing that *DNA-PK_{CS}* had similarities to members of the PI3K related family (Poltoratsky *et al* 1995). At the transcriptional and mRNA level the expression of *DNA-PK_{CS}* was similar in SCID and CB17 cells. However, there were decreased DNA-PK_{CS} protein levels in SCID mice, suggesting a defect in the stability or folding of DNA-PK_{CS} in

SCID cells (Hamantani *et al* 1996, Araki *et al* 1997, Blunt *et al* 1996, Danska *et al* 1996). In contrast, V3 cells and the equine SCID mutation have decreased *DNA-PK$_{CS}$* transcript levels, unlike the other SCID mutations, which may explain the differing V(D)J recombination defects in these cells (Hamantani *et al* 1996, Blunt *et al* 1996). The newly identified irs20 cell line has a different mutation than SCID but it also occurs in the C-terminus of *DNA-PK$_{CS}$* indicating the importance of the C-terminus for protein kinase activity (Priestley *et al* 1998).

1.7: Repair processes in mammalian cells

The above discussion has outlined the studies to date on SCID but how does this all fit into the repair pathways of IR damage that are already known. There are three categories involved in the repair of IR induced damage: excision repair and mismatch repair (which are not relevant to this discussion) and double-strand break repair (DSBR) which has two subcategories: homologous recombinational repair and non-homologous/illegitimate repair (Roth *et al* 1985, Roth and Wilson 1985, Roth *et al* 1986). Dsb are mainly repaired by homologous recombination repair in yeast, whereas higher eukaryotes repair dsb by non-homologous repair (Sargent *et al* 1997). There are two types of non-homologous repair, a novel end joining pathway that uses a fill-in mechanism to join the ends without the removal of the protruding overhangs (Thode *et al* 1990, King *et al* 1994) and a pathway involving DNA-PK, known as non-homologous end-joining (NHEJ).

1.7.1: Homologous and non-homologous end-joining in SCID cells

SCID cells are thought to be defective in the NHEJ of DNA ends in V(D)J recombination and dsb repair. Many studies have been carried out to try and elucidate the end-joining defect in SCID cells and some conflicting results have been reported. Staunton and Weaver

(1994) transfected linearised plasmid DNA into SCID and CB17 cells, using both calcium phosphate and electroporation methods. SCID cells were able to integrate the plasmid DNA into mouse chromosomes, as efficiently as CB17 cells, and integration was not dependent on homology, end structure or the addition or removal of nucleotides. In contrast, Harrington *et al* (1992) reported a 10-100 fold reduced ability of SCID cells to integrate linear plasmid DNA, using the same methodology. The conflicting results may be due to the artificial conditions under which these assays are performed. Alternatively DNA configuration and protein linkages may be important for NHEJ and these are not taken into consideration during these assays. Hairpin loops are known to accumulate at the coding ends in SCID thymocytes (Roth *et al* 1992 and Zhu and Roth 1996) which is thought to be due to a defect in the resolution of these ends. However, Staunton and Weaver (1994) developed DNA substrates with hairpin loops at the ends and the results showed that SCID cells were able to resolve hairpin ends and integrate the DNA into the genome, but it cannot be ruled out that these structures were nicked during the transfection procedure prior to integration. Another study revealed that the integration of plasmid constructs, containing antibiotic resistance genes, by non-homologous recombination was normal in SCID cells and the fidelity was similar to CB17 cells (Bühler *et al* 1985a). In addition, homologous recombination of extrachromosomal substrates also occurred at normal frequencies in SCID cells (Bühler *et al* 1985a). In conclusion, these results have shown that homologous recombination and non-homologous recombination is apparently normal in SCID cells. However, these *in vitro* assays create unusual conditions that may not represent the conditions *in vivo*. Thus, no definitive conclusions can be achieved from these studies. However, if the SCID defect is not the result of a null mutation it may explain the apparently normal recombination rates obtained in these assays (Weaver and Hendrickson 1989). The "leaky" phenotype of the SCID mouse may also be explained by the presence of low DNA-PK levels, or a recombination pathway that is usually not detected in normal cells (Weaver and Hendrickson 1989, Weaver *et al* 1996, Pennycook

1996). It has also been shown in SCID mice that meiotic recombination is normal, with no obvious defects (Heine *et al* 1996).

1.7.2: DNA-PK dependent and independent repair pathways in SCID

Recently, an interesting study suggested the presence of DNA-PK independent and dependent repair pathways in SCID pre-B lymphocytes (Lee *et al* 1997). In this study two peaks of DNA-PK activity were found corresponding to the G1 and G2 phases of the cell cycle in wildtype cells. SCID cells are known to be hypersensitive to radiation in G1 at the cellular and chromosomal levels which has been attributed to a dsb repair defect in G1 cells, whereas the dsb repair defects were not as apparent in G2 cells (Lee *et al* 1997, van Buul *et al* 1998). A biphasic cell-survival response has been shown in V3, xrs (Whitmore *et al* 1989) and XR-1 cells (Giaccia *et al* 1985), suggesting two repair pathways are involved. However, to date SCID cells have not shown a biphasic cell survival response. The same response in xrs and XR-1 cells is not suprising as they are both involved in NHEJ. xrs cells are defective in Ku80 (Ross *et al* 1995, Boubnov *et al* 1995), whilst XR-1 cells are thought to be defective in the anchorage and alignment of DNA with the DNA-PK holoenzyme due to an altered p35 protein (Critchlow *et al* 1997). V(D)J recombination occurs in the G1 phase of the cell cycle, so that may explain the defect in V(D)J recombination in mammalian mutants defective in Ku and DNA-PK (Lin and Desidero 1995). G2 SCID cells have shown a less sensitive response to IR, using chromosomal and clonogenic assays, than G1 SCID cells (Lee *et al* 1997, van Buul *et al* 1998) and PFGE studies revealed that the G2 dsb repair defect was not as apparent as the G1 dsb repair defect (Lee *et al* 1997). A recent study has shown a 3.9 fold reduced DNA rejoining ability in asynchronous SCID cells *in vitro* and a 10.9 fold reduced ability in asynchronous xrs6 cells. However, some repair occurred suggesting the presence of an alternative DNA-PK independent pathway, which appears efficient and less error prone than NHEJ (Tzung *et al*

1998). The identification of the NHEJ pathway in which the defects of SCID and xrs5 cells have been essential components does not explain the elevated chromatid response of SCID and xrs5 cells treated with IR in G2. Therefore, the proposed mechanisms of how a dsb is converted to a chromatid break will be discussed.

1.8: Mechanisms of chromosomal aberration formation

In order to understand the mechanisms of IR-induced chromosome aberrations we need to take a step back to the 1930s when the first theories of how a chromosome break was induced were proposed. The Classical theory of how chromosome damage arises in the cell was put forward by Sax in the 1930's and is still the prevailing hypothesis today (Sax 1938). A controversial "exchange" theory was proposed in the 1950's by Revell (1955) and recently, a new model was put forward by Bryant (1998) which proposes the involvement of a cellular signalling pathway converting a dsb into a chromatid break.

1.8.1: Classic breakage and reunion theory

The classic breakage and reunion or "breakage-first" theory was proposed by Sax (1938 and 1941) and elaborated by Lea and Catcheside (1942) and it is indeed still widely accepted today. Early radiobiologists thought that radiation directly severed the chromosome and the damage appeared as gaps or discontinuities in the chromosome visible at the next metaphase. Once a cell was exposed to IR many breaks occurred but 90% of the broken chromatid (or chromosome) ends were thought to be restituted (i.e. restored to re-form the original chromosome) before the next metaphase and were thus unseen. However, a small proportion of the breaks were rejoined illegitimately (mis-rejoining) with other broken ends to form various chromatid (or chromosome) exchange aberrations. This required two damaged chromosomes in the same vicinity at the same

time and the probability of such an event was dependent on the square of the radiation dose (i.e. a two hit process). The remaining chromatid breaks did not rejoin because after a certain period of time the chromatids were thought to lose their ability to rejoin. These "breaks" were assumed to be the result of a one-hit process. One hit chromatid breaks increased linearly with dose, whereas exchanges which are two-hit chromatid breaks increased as the square of the radiation dose. This model was readily accepted as experimentally there was a linear increase in chromatid breaks, whereas chromatid exchanges were dependent on the square of the dose (Sax 1940). This model still persists but it was challenged by Revell in the 50's.

1.8.2: Revell's "exchange" hypothesis

Revell proposed a then controversial theory in the 1950's of how chromatid breaks were formed (Revell 1955 and 1958). Revell suggested that radiation did not directly break the chromatids but it initiated an exchange mechanism within a chromatin loop structure, recently termed a "Revell loop" (Savage 1986). A Revell loop forms a point of cross-over between two chromatids, enabling an interaction to occur between two damaged chromatids to initiate an exchange (shown in Figure 1.4). Revell proposed two types of exchanges: inter-changes involving an exchange between sister chromatids, and intra-changes involving an exchange within a chromatid and if incomplete these exchanges result in a chromatid break. Thus, unlike the Sax breakage first model, Revell thought chromatid breaks were not formed at the time of irradiation but were the result of a failed exchange process (Revell 1974).

An assumption of Revell's model was that exchanges at the 4 cross-over points (Fig. 1.4) occur with equal frequencies and therefore the 8 incomplete forms should also occur equally. A type 1 singly incomplete (inter-chromatid) exchange will show a colour-switch

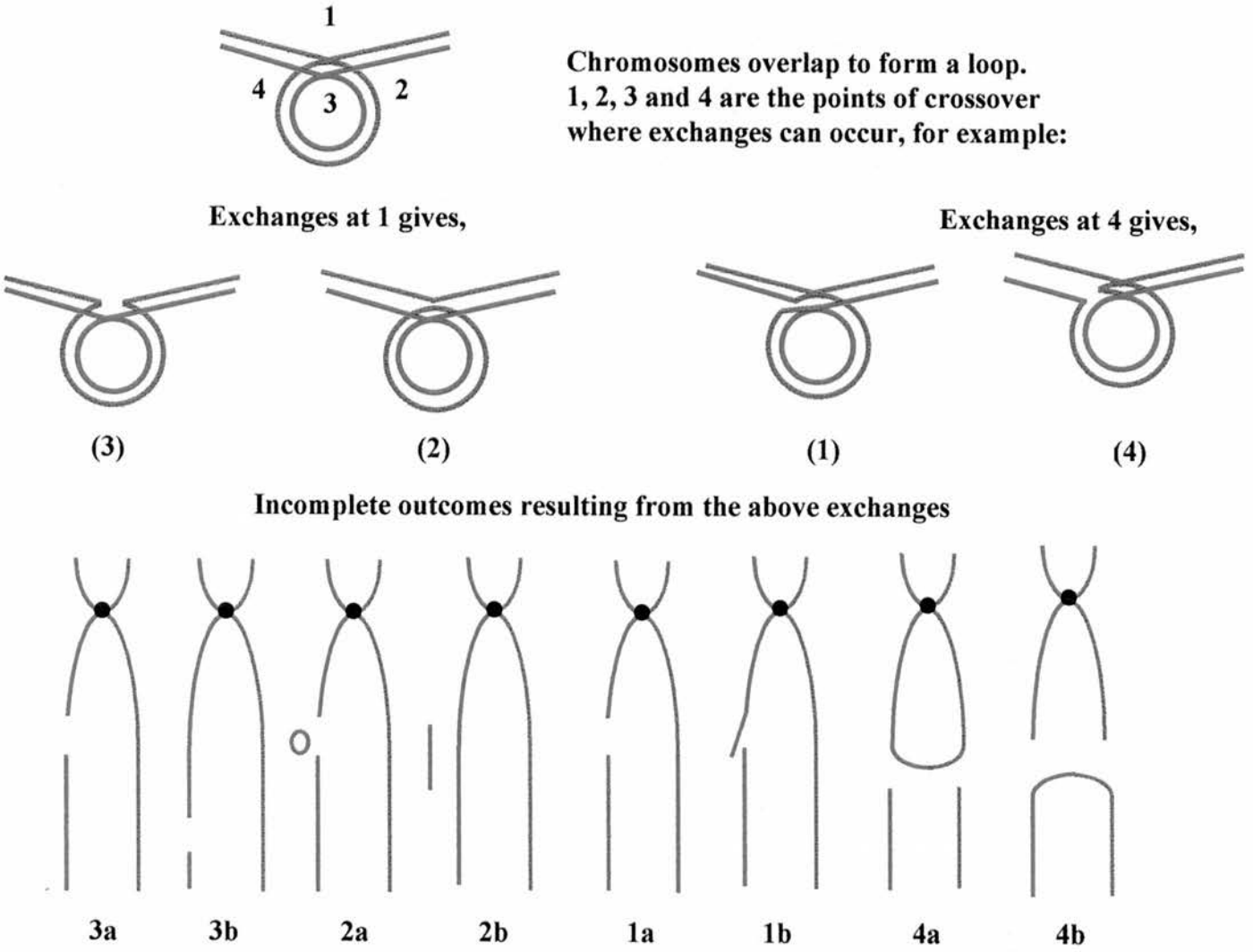

Figure 1.4: Revell's exchange hypothesis. The types of chromatid aberrations arising from the four types of exchange proposed by Revell. Types 2 and 3 are intrachanges (within a chromosome loop) and types 1 and 4 are interchanges (between chromosome loops). Chromatid aberrations 1a and 1b will be scored as chromatid breaks 3a, 3b, 2a, 1a, and 1b are equally frequent then 40% of Chromatid breaks will show a colour switch at the point of breakage. (Diagram based on Heddle and Bodycote 1969).

at the point of breakage (1a, 1b Fig. 1.4). This can be observed if the chromatids are distinguished by prior labelling with bromodeoxyuridine for two cell cycles and subsequent fluorescence plus giemsa (FPG) staining giving harlequin staining (one chromatid staining light and the other dark). If the five forms of *singly* incomplete exchange that lead to chromatid breaks (1a,1b,2a,3a,3b Fig. 1.4) are equally likely it can be predicted that 2 out of the 5 (40%) of these should have a colour-switch at the point of breakage. However, this prediction has generally not been fulfilled experimentally (e.g. Harvey and Savage 1997). The only experiment which appeared to agree with the predicted results was performed in rat kangaroo cells (*Potorus*) which showed a 38% colour-switch ratio (ratio of breaks showing a colour-switch at the break point to total breaks; Heddle *et al* 1969). However in this study only 37 breaks were analysed, making the results open to some doubt. Revell's theory also predicts a non-linear relationship for chromatid breaks since two interacting lesions are involved. This was confirmed in *Vicia fabia* cells (Revell 1966). However, more recent studies in mammalian cells have shown a linear induction of chromatid breaks (e.g. Bryant 1998).

1.8.3: The Signal Model

As previously mentioned the breakage-first model still appears to be the prevailing model for explaining chromosomal aberrations. However, it seems unlikely that the breakage-first model can account for the large size of many chromatid breaks as proposed by the exchange model. It is known that the initial dsb induced involves the loss of at most only a few base pairs, whilst the damage visible as a chromatid break with the light microscope can represent the loss of up to 40Mbp, based on the human diploid genome consisting of 6000Mbp. The signal model (Bryant 1998) proposes that a dsb is converted to a chromatid break by a process involving a signalling mechanism (Figure 1.5). The signal model attempts to explain why radiosensitive cell lines have an elevated G2 chromosomal

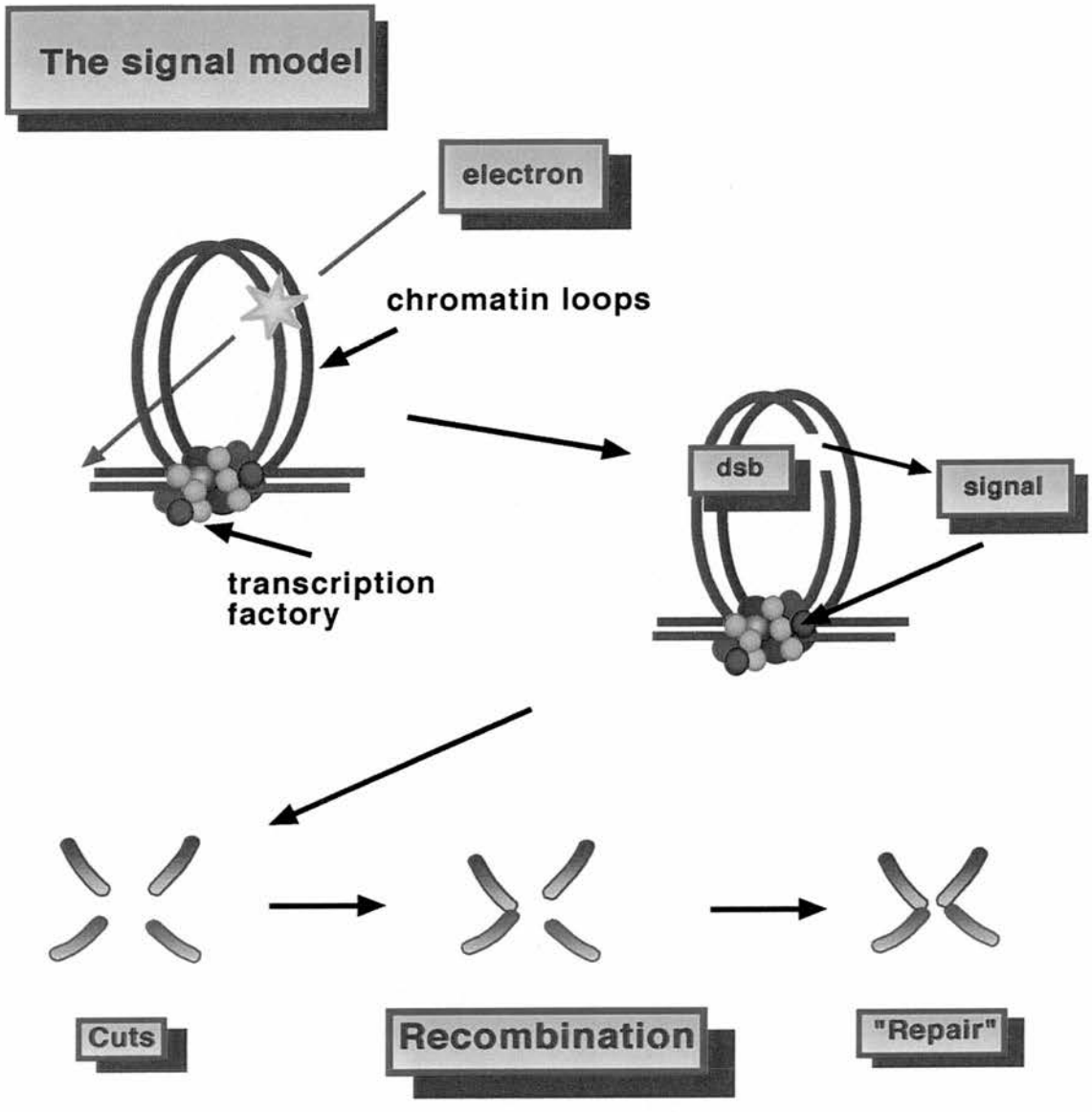

Figure 1.5: The signal model. The loops represent chromatin domains with a transcription factory (represented as small coloured circles). An electron causes a dsb in one of the loops which is recognised by a signalling protein (DNA-PK or ATM ?) which induces the cell to initiate a recombinational exchange, either within one chromatid or (as shown) between sister chromatids. The exchange process involves enzyme-mediated cuts in the DNA at the point of cross-over of the loops, with subsequent rearrangement. A chromatid discontinuity would be visible if completion of the exchange is interrupted by entry of the cell to mitosis. (adapted from Bryant 1998).

response compared with normal wild-type controls even though the induction of dsb and their repair is the same. The linear dose-response curves for IR induced dsb in mammalian cells (Bryant 1998), suggests that a single electron track causes a dsb because if two tracks were required, a dose squared relationship would be formed.

The signal model also proposes that IR induces a dsb in a chromatin loop which is detected by a signalling molecule, for example the DNA-PK holoenzyme (Figure 1.5). Once the signal has activated the "transcriptional/replication factory" repair of dsb involves the XRCC4-7 pathway which removes the dsb but these subsequent steps are not essential to the signal model (Figure 1.5). The signal model involves an exchange process between four cut ends of a chromatin loop (or loops) that are free to recombine with each other. One possible recombination is between sister chromatids, this (as mentioned already) can be detected as colour-switches at break points in harlequin stained metaphases if the cells have been previously labelled through 2 cycles with bromodeoxyuridine. If the recombinational exchange is completed the ends will be ligated together. If the recombinational exchange is not completed then a break will be observed. Colour-switches at break points have been shown to occur at a frequency of 16% in X-irradiated and restriction endonuclease treated CHO cells, (Harvey and Savage 1997) as well as in control unirradiated samples which strongly suggests they are induced by single dsb events and arise by an exchange mechanism. In the signal model the chromatid break is not a residue of the original break as in the breakage-first model, in fact the initial dsb may be deleted during the formation of the chromatid break in addition to the surrounding DNA giving rise to larger sized chromatid breaks. The signal model is a very interesting concept, although, many experiments are required before it can be fully validated and accepted. Also, it is not yet clear how differences in signalling could produce different chromatid break frequencies. It seems likely that more than one signalling protein is involved since deletion of one signalling molecule would prevent the formation of chromatid breaks. In

conclusion, the signal model introduces the concept of a single dsb signalling its presence and resulting in an incomplete exchange visualised as a chromatid break.

1.9: Aims of project

The main aims of this study were to investigate the induction and disappearance with time of chromatid breaks in SCID and wildtype CB17 G2 cells exposed to low doses of IR and the induction of chromatid breaks by restriction endonucleases. Restriction endonucleases inducing dsb with various end structures were used to treat porated cells to try and determine if the blunt or cohesive ends of a dsb had an effect on the chromosomal response of SCID and CB17 cells. As mentioned previously, a deficiency in dsb repair has been proposed as the underlying reason for SCID cell radiosensitivity, therefore, it was interesting to measure the induction and repair of dsb in SCID and CB17 cells in the G2 phase of the cell cycle and to compare this to the kinetics of disappearance of chromatid breaks with time. In addition, the response of SCID and CB17 cells to IR in the presence of 9-β-D arabinofuranosyladenine (araA; a DNA synthesis inhibitor) at the chromosomal level were investigated to test the underlying cause of the elevated G2 chromosomal response.

Two hybrid cell lines $50D^-$ (DNA-PK_{CS} complementation absent) and $100E^+$ (DNA-PK_{CS} complemented) were used to study the response elicited by IR and IR in the presence of araA at the chromosomal and DNA repair levels and to compare these results to SCID and CB17 cells.

The possible role of chromatin structure in determining frequencies of chromosomal aberrations and cellular radiosensitivity has been discussed by several authors (e.g. Schwartz *et al* 1995) who showed clear differences in the chromatin structure between

radiosensitive xrs5 cells and their parental CHO-K1 cells. It was therefore of interest to examine whether this was also the case for SCID and CB17 cells. Finally, as mentioned in relation to the signal model, DNA-PK which is defective in SCID cells is an important protein for signalling. Posing the question of whether or not another protein similar in structure may take over the function of the DNA-PK protein following irradiation in its absence, such as the ATM protein was studied in various cell lines.

Chapter Two

G2 chromatid radiosensitivity of murine SCID cells

2.1: Introduction

Chapter Two:

2.1: Introduction

50D and 100E hybrid cell lines were obtained from Dr. C. Kirchgessner (Stanford University, California) who derived them using positional cloning to create SCID cell lines containing human chromosome 8 by creating radiation-reduced hybrids (Kirchgessner *et al* 1995). The hybrid cells containing human chromosome 8 were exposed to lethal doses of IR to fragment the chromosomes and the cells containing fragmented chromosomes were fused back into the parental SCID cell line and hybrids selected that retained the human chromosome 8 fragment containing the gene complementing the SCID defect. The two cell lines that were isolated were 50D and 100E cells, the 100E cells contain the human gene encoding DNA-PK_{cs} whereas 50D cells do not, so they were used as a control for 100E cells. These two cell lines will be referred to as $50D^-$ (DNA-PK_{cs} complementation absent) and $100E^+$ (DNA-PK_{cs} complemented) in the following study. The kinetics of the disappearance of chromatid breaks with time after IR exposure, in these cells was of interest to test whether the rejoining of the dsb defect was apparent at the chromosomal level.

2.1.1: Micronucleus assay

The Mn assay has been used extensively to study the clastogenic effects of radiation and various chemicals. Therefore, the Mn assay was used to determine the radiosensitivity of the four cell lines. Micronuclei are formed from acentric chromosome fragments that remain separate from the nucleus of the cell after nuclear division. Micronuclei are indicative of chromosomal damage (Countryman *et al* 1976 and Fenech and Morley 1985) and as the radiation dose increases the frequency of micronuclei increases. The difficulty with the initial Mn assay studies was how many cell cycles the cells had gone through but the use of cytochalasin B has resolved this problem. Cytochalasin B is a fungal metabolite that prevents actin polymers forming a contractile ring between the two daughter nuclei during cytokinesis. This results in cells with two nuclei, named binucleate cells, and these cells are usually scored to determine Mn frequency because they have been through only one cell cycle. Cytochalasin B permits replication and nuclear division but it inhibits cell splitting, hence the presence of cells with multiple nuclei (Fenech and Morley 1985, 1986). The Mn assay is a rapid and convenient technique for measuring radiation-induced chromosomal damage and can be used to indicate whether or not SCID cells have reverted back to the parental phenotype, thus giving a wildtype yield of Mn. Reversion of this type has been shown to occur in xrs5 cells after long periods in cell culture (Jeggo and Kemp 1983, Denekemp *et al* 1989).

2.1.2: Double-strand breaks cause chromosome aberrations

Dsb are thought to be critical lesions caused by IR in cells (Blöcher 1982). Early theoretical and experimental measurements in yeast showed that many types of damage are induced after IR but one dsb remaining was enough to cause cell death (Ho 1975, Ho and Mortimer 1975, Frankenberg *et al* 1981). The type, dose and dose-rate of the radiation may

alter the frequency of dsb but it does not change the fact that one dsb if unrejoined is enough to cause cell killing in yeast. DNA unwinding studies investigating the repair of ssb and dsb in Ehrlich tumour acsites showed that ssb are repaired rapidly within minutes after IR exposure, whereas dsb show a half-life of 2-4h (Bryant and Blöcher 1980).

Dsb are similarly thought to be the underlying lesion that cause chromosomal aberrations (Natarajan and Obe 1984). Early experiments with CHO cells showed that ssb caused by X-rays were converted into dsb by porating the cells and treating with Neurospora endonuclease, resulting in an increase in both chromosome and chromatid break frequencies (Natarajan *et al* 1980). Other studies using restriction endonucleases have indicated that dsb are the underlying lesions that are converted to chromosome and chromatid breaks (Bryant 1984b, Natarajan and Obe 1984). There are several different types of chromatid aberrations formed after IR, the type and frequency depend on the cell line, the radiation type and the cell cycle phase. In this study chromatid aberrations induced in the G2 phase of the cell cycle were investigated, especially chromatid gaps and breaks (shown in Figure 2.1).

1. Gap: the width of the gap is not larger than the width of the chromatid

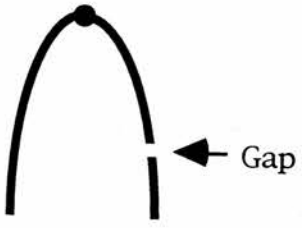

2. Breaks: the fragment is larger than the width of the chromatid and it may be aligned or displaced as shown

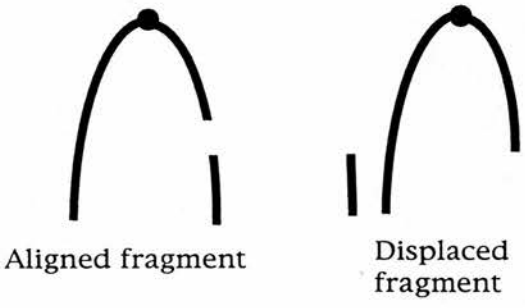

Figure 2.1. Diagramatic representation of the types of chromatid breaks and gaps scored in murine chromosomes which are mostly acrocentric

2.1.3: Chromosomal and cellular response of SCID cells to IR

Several studies have investigated the IR response of SCID cells. Clonogenic cell survival assays of several SCID cell types, such as bone marrow cells and intestinal crypt cells, have all shown a hypersensitivity to radiation (Fulop and Philips 1990, Biedermann *et al* 1991, Hendrickson *et al* 1991, Taniguchi *et al* 1993). Chromosome damage assays have shown that cells from SCID mice are 3 fold more sensitive to radiation than cells from wildtype CB17 mice. This is manifest by a higher frequency of chromatid exchanges at 4 hours after irradiation and at 24 hours there was a 5-8 fold increased frequency of chromatid fragments in bone marrow and fibroblast cells of SCID mice *in vivo* (Disney *et al* 1992). Similar results were obtained by van Buul *et al* (1995, 1998) who investigated the chromosomal response of spermatogonial and fibroblast SCID cells *in vitro*. Evans *et al* (1996) reported a 3 fold increased frequency of dicentrics formed in SCID cells (SCID sst3 fibroblast cells) compared with CB17 cells. In this study measuring the rejoining of PCC fragments showed that for every 25 breaks rejoined in CB17 cells there was a dicentric formed, but in SCID cells there was one dicentric formed for every 7-8 breaks rejoined. More recently, it was shown there were 4.3 fold more chromosome breaks in SCID fibroblast cells in G1 than CB17 cells, whereas in G2 the difference for chromatid breaks was only 1.3 fold higher in SCID cells (van Buul *et al* 1998).

Alongside these chromosome damage and clonogenic studies it has been shown that a consistently reduced or slow rejoining of dsb occurs in SCID cells which has been held as the reason for the induction of more exchange type aberrations in these cells (Biedermann *et al* 1991, Hendrickson *et al* 1991, Disney *et al* 1992, Evans *et al* 1996). However, the relationship between dsb and chromatid breaks is less than clear since dsb repair is apparently normal in G2 SCID cells (Lee *et al* 1997) although higher frequencies of chromatid breaks and exchanges are observed (Bryant *et al* 1998, van Buul *et al* 1998).

Thus, it was of great interest to study the kinetics of the disappearance of chromatid breaks in SCID cells, using the G2 assay.

The mammalian cell mutant xrs5, defective in dsb repair, shows a similar rate of disappearance of chromatid breaks with time to those of parental CHO cells (MacLeod and Bryant 1990). However, in xrs5 cells there was still a four fold increased frequency of chromatid breaks when compared to CHO cells up to five hours after IR exposure (MacLeod and Bryant 1990). This suggested there was an enhanced conversion of dsb into chromatid breaks in xrs5 cells in G2. A similar study had been carried out previously in AT cells treated with X-rays and again kinetics were similar, but break frequency was raised even at relatively short intervals (1-2h) after irradiation (Mozdarani *et al* 1989a, 1989b, 1987), in spite of the fact that AT cells are proficient in dsb repair (Lehmann and Stevens 1977, Foray *et al* 1995). A similar enhanced frequency of G2 chromatid breaks was apparent in irs2 cells, which are also dsb repair proficient (Bryant *et al* 1993). These results provide further evidence that chromatid break frequencies do not depend on dsb repair and suggest the existence of a biochemical pathway that converts dsb into chromatid breaks.

Xrs5 cells are known to be defective in Ku80 protein (Getts and Stamato 1994, Taccioli *et al* 1994b, Ross *et al* 1995, Singleton *et al* 1997) and SCID cells are defective in DNA-PK_{cs} (Araki *et al* 1997 and Blunt *et al* 1996) which is part of the same repair pathway. Therefore, it was interesting to study the kinetics of disappearance of chromatid breaks in SCID and CB17 cells for comparison with xrs5 cells. Similar experiments were repeated for $50D^-$ and $100E^+$ hybrid cells. The main question addressed in this chapter is whether the differential chromatid break frequency in SCID and CB17 cells is apparent at short time intervals (1-3h)* after IR exposure and whether or not a differential chromatid break

response is present between $50D^-$ and $100E^+$ cells. The G2 assay was used to measure the response of the four cell lines to IR at short time intervals after treatment.

* Note: While this thesis was being written a paper by van Buul *et al* (1998) was published showing an enhanced frequency of chromatid breaks at a single sampling time (2.5h).

2.2: Materials and Methods

2.2.1: Cell Culture

Murine fibroblastic cells homozygous for the SCID (severe combined immunodeficiency) mutation (SCID/st) and CB17 wildtype cell lines were obtained from Dr. Martin Brown, Stanford University, California. Cell cultures were routinely passaged and maintained in exponential growth in Waymouth's medium containing 10% foetal calf serum (GIBCO BRL), 50units/ml penicillin and 50μg/ml streptomycin.

Two transfected SCID fibroblastic cell lines $100E^{+}$ and $50D^{-}$ were obtained from Dr. Cordula Kirchgessner, Stanford University, California. These cells were routinely subcultured twice a week in Dulbecco's medium plus 10% foetal calf serum, 50units/ml penicillin, 50μg/ml streptomycin and 500μg/ml geneticin.

The cells were maintained in exponential growth by trypisinising the cells when they had reached 70-80% confluence. The media was removed from the cells that had reached 70-80% confluence and 1ml of trypsin added, the trypsin was washed over the surface of the cells by rocking the flask. This 1ml of trypsin was removed and another 1ml of trypsin added to the cells and washed over the surface. Afterwards the trypsin was removed and the cells incubated at 37°C for 3-6 min. Once the cells had detached from the surface of the flask they were resuspended in 10ml of fresh media and counted using a coulter counter. An average of three counts were used to estimate the number of cells in the final volume.

2.2.2: Irradiation

Gamma irradiation was carried out in a ^{137}Cs IBL437C γ-irradiator (CIS UK Bio-International, High Wycombe, UK). Doses were monitored by a ferrous sulphate method (Frankenberg 1969). The dose rate was approximately 4 Gy/min.

2.2.3: Growth curves

SCID and CB17 fibroblast cells after subculture were plated at 5 x 10^4 cells per petri dish ($60mm^2$) and $100E^+$ and $50D^-$ cells after subculture were plated at 5 x 10^5 cells per dish (different concentrations used because of differing growth rates). The dishes were set-up in duplicate for each time point. Every day for 14 consecutive days two petri dishes for each cell line were counted using a coulter counter. The growth curves were used to determine the doubling time, the exponential phase and growth patterns of each cell lines. For each experiment it was important to treat the cells in the log exponential phase of the cell cycle which ensured the cells were growing optimally.

2.2.4: Micronucleus assay

Petri dishes ($60mm^2$) with $5x10^5$ cells per dish after subculture were incubated at 37°C in a 5% CO_2 incubator overnight. The following day the cells were exposed to either one or two Gy of γ-rays at ambient temperature. Immediately after irradiation the medium was removed and replaced with medium containing cytochalasin B (at a final concentration of 3μg/ml, Sigma Co. UK) and cells were incubated at 37°C for 24 hours. The next day the cells were trypsinised and approximately 10^4 cells were placed into 1ml of medium and placed in a cytospin holder. The cells were cytocentrifuged for 10 min at 800 rpm. Afterwards the slides were dried, fixed in methanol for 10 min and stained with 6% giemsa (see appendix 1) for 10 min. The number of micronuclei in 100 binucleate cells were scored. Each experiment was repeated twice.

2.2.5: G2 assay

For experiments cells were seeded at a density of $2x10^6$ per 75 cm^2 flask and incubated overnight at 37°C. Following irradiation flasks were returned immediately to the incubator and incubated for various times before sampling. Samples were taken at 1, 2 and 3 hours after irradiation. Colcemid (0.04μg/ml) was added for 30 minutes in each case before fixation to block the cells in mitosis. Mitotic shake-off was used to increase the mitotic index for scoring metaphases. Usually 5 flasks were used per sample. Each experiment was repeated three times.

2.2.6: Metaphase chromosome preparations

Following mitotic shake-off cells were pooled from the 5 flasks, centrifuged at 0°C for 10 min at 1000rpm. The medium was removed and the cells were treated with ice-cold hypotonic solution (0.075M KCl, 0°C) for 10 min. The samples were centrifuged and the loosened pellets resuspended in 10ml of Carnoy's fixative (methanol: acetic acid, 3:1). Cells were washed 3 more times in fixative and collected by centrifugation each time. Cells were spread from a dilute suspension of fixative on to angled slides, that were flooded with ice-cold 70% acetic acid. Slides were dried and stained with 4% giemsa (see appendix 1) for 10 min.

2.2.7: Chromatid break analysis

Chromatid breaks and gaps were scored in 100 metaphases per sample. Scoring was always carried out under code. Each experiment was repeated at least three times.

2.3: Results

2.3.1: Analysis of growth curves for SCID, CB17, 50D$^-$ and 100E$^+$cells

The growth curves for each cell line are shown in Figures 2.2-2.3 and the data in Tables 2.1-2.2. Figure 2.2 and Table 2.1 represent the growth curves for SCID and CB17 cells. After plating, the cell concentrations were similar for both cell lines until day 2, at which point the CB17 cell concentration increased more than SCID cells. This suggests that SCID cells reached plateau phase at lower cell concentrations than CB17 (Figure 2.2, Table 2.1). The curves for SCID and CB17 cells follow an exponential growth pattern between 0-6 days, therefore, by applying the equation for exponential growth, the growth rate constant and doubling time can be calculated:

$\mathbf{N_t = N_0\, e^{\lambda t}}$ where

$\mathbf{N_t}$ represents final cell concentration;

$\mathbf{N_0}$ represents initial cell concentration;

λ represents rate constant;

and **t** represents time.

The rate constants for SCID and CB17 cells were calculated as 0.55 and 0.77 and the doubling times were 1.26 and 0.9 days, respectively. These results show a 1.4 fold slower growth for SCID cells relative to CB17 cells which is evident from Figure 2.2.

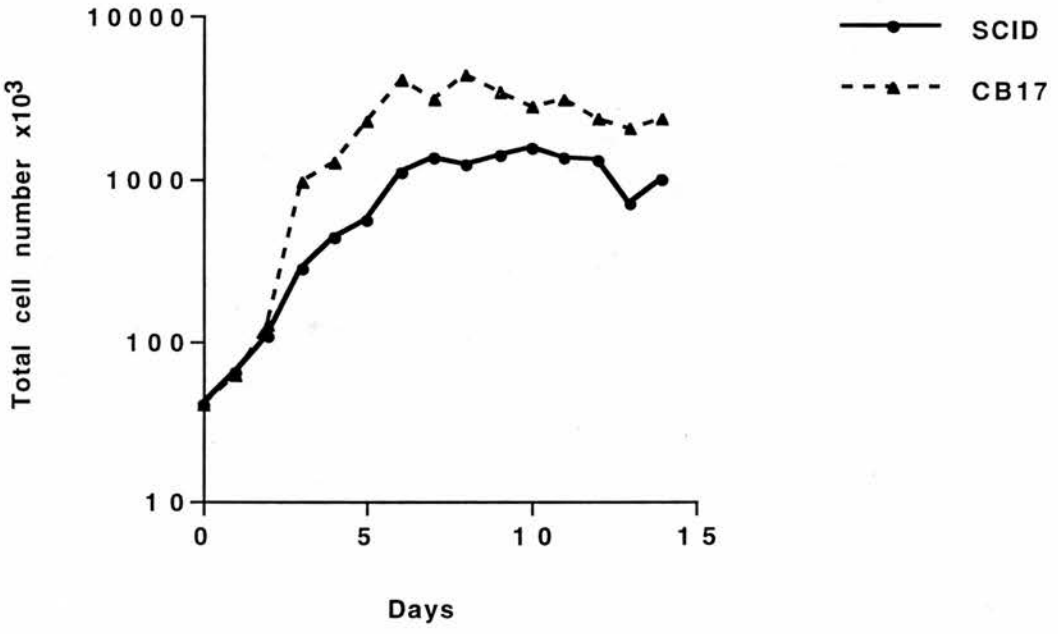

Figure 2.2: Growth curve for SCID and CB17 cells. Petri dishes were plated with $4x10^4$ cells and samples were counted every day for two weeks. Results pooled from three independent experiments, the error bars represent the standard errors.

Table 2.1: Number of cells counted from SCID and CB17 cell samples for 14 consecutive days*.

No. of days after plating	Mean number of cells x 10^{4}**	
	SCID	**CB17**
0	4.0 ± 0.0	4.0 ± 0.0
1	6.4 ± 2.0	6.2 ± 3.0
2	10.8 ± 2.0	12.6 ± 2.3
3	27.8 ± 8.4	95.9 ± 44.0
4	44.0 ± 15.9	130.0 ± 30.0
5	55.5 ± 34.0	230.0 ± 11.3
6	112.0 ± 11.2	416.0 ± 16.2
7	137.0 ± 55.0	316.0 ± 55.8
8	123.0 ± 19.7	440.0 ± 19.7
9	142.0 ± 31.8	352.0 ± 52.0
10	155.0 ± 10.6	286.0 ± 59.0
11	137.0 ± 12.4	314.0 ± 12.0
12	132.0 ± 11.9	235.0 ± 34.6
13	71.5 ± 14.9	210.0 ± 9.0
14	100.0 ± 0.0	240.0 ± 39.0

* Graphically shown in Figure 2.2

** Each value represents the mean and standard errors from three independent experiments. Cells were plated at the same concentration ($4x10^{4}$) in petri dishes and two cell samples of each cell line were counted for each experiment every day for 14 days.

The growth curves for $50D^-$ and $100E^+$ hybrid cells are shown in Figure 2.3 and Table 2.2. Both cell lines follow the same curve with similar cell numbers. An exponential growth pattern is observed between 0-3 days. The growth rate constants were 0.79 and 0.83 for $50D^-$ and $100E^+$ cells and the doubling times were 0.87 and 0.91 days, respectively. These results show a slightly faster growth rate in $100E^+$ cells which is significantly different than $50D^-$ cells ($p=0.014$ between 0-1 days, using a rank sum test). A comparison of the growth rate constants for each of the four cell lines indicated that SCID cells had the slowest growth rate.

It must be noted that the culturing of $50D^-$ and $100E^+$ was hampered by the formation of clumps and an inability to grow the cells as single cell monolayers. Usually contact inhibition prevents cells from overgrowing in culture but this was not apparent in these hybrid cells. Once clumps were formed they were difficult to disperse. Therefore, it was essential to remove clumps by pipetting or syringing the cells before setting up cultures for experiments, so that monolayers were obtained. The formation of clumps and the absence of contact inhibition appear to be characteristics of these cell lines.

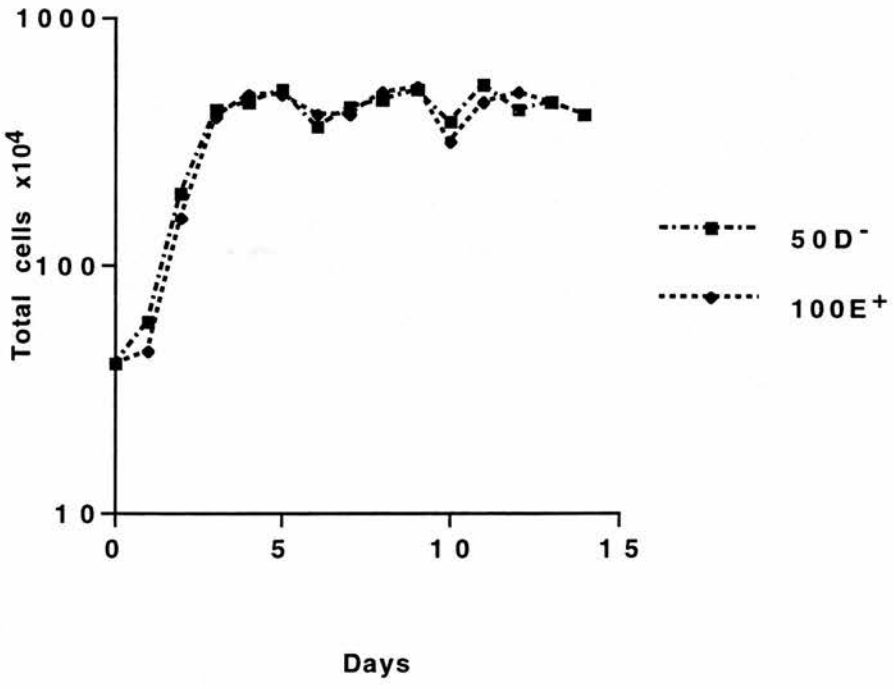

Figure 2.3: Growth curve for $50D^-$ and $100E^+$ cells. Petri dishes were plated with $4x10^5$ cells and cell samples were counted every day for two weeks. The results shown were pooled from three independent experiments and the error bars represent the standard errors.

Table 2.2: Number of cells counted from $50D^-$ and $100E^+$ cell samples for 14 days*.

No. of days after plating	No. of cells x 10^{5**}	
	$50D^-$	**$100E^+$**
0	4.0 ± 0.0	4.0 ± 0.0
1	6.0 ± 1.2	4.5 ± 1.4
2	19.7 ± 1.0	15.7 ± 1.7
3	43.0 ± 3.5	40.0 ± 3.9
4	46.7 ± 3.8	49.0 ± 3.5
5	52.3 ± 8.1	49.0 ± 8.4
6	37.0 ± 3.1	41.6 ± 8.9
7	44.0 ± 3.8	41.6 ± 2.3
8	47.4 ± 0.4	50.2 ± 3.7
9	52.4 ± 5.4	53.0 ± 1.3
10	38.6 ± 3.0	32.0 ± 3.0
11	54.0 ± 3.3	46.5 ± 0.7
12	42.9 ± 3.8	50.5 ± 1.2
13	46.0 ± 2.8	46.0 ± 1.4
14	41.0 ± 5.3	41.0 ± 1.0

* Graphically shown in figure 2.3.

** Each value represents the mean and standard errors from three independent experiments. Cells were plated at the same concentration ($4x10^5$) in petri dishes and two cell samples were counted every day for 14 days

2.3.2: Radiosensitivity of SCID, CB17, 50D$^-$ and 100E$^+$ as measured by the micronucleus assay

The micronucleus assay results shown in Figure 2.4. (Table 2.3.a), illustrate the radiosensitivities of the four cell lines, following treatment with 1 or 2 Gy of gamma radiation (Figure 2.5 a and b illustrate binucleate cells and micronuclei). SCID and 50D$^-$ cells are most sensitive to IR following 1 or 2 Gy of gamma radiation, CB17 cells are the least sensitive and 100E$^+$ cells show an intermediate radiosensitivity. In this micronucleus assay (Table 2.3.a) SCID cells were 10.5 and 7.2 fold more sensitive to ionisation radiation (1 or 2 Gy respectively, after subtracting control values) than CB17 cells which is consistent with previously published results (Fulop and Philips 1990, Biedermann *et al* 1991 and Hendrickson *et al* 1991). In addition it must be noted that the background frequency of micronuclei were approximately two fold higher in SCID cells than CB17 cells suggesting there may be a higher frequency of spontaneous chromosome damage in SCID cells. The 100E$^+$ hybrid cells complemented with the human gene which encodes for DNA-PK$_{CS}$ were expected to give a response similar to CB17 cells. However, in this Mn assay, 100E$^+$ cells displayed partial complementation of the radiosensitivity defect by showing a 5.8 and 3.4 fold elevated radiosensitivity after 1 and 2 Gy gamma radiation compared to CB17 cells. Kirchgessner *et al* (1995) reported full complementation of the radiosensitivity defect, as measured by cell survival assays. This difference may be attributed to a proportion of the 100E$^+$ cells reverting back to the SCID phenotype and this could be investigated by determining the presence of a bimodal distribution (analysis not carried out). Alternatively the difference may be due to the different end points measured by the two studies. As expected the 50D$^-$ cells showed a response similar to SCID cells as the human DNA-PK$_{CS}$ was not present to complement the SCID defect. Statistical analysis using t-tests are shown in Table 2.3b, illustrating the differences between the radiosensitivities of the four cell lines.

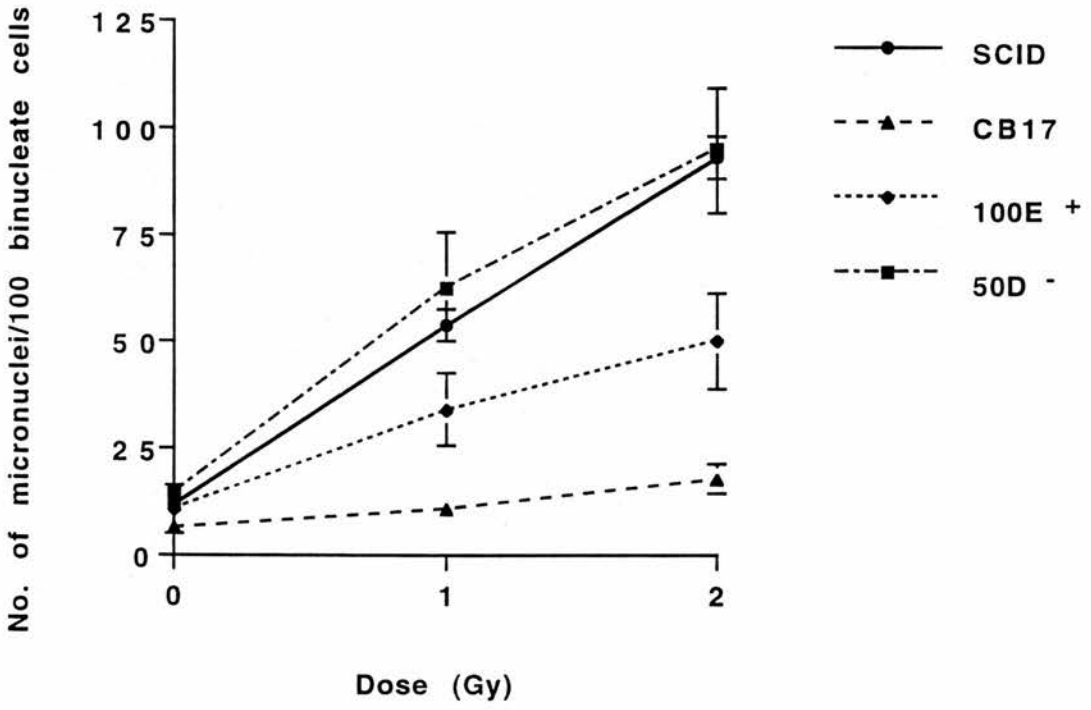

Figure 2.4: A comparison of the radiosensitivities of each cell line as measured by the micronucleus assay. Each cell sample was exposed to 1 or 2 Gy gamma rays. The cells were incubated in medium containing cytochalasin B. Each value has been adjusted for the background frequency of micronuclei. The results were pooled from three independent experiments and the error bars represent the standard errors of the mean.

Table 2.3.a: Frequency of micronuclei induced in SCID, CB17, 50D$^-$ and 100E$^+$ cells treated with 1 or 2 Gy gamma radiation.**

Treatment	No. of micronuclei per 100 cells*			
	SCID	**CB17**	**50D$^-$**	**100E$^+$**
Control cells	11.8 ± 0.5	6.5 ± 1.6	14.2 ± 2.4	10.5 ± 5.5
1 Gy γ–rays	54.0 ± 3.9	10.5 ± 1.2	62.8 ± 12.7	34.0 ± 8.2
2 Gy γ– rays	93.3 ± 3.7	17.8 ± 3.7	94.8 ± 14.8	50.0 ± 11.4

*Each value represent the means and standard errors from three independent experiments. Each cell sample was treated with gamma radiation and incubated in media containing cytochalasian B overnight. Afterwards cell samples were collected, slides were prepared and the frequency of induced micronuclei scored in 100 binucleate cells per sample.

** Graphically shown in Figure 2.4.

Table 2.3.b: Statistical analysis and comparison of Mn yields in each cell line.

T-test	P-value
SCID vs CB17 1Gy	0.002*
SCID vs CB17 2Gy	0.0002*
SCID vs 50D 1Gy	0.61
SCID vs 50D 2Gy	0.95
CB17 vs 100E 1Gy	0.032*
CB17 vs 100E 2Gy	0.0095*
50D vs 100E 1Gy	0.11
50D vs 100E 2Gy	0.053
100E vs SCID 1Gy	0.0143
100E vs SCID 2Gy	0.17

*indicates a significantly different response to IR between the two cell lines

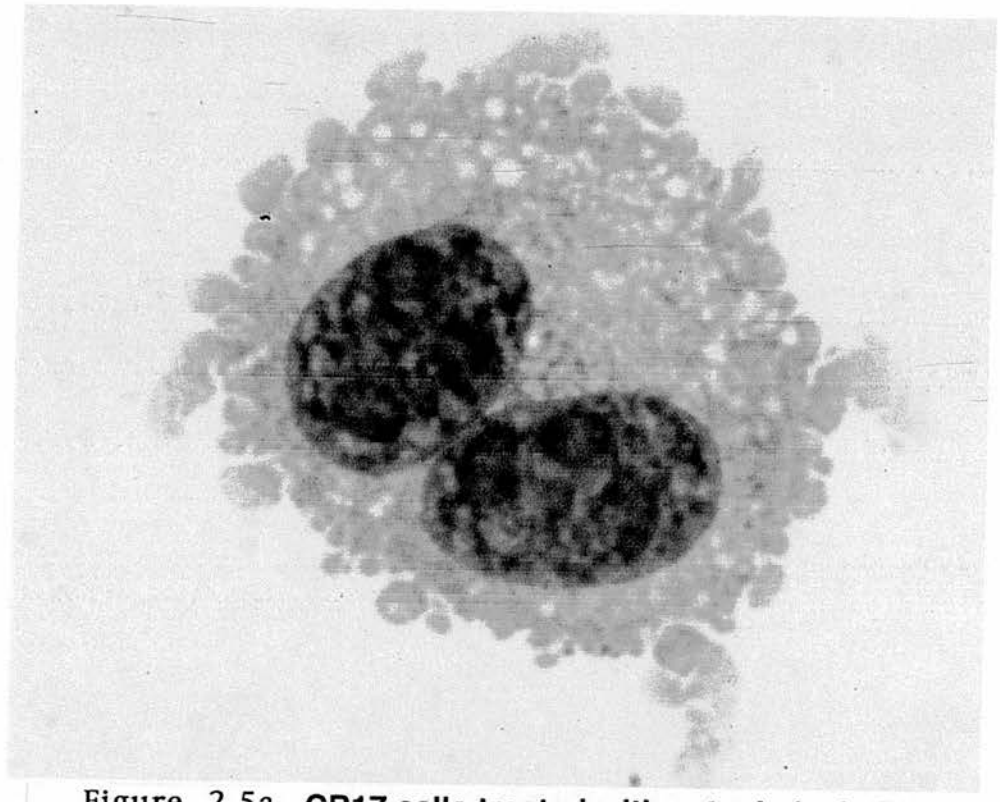

Figure 2.5a **CB17 cells treated with cytochalasin B hence the binucleated cell.**

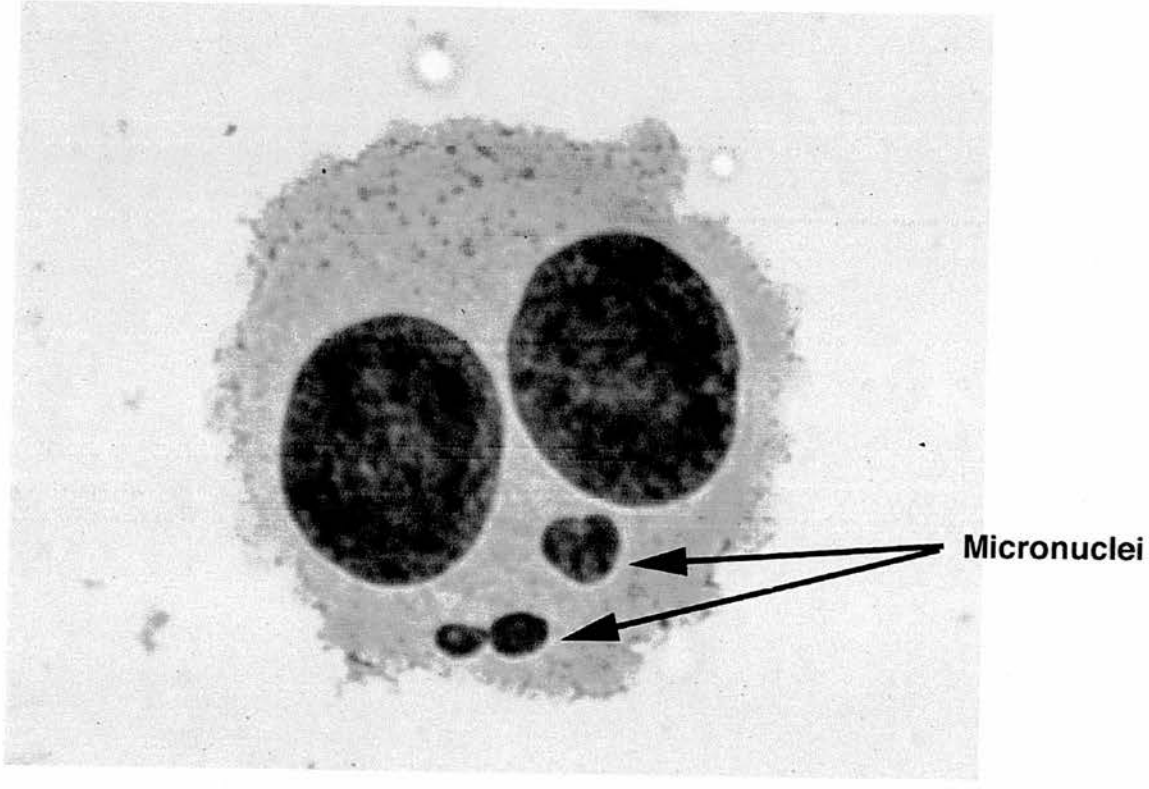

Figure 2.5b. **CB17 cells exposed to 1Gy gamma radiation, the micronuclei are marked with arrows.**

The yield of micronuclei in SCID and $50D^-$ cells was similar, which was not suprising because the $50D^-$ cell line did not contain the fragment of human chromosome 8 complementing the SCID defect. This result showed that $50D^-$ cells were useful controls for $100E^+$ cells. The SCID hybrid cells ($100E^+$, $50D^-$) did not show a significant difference in the response to IR using an analysis of variance plus coefficient of variance and regression. The reason is likely the reversion of $100E^+$ cells to the $50D^-$ phenotype. Analysis of variance plus the coefficient of variation for the response of SCID and CB17 cells to IR using the Mn assay gave an F-value of 18.75 $(df.\ 1,15)$ which was significant at $p< 0.05$. Similarly, regression analysis was also significant at $p< 0.05$. This confirmed that the response of SCID cells to increasing doses of IR, as measured by the Mn assay, was significantly different than CB17 cells.

2.3.3: Binucleate Index of SCID, CB17, $50D^-$ and $100E^+$ cells following IR treatment

The Binucleate Index (BI) was calculated for one sample of each cell line, as shown in Table 2.4.a. There were no obvious differences in the BI for the four cell lines following IR treatment. The percentage of binucleated cells in the control samples for each cell line are similar and as expected, as the radiation dose increased the number of binucleated cells decreased in each cell line. After exposure to 2 Gy of IR the BI decreased to approximately 55% in all cell lines. The normalised percentage decrease in the BI for control and irradiated samples was calculated (Table 2.4.b), to determine the overall changes in the BI before and after IR. The normalised results show a 17-28% decrease after 1 Gy of γ-radiation for each cell line and a 27-39% decrease after 2 Gy.

Table 2.4.a. The binucleate index calculations for each cell line*.

Radiation dose (Gy)	SCID	CB17	$50D^-$	$100E^+$
0	79	75	81	87
1	62	62	66	63
2	55	55	56	53

*The Binucleate index represents the number of binucleate cells per 100 cells. The binucleate index was only measured once.

Table 2.4.b. Normalised percentage decrease in the binucleate index

Cell line	Normalised decrease in the binucleate index*	
	0-1 Gy	0-2 Gy
SCID	22%	30%
CB17	17%	27%
$50D^-$	19%	31%
$100E^+$	28%	39%

*Calculated by: $100 - \frac{\text{BI after IR}}{\text{BI before IR}} \times 100\%$

2.3.4: Preliminary G2 assay studies of SCID and CB17 cells treated with gamma radiation

Preliminary experiments were carried out before the G2 assay was performed to test the appropriate radiation dose and time in colcemid (Table 2.5). Only 25 cells were scored for each sample, yet there were approximately 90 chromatid breaks in total which is approximately 4 breaks per cell. CB17 cells were exposed to 0.77 Gy of γ-rays, whereas SCID cells were exposed to 0.38 Gy which gave a similar chromatid break frequency in both cell lines. This is consistent with previous studies in which SCID cells were two fold more sensitive to ionising radiation than CB17 cells (Biedermann *et al* 1991, Hendrickson *et al* 1991 and Bryant *et al* 1998). The time period in which SCID and CB17 cells were blocked in mitosis does not appear to have any effect on the response to radiation, as there were ample mitotic cells to score at each time point. However, these preliminary results indicated that SCID cells did not produce optimally spread metaphases and many initial experiments could not be analysed. Therefore, a simple test was carried out to determine the best method for spreading SCID chromosomes, as shown in Table 2.6., treating SCID cells on ice with ice-cold hypotonic solution for 10 minutes and using ice cold slides, flooded with 70% acetic acid gave optimally spread metaphases.

Table 2.5: Preliminary G2 assay showing frequencies of chromatid breaks induced by gamma radiation in SCID and CB17 cells.

Cell line	Treatment Radiation dose (Gy)	Time in colcemid (h)**	Chromatid breaks per 25 cells*
SCID	Control	1.0	2.0
CB17	Control	1.0	1.0
SCID	0.38 γ-rays	1.0	96.0
CB17	0.77 γ-rays	1.0	79.0
SCID	Control	2.0	8.0
CB17	Control	2.0	4.0
SCID	0.38 γ-rays	2.0	92.0
CB17	0.77 γ-rays	2.0	102.0

*Results of a single experiment.
**Colcemid was added to the cells 30 min after IR

Table 2.6: Various methods used to separate untreated SCID chromatids*.

Temperature of hypotonic solution	Time of hypotonic treatment	Clarity of chromosomes
37 degrees	5min	No metaphases
Room temperature	10min	Fuzzy chromosomes poor definition
Ice-cold	10min	Good staining and clear chromosomes
Ice-cold	20min	Good staining poor metaphases

*Each sample was treated with colcemid for 1.5 hours.

2.3.5: Disappearance with time of chromatid breaks in G2 SCID and CB17 cells following IR exposure

The G2 assay results are shown in Figure 2.6 and Table 2.7. An example of the type of chromatid breaks and gaps scored are shown in Figure 2.7. The disappearance of chromatid breaks with time following IR appears to be the same in SCID and CB17 cells between 1-2 h, after which time the disappearance of chromatid breaks in CB17 cells is reduced. SCID cells display a 1.3, 1.7 and 1.5 fold elevated chromatid break frequency compared to CB17 cells at 1, 2 and 3 hours respectively, after irradiation. The graph in Figure 2.6 suggests first order kinetics of disappearance of chromatid breaks in SCID and CB17 cells between 1-3 h. The results can be fitted to the expression for exponential decay $\mathbf{N_t = N_0\, e^{-\lambda t}}$ where,

Nt represents final frequency of chromatid breaks;

$\mathbf{N_0}$ represents initial frequency of chromatid breaks;

λ represents rate constant;

and **t** represents time.

Regression analysis of the disappearance of chromatid breaks with time yielded similar $t_{1/2}$ values (1.3 and 1.2h for SCID and CB17 cells respectively see appendix 5 for details).

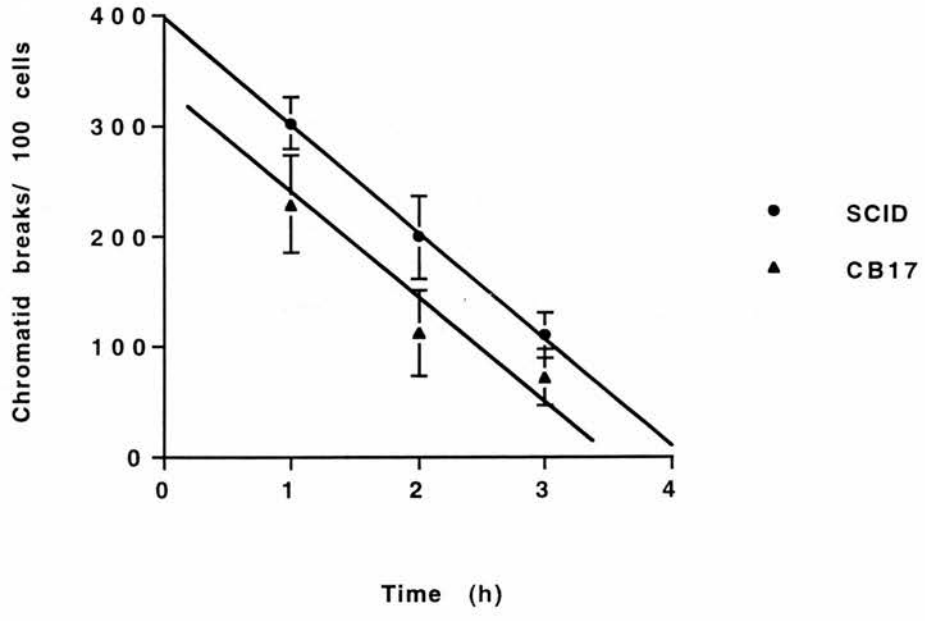

Figure 2.6: Kinetics of disappearance of chromatid breaks in SCID and CB17 cells. Each cell line was exposed to 0.24 Gy of gamma radiation and samples were taken at 1, 2 and 3h after irradiation. Control values have been subtracted from each value. The values plotted represent the means and standard errors from three independent experiments. Data shown in Table 2.7.

Table 2.7: Frequencies of chromatid breaks in G2 SCID and CB17 cells as measured by the G2 assay at short time intervals after gamma radiation*.

Cell line	Treatment	Time after irradiation (h) ***	Chromatid breaks per 100 cells**
SCID	Control	1.0	12.3 ± 2.4
CB17	Control	1.0	9.6 ± 00.3
SCID	0.24 γ-rays	1.0	315.0 ± 23.5
CB17	0.24 γ-rays	1.0	239.0 ± 44.4
SCID	Control	2.0	9.0 ± 6.1
CB17	Control	2.0	9.6 ± 0.3
SCID	0.24 γ-rays	2.0	209 ± 37.7
CB17	0.24 γ-rays	2.0	121.6 ± 38.7
SCID	Control	3.0	8.3 ± 1.2
CB17	Control	3.0	5.3 ± 0.9
SCID	0.24 γ-rays	3.0	118.0 ± 20.4
CB17	0.24 γ-rays	3.0	77.7 ± 25.1

* Graphically shown in Figure 2.6.

**Data represent the means and standard errors from three independent experiments in which a total of 300 cells were scored.

***Time after irradiation represents the time interval after IR exposure before the cells were treated with colcemid (30 min) to block the cells in mitosis before fixation.

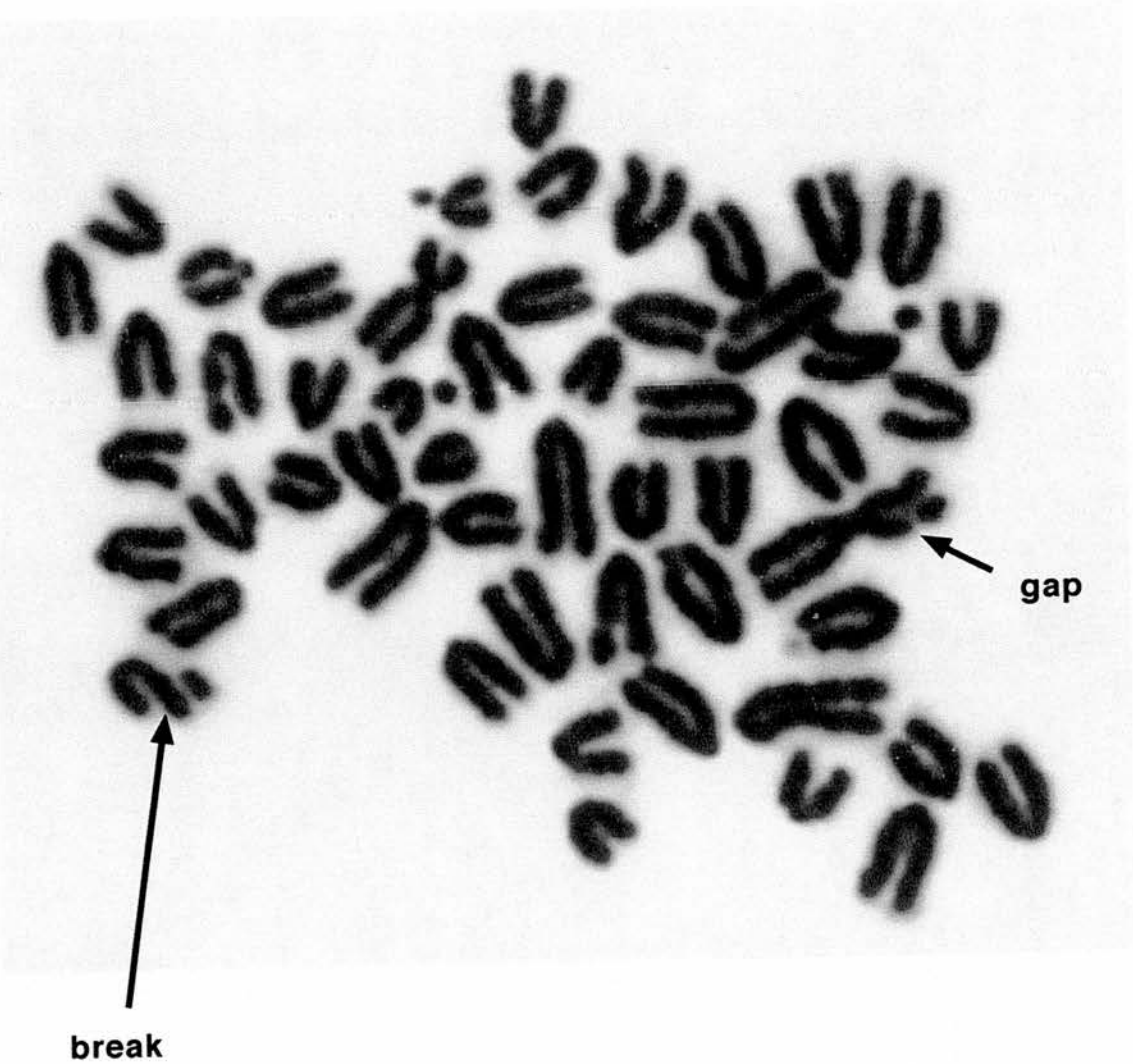

Figure 2.7: Murine SCID cells treated with 0.24Gy gamma radiation and blocked in mitosis by colcemid 30 mins prior to harvesting.

2.3.6: Disappearance of chromatid breaks in G2 50D$^-$ and 100E$^+$ cells after IR

Similar kinetics of disappearance of chromatid breaks with time were obtained for 50D$^-$ and 100E$^+$ cells, as shown in Figure 2.8 and Table 2.8, however, the overall frequency of chromatid breaks per 100 metaphases were unexpectedly lower, by approximately 2 fold in 50D$^-$ and 100E$^+$ cells relative to SCID and CB17 cells, although a difference between 50D$^-$ and 100E$^+$ was still evident. The reasons for difference between the two pairs of lines are not understood. These results exhibited a first order exponential decay rate of chromatid breaks with time, hence, the use of the equation as shown previously. The $t_{1/2}$ values were 1.4 h and 1.5 h for 50D$^-$ and 100E$^+$ cells, respectively, between 1-3 h (calculations shown in appendix 5). Regression analysis of the disappearance of chromatid breaks in both hybrid cell lines with time was not significantly different suggesting the same "repair" rate in both cell lines. Even though the "repair" rates were the same for these hybrid cells, the 50D$^-$ cells had a 1.6, 1.7 and 2.8 fold elevated chromatid break frequency at 1, 2 and 3 h respectively following irradiation which was higher than the differential response exhibited by SCID cells compared with CB17 cells.

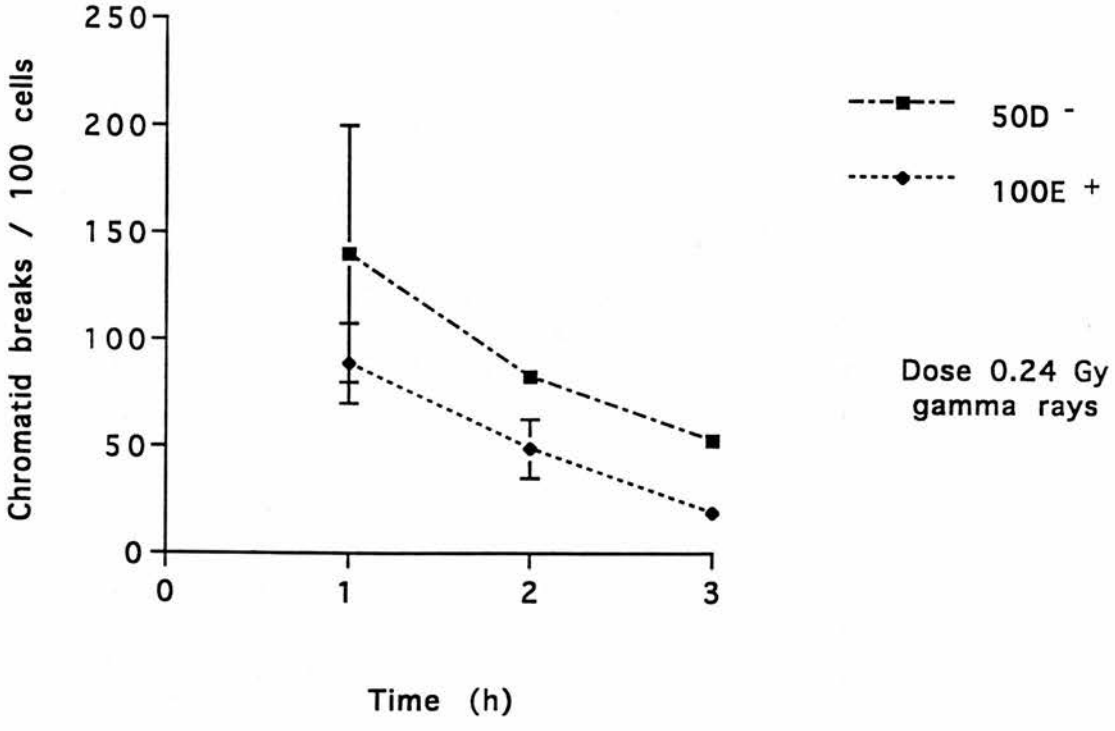

Figure 2.8: Kinetics of the disappearance of chromatid breaks in $50D^-$ and $100E^+$ cells. Each cell line was exposed to 0.24Gy of gamma radiation and samples taken at 1, 2 and 3 h after irradiation. Control values have been subtracted from the plotted values and are shown in Table 2.8. The values plotted represent the means and standard errors from three independent experiments.

Table 2.8: Frequencies of chromatid breaks in $50D^-$ and $100E^+$ cells as measured by the G2 assay at short time intervals after γ-radiation*.

Cell Line	Treatment	Time after irradiation (h)**	Chromatid breaks per 100 cells***
$50D^-$	Control	1.0	16.0 ± 8.9
$100E^+$	Control	1.0	23.0 ± 1.5
$50D^-$	0.24 γ-rays	1.0	156.0 ± 60.0
$100E^+$	0.24 γ-rays	1.0	112.0 ± 19.0
$50D^-$	Control	2.0	21.0 ± 3.6
$100E^+$	Control	2.0	25.0 ± 6.0
$50D^-$	0.24 γ-rays	2.0	104.0 ± 2.0
$100E^+$	0.24 γ-rays	2.0	74.0 ± 14.0
$50D^-$	Control	3.0	15.0 ± 6.0
$100E^+$	Control	3.0	21.0 ± 9.0
$50D^-$	0.24 γ-rays	3.0	68.0 ± 6.0
$100E^+$	0.24 γ-rays	3.0	40.0 ± 6.0

*Graphically shown in Figure 2.7.

**Time after irradiation represents the time interval after IR exposure before the cells were treated with colcemid (30 min) to block the cells in mitosis before fixation.

***Data represent the means and standard errors from two independent experiments in which 200 cells were scored.

2.4: Discussion

2.4: Discussion

The growth curves (Figure 2.2 & 2.3) were used to determine the optimal cell concentration to use in experiments. The initial cell concentrations for seeding the petri dishes were the same for SCID and CB17 cell lines (Table 2.1). After 3 days in culture there was a decreased growth rate in SCID cells relative to CB17 cells (Figure 2.2). SCID cells reached plateau phase at lower cell concentrations than CB17 cells and this may be explained by SCID cells appearing larger and more spread out with longer cell processes. CB17 cells gave a more rounded appearance enabling more cells to grow within the same area before reaching confluence (a point reached when the cells contact each other and stop growing). For experiments $2x10^6$ cells were seeded in tissue culture flasks ($75mm^3$) overnight maintaining the cells in exponential growth.

The $50D^-$ hybrid cells had a significantly higher initial growth rate than $100E^+$ hybrid cells, resulting in a slightly shorter log phase for $50D^-$ hybrid cells. However, after 2 days in culture both hybrid cell lines had similar growth rates and growth patterns (Figure 2.3 and Table 2.2.). These two cell lines showed a dependency on neighbouring cells for optimal growth, as conditions in which low cell concentrations were used resulted in no growth or small groups of cells growing in colonies

The preparation of metaphase chromosomes for SCID cells in the G2 assay proved difficult initially. The chromosomes of SCID cells are very "sticky" and appear smaller than CB17 chromosomes. The individual SCID chromatids were difficult to separate and the clarity of small chromatid breaks was poor, making it difficult to score the damage accurately. However, several different techniques were tried until a method was found that produced clear chromatids (Figure 2.7). A difference in chromatid appearance has also been shown for xrs5 cells when compared to parental CHO cells (Schwartz *et al* 1993).

Schwartz *et al* (1995) reported that xrs5 chromatids appeared over-condensed, shorter and thicker than CHO chromatids which may be due to differences in the phosphorylation of nuclear proteins. This may be the reason for the "sticky" chromatids in SCID cells, as DNA-PK_{cs} is defective, and one function of DNA-PK is the phosphorylation of proteins involved in transcription and replication (see Chapter 6 for measurements of chromatid lengths).

The Mn assay is a quick and easy method to determine radiosensitivity. It ensured that the SCID cell line had not reverted back to the CB17 phenotype, or $100E^+$ cells had not reverted to the $50D^-$ phenotype, an effect which has been observed previously in xrs5 cells (Jeggo and Kemp 1983 and Denekemp *et al* 1989). In this study, the Mn assay was useful because it showed that the $100E^+$ cell line had partially reverted back to the SCID phenotype. Previously Kirchgessner *et al* (1995) showed a slight degree of reduced complementation, using the colony assay, when the cell line was first produced but not to the same extent as presented here which was 5.8 and 3.4 fold elevated after 1 and 2Gy gamma radiation compared with CB17 cells. This difference may be explained by the $100E^+$ cell line having a reduced DNA-PK complementation after long periods in culture, due to a subpopulation of cells retaining the neomycin resistance but not DNA-PK complementation. This is consistent with previously published results in which $100E^+$ cells exhibited an intermediate radiosensitivity as measured by the colony assay (Johnston *et al* 1998). Therefore, it is necessary to regularly use the Mn assay, in addition to FISH analysis, to confirm the presence of human chromosome 8 in $100E^+$ cells. Other complementation studies of SCID cell lines have shown full restoration of the V(D)J recombination defect but not the radiosensitivity deficiency. This may be due to another gene defective in these cells, it may be a characteristic of the SCID cell line or an interspecies effect, such that the human gene fails to fully complement the mouse mutation.

SCID cells exhibited an enhanced radiosensitivity after exposure to IR relative to wildtype CB17 cells, as measured by the production of micronuclei in an asychronous cell culture and chromatid breaks in the G2 assay. This agrees with previously published results showing an enhanced chromosomal (Disney *et al* 1992, van Buul *et al* 1995, 1998, Evans *et al* 1996) and cellular (Fulop and Philips 1990, Biedermann *et al* 1991, Hendrickson *et al* 1991) radiosensitivity in SCID cells relative to CB17 cells. The G2 assay results shown here (Figure 2.5) demonstrate a 1.3-1.7 fold enhanced radiosensitivity in SCID cells that is consistent with recently published results showing a 1.3 fold elevated frequency of chromatid breaks in G2 SCID cells (van Buul *et al* 1998). Similarly $50D^-$ cells showed a 1.7-2.8 fold enhanced frequency of chromatid breaks relative to $100E^+$ cells within G2.

SCID and CB17 cells showed a decrease in the binucleate index as the radiation dose increased (BI). This may be attributed to an increased cell cycle inhibition. However, measurement of multinucleate cells as opposed to just binucleate cells would provide a better idea of cell cycle variations and growth differences. Further investigations are required to provide a greater insight into the possible cell cycle variations.

This study was mainly concerned with investigating the kinetics of the disappearance of chromatid breaks in G2 SCID and CB17 cells at short time intervals following IR. The $t_{1/2}$ values obtained for SCID and CB17 cells were 1.3 and 1.2 h respectively. These $t_{1/2}$ values are consistent with a recent report, by Bryant *et al* (1998), showing a $t_{1/2}$ value of 1.5 h for SCID and CB17 cells. A similar disappearance of chromatid breaks (between 1-3 h) was shown in this study for SCID and CB17 cells at short time intervals following IR treatment (Figure 2.6). This suggests that both cell lines were "repairing" chromatid breaks. The 1.3-1.7 fold elevated chromatid break response detected in SCID cells remained consistent between 1-3 h. This elevated response has also been observed in other mammalian cell mutants that are dsb repair deficient, such as xrs5 cells (Mateos *et al*

1994), as well as cells known to be proficient in dsb repair, e.g. AT or irs2 cells (Mozdarani *et al* 1989a, 1989b, Bryant *et al* 1993). The elevated chromosomal response exhibited by these mutants has been proposed to be the result of an enhanced conversion of dsb into chromatid breaks (Bryant 1998). However, in this study the elevated chromatid break response in SCID cells is likely explained by the G2 dsb repair deficiency, as shown in Chapter 5 (Figure 5.5). G2 dsb repair analysis shows a reduced rejoining of dsb 10 min after irradiation in SCID cells relative to CB17 cells. Therefore, the elevated chromatid break response shown in SCID cells at 1 h post-irradiation suggests the dsb rejoining deficiency is directly related to the frequency of induced chromatid breaks.

An elevated chromatid break frequency was also apparent for $50D^-$ cells (1.6-2.8 fold) relative to $100E^+$ cells and may be explained by the signal model (Bryant 1998). However, it should be noted that chromatid break frequencies were two fold lower in both $50D^-$ and $100E^+$ (Fig.2.6 and 2.8). It is not clear why $50D^-$ should show lower chromatid break frequency than SCID, since $50D^-$ is a non-complemented line. Further experiments are clearly required to fully understand the mechanisms of the conversion of dsb to chromatid breaks in these hybrid cells.

Chapter Three

The chromosomal response of murine SCID cells to 9-β-D arabinofuranosyladenine (araA; a DNA synthesis inhibitor).

3.1: Introduction

Chapter Three:

3.1 Introduction

The aim of the work described in this chapter was to investigate the G2 response of SCID and CB17 cells to IR in the presence of 9-β-D arabinofuranosyladenine (araA). The kinetics of the disappearance of chromatid breaks in SCID and CB17 cells were reported in the previous chapter, and although more breaks were observed in SCID cells the disappearance of breaks were the same for both cell lines (i.e. parallel to one another between 1-3 h Figure 2.6 Chapter 2), suggesting that "repair" of an underlying lesion was occurring at a similar rate in both cell lines. AraA is a DNA synthesis (Furth and Cohen 1967, 1968, Müller *et al* 1975) and DNA dsb repair inhibitor in murine Ehrlich ascites tumour cells (Bryant and Blöcher 1982). Therefore, it was interesting to investigate the response of SCID and CB17 cells to IR in the presence of araA and to see the effects on the disappearance of chromatid breaks with time (Figure 2.6 Chapter 2). If a response was present in SCID and CB17 cells treated with araA, then it may be interpreted either as an inhibition of dsb repair, or as an effect on the rejoining of DNA ends to form recombinational exchanges, as this process is thought to require DNA synthesis. The reports to date suggest that SCID cells are deficient in dsb repair (Biedermann *et al* 1991, Hendrickson *et al* 1991). Thus, it might be expected that the addition of araA would cause an increase in the frequency of chromatid breaks in CB17 cells (due to inhibition of dsb repair) but the response of SCID cells might remain the same due to the already deficient dsb repair in these cells. This experiment was also used to investigate the response of $50D^-$ and $100E^+$ cells (SCID hybrid cell lines) to IR in the presence of araA. Initially, preliminary experiments were carried out to determine the optimal concentration of araA to use, i.e. that which had a minimum effect on the background levels of chromatid damage. The effect of araA after IR exposure was studied in G2 cells of SCID, CB17, $50D^-$ and $100E^+$ lines by the G2 assay.

3.1.1: Discovery of araA

AraA was first recognised by its cytostatic action (Lee *et al* 1960) and it was viewed as a potential antitumor (Müller *et al* 1977) and antiviral agent (Shannon 1975). AraA has been used in the treatment of herpes infections as an antiviral agent because araA is incorporated into viral DNA causing chain termination (Shannon 1975). Therefore, araATP molecules have to be incised from the DNA chain before viral replication can proceed. Unlike the chain termination effects that occur in viral DNA, in mammalian cells the incorporation of araATP into DNA is limited, as only 1 molecule of araA was incorporated per 8000 molecules of deoxyadenosine, as an internucleotide linkage during DNA synthesis (Müller *et al* 1975, Plunkett *et al* 1975). However, it has been shown that araA is mainly incorporated at 3' termini and it may alter the addition of nucleotides thereby acting as a relative chain terminator (Müller *et al* 1977).

AraA was first identified as an antitumor agent when it was added to mouse lymphoma cells in which there was a reduced growth rate as the AraA concentration increased (Müller *et al* 1977). AraA is a nucleoside analogue of deoxyadenosine and it differs from adenosine at the 2' position of the sugar moiety [Figure 3.1] (Müller and Zahn 1978). AraA acts on DNA synthesis by having a direct effect on DNA polymerase, and it has been shown to reduce DNA synthesis even in the presence of deoxynucleotides (Brink and Lepage 1965).

3.1.2: Uptake and action of araA

The action of araA on the cell was initially studied in mouse lymphoma cells which showed that araA was phosphorylated on entering the cell to form araATP which competes with dATP at the binding sites of DNA polymerase α and β (Tseng *et al* 1982, Parker *et al*

Adenosine

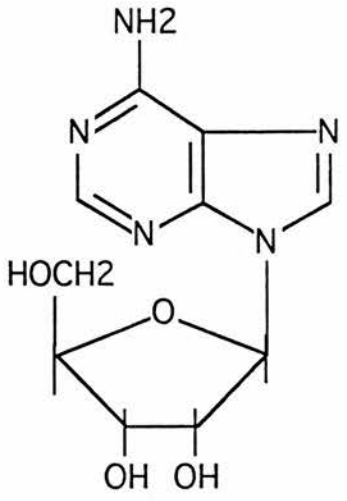

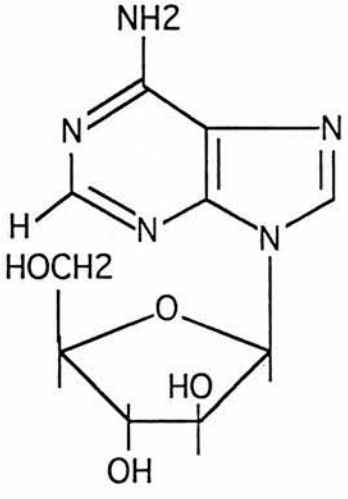

Arabinofuranosyladenine

(araA)

Deoxyadenosine

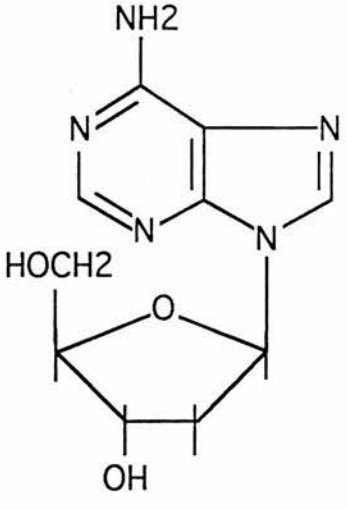

Figure 3.1. Structures of adenosine, arabinofuranosyladenine (araA) and deoxyadenosine

1988 and White 1982). Other polymerases affected by araA are δ and ε (Parker *et al* 1988). A study of the pool size of dATP and araATP was investigated in synchronised mouse lymphoma L5178Y cells, which showed a usual pool size of 1-3 pmoles/10^6 cells for dATP during G1 which increased to 4 pmoles/10^6 cells during S phase (Müller *et al* 1977). The addition of araA to mouse lymphoma cells showed that 61% of araA was taken up by the cells as araATP forming a pool size of 1 pmole/10^6 cells. In calf thymus cells the Ki value (inhibition constant for DNA synthesis rate) for araATP was 45μM for polymerase β which was 15 fold higher than the Ki value for α polymerase (3μM) (Okura and Yoshida 1978). This suggested that araATP competed with dATP at the polymerase binding sites, inhibiting α more than β. However, other studies have shown that β polymerase is inhibited more than α (Müller *et al* 1975). Therefore, the extent of inhibition of individual polymerases by araA is not fully known. As mentioned previously the reaction between araATP and dATP was thought to be competitive and this has been confirmed by increasing the pool size of dATP which decreased the inhibitory effect of araATP (Müller *et al* 1975).

3.1.3: Incorporation of araA and effects on DNA structure

A later study by Ohno *et al* (1989) investigating the effects of araA on β polymerase showed that araA was incorporated at specific sequences depending on the concentration of araATP and dATP. AraA was shown to be incorporated into the elongating strand at adenine sites (Tseng *et al* 1980). At paired adenine sites there was DNA strand accumulation due to the reinitiation of strand synthesis which may contribute to the cytotoxicity of the drug (Kufe *et al* 1983). Relative chain termination was more evident at multiple adenine sites because of hydrogen bonding in the arabinose sugar and the incorporation of several araA residues increased the distortion of the DNA strand. Therefore, as more araATP was incorporated into the DNA the greater the distortion of the

DNA helix resulting in chain termination (Ohno *et al* 1989). However, it has been shown that the effects of araA can be reversed by increasing the ratio of dATP to araATP (Müller *et al* 1975, Kufe *et al* 1983).

Further studies have shown a varied cytostatic action of araA varied cell line to cell line and this has been attributed to the differing levels of adenosine deaminase in mammalian cells (Plunkett *et al* 1975, Cohen and Plunkett 1975). High levels of adenosine deaminase (ADA) transform araATP into 9-β-D-adeninefuranosylhypoxanthine (araHX) which reduces the inhibition effects on DNA synthesis (LePage 1970). This has been shown in KB cells which have high levels of ADA, after a 5 hour incubation period with araA there were 15 pmoles/10^6 cells araATP formed in KB cells in contrast to 60 pmoles araATP/10^6 cells formed in mouse lymphoma cells which have low ADA levels (Cohen and Plunkett 1975, Müller *et al* 1977). Similarly, the effect of araA on chromatid break rejoining was reduced in human peripheral blood lymphocytes due to high ADA levels because in the presence of coformycin (an ADA inhibitor) there was a higher frequency of chromatid breaks unrejoined due to the inhibition of dsb repair by araA (MacLeod and Bryant 1992).

3.1.4: AraA as a DNA synthesis inhibitor and effects on dsb repair

AraA has been useful from a radiobiological view point because it inhibits DNA synthesis and it has been shown to potentiate the effects of IR. The shoulder of the survival curves for Ehrlich ascites tumour cells was removed after the addition of araA (Iliakis 1980) that was interpreted as an inhibition of repair of potentially lethal damage (PLD). Bryant and Blöcher (1982) showed that 30% of single-strand breaks were repaired in the presence of araA (200μm) whereas dsb repair was totally blocked. This indicated that DNA synthesis was required for the repair of dsb whereas the majority of ssb did not require DNA synthesis. In this study, it was also shown that the inhibitory effects of araA can be

partially reversed by washing away the drug and replacing with fresh medium. However, the inhibitory effects were not fully restored possibly due to the cell killing effects of araA (Bryant and Blöcher 1982). The reversible effects of araA have also been shown, by Iliakis (1980), in Ehrlich ascites tumour cells which were exposed to araA and the inhibitory effects of dsb repair were removed when araA was washed from the cells. However, the cells only showed partial reversible effects on PLD repair which has been attributed to araA fixing a percentage of PLD damage, whereas the inhibition of polymerases α and β was fully reversible (Iliakis 1980).

3.1.5: Effects of araA on the chromosomal response of mammalian mutants

As mentioned previously, dsb are thought to be the underlying lesions responsible for the formation of chromatid breaks (Bender *et al* 1974, Natarajan *et al* 1983). Therefore, it was interesting to investigate the chromosomal response of mammalian cells to IR in the presence of araA. Studies in which the cells were exposed to IR in the presence of araA illustrated an increase in the frequency of chromosomal breaks (Bryant 1983, 1984a). In Ehrlich ascites tumour cells the frequency of anaphase bridges and chromosome fragments increased when cells were treated after irradiation with araA, which implied an increase in the misrepair and inhibition of dsb rejoining in the presence of araA (Bryant and Blöcher 1982). Chinese hamster ovary (CHO) cells exposed to X-rays exhibited an increased frequency of chromosome fragments in the presence of araA as measured by the PCC technique and this has been attributed to an effect of araA on the repair of chromosomal damage (Iliakis 1989).

Other mammalian mutants deficient or proficient in dsb repair have been treated after irradiation with araA and the frequency of chromatid aberrations has been shown to increase. For example, xrs5 cells deficient in dsb repair due to a Ku80 defect, which is a

component of the DNA-PK holoenzyme that is deficient in SCID cells, have shown an elevated chromosomal response when treated with araA and IR as measured by PCC (Okayasu and Iliakis 1994). Okayasu and Iliakis identified two components of dsb repair in CHO and xrs5 cells: α is a fast repairing component and is sensitive to hypertonic treatment, whereas β is the slow repairing component and is sensitive to araA (Okayasu and Iliakis 1993, 1994). AraA inhibited the rejoining of interphase chromosome breaks in xrs5 cells and there was an enhanced cell killing effect which has been attributed to the inhibition of DNA synthesis in xrs5 cells by araA (Okayasu and Iliakis 1994). Similarly, another radiosensitive line: AT cells treated with araA after radiation exposure showed an increase in the chromatid break frequency compared to irradiated AT controls (Mozdarani *et al* 1989b).

In this study, preliminary experiments were used to determine the optimal concentration of araA to use on murine SCID and CB17 cells, and then the G2 assay in the presence and absence (Chapter 2) of araA was carried out on all four cell lines.

3.2: Materials and Methods

Cell culture, irradiation and chromosome preparation details in Chapter 2 section 2.2.

3.2.1: G2 assay

Cells were seeded at $2x10^6$ per $75cm^2$ flasks and incubated overnight at 37°C. 30 min prior to irradiation 100μM of araA (Sigma Co. UK) was added to the samples to allow the phosphorylation of araA to form araATP. Following irradiation the samples were incubated for various times before sampling. Samples were taken at 1, 2 and 3 h after irradiation. In each case colcemid (0.04μg/ml) was added for 30 min before mitotic shake-off. Usually 5 flasks were employed per sample.

3.3: Results

3.3.1: Preliminary G2 assay studies of SCID and CB17 cells treated with araA and IR

Preliminary experiments were carried out to determine the effects of IR in the presence of araA in SCID and CB17 cells. SCID cells were exposed to 0.38 Gy of γ- rays and CB17 cells 0.77 Gy and both cell lines were treated with 1000μM araA (Table 3.1). The frequency of chromatid breaks in SCID and CB17 cells was similar, even though CB17 cells were exposed to a higher radiation dose. The results show that araA potentiates the effects of IR by increasing the chromatid break frequencies. Assuming there is a linear relationship between chromatid break frequency and radiation dose (Bryant *et al* 1998), the frequency of breaks induced by 0.38Gy can be multiplied by 2 to give an estimate of the frequency of breaks induced by 0.77Gy. On this basis a difference of a factor of approximately 2 between SCID and CB17 is evident both in the presence and absence of araA (fold differences were: -araA/1h 2.4; -araA/2h 1.7; +araA/1h 2.1; +araA/2h 1.9; Table 3.1b, 3.1c). However, there were many heavily damaged cells that were difficult to score accurately because in 25 metaphase cells there were approximately 190 breaks (7.6 breaks per cell), therefore 0.24 Gy γ-rays was adopted as the radiation dose for each cell line.

Table 3.1: Preliminary G2 assay results. Frequencies of chromatid breaks measured in SCID and CB17 cells treated with araA and gamma radiation.

Cell line	Treatment**	Time in colcemid (h) ***	Chromatid breaks per 25 cells*
SCID	Control	1.0	2.0
CB17	Control	1.0	1.0
SCID	Gamma rays (0.38 Gy)	1.0	96.0
CB17	Gamma rays (0.77 Gy)	1.0	79.0
SCID	araA alone	1.0	45.0
CB17	araA alone	1.0	52.0
SCID	Gamma rays (0.38 Gy) + araA	1.0	186.0
CB17	Gamma rays (0.77 Gy) + araA	1.0	188.0
SCID	Control	2.0	8.0
CB17	Control	2.0	4.0
SCID	Gamma rays (0.38 Gy)	2.0	92.0
CB17	Gamma rays (0.77 Gy)	2.0	102.0
SCID	araA alone	2.0	83.0
CB17	araA alone	2.0	149.0
SCID	Gamma rays (0.38 Gy) + araA	2.0	285.0
CB17	Gamma rays (0.77 Gy) + araA	2.0	352.0

* Data are representative of a single experiment.
** Cells were treated with 1000μM araA 30 min before IR.
*** Colcemid was added to the cells 30 min after IR.

Table 3.1b. Fold differences between cell lines in the presence and absence of araA (assuming linearity between chromatid break frequency and radiation dose values. CB17 cells treated with 0.38Gy can be multiplied by 2 to compare with SCID cells treated with 0.77Gy).

Cell line	Time (h)	Treatment with AraA	Fold Difference
SCID vs. CB17	1	Control	2.4
SCID vs. CB17	2	Control	1.7
SCID vs. CB17	1	1000μM araA	2.1
SCID vs. CB17	2	1000μM araA	1.9

Table 3.1c. Enhancement ratio of chromatid break frequencies in the presence of araA.

Cell line	Time (h)	Chromatid break frequency		Enhancement Ratio
		Control	1000μM araA	
SCID	1	96	141	1.5
SCID	2	84	202	2.4
CB17	1	78	136	1.7
CB17	2	98	206	2.1

3.3.2: Effects of increasing araA concentrations on unirradiated SCID and CB17 cells

The effects of increasing araA concentrations on SCID and CB17 cells are shown in Table 3.2. As the concentration of araA increased, the background damage in unirradiated SCID and CB17 cells increased. Therefore, minimum concentrations of araA were used to reduce the toxic effects (araA concentrations higher than 120μM/l are toxic as shown by Bryant and Iliakis 1984). The mitotic index was also calculated (Figure 3.2). The mitotic index decreased from approximately 7% to 3.5% after the addition of 125μM araA and remained at this value even though the araA concentration was increased. A dose dependent response shown previously in mammalian cells, such as AT, was not apparent in this study (N.Liu Ph.D. thesis).

Table 3.2: Effect of increasing araA concentrations on unirradiated SCID and CB17 cells.

Cell line	Treatment*	Chromatid breaks per 100 cells
SCID	Control	11.0
CB17	Control	9.0
SCID	100 μM araA	22.0
CB17	100 μM araA	39.0
SCID	250 μM araA	71.0
CB17	250 μM araA	146.0

* Cells were treated with araA for 2.5h (equivalent to 1.5h after IR treatment since araA is added to the cells 30 min prior to IR and colcemid is added to the cells 30 min prior to fixation).

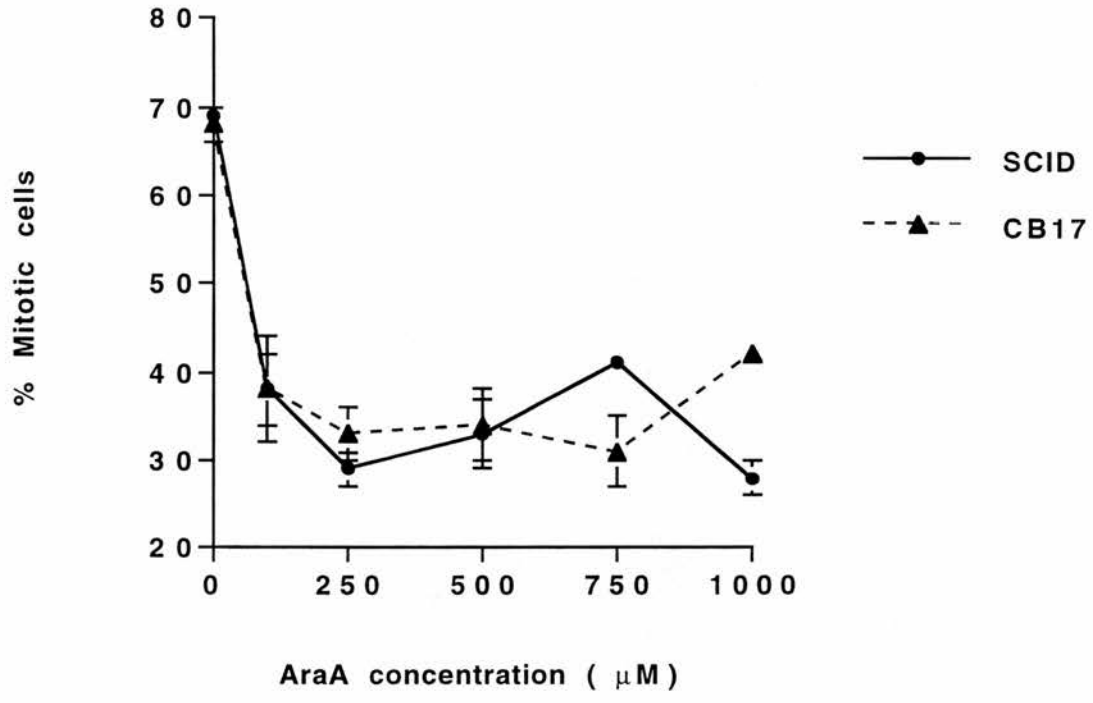

Figure 3.2: Mitotic index of unirradiated SCID and CB17 cells treated with increasing concentrations of araA for 2h before adding colcemid for 30 mins prior to fixation. The results shown represent the mean score from three independent experiments and the errors bars represent the standard errors of the mean.

3.3.3: Chromatid break response of SCID and CB17 cells to IR in the presence of araA

An araA concentration of 100μM was adopted for this study, so as to keep the toxic effects of araA to a minimum. The results from the G2 assay of SCID and CB17 cells treated with IR in the presence of araA show a two fold difference in the chromatid break frequency at 1h after treatment (Figure 3.3, Table 3.3). The original 1.3 fold difference present between SCID and CB17 cells in the absence of araA was, thus, still apparent at the first hour time point and elevated to two fold in the presence of araA. However, between two and three hours the frequency of chromatid breaks decreased in SCID cells whereas in CB17 cells it increased. Regression analysis revealed that SCID and CB17 cells had a significantly different response to IR when treated with araA over the 3 h period ($p=0.0004$), which is evident in Figure 3.3. The response of SCID cells to araA and radiation at 1 and 2 h was increased 2.05 and 1.4 fold respectively, compared to wildtype CB17 cells and no difference apparent at 3 h.

The increased frequency of chromatid breaks in the presence of araA was compared to the response induced by radiation alone in SCID and CB17 cell lines at the first hour time point. SCID cells gave a 2.1 elevated response, whereas CB17 cells showed a 1.4 fold elevated response, that was significantly different at 95% confidence levels. The potentiation of chromatid break frequencies by araA on SCID cells was the same at all three sampling times (Fig.3.3). Thus, analysing the kinetics of SCID cells after IR in the presence and absence of araA between 1-3 h by regression did not reveal a significantly different slope (p-value 0.94). In CB17 cells chromatid break frequencies were potentiated. However, the frequency of breaks remained essentially constant over the time period investigated.

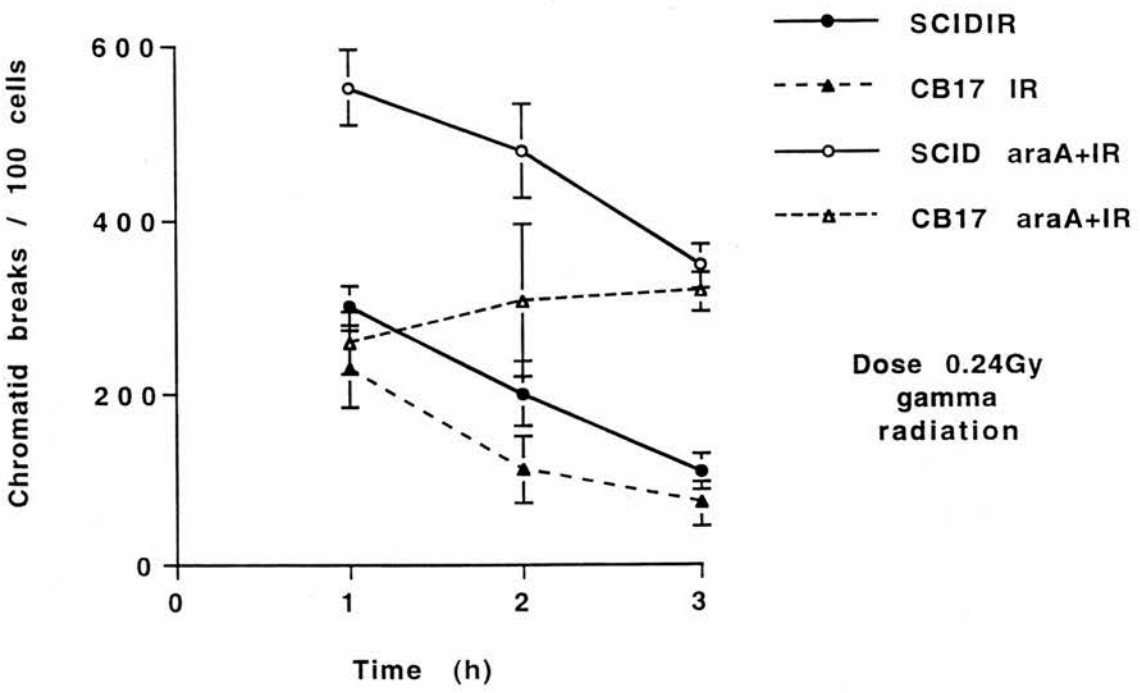

Figure 3.3: Frequencies of chromatid breaks measured in SCID and CB17 cells treated with gamma radiation in the presence and absence of araA (100μM). Control values in the presence and absence of araA have been subtratced from the appropiate value and the data shown in Table 3.3. The results were pooled from three independent experiments and the error bars represent the standard errors of the mean.

Table 3.3: Frequencies of chromatid breaks in SCID and CB17 cells in response to γ-rays in the absence and presence of araA (100μM) measured by G2 assay*.

Cell line	Treatment	Time after irradiation (h)**	Chromatid breaks per 100 cells***
SCID	Control	1.0	12.3 ± 2.4
CB17	Control	1.0	9.6 ± 0.3
SCID	γ-rays (0.24 Gy)	1.0	315.0 ± 23.5
CB17	γ-rays (0.24 Gy)	1.0	239.7 ± 44.4
SCID	araA control	1.0	107.3 ± 40.9
CB17	araA control	1.0	65.0 ± 18.5
SCID	γ-rays (0.24 Gy) + araA	1.0	661.7 ± 44.4
CB17	γ-rays (0.24 Gy) + araA	1.0	323.0 ± 36.0
SCID	Control	2.0	9.0 ± 6.1
CB17	Control	2.0	9.6 ± 0.3
SCID	γ-rays (0.24 Gy)	2.0	209.0 ± 37.7
CB17	γ-rays (0.24 Gy)	2.0	121.6 ± 38.7
SCID	araA control	2.0	101.3 ± 34.1
CB17	araA control	2.0	93.0 ± 33.0
SCID	γ-rays (0.24 Gy) + araA	2.0	581.7 ± 54.4
CB17	γ-rays (0.24 Gy) + araA	2.0	401.7 ± 88.5
SCID	Control	3.0	8.3 ± 1.2
CB17	Control	3.0	5.3 ± 0.9
SCID	γ-rays (0.24 Gy)	3.0	118.0 ± 20.4
CB17	γ-rays (0.24 Gy)	3.0	77.7 ± 25.1
SCID	araA control	3.0	107.3 ± 40.5
CB17	araA control	3.0	128.7 ± 49.4
SCID	γ-rays (0.24 Gy) + araA	3.0	455.3 ± 24.5
CB17	γ-rays (0.24 Gy) + araA	3.0	446.7 ± 22.5

*Graphically shown in Figure 3.3

**Time interval after IR exposure, before colcemid treatment. Cells were treated with araA 30 min prior to IR exposure to allow the incorporation of araATP.

***Each value represents the mean and standard errors from three independent experiments.

3.3.4: Chromatid break response of 50D$^-$ and 100E$^+$ cells to IR in the presence of araA

The same G2 assay was carried out with 50D$^-$ and 100E$^+$ cells to investigate their response to IR in the presence and absence of araA (Figure 3.4 and Table 3.4). In this case, the addition of araA increased the frequency of chromatid breaks by a factor of approximately 2 in 50D$^-$ and 100E$^+$ cells at 1 h post irradiation (Figure 3.4). The results were similar to those for CB17 in that the frequency of chromatid breaks in the presence of araA remained essentially constant between 1-3 h in both cell lines.

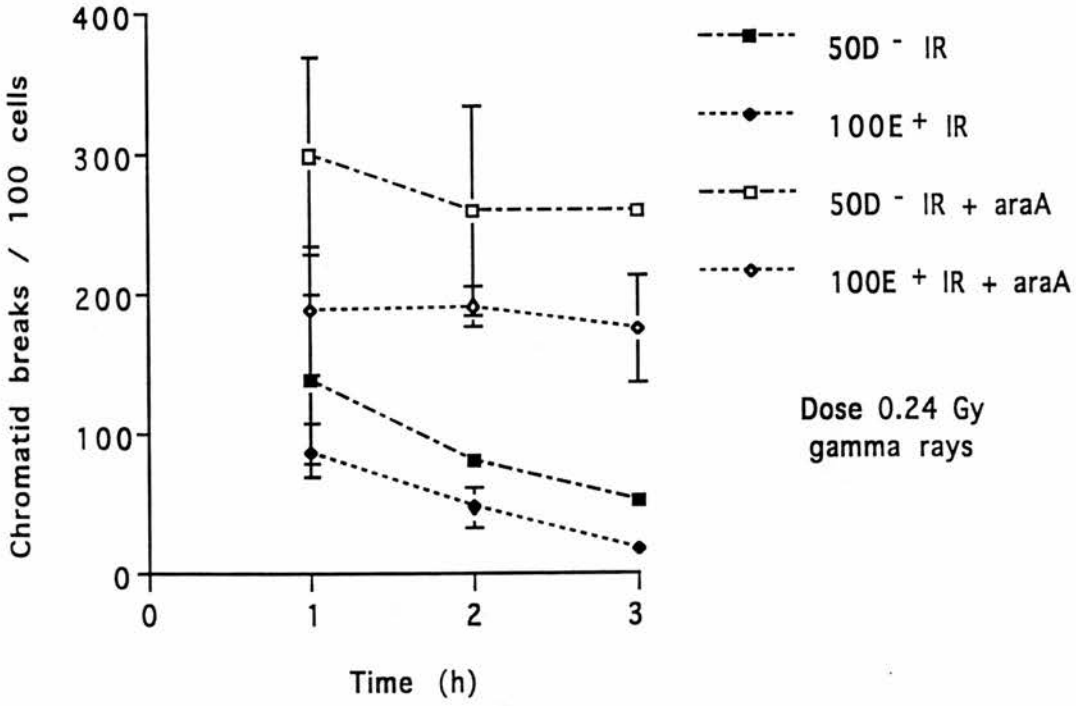

Figure 3.4: Chromatid breaks induced in 50D⁻ and 100E⁺ cells treated with IR in the presence and absence of araA (100μM) as measured by the G2 assay. Each valus had been adjusted for background damage in the presence and absence of araA as appropiate and the data shown in Table 3.4. The results were pooled from three independent experiments and the error bars represent the standard errors of the mean.

Table 3.4: Frequencies of chromatid breaks in $50D^-$ and $100E^+$ cells in response to γ-rays in the absence and presence of araA (100μM)*.

Cell Line	Treatment	Time after irradiation (h)**	Chromatid breaks per 100 cells***
$50D^-$	Control	1.0	16.0 ± 8.9
$100E^+$	Control	1.0	23.0 ± 1.5
$50D^-$	γ-rays (0.24 Gy)	1.0	156.0 ± 60.0
$100E^+$	γ-rays (0.24 Gy)	1.0	112.0 ± 19.0
$50D^-$	araA control	1.0	65 ± 35.0
$100E^+$	araA control	1.0	56 ± 7.0
$50D^-$	γ-rays (0.24 Gy) + araA	1.0	366 ± 70.0
$100E^+$	γ-rays (0.24 Gy) + araA	1.0	247 ± 46.0
$50D^-$	Control	2.0	21.0 ± 3.6
$100E^+$	Control	2.0	25.0 ± 6.0
$50D^-$	γ-rays (0.24 Gy)	2.0	104.0 ± 2.0
$100E^+$	γ-rays (0.24 Gy)	2.0	74.0 ± 14.0
$50D^-$	araA control	2.0	43 ± 7.6
$100E^+$	araA control	2.0	97.0 ± 00.0
$50D^-$	γ-rays (0.24 Gy) + araA	2.0	304.0 ± 75.0
$100E^+$	γ-rays (0.24 Gy) + araA	2.0	290 ± 27.0
$50D^-$	Control	3.0	15.0 ± 6.0
$100E^+$	Control	3.0	21.0 ± 9.0
$50D^-$	γ-rays (0.24 Gy)	3.0	68.0 ± 6.0
$100E^+$	γ-rays (0.24 Gy)	3.0	40.0 ± 6.0
$50D^-$	araA control	3.0	56.0 ± 0.5
$100E^+$	araA control	3.0	110.5 ± 35.0
$50D^-$	γ-rays (0.24 Gy) + araA	3.0	317 ± 0.5
$100E^+$	γ-rays (0.24 Gy) + araA	3.0	287.0 ± 38.0

*Graphically shown in Figure 3.4.

**This is the time interval after IR exposure and before colcemid treatment. AraA was added to the samples 30 min prior to IR allowing time for araA to be incorporated as araATP.

***Data represent the means and standard errors from two independent experiments in which 200 cells were scored.

3.4: Discussion

3.4: Discussion

Preliminary experiments with radiation doses between 0.38-0.77 Gy- radiation showed high levels of chromatid breaks which were difficult to score, hence, the use of 0.24 Gy γ-radiation for each cell line. The preliminary experiment in which SCID cells were exposed to 0.38 Gy γ- radiation plus 1000μM araA showed a similar chromatid break frequency to that of CB17 cells exposed to 0.77 Gy γ- radiation plus 1000μM araA. This indicates an approximate two fold difference between SCID and CB17 cells in the presence or absence of araA at 1h. These results are reminiscent of those for AT and normal fibroblasts (Mozdarani *et al* 1987 and 1989b). The reasons for this elevated chromatid break frequency in the presence of araA are at present unknown. However, it has been suggested that araA affects the final stage in the putative recombinational rearrangement process leading to chromatid breaks proposed by the signal model (Bryant 1998 and personal comm.).

The preliminary results showed that high concentrations of araA increased the background chromatid break frequency in unirradiated controls, so a lower concentration (100μM) was adopted (Table 3.2). At this lower concentration araA also potentiated the chromatid break frequency. In CB17 this resulted in an essentially level response (Figure 3.3). $50D^-$ and $100E^+$ cells showed a similar potentiation and level chromatid break response when treated with araA (Figure 3.4). These results agree with previous data on AT fibroblasts (Mozdarani *et al* 1987), CHO cells (Bryant *et al* 1993) and normal human lymphocytes (MacLeod *et al* 1992) where a similar level chromatid break response was seen during treatment with araA.

In contrast to CB17, the frequency of breaks in SCID cells was potentiated and the degree of potentiation was constant at all three time points investigated. Thus, the frequency of

breaks in SCID cells decreased with increasing time. These results are clearly different from those of the other three lines investigated and it is possible that the different response of SCID to araA may be due to a higher level of adenosine deaminase (ADA), leading to progressive deamination of araA to araHX, possibly allowing the completion of recombinational rearrangements and subsequent disappearance of chromatid breaks with time. Treatment of SCID cells with araA at 1000μM (Table 3.1) led to a potentiation with a slight increase in chromatid breaks between 1-2h supporting the notion of deamination of araA at the lower concentration of 100μM. A similar deamination of araA was seen in normal human lymphocytes, and treatment with coformycin (ADA inhibitor) was necessary in order to achieve a level chromatid break response (MacLeod and Bryant 1992).

In contrast, to the chromatid break kinetic data, analysis of dsb rejoining in partially synchronised (70%) G2 cells was not affected by araA at 100μM (Fig. 5.6 and 5.7). Thus, it is unlikely that the elevated chromatid break frequency and level responses in the presence of araA can be explained by an inhibition of dsb rejoining. As explained above, it is possible that the putative inter- and intra- recombinational rearrangement process leading to chromatid breaks requires a small amount of DNA synthesis prior to ligation, which is highly sensitive to araA.

Chapter Four

The role of double-strand break end-structure in chromatid break response : use of restriction endonucleases

4.1 Introduction

Chapter Four:

The role of double-strand break end-structure in chromatid break response : use of restriction endonucleases.....100

4.1: Introduction

The end structure of a dsb may effect the signal perceived by the cell in response to the damage, resulting in different frequencies of chromatid breaks. The use of restriction endonucleases (RE) which induce dsb with different end-structures have been useful to study the effects of different molecular configurations on the chromatid break response in mammalian mutant cells. Initially, the optimal poration concentration of streptolysin-O (SLO) was investigated, using the micronucleus assay. The G2 chromatid break response of SCID and CB17 cells to RE which induce specific types of dsb (blunt or cohesive) were investigated. The aim was to determine whether the end-structure of the dsb elicited different signals and produced a different chromatid break response in SCID and CB17 cells. If different responses are found then the importance of DNA-PK as a signalling protein in response to DNA damage may be revealed.

4.1.1: The use of restriction endonucleases

RE were first shown to induce chromosomal fragments in the root tips of barley and more recently, they have been used to mimic IR responses in mammalian cells. RE are bacterial enzymes that remove intrusive DNA from a cell by cleavage at specific sites. RE recognise specific base sequences in the DNA and generate dsb at these sites with blunt- (no overlapping bases) or cohesive- (varying degrees of overlap at 3' or 5' termini) ended dsb.

4.1.2: Methods used for the introduction of RE into mammalian cells

Many different methods have been used to porate cells, enabling RE to enter the cell and cleave the DNA. Initially, inactivated Sendai Virus (ISV) was used to porate cells, producing pores 1nm in diameter in the cell membrane (Bryant 1984b). Other methods

included: (a) the "pellet" method in which cells were centrifuged to a pellet and treated with RE in a small volume: (b) the transportation of pinocytic vesicles containing RE into the cell and once inside the vesicles were lysed by osmotic shock releasing the RE (Obe and Winkel 1985, Johannes *et al* 1992): (c) the construction of a plasmid assay containing a selectable marker and the bacterial RE (EcoRI) gene attached to the mouse metallothionein gene promoter, so that in the presence of heavy metals, such as Cd^{++}, the cell up-regulated the production of EcoRI (Morgan *et al* 1988, Winegar *et al* 1989). However, one disadvantage with the last method was the inability to switch the EcoRI gene on and off as required, resulting in no control over the RE treatment period. The main disadvantage with all of these techniques was an overdispersion of damage in cells. This has been interpreted as a difference in cell permeability or more RE entering some cells and not others.

The most widely used method has been electroporation (Winegar 1989, Costa and Bryant 1990a, Moses *et al* 1990) in which a high voltage discharge generates pores 2-4 nm in diameter enabling the RE to enter the cell. The main disadvantage of this technique is that many cells were lysed and only 30% remain viable after treatment (Lambert *et al* 1990, Bryant 1992b). However, more recently Streptolysin-O (SLO), a bacterial cytolysin, has been used to porate cells facilitating the uptake of RE by cells and there is a much increased percentage of live porated cells enabling better cytogenetic analysis of damage at the next metaphase. SLO is a 69Kda protein produced by bacterial *streptococcus pyogenes* that porates the cell membrane by targeting cholesterol molecules (Duncan *et al* 1975, Bhakdi *et al* 1985) and produces pores as large as 12nm at high SLO concentrations (Buckingham and Duncan 1983).

4.1.3: RE mimic IR by inducing dsb and chromosome damage

RE were first used to mimic the effects of IR in Chinese hamster V79 cells (Bryant 1984b) permeabilised with ISV and the type of chromosome aberrations produced were similar to those induced by IR. There was a linear dose-dependent increase in the induction of chromosome aberrations with increasing RE concentrations (Bryant 1984b, Obe *et al* 1993) and the induction of complex aberrations, such as exchanges after RE treatment, was increased and has been attributed to isochromatid breaks interacting with single chromatid breaks to produce triradials. The type of aberration induced by RE was influenced by the cell cycle phase (Obe and Winkel 1985, Winegar 1988): chromatid aberrations were produced after exposure in S/G2, whereas chromosome type aberrations were induced after treatment in G1/early S phase (Obe and Winkel 1985). Interestingly, cells treated with RE in G1 and incubated before sampling produced both chromosome (G1/early S phase) and chromatid (S/G2 phase) aberrations in the cell, suggesting that RE are active for long periods after treatment, whereas IR only causes damage in the cell at the time of treatment. (Natarajan and Obe 1984). This was confirmed in xrs5 cells treated with PvuII in which dsb were shown to accumulate over a 24 hour period after treatment, as measured by neutral filter elution (Costa *et al* 1991b). Synchronised mitotic cells treated with RE show no induction of chromosome damage which is also true for mitotic cells treated with IR (Morgan *et al* 1991). A possible reason for the lack of chromosomal damage in mitotic cells may be that decondensation, DNA replication and chromosome recondensation are required before chromosome damage is visible. Interestingly, DNA damage was detected by PFGE in the mitotic cells treated with RE (Morgan *et al* 1991). In addition to RE inducing chromosome damage in mammalian cells, micronuclei have been induced in CHO cells treated with PvuII (Moses *et al* 1990, Bryant 1992a). Other studies showing that RE mimic the effects of IR include: increased levels of SCE (Natarajan *et al* 1985, Stoilov *et al* 1986, Folle *et al* 1992), an increase in mutations at the *hprt* and the *tk* loci (Obe *et al*

1986a, Singh *et al* 1991) and an increase in oncogenic transformations (Bryant and Riches 1989) in mammalian cells. The induction of SCE by RE is under debate as other studies have not shown an elevated SCE in response to RE. However, this is likely explained by SCE induction being dependent on the cell cycle phase (Morgan *et al* 1985, 1989, Folle *et al* 1992).

Attempts have been made to measure the amount of damage induced by PvuII in permeabilised cells and to compare this with the damage induced by IR (Bryant 1984b, Natarajan *et al* 1985). In mammalian V79 cells the induction of dsb after treatment with 500 units of PvuII was found to be equivalent to 2 Gy of IR, as measured by DNA unwinding assays (Bryant 1984b). Similar, investigations using a nucleoid sedimentation method to measure dsb induction showed that 60-120 units of PvuII induced damage that was equivalent to the damage induced by 0.25 Gy in CHO cells (Natarajan *et al* 1985). These studies suggested that 100 units of PvuII induced 400 dsb per cell which is equivalent to 10 Gy of IR (Bryant 1988), illustrating that higher concentrations of RE are required to induce the same effects as IR. However, it is difficult to equate RE treatment and IR exposure as the type of damage induced by each treatment differs and damage induced by RE is dependent on the type of RE used. The type of dsb induced by RE are different than those induced by IR; dsb induced by RE have "clean" ends with 5' phosphoryl and 3' hydroxyl ends that can be readily ligated. In contrast, the formation of dsb by IR is caused by a single track in which radicals are generated that attack both strands of the DNA to form a blunt dsb or two closely generated ssb with staggered ends in either the 5' or 3' direction and these "dirty" termini require endonuclease activity before ligation can proceed. After IR exposure it is thought that dsb are mostly of the cohesive type as the chance of two ssb at sites exactly opposite one another in the DNA helix is low (Bryant 1989). These findings suggest that although the dsb structures are different there

are many aspects of dsb induction by RE that are similar to IR-induced dsb, illustrating how useful RE can be for studying the response of mammalian cells to different ended dsb.

4.1.4: The differential effects of RE inducing various end-structures on mammalian cells

The end-structure of RE induced dsb has been shown to influence the induction of chromatid aberrations in mammalian cells. In particular blunt-ended dsb (PvuII) have been shown to be more effective at inducing chromatid aberrations than cohesive-ended dsb (BamHI) in V79 cells, even though the initial levels of dsb induction were the same as measured by DNA unwinding studies (Bryant 1984b). CHO cells treated with PvuII, PstI and XbaI which induce blunt, 5' cohesive and 3' cohesive ended dsb respectively, showed that PuvII was the most effective at inducing chromatid aberrations and analysis of dsb induction by PFGE showed that PvuII produced the lowest yield of dsb confirming how effective PvuII was at inducing chromosome aberrations (Morgan *et al* 1990). Similar results were obtained with CHO cells treated with PvuII and EcoRI, in which there were more chromosome aberrations induced after treatment with PvuII than EcoRI (Moses *et al* 1990). Other studies have shown that RE inducing blunt-ended dsb (e.g. PvuII, EcoRV) induce more chromosome aberrations than RE inducing cohesive-ended dsb (BamHI, NunII and AsuIII) (Natarajan and Obe 1984). Cell survival analysis has shown that cell death is also induced more by blunt-ended dsb than cohesive-ended dsb (Bryant 1985, Giaccia *et al* 1990b). Similarly, the mutagenic effect of PvuII (blunt-ended dsb) was greater than EcoRI (cohesive-ended dsb) at the *tk* gene (Singh and Bryant 1991), even though the *tk* gene had more cutting sites for EcoRI. Not only are blunt-ended dsb more effective at inducing chromosome aberrations but 3' dsb with overhangs (PstI) have been shown to be more effective at inducing chromosome aberrations than 5' cohesive-ended dsb in CHO cells (Zhang and Dong 1987). It has also been shown that the frequency of aberrations increase when the degree of overlap decreases from 4 to 1 bp in mammalian

cells (Bryant 1989). These studies have all indicated that the end-structure of dsb are relevant to the induction of chromosome aberrations. In contrast, other studies have shown no differences between the induction of chromosome aberrations in mammalian cells treated with RE inducing cohesive- or blunt-ended dsb (Obe *et al* 1985, Winegar and Preston 1988, Johannes and Obe 1991). However, the possible reasons for these contradictory results are: the methods used to treat the cells, such as the pellet method which requires much higher concentrations of RE (Bryant and Christie 1989) and the presence of glycerol in the storage buffer may affect the induction of chromosome aberrations (Obe *et al* 1985). In conclusion, these findings suggest that the end-structure of dsb may influence the chromosome aberration frequencies in mammalian cells. In particular, blunt-ended dsb appear to be the most effective at inducing chromosome damage.

4.1.5: Action of RE inside mammalian cells

The mode of entry and action of RE inside the cell are largely unknown and this may contribute to the contradictory results reported above. Initially, it was not known if RE once inside the cell cut at their specific recognition sites, but an analysis of DNA molecules exposed to RE showed that RE did in fact cut at their specific recognition sites (Winegar *et al* 1992). Cells treated with IR have randomly distributed chromosome damage, but with RE there has been a problem with overdispersion of chromosome damage in some cells and no damage in other cells. This problem may be attributed to DNA accessibility, nucleosome position or DNA methylation (Obe *et al* 1986b, Higurashi and Cole 1991). Cells grown in BrdU to substitute thymine bases show reduced chromosome breakage after treatment with EcoRI, ScaI and DraI than untreated cells because these RE recognise thymine rich sequences in comparison with HpaII, for which BrdU substitution had no effect, as this RE does not recognise thymine rich sequences

(Cortes and Ortiz 1992). Cells treated with high salt concentrations show an increased frequency of chromosome aberrations after treatment with AluI which has been attributed to an alteration in chromatin structure thereby, revealing more recognition sites (Obe and Kumara 1986b). More recently, Folle *et al* (1998) have investigated the location of chromosome break points in cells exposed to RE. These studies have shown that RE- and IR-induced dsb are located in the giemsa (G) light stained bands and the localisation of damage in S and G1 cells was the same, illustrating that the same areas of the chromosome are damaged irrespective of the cell cycle phases (Folle and Obe 1995, 1996). G-light areas are active areas of chromatin, including the house keeping genes, suggesting that active chromatin is more easily damaged (Folle *et al* 1998).

4.1.6: Repair of RE induced dsb

Repair is difficult to measure after RE treatment because RE often remain active in cells for long periods after treatment, thereby inducing more dsb. Neutral filter elution studies have shown a linear accumulation of dsb in xrs5 cells treated with PvuII for up to 24 hours after treatment when the curve reaches a plateau (Costa and Bryant 1990a, 1991b). BamHI produced an accumulation of dsb but it was reduced in comparison with dsb accumulation after treatment with PvuII (Costa and Bryant 1990a, 1991b). The induction of chromatid breaks in mammalian cells by RE have been interpreted as representing a competition between DNA excision and DNA repair. It has been proposed that RE which induce blunt-ended dsb have a higher rate of DNA excision than the rate of DNA repair which leads to an accumulation of dsb. In contrast, RE which induce cohesive-ended dsb have similar DNA excision and DNA repair rates, thereby reducing the accumulation of dsb and induction of chromosome aberrations. This suggests there may be different pathways for the repair of dsb depending on the end-structure. Alternatively, staggered ends may be more easily rejoined as the cell may view them as two ssb and use a rapid rejoining

mechanism in which polynucleotide ligases join the RE induced 3' OH and 5' phosphate ends (Bryant 1989).

The use of DNA repair inhibitors has been used to investigate the process of RE dsb induction in mammalian cells. The addition of araC which is known to inhibit DNA synthesis and ligation has been shown to potentiate the effects of PvuII, EcoRI and AluI (Natarajan and Obe 1984, Obe and Natarajan 1985). DNA repair inhibitors, such as 3 aminobenzamide (3AB), aphidicolin, araC and caffeine were used to examine the effects of RE on chromosome aberration and dsb induction in CHO-KI cells (Chung *et al* 1991). The results showed that 3AB and araC increased the frequency of chromosome aberrations in cells treated with AluI and Sau3A I whereas caffeine had no effect on the yield of chromatid aberration induction by either RE. Aphidicolin increased the yield of chromosome aberrations with Sau3A I but it had no effect on the response to AluI. Analysis by PFGE showed a transient increase of dsb induction in cells treated with AluI or Sau3A I and 3AB. These results indicate that poly (ADP-ribose) polymerases and polymerases α and δ are important for the repair of RE induced dsb but there may be different cellular repair pathways required for the repair of the specific end-structures (Chung *et al* 1991).

4.1.7: Effect of RE on radiosensitive mutant mammalian cell lines

Mammalian cells defective in dsb repair have shown elevated frequencies of chromosome aberrations in response to IR when compared with normal wild type cells and this has been attributed to the dsb repair defect. Analysis of the effects of different dsb end-structures induced by RE have shown a more elevated response to blunt-ended dsb than to cohesive-ended dsb in mutant mammalian lines. As mentioned previously, xrs5 and CHO cells treated with BamHI and EcoRI (inducing cohesive-ended dsb) did not show as many

chromosome breaks than treatment with PvuII or EcoRV which induce blunt-ended dsb (Bryant *et al* 1987). In addition, when treated with PvuII xrs5 cells showed a 3-4 fold elevated frequency of chromosome aberrations compared to CHO cells, whereas BamHI did not produce a significantly enhanced chromatid break frequency in xrs5 cells relative to CHO cells (Bryant *et al* 1987). Similarly, all types of chromosome aberrations were 2-4 fold more elevated in xrs5 and xrs6 cells treated with PvuII, EcoRV, HaeIII and AluI (blunt ended-dsb) than CfoI, EcoRI and ApaIII inducing cohesive-ended dsb (Darroudi and Natarajan 1989). This indicates a higher conversion of blunt-ended dsb only into chromatid breaks in mammalian mutants compared with wildtype cells which is similar to the response exhibited when mutant mammalian cells were treated with IR. XR-1 cells have shown an enhanced clonogenic sensitivity to AluI (blunt-ended dsb) and Sau3AI (cohesive-ended dsb) compared with CHO cells, even though the yield of dsb were the same (Giaccia *et al* 1990b). However, there was no difference in the response of XR-1 cells to the type of end-structure, as both RE gave comparable clonogenic sensitivity, even though the dsb end-structures were different.

Other mammalian cells which have elevated chromosomal responses to IR but are dsb repair proficient have also shown elevated responses to blunt-ended dsb. AT cells show a 2-4 fold increase in the frequency of deletions and exchanges in response to PvuII (Liu and Bryant 1994). The chromosomal response to BamHI was elevated but it was not as pronounced as the response exhibited after treatment with PvuII (Liu and Bryant 1994). Similarly, irs2 and VC-4 cells have shown a 2-4 fold elevated frequency of chromosome damage after exposure to PvuII (Bryant *et al* 1993a, Bryant and Liu 1994). More recently, AT cells were exposed to PvuII, PstI and BamHI by SLO poration and PvuII was found to be the most clastogenic, inducing the most chromosomal damage and producing an elevated response in comparison with normal cells (Liu and Bryant 1997a). Also in this study, araA was added to the cells prior to RE treatment. PvuII and PstI gave increased

responses in the presence of araA whereas, there was no effect of araA after treatment with BamHI (Liu and Bryant 1997a). This suggested that the dsb end-structure was important in DNA repair and damage recognition and each type of structure may be repaired by different mechanisms. The elevated response seen with PvuII and PstI may be attributed to the blunt- and 5' end- structures requiring exonuclease action or a fill-in mechanism at the termini involving DNA synthesis. The 3' ends induced by BamHI may be treated as two ssb enabling the damage to be repaired more easily. In conclusion, it can be postulated that the enhanced frequencies of chromosome aberrations are due to an enhanced conversion of blunt-ended dsb into chromatid breaks in these mammalian mutants. This conversion has been explained by the signal model (Bryant 1998) in which a single dsb generates a signal which initiates a recombinational rearrangement which, if incomplete, results in a visible chromatid break. It was postulated that deletion of a signalling protein (e.g. DNA-PK or ATM protein) might alter the signal effectiveness, i.e. deletion of ATM might result in an increased chromatid break frequency due to the alternative, over compensating DNA-PK signal pathway.

4.1.8: Response of SCID cells to RE

To date, the only study investigating the response of SCID cells to RE was by Chang *et al* (1993). They used electroporation to introduce RsaI and Sau3AI into SCID and CB17 cells. RsaI induces blunt-ends and Sau3A I induces 5' overhangs. A dose-dependent cytotoxicity in both cell lines was observed and SCID cells were 2 fold more sensitive than CB17 cells to both blunt- and staggered-ended dsb, even though the initial induction of dsb, as measured by PFGE, were the same in both cell lines. This study showed a two-fold elevated cytotoxicity to RE in SCID cells compared with CB17 cells but the dsb end-structure had no differential effect on the surviving fraction of SCID cells. However, they did not look at the G2 or G1 response in particular, so in the present study it was decided

to investigate the G2 chromatid break response in SCID and CB17 cells, using RE inducing different dsb end structures to see if there were different induced chromatid break responses.

In this chapter the aim was to use six different RE, three of which induced blunt-ended dsb, 2 inducing 3' dsb and PstI which induces 5' dsb. The various RE were introduced to SCID and CB17 cells by SLO poration. Optimisation of poration conditions was carried out in preliminary experiments, using micronuclei (Mn) as an endpoint.

4.2 Materials and Methods

Cell culture, irradiation and chromosome preparation details in Chapter 2 section 2.2.

4.2.1: Micronucleus assay

$5x10^5$ cells were plated per petri dish ($60mm^3$) and incubated at 37°C in a 5% CO_2 incubator overnight. The following day the medium was removed from the dishes and the cells were treated with PvuII and SLO in HBSS for 5 minutes to porate the cells and enable the RE to enter the cells. Afterwards the cells were washed with HBSS and fresh medium containing cytochalasin B was added to the cells at a final concentration of 3µg/ml, (Sigma, Co. UK). Further experimental details are given in Chapter 2 section 2.2.4.

4.2.2: Purification and assay to determine the activity of the restriction endonucleases

Restriction endonucleases (RE) PvuII, EcoRV, AluI, HindIII, EcoRI and PstI (Table 4.1 shows recognition sequences) were purchased from Gibco-BRL and purified by ultrafiltration using Centricon-10 (Amicon) filters. RE were added to filters after addition of 50ml bovine serum albumin in HBSS (1% w/v), mixed with 1 ml HBSS and centrifuged at 8000g for 2 h at 4°C. RE were recovered from filters by centrifugation (4°C) and diluted to 50 unit/ml in HBSS/BSA. The activity of purified RE was assayed using a titration digest of lambda DNA. Various amounts of RE were incubated at 37°C with 0.35µg lambda DNA for 1h, the reaction was terminated by adding 1% SDS and bromophenol blue, and the digests run on a 0.7% agarose electrophoresis gel.

Table 4.1: Recognition sequences and end-structures of DNA double-strand breaks induced by restriction endonucleases

Restriction endonucleases	Recognition sequence and cutting site	End structure of dsb
PvuII	CAG/CTG	Blunt
EcoRV	GAT/ATC	Blunt
AluI	AG/CT	Blunt
HindIII	A/AGCTT	Cohesive with 5' overhang
EcoRI	G/AATTC	Cohesive with 5' overhang
PstI	CTGCA/G	Cohesive with 3' overhang

4.2.3: Assay of purified restriction endonucleases

Figure 4.1 shows an example of a gel illustrating the titration of cutting activity of HindIII. The first well contains undigested control lambda DNA, therefore, only one DNA band is visible. In wells 2-5 (2, 1, 0.5 and 0.25 units HindIII) digestion of lambda DNA into bands produces the observed laddering effect. As the concentration of HindIII decreased from 0.125 units to 0.065 units (lanes 6&7) there is a reduced cleavage of the DNA. RE concentrations lower than 0.125 units/ml fails to cleave the DNA, suggesting the RE is not active enough to cut the DNA.

4.2.4: Cell poration with streptolysin-O and restriction endonuclease treatment

Reduced streptolysin-O (SLO, Murex, UK) was used to porate cells. Medium was removed and cell monolayers washed with HBSS. Cell monolayers were treated with SLO (0.3 units/ml) and the appropriate RE (100 units/ml) for 5 min at ambient temperature. Treatment was terminated by washing the monolayers with medium, replenishing the cells with fresh medium and incubating for a total of 5 h. 5h was used to harvest the cells because it allowed enough time for the mitotic index to recover following SLO treatment. Harvested mitotic cells were in the G2 phase of the cell cycle at the time of treatment because G2 lasts for approximately 5 h (Bryant *et al* 1998). Colcemid was added for 1 h before harvesting.

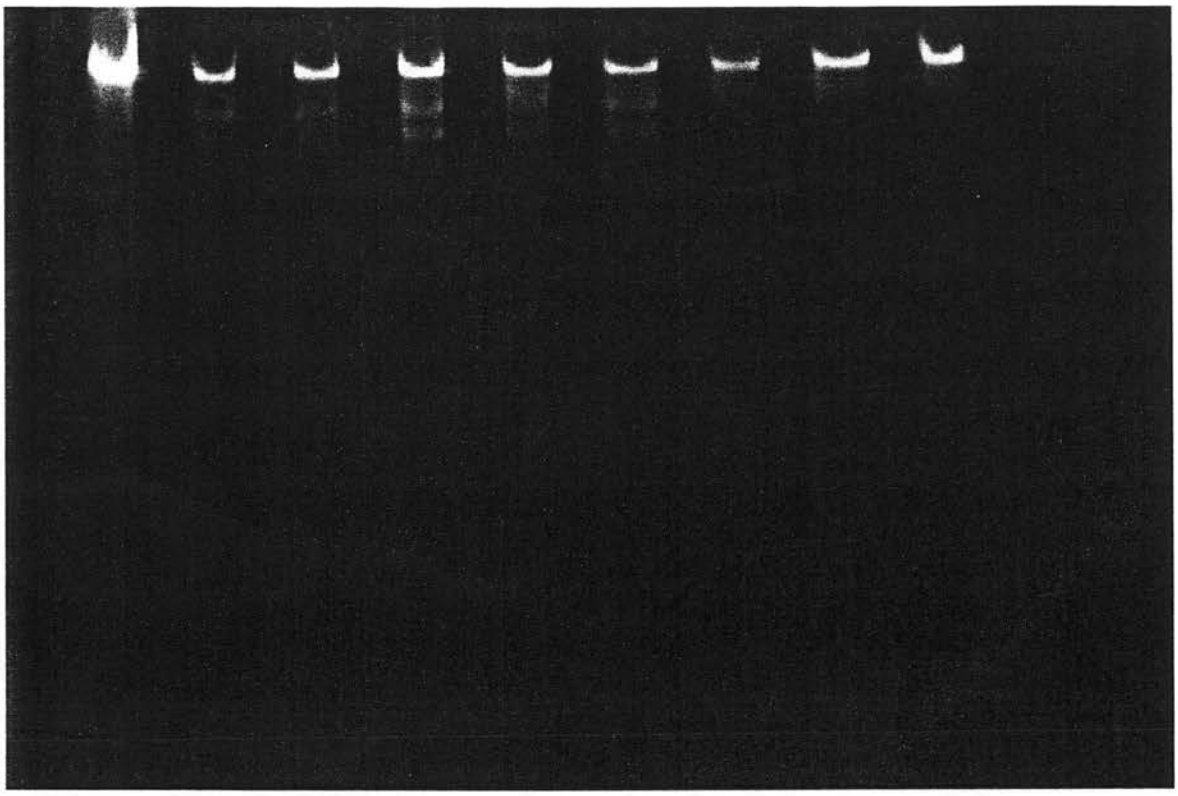

1 2 3 4 5 6 7 8 9

Figure 4.1: Agarose gel illustrating the titration of cutting activity of HindIII.
Well 1: undigested lambda DNA.
Well 2: 2 units HindIII + lambda DNA.
Well 3: 1 unit HindIII + lambda DNA.
Well 4: 0.5 units HindIII + lambda DNA.
Well 5: 0.25 units HindIII + lambda DNA.
Well 6: 0.125 units HindIII + lambda DNA.
Well 7: 0.065 units HindIII + lambda DNA.
Well 8: 0.032 units HindIII + lambda DNA.
Well 9: 0.016 units HindIII + lambda DNA.

4.3 Results

4.3.1: Preliminary micronucleus assay studies

4.3.1.1: Effects of increasing SLO concentrations on SCID and CB17 cells

Preliminary experiments were used to determine the optimal poration concentration of SLO in murine SCID and CB17 cells. Cells were treated with 10 units PvuII and increasing SLO concentrations from 0.05-0.5 units/ml to determine the poration ability of SLO. The results, as shown in Table 4.2, illustrate that increasing concentrations of SLO enables more RE to enter the cell, hence the increase in the frequency of induced micronuclei. In this experiment (Table 4.2.) micronucleus frequency increased up to 0.25units/ml and remained constant up to 0.5units/ml. Therefore, for further experiments an intermediate value of 0.33units/ml of SLO were used to porate the cells of both lines.

Having established that SLO was able to porate SCID and CB17 cells, this experiment was repeated with 25 units/ml PvuII (Table 4.3) resulting in a clear increase in Mn frequency indicating that the RE was gaining entry into cells.

4.3.1.2: Effects of SLO on the binucleate index of SCID and CB17 cells

The binucleate index was also calculated for the results shown Table 4.3. The results (Table 4.4) indicate a decrease in the percentage of binucleate cells in SCID and CB17 cells after SLO treatment. The percentage of binucleate cells decreased from 70% to 23% in SCID cells treated with SLO and for CB17 cells the percentage of binucleate cells decreased to 41% after SLO treatment.

Table 4.2: Frequency of micronuclei induced in SCID and CB17 cells treated with 10units/ml PvuII and increasing concentrations of SLO.**

Cell line	Treatment	No. of micronuclei/100 binucleate cells
SCID	Control	12.0
CB17	Control	2.0
SCID	0.05 units/ml SLO	18.0
CB17	0.05 units/ml SLO	3.0
SCID	0.15 units/ml SLO	23.0
CB17	0.15 units/ml SLO	18.0
SCID	0.25 units/ml SLO	53.0
CB17	0.25 units/ml SLO	21.0
SCID	0.40 units/ml SLO	50.0
CB17	0.40 units/ml SLO	20.0
SCID	0.50 units/ml SLO	58.0
CB17	0.50 units/ml SLO	25.0

**This was a single experiment to determine the poration ability of SLO on SCID and CB17 cells.

*Each sample was set up overnight and the following day each sample was treated with the appropriate SLO concentration in HBSS for 5 min. After treatment the dishes were washed with HBSS and incubated at 37°C in medium containing cytochalasian B for 24 hours. Samples were prepared and the frequency of micronuclei scored.

Table 4.3: Frequency of micronuclei induced in SCID and CB17 cells treated with 25 units/ml PvuII and 0.33units/ml SLO.

Cell line	Treatment SLO concentration units/ml*	No. of micronuclei/100 binucleate cells**
SCID	Control	8.5 ± 2.4
CB17	Control	5.5 ± 2.8
SCID	Control + 0.33 units/ml SLO	12.5 ± 1.5
CB17	Control + 0.33 units/ml SLO	8.0 ± 1.0
SCID	0.33 units/ml SLO + 25 units/ml PvuII	40.0 ± 4.0
CB17	0.33 units/ml SLO + 25 units/ml PvuII	27.0 ± 0.9

**Data represent the means and standard errors from three independent experiments.
*Each sample was set up overnight and the following day each sample was treated with the appropriate SLO concentration and PvuII in HBSS for 5 min. After treatment the dishes were washed with HBSS and incubated at 37°C in medium containing cytochalasian B for 24 hours. Samples were prepared and the frequency of induced Mn scored.

Table 4.4: Binucleate index for SCID and CB17 cells treated with 25 units/ml PvuII and 0.33units/ml SLO. These results were calculated from the experiment in Table 4.3.

Cell line	Treatment SLO concentration units/ml	Percentage of binucleate cells per 100 cells*
SCID	Control	71.0 ± 0.9
CB17	Control	69.0 ± 0.9
SCID	Control + 0.33 units/ml SLO	67.0 ± 1.0
CB17	Control + 0.33 units/ml SLO	69.0 ± 0.9
SCID	0.33 units/ml SLO + 25 units/ml PvuII	22.5 ± 1.2
CB17	0.33 units/ml SLO + 25 units/ml PvuII	41.0 ± 1.2

*Data represent the mean and standard errors from three independent experiments.

4.3.1.3: Effects of increasing PvuII concentrations on SCID and CB17 cells

The next investigation was to study the effects of increasing PvuII concentrations on SCID and CB17 cells porated with 0.33 units/ml SLO (Figure 4.2 and Table 4.5). The results, as shown in Figure 4.2, indicate a linear induction of micronuclei as the concentration increased from 10-40 units/ml PvuII. SCID cells compared to CB17 cells had a 2.1, 1.7, 2.0 and 1.8 fold higher frequency of induced Mn following treatment with 10, 20, 30 and 40 units/ml PvuII respectively.

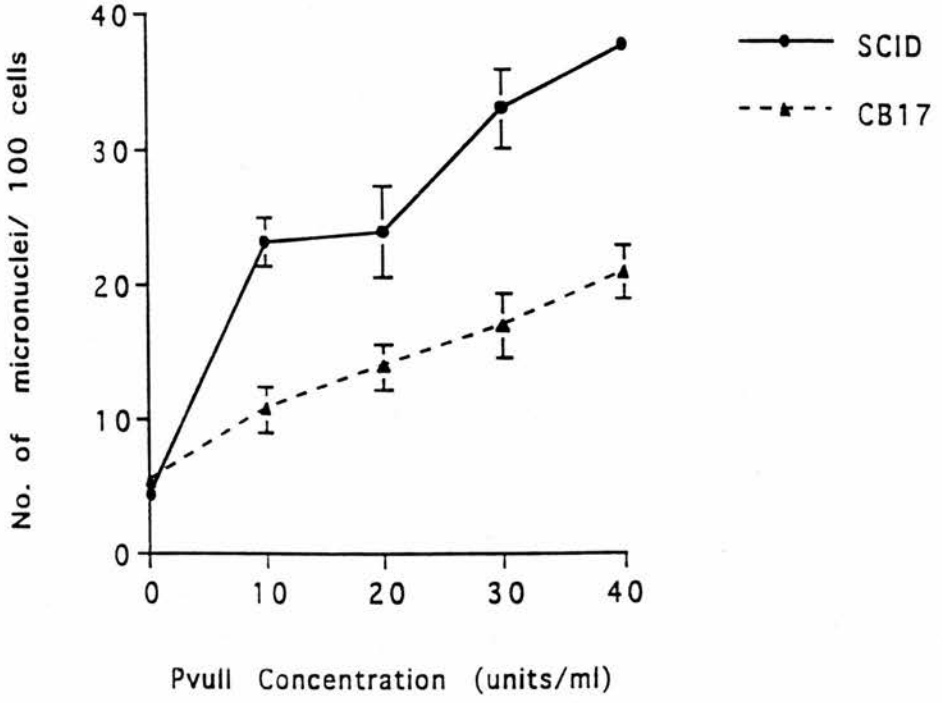

Figure 4.2: Response of SCID and CB17 cells to increasing concentrations of PvuII and 0.33 units/ml SLO. Each sample was treated with SLO and PvuII for 5 min and then incubated in medium containing cytochalasin B for 24h. The results were pooled from three independent experiments and the error bars represent the standard errors of the mean.

Table 4.5: Micronuclei yields in SCID and CB17 cells treated with increasing concentrations of PvuII and porated with 0.33 units/ml SLO.

Cell line	Treatment	Frequency of micronuclei per 100 binucleate cells*
SCID	SLO only (0.33 units/ml)	4.5 ± 0.8
CB17	SLO only (0.33 units/ml)	5.4 ± 0.7
SCID	SLO (0.33 units/ml) + PvuII (10 units/ml)	23.2 ± 1.8
CB17	SLO (0.33 units/ml) + PvuII (10 units/ml)	10.8 ± 1.7
SCID	SLO (0.33 units/ml) + PvuII (20 units/ml)	24.0 ± 3.4
CB17	SLO (0.33 units/ml) + PvuII (20 units/ml)	14.0 ± 1.7
SCID	SLO (0.33 units/ml) + PvuII (30 units/ml)	33.2 ± 2.9
CB17	SLO (0.33 units/ml) + PvuII (30 units/ml)	17.0 ± 2.3
SCID	SLO (0.33 units/ml) + PvuII (40 units/ml)	37.8 ± 0.4
CB17	SLO (0.33 units/ml) + PvuII (40 units/ml)	21.0 ± 2.0

* Data represent the mean and standard errors from three independent experiments.

4.3.2: Disappearance of chromatid breaks with time in SCID and CB17 cells treated with PvuII

The G2 assay was used to investigate the response of SCID and CB17 cells to RE inducing different types of dsb. In order to establish an optimal sampling time for the G2 assay with SLO and restriction endonucleases a preliminary experiment was carried out (Figure 4.3). At 2.5 h there was a high induction of chromatid breaks in both cell lines and at 5 and 7.5 h after treatment this value had decreased. Although giving high frequencies of chromatid breaks, scoring samples taken at 2.5 h was difficult, because the mitotic index was very low at this early time after treatment. Therefore, 5 h was chosen as a sampling time, when the mitotic index had returned to near normal after SLO treatment.

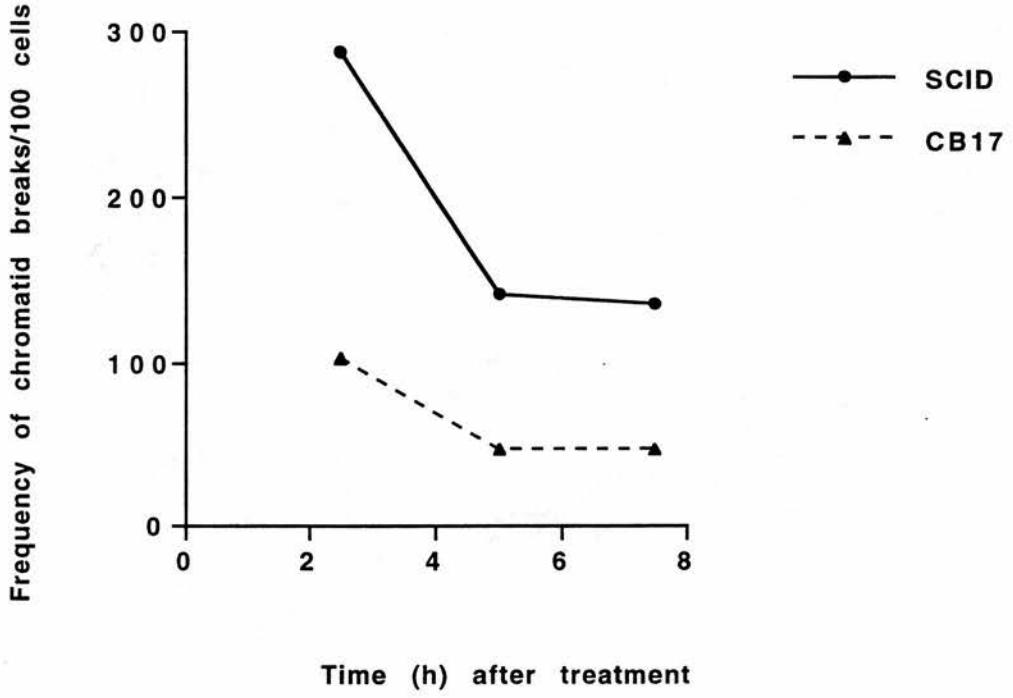

Figure 4.3: Disappearance of chromatid break frequencies in SCID and CB17 cells treated with 100units/ml PvuII and 0.33units/ml SLO for 5 min and samples taken at 2.5, 5 and 7.5h. Results of a single experiment

4.3.3: Induction of chromatid breaks in SCID and CB17 cells treated with restriction endonucleases inducing various dsb-end structures

The chromatid break response of SCID and CB17 cells at t=5h to the RE; PvuII, EcoRV and AluI inducing blunt-ended dsb is shown in Figure 4.4 and Figure 4.5 shows the response to HindIII, EcoRI and PstI inducing dsb with 5' or 3' overhanging bases. Figure 4.4 shows that SCID cells are more sensitive than CB17 cells to all three types of blunt-ended dsb. The difference in chromatid break frequency between SCID and CB17 cells for each of the RE that induce blunt-ended dsb were: PvuII: 2.25, EcoRV: 4.3 and AluI: 1.6 (Figure 4.4). In contrast, there was a relatively small difference between the response of SCID and CB17 cells to HindIII and EcoRI which induce 5' cohesive-ended dsb whereas PstI (3' cohesive ends) gave a 2.5 fold elevated response in SCID cells (Figure 4.5). The overall frequency of chromatid break induction in response to cohesive-ended dsb was reduced relative to the response exhibited by blunt-ended dsb in both cell lines. The addition of SLO to SCID and CB17 cells did not significantly ($p>0.05$) affect the chromatid break response as shown in Table 4.6. SCID cells treated with RE inducing blunt-ended dsb gave a significantly different response than CB17 cells (Table 4.6). In addition, SCID cells treated with PstI produced a significantly different response ($p=0.0023$), whereas HindIII and EcoRI did not. The results showed a significant enhancement in the response exhibited by SCID cells relative to CB17 cells when treated with RE which induce blunt- and 3' cohesive-ended dsb but not with 5' cohesive-ended dsb.

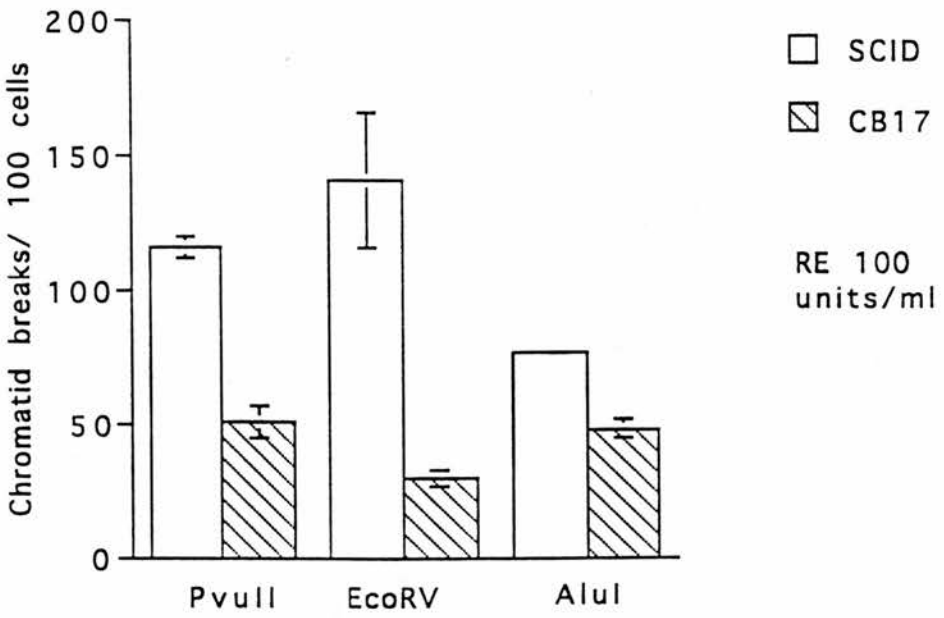

Figure 4.4: Chromatid break response of SCID and CB17 cells treated with various restriction endonucleases inducing blunt-ended dsb during SLO treatment. Each cell sample was treated with 0.33 units/ml SLO and 100units/ml restriction endonuclease. Each value has been adjusted for background chromatid break frequencies, the data is shown in Table 4.6. The results were pooled from at least three independent experiments and the errors bars represent the standard errors of the mean.

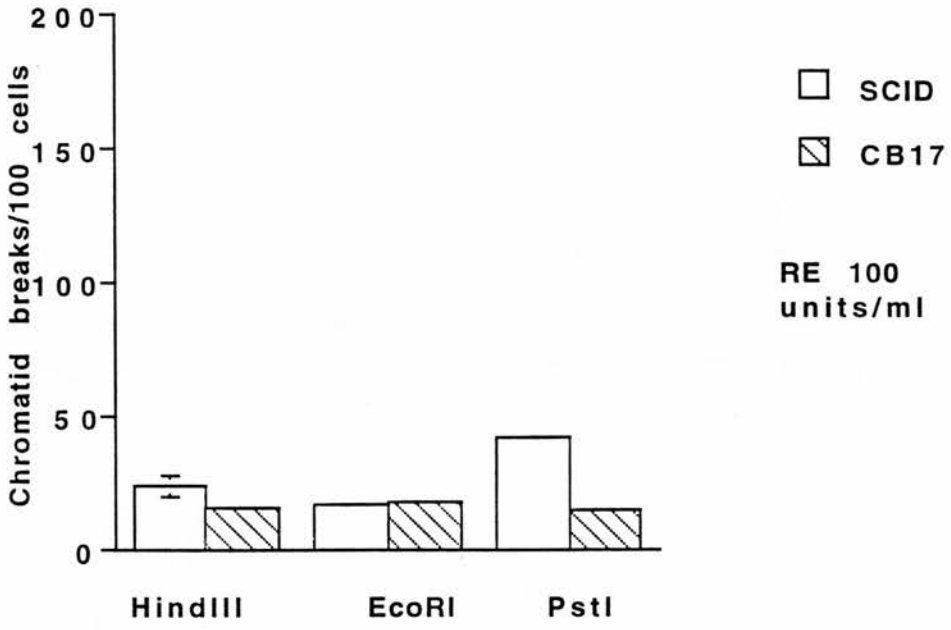

Figure 4.5: Chromatid break response of SCID and CB17 cells treated with various restriction endonucleases inducing cohesive-ended dsb during SLO treatment. Each cell sample was treated with 0.33 units/ml SLO and 100units/ml restriction endonuclease. Each value has been adjusted for background chromatid break frequencies, the data is shown in Table 4.6. The results were pooled from three independent experiments and the errors bars represent the standard errors of the mean.

Table 4.6: The frequency of chromatid breaks induced in SCID and CB17 cells by different restriction endonucleases and the significance of the response of each cell line to different RE.

Cell line	Treatment	No. of metaphases scored	Mean breaks per 100 cells**	P-value
SCID	Control	500	10.0 ± 03.8	
CB17	Control	500	5.0 ± 00.7	
SCID	SLO (0.33 units/ml)	500	10.0 ± 02.2	
CB17	SLO (0.33 units/ml)	500	5.0 ± 00.5	
SCID	SLO + PvuII (100 units/ml)	400	126.0 ± 03.7	0.0006*
CB17	SLO + PvuII (100 units/ml)	400	56.0 ± 06.2	
SCID	SLO + EcoRV (100 units/ml)	300	152.0 ± 25.0	0.043*
CB17	SLO + EcoRV (100 units/ml)	300	35.0 ± 03.2	
SCID	SLO + AluI (100 units/ml)	300	87.0 ± 02.3	0.0036*
CB17	SLO + AluI (100 units/ml)	300	54.0 ± 03.2	
SCID	SLO + HindIII (100 units/ml)	300	34.0 ± 04.2	0.11
CB17	SLO + HindIII (100 units/ml)	300	22.0 ± 01.5	
SCID	SLO + EcoRI (100 units/ml)	300	27.0 ± 01.2	0.27
CB17	SLO + EcoRI (100 units/ml)	300	24.0 ± 01.9	
SCID	SLO + PstI (100 units/ml)	300	52.0 ± 01.5	0.0023*
CB17	SLO + PstI (100 units/ml)	300	20.0 ± 00.4	

** Data represent the mean and standard errors from at least three independent experiments.

* indicates a significant difference at 95% confidence intervals meaning that SCID and CB17 cells responded different to the RE treatment.

4.4: Discussion

4.4: Discussion

The preliminary Mn studies (Table 4.2 and 4.3) show that SLO was able to porate SCID and CB17 cells allowing PvuII to penetrate cells. An optimal concentration of 0.33 units/ml of SLO was adopted for both cell lines. Analysis of the binucleate index (Table 4.4) showed a decrease after SLO treatment. 0.33units/ml of SLO reduced the BI by approximately 2 fold compared to controls but was still adequate for scoring cells with Mn. There was an increasing Mn frequency in cells treated with increasing PvuII concentrations in SCID and CB17 cells (Figure 4.2), with SCID cells showing higher frequencies of Mn than CB17, consistent with previously published results in other mammalian mutant radiosensitive cells lines, such as irs2, xrs5 and AT (Bryant *et al* 1993a, Darroudi and Natarajan 1989, Liu and Bryant 1993).

The main focus of this study was to determine the response of G2 SCID and CB17 cells to dsb with different end structures and Figures 4.4 and 4.5 illustrate the G2 chromatid sensitivity of SCID and parental CB17 cells to RE which induce either blunt-ended or cohesive-ended dsb with 5' or 3' 5 base pair overhangs. The results show that PvuII gave a 2.25 fold elevated frequency of chromatid breaks, EcoRV produced an even higher (4.3 fold) frequency of chromatid breaks, but in contrast AluI only produced an enhancement of 1.6. A possible reason for the lower, but still elevated frequency, with AluI is a difference in the stability of AluI in the cells relative to the two other REs. However, it may reveal a difference in the nature of the recognition sequence and cutting site of AluI compared to PvuII and EcoRV (Lutze *et al* 1993). The higher frequency of chromatid breaks in SCID cells treated with EcoRV is likely the result of the DNA sequence at or near the break influencing the end-joining process (Kinashi *et al* 1995, reviewed by Morgan *et al* 1998). Blunt-ended dsb induced by various RE in the APRT gene of CHO cells were shown to be repaired by different end processing events before religation. Single base pairs were

inserted to repair dsb induced by PvuII, whereas StyI and EcoRV induced dsb were repaired by DNA deletions of short complementary nucleotide sequences 1-6bp at or near the termini of the break (Philips and Morgan 1994, reviewed in Morgan *et al* 1998). However, *in vivo* the case may be very different and the spatial orientations of the dsb may be a determining factor for selecting the repair mechanism (Yates and Morgan 1993).

The elevated chromatid break frequencies in response to blunt-ended dsb in SCID cells is likely the result of a defective NHEJ repair pathway, due to the absence of DNA-PK. DNA-PK has been proposed as a DNA damage signalling protein (Jeggo 1999) and it may be required for the recruitment of the MRE11-RAD50-Nbs1 complex that acts as a nuclease preparing the DNA ends for religation (Petrini 1999). Recent studies have shown the relocalisation of the MRE11-RAD50-Nbs1 complex from a uniform distribution within the cell to nuclear foci after IR exposure (Nelms *et al* 1998, reviewed by Petrini 1999). These nuclear foci are thought to be the sites of ongoing DNA repair. Furthermore, Ku70 has been shown to regulate the activity of NHEJ because in the absence of Ku70, Mre11 does not localise as discrete nuclear foci after IR treatment(Nelms *et al* 1998, Goedecke *et al* 1999, Lustig 1999). These studies illustrate the importance of signalling DNA damage so that repair proteins are recruited to the damaged DNA. The importance of DNA-PK and ATM as potential signalling proteins remains to be elucidated. In the absence of DNA-PK, Ku can bind DNA ends, so the MRE11-RAD50-Nbs1 complex should be able to resect the blunt-ended dsb. However, the stability of the resected DNA end will influence the ease with which the dsb can be repaired (Lutze *et al* 1993).

Dsb with cohesive-termini were not as clastogenic as those with blunt-termini and the overall frequency of chromatid breaks in both SCID and CB17 cells was greatly reduced (Figure 4.7 and Table 4.1). This is consistent with previous results in other radiosensitive hamster and human cell lines (Bryant 1984, Bryant and Christie 1989, Liu and Bryant

1994), suggesting that cohesive-ended dsb are repaired more readily than blunt-ended dsb (i.e. possibly as two ssb). There was virtually no difference in the G2 chromatid break response of CB17 and SCID cells to EcoRI and only a relatively small differential response to HindIII ($p>0.05$), suggesting that the repair of 5' cohesive-ended dsb is normal in both cell lines. However, PstI yielded a significant enhancement ratio of 2.5 in SCID cells compared to parental cells ($p=0.0023$). PstI induces cohesive ends with a 5 base pair 3' overhang, whereas the other REs induced breaks with a 5 base pair 5' overhang. It has previously been suggested that 5' cohesive termini with a 5 base-pair overhang may be recognised as two single-strand breaks, so that these damaged sites are repaired with ease. Previous studies, have shown that cohesive-ended dsb are not as clastogenic and it was suggested that the ends induced may be held together by hydrogen bonds and repaired by simple ligation (Bryant 1988).

Possible reasons for the differential response of SCID cells to PstI treatment are a difference in the effectiveness by which different end structures of dsb are signalled. Similar to the repair of blunt-ended dsb induced by RE, cohesive ends induced by RE are repaired differently dependent on the RE. Winegar *et al* (1992) have shown that the repair of cohesive-ended dsb is dependent on the RE, by studying the spectra of alterations in a plasmid, pHAZE, that is stably maintained in human lymphoblastoid cells. Similar to PstI, PvuI induces dsb with 3' overhangs and induced breaks are repaired by inversions and deletions. PvuI site inversions are thought to be mediated by a looping-out structure (Winegar *et al* 1992). If this looping-out structure is a feature common for all 3' overhangs *in vivo* it is likely the underlying cause for the elevated chromatid break frequency in SCID cells treated with PstI. SCID cells are unable to resolve coding ends during V(D)J recombination and this process involves looping-out DNA segments (Jeggo *et al* 1999).

Thus, both the position and overhang of the termini of a dsb are likely determinants of how the dsb is perceived by the DNA repair processing enzymes. SCID cells appear to repair 5' dsb but not 3' dsb nor blunt-ended dsb possibly due to the dsb repair deficiency in SCID cells. Different pathways are likely required for each dsb induced and those pathways that repair 3' and blunt-ended dsb appear to be defective in SCID cells. Alternatively, it may be speculated that the DNA-PK signalling pathway which is deficient in SCID cells may use another pathway for e.g. ATM, as a signalling protein, and in doing so may over compensate for DNA-PK, so that more chromatid breaks are induced in SCID cells in response to 3' and blunt-ended dsb.

In contrast, to the results presented here, Chang *et al* (1993), showed a reduced survival in SCID cells treated with blunt- and cohesive- ended dsb than CB17 cells. The reason for these differences are likely attributed to the different end points measured. Chang *et al* measured the survival of SCID cells 8 days after treatment, whereas the G2 assay studied the affects 5h following treatment. The G2 assay gives a better insight into the initial differences between the response of the two cell lines to various RE induced breaks. Furthermore, the methods of poration were different. SLO was chosen to porate the cells in this study because cell killing and the overdispersal of damage in cells is reduced, whereas these problems are encountered when using electroporation.

In conclusion, the chromatid break response in both SCID and normal fibroblasts is determined by dsb end-structure which is consistent with previously published reports (Lutze et al 1993, Winegar *et al* 1992, Kinashi *et al* 1995). It may be speculated that this specificity may result from the effectiveness with which dsb of a given end-structure are signalled. Blunt-ended and cohesive-ended dsb with 3' overhangs seem to be more readily signalled than cohesive-ends with 5' overhangs.

An interesting study would be to measure the induction and repair of dsb by RE, using PFGE, and to compare these results with the chromatid break results presented here. Furthermore, the effects of RE on $50D^-$ and $100E^+$ cells were not measured because time did not permit these studies, but it would be an interesting study. In addition, investigating the localisation of the MRE11-RAD50-Nbs1 complex, by in situ hybridisation assays, in DNA-$PK^{-/-}$ and $ATM^{-/-}$ cell lines treated with various RE is likely to give an insight into the signalling mechanisms and the proteins required for signalling DNA damage.

Chapter Five

Induction and repair of dsb in SCID and CB17 fibroblast cells

5.1: Introduction

Chapter Five:

5.1: Introduction

The aim of the work described in this chapter was to measure the repair of DNA dsb in SCID, CB17, $50D^-$ and $100E^+$ lines. At the chromosomal level there was an enhanced frequency of chromatid breaks in SCID and $50D^-$ cell lines in response to IR compared with parental cells (Chapter 2). Chromosomal radiosensitivity in mutant lines has been attributed to a dsb repair deficiency (e.g. Biedermann *et al* 1991) and to confirm this it was necessary to study the induction and repair of dsb in SCID, CB17, $50D^-$ and $100E^+$ cells.

Previous chapters have shown similar kinetics of disappearance of chromatid breaks with time in G2 SCID and CB17 cell lines (Chapter 2) and the DNA synthesis inhibitor araA resulted in potentiation of chromatid damage (Chapter 3). In order to understand the degree of involvement of dsb rejoining in these processes, repair kinetics of dsb were studied in SCID and CB17 cells with and without araA. Rotating orthogonal field gel electrophoresis (ROFE) and constant-field gel electrophoresis(CFGE) were used to determine if there was a dsb repair defect observable in G2 cells. Initially, the induction of dsb was measured in exponential SCID and CB17 cells to determine the optimal electrophoresis conditions. The induction and repair of dsb was then studied in synchronised G2 populations of SCID and CB17 cells to compare with the results obtained at the (G2) chromosomal level. Finally, the induction of dsb in exponential $50D^-$ and $100E^+$ cells was also investigated.

5.1.1: Eukaryotic chromatin structure

Chromosomes are made up of different regions including the centromere and the telomere. The centromere is involved in cell division and the telomere prevents the ends of chromosomes from fusing with each other (Alberts *et al* 1989). DNA is the fundamental component of chromosomes. Each diploid nucleus contains approximately $6x10^9$

nucleotides which measure 1 metre in length when unravelled, however, due to the highly organised structure of DNA it is folded into a 10μm nucleus (shown in Figure 5.1). The basic level is the DNA β helix which wraps around a central protein complex to form nucleosomes and each nucleosome is separated by linker chromatin which varies in length from 0-70 bp. The nucleosomes form a "beads on a string" structure, known as the 10nm fibre. The next level of organisation requires linker histones which enable further packaging of the nucleosomes to form the 30nm chromatin fibre visible in interphase nuclei, using electron microscopy (Bohr *et al* 1987). The 30nm chromatin fibre forms looped domains evident in interphase nuclei and these looped domains may be supercoiled to enable further condensation (Cook and Brazell 1975) [Figure 5.1]. These looped domains are attached to a supporting skeletal structure known as the nuclear "matrix" at specific points called matrix attachment sites (MARs). MARs are not stable structures as attachment to the matrix lamina and nuclear envelope is disrupted at metaphase enabling further condensation along the central axis of a chromosome. The binding of histones to DNA can be modified by post-translational alterations such as phosphorylation or acetylation, which may be relevant to the accessibility of DNA resulting in changes to transcriptional status, structure and repair of DNA (Bohr *et al* 1987, Alberts *et al* 1989).

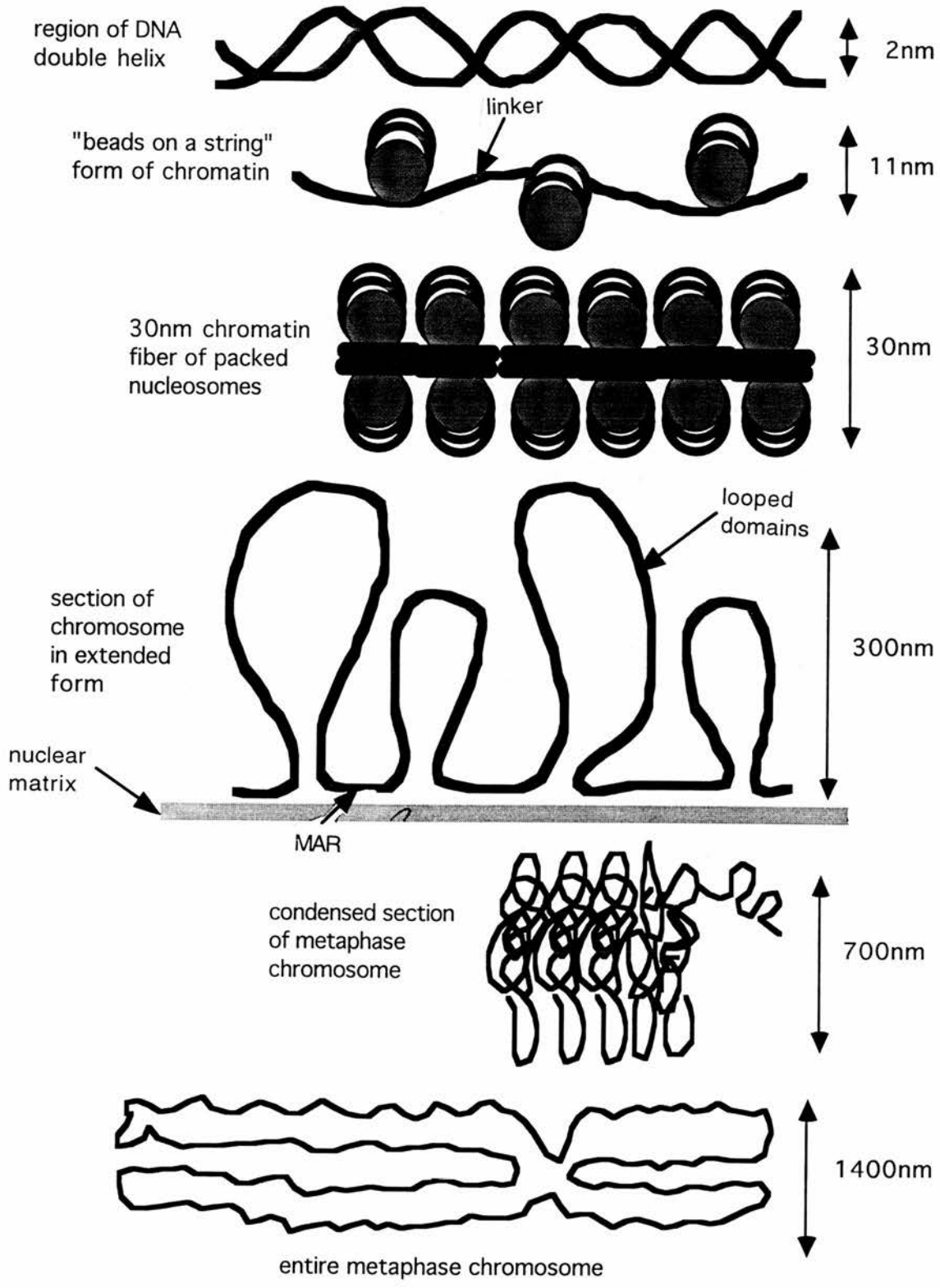

Figure 5.1: Diagrammatic representation of the organisation levels in chromatin to give rise to a highly condensed metaphase chromosome (adapted from Alberts et al 1989).

Only a small fraction of chromosomal DNA is actively transcribed, and this is packaged in an altered nucleosomal structure that is less condensed than transcriptionally inactive DNA. Active DNA known as euchromatin is associated with nonhistone proteins which may establish the transcriptionally active state. Therefore, the accessibility of some DNA regions to repair enzymes depends upon the local "openness" of the chromatin structure and an essential step in repair may control the accessibility of the damaged DNA region to the repair enzymes (Bohr *et al* 1987). It has been shown that DNA-bound proteins (especially histones) are essential for DNA protection against radical attack and these conditions are also important when investigating repair (Ljungman *et al* 1991).

5.1.2: Methods for measuring induction and repair of dsb

The velocity sedimentation method was used initially for the detection of dsb in mammalian cells but it was relatively insensitive, laborious (Lehmann and Stevens 1977, Blöcher 1982) and ambiguous results were difficult to interpret (Okayasu *et al* 1988). The original DNA filter assays (Kohn *et al* 1976) were adapted by pH adjustment, lysis conditions and temperature to measure dsb induction and repair in mammalian cells (Bradley and Kohn 1979). However, DNA shearing and chromatin configuration effects during the lysis procedure were unknown (Wlodek *et al* 1990). Therefore, the development of pulsed-field gel electrophoresis (PFGE) was advantageous because the cells could be embedded in a gel matrix to prevent mechanical shearing of DNA during the lysis procedure, the method was relatively sensitive and the effects of low biologically relevant radiation doses could be measured.

5.1.3: Pulsed-field gel electrophoresis

Pulsed-field gel electrophoresis (PFGE) emerged as a powerful tool for the study of high molecular weight DNA which could not be measured by conventional electrophoresis. PFGE was initially introduced for the separation of yeast DNA molecules of up to several million bp (Schwartz and Cantor 1984), but more recently it has been used to study the induction and repair of dsb in mammalian cells (Blöcher *et al* 1989, Stamato and Denko 1990).

Conventional electrophoresis is limited to the separation of DNA molecules of up to 0.75Mbp in size whilst larger molecular weight DNA "reptated" through the gel (Fangman 1978). "Reptation" is a term used to describe the movement (reorientation) of DNA molecules through a gel matrix as the field direction is shifted, regardless of the molecular weight (Lerman and Firsh 1982, Lumpkin *et al* 1985). However, the use of two electric fields parallel to each other has resolved the problem of large molecular weight DNA reptating very slowly through the gel. Altering the direction of the electric field and varying the pulse time of the applied electric field has enabled the separation of DNA molecules by size. Small molecular weight DNA migrate faster through the gel as reorientation to the new direction of the electric field requires a shorter time, whereas large molecular weight DNA requires a much longer time period to reorientate. This method enabled the successful separation of yeast and parasite chromosomes of up to 10Mbp (Schwartz and Cantor 1984, Carle and Olsen 1984, Snell and Wilkin 1986, Smith *et al* 1987). Since PFGE was introduced, many other electrophoresis techniques have been developed including: field inversion gel electrophoresis (FIGE, Carle *et al* 1986), orthogonal field alternating gel electrophoresis (OFAGE, Carle and Olsen 1984), contour clamped homogenous electrophoresis (CCHE, Chu *et al* 1986), transverse alternating field gel electrophoresis (TAFE, Gardiner 1986), continuos homogenous field gel

electrophoresis (CHEF, Blöcher *et al* 1989), programmable autonomously controlled electrode electrophoresis (PACE, Elia and Nichols 1993) and graded field gel electrophoresis (GFGE, Zhou *et al* 1997). These techniques are named according to the electric field applied and each has improved the separation of large molecular weight DNA. CHEF separates DNA up to 10Mbp in size and DNA damage induced by 1Gy of radiation can be measured, which is useful for measuring the repair of dsb in mammalian cells exposed to biological relevant doses (Blöcher *et al* 1989). The underlying principle of PFGE is measurement of the fraction of activity released (FAR; radioactively labelled DNA) from the well into the gel. This is used as a measure of the amount of radiation induced DNA damage (dsb). Quantification can be accomplished by using radioactively labelled cells in which the DNA bands can be first visualised by fluorescence, cut out and the radioactivity counted, using a liquid scintillation counter. More recently, analysis of FAR using fluorescent dyes and image analysis systems has enabled the measurement of dsb induction and repair in tissue samples and nondividing cells (Rosemann *et al* 1993). Constant-field gel electrophoresis has recently been used to measure dsb induction in mammalian cells (Wlodek *et al* 1991). CFGE has many advantages, including a short time of 26 hours to resolve the damaged DNA into lanes, the apparatus is cheaper and simpler to use than PFGE and the fragmented DNA migrates into the gel to form a compression zone just below the well making it easier to measure the damage (Ager *et al* 1990, Wlodek *et al* 1991). CFGE is dependent on low voltage and low agarose gel concentrations to achieve maximum separation, but does not separate the DNA according to molecular weight (Fangman 1978, Wlodek *et al* 1991).

5.1.4: Induction and repair of dsb in mammalian mutants

Recently, PFGE has become a useful technique for measuring dsb induction and repair in mammalian cells. The repair of dsb has been investigated in mammalian mutant cells using

a variety of techniques and two repair phases were identified, an initial fast phase which occurs within minutes and a second much slower phase which can take several hours.

AT cells have shown similar repair kinetics compared with normal cells, as measured by velocity sedimentation (Lehmann and Stevens 1977) and pulsed field gel electrophoresis (Blöcher *et al* 1991). A fast repair rate was observed in the first few minutes followed by a second much slower repair phase, in both AT and normal cells, but the residual dsb fragments remaining in AT cells was higher than normal cells. However, more recently, it has been reported that the initial repair in AT cells is faster than wildtype cells (Foray *et al* 1995). xrs5 cells, deficient for Ku80 protein, have shown similar initial repair rates to those in CHO cells, but the slow repair component is reduced in xrs5 cells, hence the higher frequency of unrejoined dsb remaining in xrs5 cells compared to CHO cells (Kemp *et al* 1986, Costa and Bryant 1988, Iliakis *et al* 1992, Dahm-Daphi *et al* 1993). However, Mateos *et al* (1994) studied the repair of dsb in G1 and G2 xrs5 cells using neutral filter elution. The repair rate was apparently normal in G2 xrs5 cells which may explain the apparently normal rate of disappearance of chromatid breaks in these cells as measured by the G2 assay. The repair rate of dsb was reduced in G1, suggesting that the dsb repair deficiency is specific to G1 cells. Even though the G2 repair of dsb is apparently normal in G2 xrs5 cells, there remains a 2-fold elevated frequency of chromatid breaks which has been attributed to an enhanced conversion of dsb into chromatid breaks, which may be due to an altered initiating signal as proposed under the signal model (Bryant 1998).

5.1.5: Repair of dsb in SCID cells

Repair of dsb as measured by neutral filter elution shows a reduced rejoining of dsb in asynchronous SCID cells compared with asynchronous wildtype cells (Biedermann *et al* 1991). BALB/C cells are the parental cells of CB17 cells and can be used as a control for

SCID cells. BALB/C cells repaired 75% of the initial DNA damage by 2 h post irradiation, whereas SCID cells only repaired 50% of the initial DNA damage after 2 h. The initial DNA dsb levels were the same in SCID and wildtype (BALB/C) cells (Hendrickson *et al* 1991). This suggested that the slow dsb repair phase was reduced in SCID cells relative to BALB/C cells. SCID cells have also shown a reduced repair capacity compared with CB17 cells as measured by FIGE (Chang *et al* 1993). In addition, there was a dose dependent repair rate in SCID cells as 75% of the initial DNA damage was repaired in SCID cells 3h after 10 Gy, in comparison to 40% repaired 3h after 50 Gy γ-rays. In contrast, CB17 cells repaired 90% of the initial damage by 3h which was independent of the initial dose administered. xrs5 cells also have a reduced slow dsb repair phase in G1 cells and a dose dependent repair rate, suggesting that these are characteristics of mammalian mutants deficient in dsb repair (Kemp *et al* 1984, Giaccia *et al* 1985, Zdzienicka *et al* 1988, Dahm-Daphi *et al* 1993).

More recently, Nevaldine *et al* (1997) used a dsb repair assay to measure IR-induced DNA fragments of 2-6 Mbp in size. The report stated that SCID and CB17 cells had similar repair rates for the initial 15 min, after which SCID cells exhibited a slower rejoining rate, but by 24 h post irradiation no residual or unrepaired dsb were apparent in SCID cells even with doses as high as 10 Gy and SCID cells did not have a dose dependent repair rate. This is in contrast to the study by Chang *et al* (1993) and the differences have been attributed to the different methods used as the residual unrejoined dsb reported by Chang *et al* (1993) may be due to necrosis or degradation.

A recent study by Lee *et al* (1997) investigated the repair of dsb in G2 SCID and CB17 pre-B lymphocyte cells and it was reported that 65% of DNA damage was repaired in G2 SCID cells whereas only 35% was repaired in G1 SCID cells, again indicating that the dsb

repair deficiency was mainly apparent in the G1 phase of the cell cycle which is similar to the response exhibited by xrs5 cells (Mateos *et al* 1994).

At the onset of the project, the G2 repair of SCID and CB17 fibroblast cells had not been investigated. Therefore, the repair of dsb in G2 SCID and CB17 fibroblast cells after 30 Gy γ-rays was investigated. Also dsb repair in G2 SCID and CB17 cells treated with araA was studied up to 1-3 h post-irradiation, enabling a comparison between the chromosomal and DNA levels. Rotating orthologonal gel electrophoresis (ROFE) and constant-field gel electrophoresis (CFGE) were used to measure the induction and repair of dsb in G2 SCID and CB17. ROFE was also used to investigate the induction of dsb in exponentially growing $50D^-$ and $100E^+$ cells.

5.2 Materials and Methods

Cell culture and irradiation details in Chapter 2 section 2.2.

5.2.1: Cell synchronisation in G2

Confluent cell cultures of CB17 and SCID cells were passaged and seeded at $2x10^6$ per $75cm^2$ flasks in the presence of araC (final concentration 2.5µg/ml). The addition of araC to an asynchronous population of cells causes the cells to stop cycling and arrest at the G1/S border. After 18 h the monolayers were washed three times with fresh medium and samples were taken every hour for up to 12 h. Subsequential removal of araC enabled the cells to progress through the cell cycle almost in synchrony.

5.2.2: Flow cytometry

Samples of $5x10^5$ cells in 4 ml of ice-cold PBS were washed twice with PBS, resuspended in 70% ethanol and held on ice for 30 min, after fixation in ethanol 2 ml of ice-cold PBS were added, the samples centrifuged at 1000 rpm for 10 min, resuspended in 1 ml of cold PBS and held on ice for a further 30 min. After which 3 ml of cold PBS were added to the samples prior to centrifugation. The pelleted cells were resuspended in PBS at a concentration of $1x10^6$/ml containing propidium iodide (25µg/ml) and stored at 4°C ready for analysis. Cell cycle analysis was performed using a "Cell Fit" programme on a Becton Dickinson FACScan.

5.2.3: Radioactive labelling of cells and irradiation

Cells were grown in media containing tritiated thymidine for 24h, to substitute the thymidine bases with radiolabelled thymidine, enabling detection by a scintillation counter. Thymidine was also added at the same time to prevent the incorporation of nonspecific

radiolabel, resulting in a misrepresentation of the amount of DNA present. After each cell sample was exposed to IR and allowed to repair, the damaged DNA was separated from the undamaged DNA by electrophoresis. The relative amounts of DNA in the wells and lanes of the gel was estimated by the presence of incorporated tritiated thymidine in the DNA.

Cells were seeded at a concentration of $2x10^6$ and labelled with $3.7x10^2$ Bq/ml ^{3}H-Tdr (specific activity $1.63\ x10^{11}$/ mmol: Amersham, Life Sciences UK) and 5μM thymidine 24 hours before experiments with exponential cells. For G2 cultures the cells were labelled with tritiated thymidine and thymidine prior to blockage with araC. Irradiation was performed on ice using a ^{137}Cs IBL437C γ-irradiator (CIS Bio-International, High Wycombe, UK).

5.2.4: Preparation of cells for gel electrophoresis

Cells were harvested by trypsination, washed, centrifuged, resuspended in PBS and mixed with low melting point agarose (0.8% LMP-agarose, Sigma, Co. UK) resulting in a concentration of $3x10^5$ cells per/ml . The liquid gel suspension was immediately pipetted into rectangular 100μl moulds (10mm x 5mm) and allowed to solidify on ice for 5 min. The agarose plugs were transferred to bijou bottles containing ice-cold PBS. The plugs were exposed to doses of radiation ranging from 0-30 Gy. Immediately after irradiation the gel plugs were placed in ice-cold lysis solution (appendix 2). Experiments in which the cells were allowed to repair, cells were irradiated (30Gy) as a monolayer followed by incubation at 37°C for up to 3 h. Repair was stopped by rapid chilling on ice, cells were harvested and embedded in agarose as described above. Cell lysis was started on ice for 30 min and continued overnight (at least 16 h) at 37°C. Subsequently, the plugs were washed

three times in TE (pH 8.0) and once in TE plus 0.1mg/ml RNase and incubated at 37°C for 1h.

5.2.5: Constant-field gel electrophoresis

The plugs were inserted into a 0.7% agarose gel (ultrapure, GIBCO BRL) containing 0.5µg/ml ethidium bromide for electrophoresis. Gel electrophoresis was performed in 0.5% TBE buffer (Bio-Rad) at ambient temperature for 26 h at a constant field strength of 1.8V/cm. The gel was viewed using a UV transilluminator. *S. pombe* (Bio Rad) was used as a marker.

5.2.6: Rotating orthogonal field gel electrophoresis

In these experiments the cell preparation procedures were similar to those in 5.2.4, except for the following changes. Lysis took place at 50°C overnight (for details of lysis solution see appendix 2). The plugs were inserted into a 0.5% ultrapure agarose gel (GIBCO BRL) containing 0.1µg/ml ethidium bromide. Gel electrophoresis was performed in 0.5% TBE buffer at 11°C, using the Rotaphor apparatus. The gel was electrophoresed for 72 h at a constant field strength of 50V, the angle was 110° with a switch interval of 1000-5000s and rotor speed of 5. *S. pombe* (Bio Rad) was used as a marker.

5.2.7: Gel analysis after electrophoresis

The gel was sliced into sections separating the wells from the lanes and melted at 95°C in 1M HCl. The samples were mixed with Instagel II (Packard, Ltd) for scintillation counting of incorporated tritiated thymidine. The fraction of DNA released into the gel (FAR) corresponded to fragmented damaged DNA and the fraction of this was calculated by

$$FAR = \frac{\text{dpm in lane}}{\text{dpm in lane} + \text{dpm in well}}$$

Each datum point was duplicated in the experiments and each experiment was repeated at least three times. The results represent the average of these repeats.

5.3: Results

5.3.1: The induction of dsb in exponential SCID and CB17 cells

The dose-response curves for exponential SCID and CB17 cells as measured by ROFE and CFGE are shown in Figures 5.2 and 5.3 respectively (Tables 5.1 and 5.2). There is a linear induction of dsb between 0-30 Gy gamma radiation and the frequency of induced dsb is the same for both cell lines. These results are consistent with previously published reports, using FIGE (Hendrickson *et al* 1991, Chang *et al* 1993). The results show that as the radiation dose increased the frequency of induced dsb increased, as expected. Statistical analysis by regression showed no statistically significant differences between the response of SCID and CB17 cells to IR either with ROFE (Fig.5.2; p=0.37) or with CFGE (Figure 5.3; p=0.33).

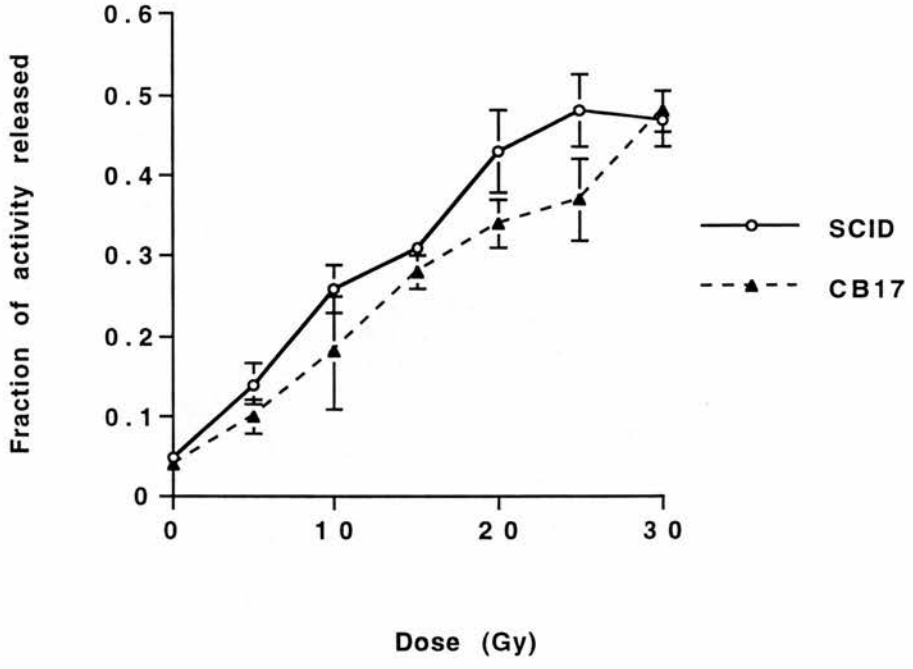

Figure 5.2: Dose response curve for exponential SCID and CB17 cells treated with gamma radiation and measured by rotating field gel electrophoresis (ROFE). The results plotted represent the mean values from at least three independent experiments and the error bars represent the standard errors. Data shown in Table 5.1.

Table 5.1: Induction of double-strand breaks measured by Rotating orthologonal field gel electrophoresis (ROFE) in exponential SCID and CB17 cells treated with increasing doses of γ-radiation.

Cell Line	Treatment	Fraction of activity released ± SEM*
SCID	Control	0.05 ± 0.010
CB17	Control	0.04 ± 0.005
SCID	5 Gy γ-rays	0.14 ± 0.025
CB17	5 Gy γ-rays	0.10 ± 0.020
SCID	10 Gy γ-rays	0.26 ± 0.030
CB17	10 Gy γ-rays	0.18 ± 0.070
SCID	15 Gy γ-rays	0.31 ± 0.005
CB17	15 Gy γ-rays	0.28 ± 0.020
SCID	20 Gy γ-rays	0.43 ± 0.050
CB17	20 Gy γ-rays	0.34 ± 0.030
SCID	25 Gy γ-rays	0.48 ± 0.045
CB17	25 Gy γ-rays	0.37 ± 0.050
SCID	30 Gy γ-rays	0.47 ± 0.035
CB17	30 Gy γ-rays	0.48 ± 0.025

* Data represent the means and standard errors from four independent experiments. Each sample was set up in duplicate. The cells were mixed with PBS plus low melting point agarose (final concentration 0.8%) and placed into moulds to from agarose plugs. The agarose plugs were treated with radiation, lysed overnight and electrophoresed on a 0.7% agarose gel.

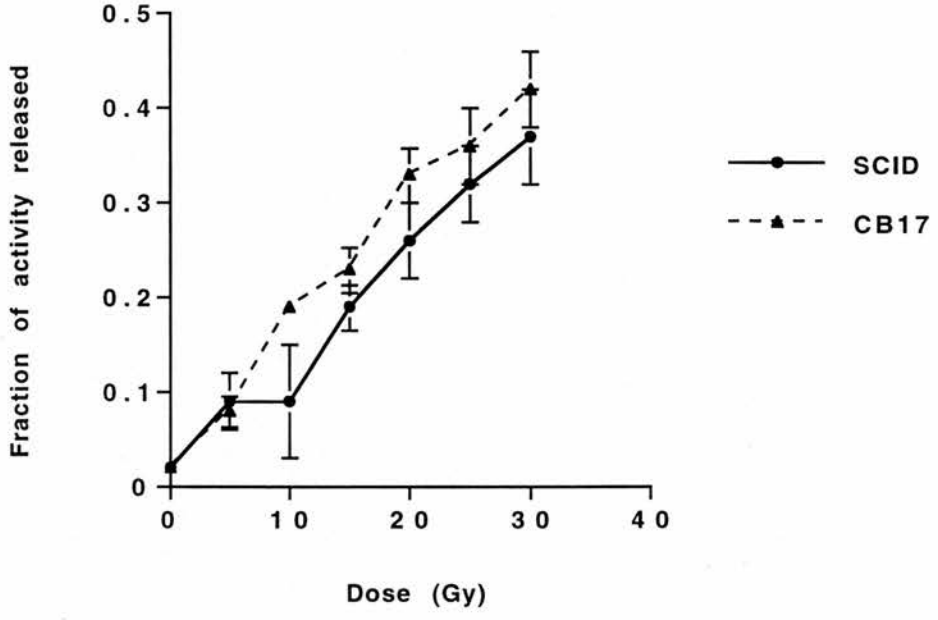

Figure 5.3: Dose-response curve for exponential SCID and CB17 cells treated with gamma radiation and measured by constant-field gel electrophoresis (CFGE). The plotted values represent the means and standard errors from at least three independent experiments. Data shown in Table 5.2.

Table 5.2: Induction of double-strand breaks in exponential SCID and CB17 cells treated with increasing doses of gamma radiation. Constant-field gel electrophoresis (CFGE) was used to measure the induced DNA damage.

Cell Line	Treatment (dose of gamma radiation)	Fraction of activity released ± SEM*
SCID	Control	0.020 ± 0.001
CB17	Control	0.022 ± 0.009
SCID	5 Gy γ-rays	0.090 ± 0.030
CB17	5 Gy γ-rays	0.080 ± 0.017
SCID	10 Gy γ-rays	0.090 ± 0.070
CB17	10 Gy γ-rays	0.190 ± 0.012
SCID	15 Gy γ-rays	0.190 ± 0.023
CB17	15 Gy γ-rays	0.230 ± 0.023
SCID	20 Gy γ-rays	0.260 ± 0.040
CB17	20 Gy γ-rays	0.330 ± 0.029
SCID	25 Gy γ-rays	0.320 ± 0.040
CB17	25 Gy -rays	0.360 ± 0.040
SCID	30 Gy γ-rays	0.370 ± 0.050
CB17	30 Gy γ-rays	0.420 ± 0.040

* Data represent the means and standard errors from three independent experiments. Each sample was set up in duplicate. The cells were mixed with PBS plus low melting point agarose (final concentration 0.8%) and placed into moulds to from agarose plugs. The agarose plugs were treated with radiation, lysed overnight and electrophoresed on a 0.7% agarose gel.

5.3.2: FACScan analysis to determine the percentage of cells in G2 for SCID and CB17 cells (Mateos et al 1994)

SCID and CB17 cells were synchronised in S phase of the cell cycle using araC. After which araC was washed from the cells and they were incubated with fresh medium and samples were taken every 4 hours. Analysis of the cell samples using the "Cell Fit" programme on the FACScan revealed that 68-72% of SCID and CB17 cells were in G2 8 h after removing araC (results shown in appendix 6 Table1). Therefore, this procedure was used prior to each experiment to ensure that a high proportion of the cells were indeed in the G2 phase of the cell cycle (results shown in appendix 6 Table 2). The results in Table 2 appendix 6 show how reproducible and accurate araC was for separating SCID and CB17 cells. These separation methods enabled induction and repair of dsb in G2 SCID and CB17 cells to be measured. Due to the presence of some mitotic cells the population of cells will be referred to as G2/M.

5.3.3: Induction of dsb in G2 /M SCID and CB17 cells

ROFE was used to analyse dsb induction in G2/M SCID and CB17 cells exposed to a range of γ-ray doses between 0-30 Gy (Figure 5.4 and Table 5.3). The results in Figure 5.4 for G2/M cells are similar to the results presented in Figures 5.2 and 5.3 for exponential growing cells in that no significant differences in the induction of dsb was evident in SCID and CB17 cells. Differences between the response of SCID and CB17 cells to increasing doses of radiation were tested using a one way analysis of variance (ANOVA) and no significant differences were found between the two cell lines at each point at 95% confidence limits (no values less than $p=0.05$).

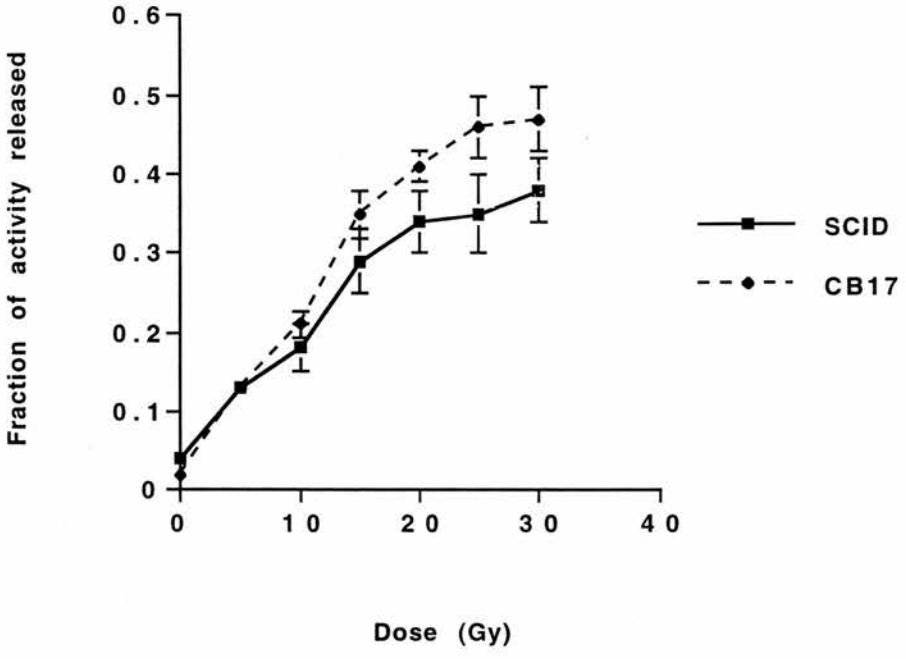

Figure 5.4: Dose-response curve for SCID and CB17 cells synchronised in G2 treated with gamma radiation and measured by rotating field gel electrophoresis (ROFE). The values plotted represent the means and standard errors from at least three independent experiements. Data shown in table 5.3.

Table 5.3: Induction of double-strand breaks in G2/M SCID and CB17 cells treated with increasing doses of gamma radiation. Rotating orthologonal field gel electrophoresis (ROFE) was used to measure the induced damage.

Cell Line	Treatment	Fraction of activity released ± SEM
SCID	Control	0.04 ± 0.006
CB17	Control	0.02 ± 0.003
SCID	5 Gy γ-rays	0.13 ± 0.012
CB17	5 Gy γ-rays	0.13 ± 0.012
SCID	10 Gy γ-rays	0.18 ± 0.030
CB17	10 Gy γ-rays	0.21 ± 0.016
SCID	15 Gy γ-rays	0.29 ± 0.040
CB17	15 Gy γ-rays	0.35 ± 0.030
SCID	20 Gy γ-rays	0.34 ± 0.040
CB17	20 Gy γ-rays	0.41 ± 0.020
SCID	25 Gy γ-rays	0.35 ± 0.050
CB17	25 Gy γ-rays	0.46 ± 0.040
SCID	30 Gy γ-rays	0.38 ± 0.040
CB17	30 Gy γ-rays	0.47 ± 0.040

*Data represent the means and standard errors from six independent experiments. Each sample was set up in duplicate. The cells were synchronised by treating with araC overnight to block the cells in G1 phase. Removal of araC allowed the cells to continue cycling almost in synchrony. After 8 hours 65-75% of SCID and CB17 cells were in G2. The cells were mixed with PBS plus low melting point agarose (final concentration 0.8%) and placed into moulds to from agarose plugs. The agarose plugs were treated with radiation, lysed overnight and electrophoresed on a 0.7% agarose gel.

5.3.4: Repair kinetics of dsb in G2 /M SCID and CB17 cells

The repair of dsb in G2/M SCID and CB17 cells, as measured by CFGE, is shown in Figure 5.5 and Table 5.4. There appear to be at least two phases of rejoining rate in SCID and CB17 cells; an initial fast phase followed by one or more slower phases. These results are consistent with previously reported studies in mammalian cells (Dahm-Daphi *et al* 1993). An alternative interpretation of the kinetics of dsb rejoining in G2/M cells is that a higher frequency of dsb remain unrejoined in SCID cells than CB17 cells. The results in figure 5.5 show higher frequencies of dsb between 10min and 3h in SCID cells than CB17 cells.

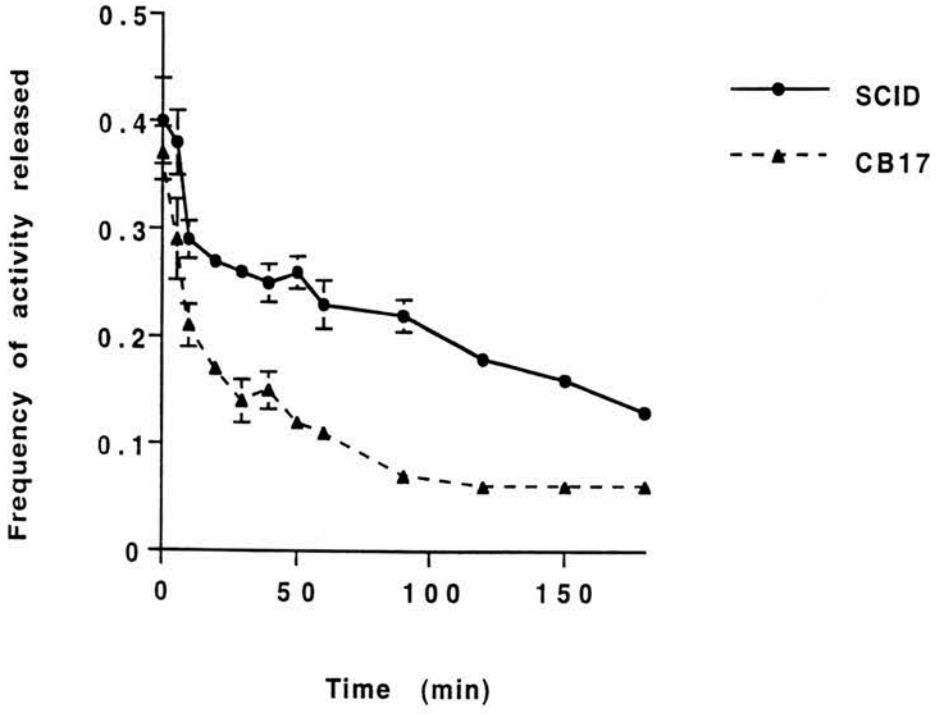

Figure 5.5: The induction and repair of dsb after 30Gy gamma radiation in SCID and CB17 cells synchronised in G2 as measured by constant field gel electrophoresis (CFGE). The values plotted represent the means and standard errors from at least three independent experiments. Data shown in Table 5.4.

Table 5.4: Frequency of double-strand breaks induced and repaired with time in G2/M SCID and CB17 cells treated with 30Gy gamma radiation as measured by Constant-field gel electrophoresis.

Cell Line	Time (min)	Fraction of activity released ± SEM*
SCID	0	0.40 ± 0.040
CB17	0	0.37 ± 0.026
SCID	5	0.38 ± 0.030
CB17	5	0.29 ± 0.038
SCID	10	0.29 ± 0.017
CB17	10	0.21 ± 0.020
SCID	20	0.27 ± 0.008
CB17	20	0.17 ± 0.020
SCID	30	0.26 ± 0.008
CB17	30	0.14 ± 0.020
SCID	40	0.25 ± 0.017
CB17	40	0.15 ± 0.017
SCID	50	0.25 ± 0.014
CB17	50	0.12 ± 0.008
SCID	60	0.229 ± 0.022
CB17	60	0.11 ± 0.007
SCID	90	0.22 ± 0.016
CB17	90	0.07 ± 0.008
SCID	120	0.18 ± 0.003
CB17	120	0.06 ± 0.002
SCID	150	0.16 ± 0.006
CB17	150	0.06 ± 0.005
SCID	180	0.131 ± 0.003
CB17	180	0.06 ± 0.005

* Data represent the means and standard errors from five independent experiments. Each sample was set up in duplicate. The cells resuspended in media were treated with 30Gy gamma radiation and allowed to repair at 37 degrees for the required time period. Afterwards the cells were centrifuged and resuspended in PBS plus low melting point agarose (final concentration 0.8%) and placed into moulds to from agarose plugs. The agarose plugs were lysed overnight and electrophoresed on a 0.7% agarose gel

5.3.5: Kinetics of dsb repair in the presence of araA in SCID and CB17 cells

The repair kinetics of DNA dsb were investigated in the presence of araA (100μM) in SCID and CB17 cells (Figures 5.6, 5.7 and Table 5.5). The rejoining of dsb in the presence of araA at this concentration were essentially the same as that in the absence of araA. The similarities in the kinetics of dsb rejoining (Figures 5.6 and 5.7) in the presence and absence of araA show that araA had no effect on dsb induction and repair in SCID and CB17 cells.

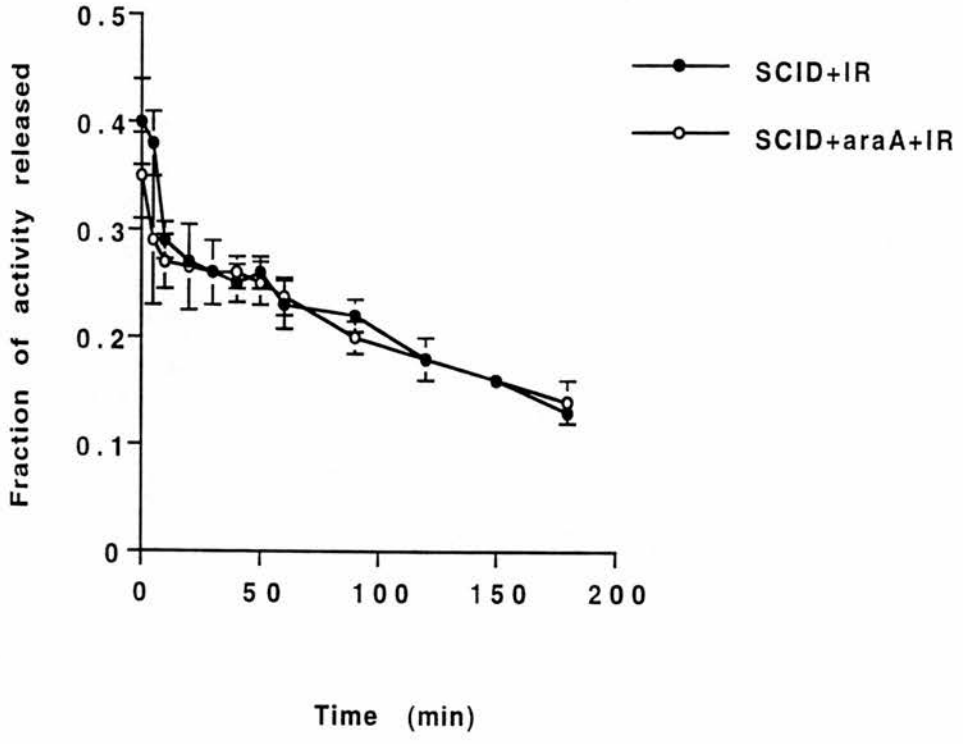

Figure 5.6: The response of G2/M SCID cells to 30Gy gamma radiation in the presence and absence of araA as measured by constant field gel electrophoresis (CFGE). The values plotted represent the means and standard errors from at least three independent experiments. Data given in Table 5.4 and 5.5.

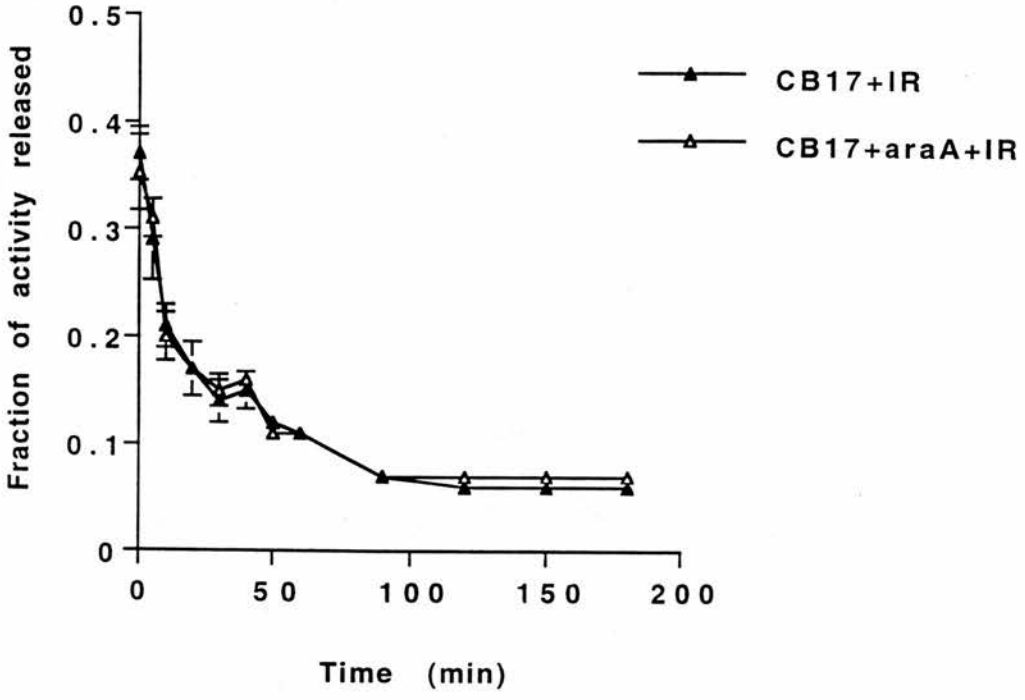

Figure 5.7: The response of G2/M CB17 cells to 30Gy gamma radiation in the presence and absence of araA as measured by constant field gel electrophoresis (CFGE). The values plotted represent the means and standard errors from at least three independent experiments. Data given in Table 5.4 and 5.5.

Table 5.5: Repair of double-strand breaks induced in G2/M SCID and CB17 cells treated with 30Gy gamma radiation and araA as measured by Constant-field gel electrophoresis.

Cell Line	Time (min)	Fraction of activity released ± SEM*
SCID	0	0.35 ± 0.040
CB17	0	0.35 ± 0.035
SCID	5	0.27 ± 0.060
CB17	5	0.31 ± 0.018
SCID	10	0.20 ± 0.025
CB17	10	0.20 ± 0.022
SCID	20	0.31 ± 0.040
CB17	20	0.17 ± 0.025
SCID	30	0.29 ± 0.030
CB17	30	0.15 ± 0.016
SCID	40	0.26 ± 0.016
CB17	40	0.16 ± 0.004
SCID	50	0.25 ± 0.020
CB17	50	0.11 ± 0.006
SCID	60	0.238 ± 0.018
CB17	60	0.11 ± 0.008
SCID	90	0.20 ± 0.016
CB17	90	0.07 ± 0.008
SCID	120	0.18 ± 0.019
CB17	120	0.07 ± 0.004
SCID	150	0.16 ± 0.006
CB17	150	0.07 ± 0.003
SCID	180	0.14 ± 0.019
CB17	180	0.07 ± 0.006

* Data represent the means and standard errors from five independent experiments. Each sample was set up in duplicate. The cells resuspended in media were treated with araA 30 minutes prior to treatment with 30Gy gamma radiation and allowed to repair at 37 degrees for the required time period. Afterwards the cells were centrifuged and resuspended in PBS plus low melting point agarose (final concentration 0.8%) and placed into moulds to from agarose plugs. The agarose plugs were lysed overnight and electrophoresed on a 0.7% agarose gel.

5.3.6: 50D$^-$ and 100E$^+$ dose response curve

The induction of dsb in 50D$^-$ and 100E$^+$ cells, as shown in Figure 5.8 and Table 5.6, exhibit a linear induction of dsb between 0-30 Gy gamma radiation, as measured by ROFE. The induction of dsb in the two cell lines are the same with no significant differences. This was also shown for SCID and CB17 cells (Figures 5.2 and 5.3).

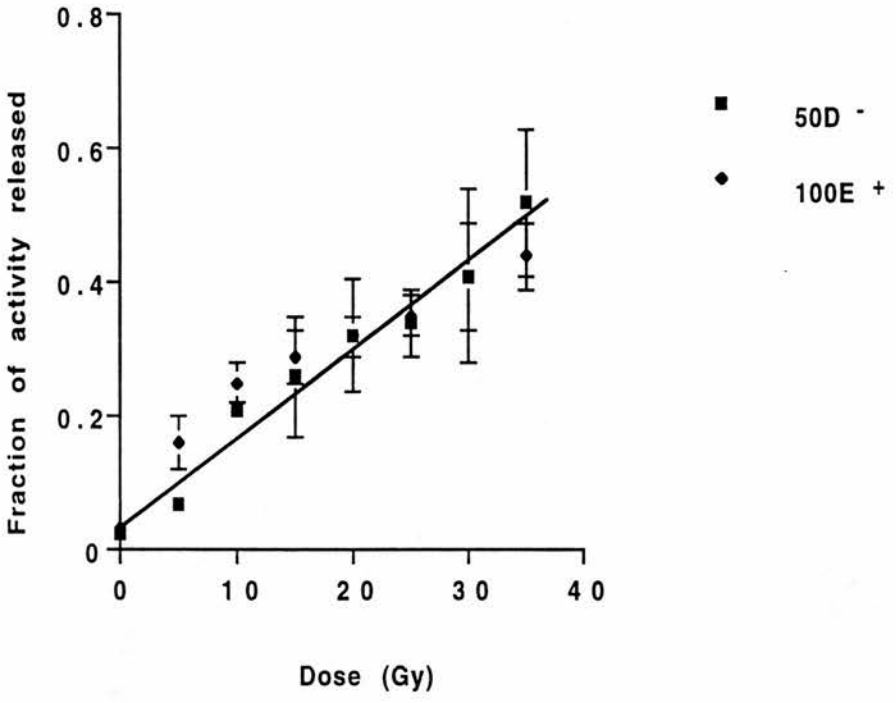

Figure 5.8: Dose-response curve for exponential 50D⁻ and 100E⁺ cells exposed to increasing dosese of gamma radiation as measured by rotating orthologonal field gel electrophoresis (ROFE). The values plotted represent the means and standard errors from at least three independent experiments. Data shown in Table 5.6.

Table 5.6: Induction of double-strand breaks in exponential 50D$^-$ and 100E$^+$ cells treated with increasing doses of gamma radiation. Rotating field orthologonal gel electrophoresis was used to measure the DNA damage induced.

Cell Line	Treatment	Fraction of activity released ± SEM
50D$^-$	Control	0.02 ± 0.006
100E$^+$	Control	0.03 ± 0.005
50D$^-$	5 Gy γ-rays	0.07 ± 0.013
100E$^+$	5 Gy γ-rays	0.16 ± 0.040
50D$^-$	10 Gy γ-rays	0.21 ± 0.018
100E$^+$	10 Gy γ-rays	0.25 ± 0.030
50D$^-$	15 Gy γ-rays	0.26 ± 0.090
100E$^+$	15 Gy γ-rays	0.29 ± 0.040
50D$^-$	20 Gy γ-rays	0.32 ± 0.085
100E$^+$	20 Gy γ-rays	0.32 ± 0.030
50D$^-$	25 Gy γ-rays	0.34 ± 0.050
100E$^+$	25 Gy γ-rays	0.35 ± 0.030
50D$^-$	30 Gy γ-rays	0.41 ± 0.130
100E$^+$	30 Gy γ-rays	0.41 ± 0.080
50D	35 Gy γ-rays	0.52 ± 0.110
100E$^+$	35 Gy γ-rays	0.44 ± 0.050

* Data represent the means and standard errors from four independent experiments. Each sample was set up in duplicate. The cells were mixed with PBS plus low melting point agarose (final concentration 0.8%) and placed into moulds to from agarose plugs. The agarose plugs were treated with radiation, lysed overnight and electrophoresed on a 0.7% agarose gel.

5.4: Discussion

5.4 Discussion

The frequency of induced dsb was linear between 10-30 Gy gamma radiation for SCID and CB17 cells (Figures 5.2 and 5.3) which agrees with previously published results showing similar findings between 10-50 Gy, as measured by asymmetric-field inversion gel electrophoresis (Hendrickson *et al* 1991, Chang *et al* 1993). Even though the frequency of dsb induced are the same for SCID and CB17 cells there is a 1.3-1.7 fold elevated frequency of chromatid breaks in SCID cells (Chapter 2 Figure 2.5, Bryant *et al* 1998, van Buul *et al* 1998). The reason for this result is unknown but a possible cause is an elevated conversion of dsb into chromatid breaks and measuring dsb repair in SCID and CB17 cells will test this hypothesis, as shown in the following paragraphs. A linear induction of dsb has also been shown for other mammalian mutants, such as xrs5 cells (Iliakis *et al* 1992, Dahm-Daphi *et al* 1993). In the present study two methods were used (ROFE and CFGE). Neither method showed a difference in the total dsb induced in SCID and CB17 cells (e.g. Figure 5.2 and 5.3). CFGE was the method used for measuring repair of dsb. ROFE applies four electrodes placed at right angles to each other and by varying the pulse time and the on and off phases large molecular weight DNA, e.g. that of yeast chromosomes, could be separated according to size. One disadvantage with ROFE was the long time required for optimal separation, 3 days. Therefore, the method of choice was CFGE which applies a constant field for 26 hours and separates the fragmented DNA into a compression band just below the well.

AraC was used to block actively growing cells at the G1/S border. Once araC was removed from the cells they resumed cycling, such that 8 h after removal of araC 65-75% SCID and CB17 cells were in G2. The synchronisation of cells in G2 has always been a problem as it cannot be easily achieved using chemicals. Many chemicals are available to block cells in S phase and mitosis but there are none available to specifically block cells in G2. In this study timed experiments were used and even then a population with 90% of G2 cells was

difficult to achieve because a proportion of the cells had progressed to mitosis. Therefore, cell populations with 65-75% of cells in G2 were used to investigate the induction and repair of dsb. Another method, centrifugal elutriation, has been used to synchronise cells in different cell cycle phases and an advantage with this method is no drugs are required to synchronise the cells. This method separates the cells by size and populations of cells with >70% in G2 have been obtained (L.Thompson personal comm.).

The induction of dsb in G2/M SCID and CB17 cells as measured by ROFE shows no differences. However, at the chromosomal level the frequency of chromatid breaks was 1.3-1.7 fold elevated in SCID cells (Chapter 2), even though the frequency of induced dsb was the same for both lines. The rejoining kinetics of dsb in G2 SCID cells after 30Gy (Figure 5.5) were different from those for CB17. The rejoining kinetics were complex, indicating the possibility of more than one component. The dsb rejoining kinetics appear to reflect the disappearance with time of chromatid breaks (Figure 2.6), albeit at a very much lower dose (0.24Gy). Furthermore, CB17 cells do not appear to rejoin dsb after 2 h. Even though the rejoining rate appears faster in SCID cells between 2-3h there remains a 2-3 fold higher frequency of dsb. SCID cells appear to have a continual slow rejoining rate between 2-3 h and it may be speculated that further incubation would have seen the convergence of the two lines. In agreement with this, Nevaldine *et al* (1997) showed that SCID cells have a reduced repair rate, however 24 hours after treatment the DNA damage had been repaired equally in mutant and wildtype lines.

In contrast, to the results mentioned above (Figure 5.5) the repair kinetics for SCID and CB17 cells treated with araA prior to IR (Figure 5.6 and 5.7) show a lack of correlation between dsb rejoining and chromatid break frequency. In this study dsb rejoining in SCID and CB17 cells was not significantly altered in the presence of araA, whereas araA strongly potentiated chromatid break frequency (Figure 3.3).

The results presented here disagree with published reports for Ehlrich ascites tumour cells showing that araA inhibited dsb repair (reviewed by Bryant and Iliakis 1984). These differences are likely explained either by the different methods of measurement or the use of different cell lines. Previously, neutral filter elution (Iliakis and Okayasu 1990) and alkaline unwinding assays (Bryant and Iliakis 1984) were used and these methods cannot be directly correlated to CFGE. CFGE maintains the structural integrity of DNA by forming a homogenous gel but after neutral filter elution and alkaline unwinding assays the integrity of the DNA is unknown (Kinashi *et al* 1995). In addition, the damage being measured by the latter assays may not be specifically dsb. Furthermore, the present study measured the effects of araA on dsb repair at short time intervals after treatment, whereas previous studies measured dsb repair 2 h after treatment (Iliakis and Bryant 1984). Short time intervals after IR were used in this study so that they could be related to the G2 assay results and aid in the understanding of the initial effects araA had on dsb rejoining. In conclusion, the present study shows that at 100μM araA had no effect on dsb induction or repair following 30Gy IR in SCID and CB17 cells.

A linear and similar induction of dsb were observed in exponential $50D^-$ and $100E^+$ cells. Further experiments are required to measure repair in these cell lines.

Chapter Six

Chromatin structural differences between SCID and CB17 cells

6.1: Introduction

Chapter 6

6.1: Introduction

The aim of the work described in this chapter was to determine possible differences between chromatin structure in SCID and CB17 cells. Radiosensitivity is thought to be influenced by chromatin structure (e.g. Malyapa *et al* 1994, Roti Roti *et al* 1987). Thus, chromatin structure may be a factor leading to the increased radiosensitivity in SCID cells. Differences in the chromatin structure between SCID and CB17 cells was investigated by the fluorescent nucleoid assay and by measuring the length of metaphase chromosome one *in vivo* from bone marrow cells and fibroblast cells *in vitro*. In addition, to these experiments the levels of mitosis promoting factor (MPF) were measured to determine whether differences exist in the amount of MPF, and consequently in the potential rate of chromatin condensation in mitotic cells, which may play a role in the radiosensitivity of SCID cells.

The structure of chromatin has previously been discussed in Chapter 5 (Introduction section 5.1.2) and in this chapter the higher order structures of chromatin, especially the looped domains are discussed. When attempting to study chromatin differences the higher order structure of chromatin is important, as it may affect the accessibility of DNA to IR induced damage and repair enzymes.

6.1.1: Eukaryotic chromatin structure

Supercoiled human DNA was first identified by Cook and Brazell (1975) in interphase Hela cells treated with high salt concentrations to remove the chromatin associated proteins. The removal of histones H2A and H2B from Hela cells by treatment with low salt concentrations did not affect the supercoils in DNA and at high salt concentrations (0.92-0.95M NaCl) negatively supercoiled DNA was more apparent with histones 3 and 4

attached. The stable attachment of histones 3 and 4 to the base of DNA loops suggested that they were involved in the formation of supercoiled loops.

6.1.2: Attachment of "Looped" chromatin domains

The "looped" domains are constrained to a structural nuclear matrix in interphase cells and a scaffold matrix in mitotic cells. The DNA segments located at the base of each looped domain are known as, matrix attachment regions (MAR) in interphase cells and scaffold attachment regions (SAR) in mitotic cells (Mirkorvirtch *et al* 1987, Yanagisawa *et al* 1996). The looped domains are 80-90 Kbp in size in Hela cells and are stably attached by 1 Kbp of DNA that is protected from nuclease attack (Jackson *et al* 1990b). SAR sites were also stable after treatment with 2M salt and it has been proposed that 1% of total DNA is attached to the nuclear matrix.

Hela cells treated with micrococcal nuclease before removing the histones enabled isolation of the protein scaffold and electron microscopic analysis revealed that DNA was attached to the scaffold transversely, forming loops that originate from adjacent points on the scaffold. The scaffold retains the general shape and size of the intact chromosomes and exhibits a loose fibrous structure, comprising non histone proteins (Adolph *et al* 1977). The use of the term scaffold can be misleading, because it portrays the presence of a rod like structure which forms in the centre of each chromatid, which is in fact not the case, because the central scaffold consists of an aggregation of discrete anchoring complexes for the loops of the fibre (Earnshaw 1988).

6.1.3: Giant loops

The next level of organisation is the formation of giant loops 2-4 Mbp in size that are flexible, randomly formed throughout the DNA and are not attached to the structural scaffold (these structures are not shown in Figure 5.1; Sachs *et al* 1995, Yokota *et al* 1995). These loops are formed by intrastrand protein connections linking sites that are several Mbp apart and in mitotic chromatin further condensation of these loops is achieved by protein-protein and protein-DNA interactions along the central scaffold. The giant loops are formed at or near the same DNA sequences in different regions and these "loop attachment points" are randomly located enabling chromatin interaction between neighbouring loops.

6.1.4: DNA accessibility, dsb induction and repair

Transcriptionally active DNA is not as highly condensed as transcriptionally inactive DNA and it has been shown that active chromatin has a greater yield and rate of repair of IR induced base lesions than total DNA (Patil *et al* 1985). Recently, Fluorescent In Situ Hybridisation (FISII) analysis of nucleoid preparations revealed that most active genes remain highly associated with the nuclear matrix, whereas inactive genes remain in the loops (Gerdes *et al* 1994). Therefore, DNA accessibility may be important when investigating dsb break induction and repair (Chiu and Olenick 1982).

Packaging and accessibility of DNA in chromatin loops may be factors which contribute to the radiosensitivity and repair capacity of mammalian cells, as the extent of radiation damage and the sites are influenced by chromatin structure. Therefore, the supercoiling of DNA may be relevant when investigating radiosensitivity.

6.1.5: Methods used to investigate supercoiling in DNA

Supercoiling of DNA in mammalian cells can be studied by treating cells with non-ionic detergents and high salt concentrations to produce structures which resemble the nucleus minus the protein, known as nucleoids (Cook and Brazell 1976a). Nucleoids maintain the superhelical conformations of DNA enabling analysis of these conformations in radiosensitive cells. High molecular weight DNA is easily sheared whereas superhelical DNA packaged into nucleoids may be pipetted without the loss of supercoils due to the highly compact structure, illustrating the usefulness of nucleoids for studying higher order chromatin structures (Cook and Brazell 1976a). It has been shown that DNA associated with histones *in vivo* is underwound in comparison with the DNA in nucleoids and may explain the increased shearing effects of mammalian DNA *in vivo*.

Intercalating dyes, such as ethidium bromide (EB), propidium iodide (PI) and aminoacridines, bind to DNA and effect the negative supercoils. EB is thought to intercalate between the bp of DNA changing the rotational angle between the base pairs whilst unwinding the right handed Watson-Crick helix (Hinton and Bode 1975). One EB molecule intercalated into the DNA duplex is thought to unwind the helix by 26-28°. Nucleoids containing intercalated EB have a "halo" appearance and the increase and decrease in the size of the halo can be used to measure the relative number of supercoils in mammalian cells.

Hela cells treated with high salt concentrations and increasing EB concentrations showed significant changes in the shape and supercoiling of Hela nucleoids (Figure 6.1). The addition of increasing concentrations of EB caused a continuous but reversible reduction of DNA winding, as measured by sucrose gradient sedimentation. At low EB concentrations the halo increased in size due to the unwinding of the supercoils, reflected by a reduction

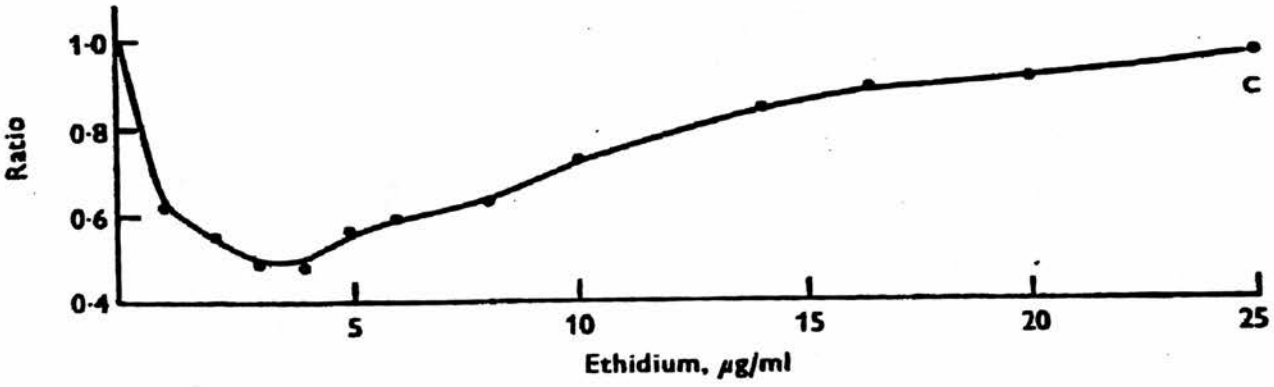

Figure 6.1: The graph shows the effect of ethidium bromide on Hela nucleoids treated with 1.95M NaCl. The ratio is the distance sedimented by Hela nuceloids expressed as a ratio relative to that of nucleoids sedimenting in a reference tube (Taken from Cook, Brazell and Jost 1976).

in nucleoid sedimentation rate (Figure 6.1). The minimum nucleoid sedimentation value reflected the point at which the supercoils were removed which was the same for linear, circular and nicked DNA (Hinton and Bode 1975). However, after this point as the EB concentration increased the supercoiling orientation reverted to the opposite conformation, positively supercoiled DNA, and was reflected by an increase in nucleoid sedimentation rate due to an increased condensation of the nucleoid and a reduction in halo size (Figure 6.1). The minimum nucleoid sedimentation value (Figure 6.1) suggested the relative superhelical density of the cells.

The higher the concentration of EB required to remove the supercoils the greater the degree of supercoiling in the nucleoids. Hela cells treated with 1.0 and 1.95M NaCl had the same minimum nucleoid sedimentation values indicating the same degree of supercoiling regardless of the NaCl concentration (Cook and Brazell 1976a). Protein analysis has shown that some histones are still present at 1.0M NaCl but treatment with 1.95M NaCl removed all histones (Cook and Brazell 1976a). The nucleoid sedimentation profile of DNA also followed similar curves in chicken fibroblasts, and epithelial cells from *Xenopus* and *Drosophila* in response to increasing concentrations of EB (Cook and Brazell 1976b). The biphasic nucleoid sedimentation curves exhibited in response to intercalating dyes was abolished when DNA was treated with nicking agents because in nicked DNA there were topological restrictions preventing the free rotation of one strand of the duplex about the other, hence the absence of rewinding nucleoid DNA to positive supercoils (Hinton and Bode 1975b).

Exposure of Hela nucleoids to radiation causes an expansion of the nucleoid halo and the increase in halo size is related to IR dose. IR causes breakage of the phosphodiester bonds in the backbone of the duplex, removing the superhelical turns, so that the nucleoid sedimentation values were similar to DNA without supercoils (Hinton and Bode 1975,

Cook and Brazell 1975). It has been shown that 10^4 single-strand breaks were required to remove all the supercoils from Hela cells (Cook and Brazell 1975).

6.1.6: Supercoiling in radiosensitive mammalian cells

The degree of supercoiling in DNA may be relevant when investigating the radiosensitivities of mammalian cells. A reduced degree of supercoiling may open more DNA sites to IR-induced damage or it may affect the accessibility of DNA to repair enzymes. Several studies have investigated the extent of supercoiling in radiosensitive cells, using the fluorescent nucleoid assay and these studies have generally shown an increased inhibition of DNA loops rewinding to the positive conformation after IR exposure in radiosensitive cells in comparison with radioresistant cells. Evidence for this has been shown with radiosensitive LY5178-S (LY-S) cells which exhibited a greater inhibition of DNA loop rewinding than LY5178-R (LY-R) cells after IR exposure, as measured by nucleoid sedimentation (Kapiszewska *et al* 1989). The greater inhibition of DNA loop rewinding in LY-S cells has been attributed to the greater loss of topological constraint on the DNA loops of LY-S cells, as the induction of DNA dsb was the same initially. Similarly, Hela cells exposed to IR were unable to rewind DNA loops and a 55-60 Kda protein was absent in irradiated Hela cells. This protein was thought to be involved with the supercoiling of DNA however, further protein analysis is required to determine it's exact function.

AT immortalised diploid fibroblasts proficient in dsb repair showing an increased frequency of chromatid breaks after IR in comparison to normal cells have shown an increased amount of DNA loop unwinding compared with normal fibroblasts. The increased DNA loop unwinding in AT cells has been explained by an instability of the nuclear matrix attachment protein in AT fibroblasts exposed to IR (Taylor *et al* 1991).

Irradiated chinese hamster mutant XR-1 cells, deficient in dsb repair involving the DNA-PK pathway (also defective in SCID cells), have shown a dose dependent reduction in loop rewinding of nucleoids to the positive conformation when treated with EB relative to irradiated CHO wildtype cells. Protein analysis revealed that 13 proteins were absent in XR-1 cells compared to wildtype cells, whereas XR122 cells containing human chromosome 5, to complement the radiosensitivity defect of XR-1 cells, contained 5 of the 13 proteins missing from XR-1 cells, suggesting that these proteins may be involved in the supercoiling of DNA in XR-1 cells (Malyapa *et al* 1994). The reduced rewinding of radiosensitive XR-1 cells may be due to altered DNA-matrix anchor points, so that supercoils near to the DNA damaged site are unable to rewind the DNA loops. Alternatively, the DNA-matrix anchor points in radioresistant cells may change the DNA supercoiling conformation, so that damaged DNA is isolated from neighbouring loops, enabling the remaining DNA loops to rewind.

More recently, supercoiling differences in radioresistant cells has been measured by the differences in the light scatter of nucleoids and may be used as a predictive assay, producing results within 24 hours and eliminating the difficulties of culturing cells (Schwartz *et al* 1995). A flow cytometer was used to measure nucleoid size by the scattering of a focused laser beam. The mean forward angle scatter can be related to size alterations in DNA configurations in response to IR induced damage. The fluorescence profile observed for xrs5 nucleoids was much broader and less resolved than CHO nucleoids and at high EB concentrations CHO cells had a significantly smaller nucleoid size than xrs5 cells suggesting a constraint on the positive supercoiling in xrs5 cells. However, treatment with IR did not produce any significant differences in nucleoid supercoiling between CHO and xrs5 cells (Schwartz *et al* 1995). In CHO and xrs5 cells there may be a difference in the organisation of the supercoiled loops of DNA attached to the nuclear matrix or a difference in the nature of the proteins that attach DNA to the

matrix. However, the relevance of these suggestions to the radiosensitivity of xrs5 cells remains to be elucidated.

Wilks *et al* (1996) used FACScan analysis to investigate the supercoiling differences between several carcinoma cell lines, CHO and xrs6 cells. This study showed no significant differences between the radiosensitive and radioresistant carcinoma cell lines. However, a significant difference in nucleoid size between CHO and xrs6 cells was present with increasing IR doses that may indicate a difference in chromatin structure.

6.1.7: Chromatin structure of radiosensitive xrs5 cells

Another index of chromatin configuration is chromosome length. A comparison of lengths of metaphase chromosomes in radioresistant and radiosensitive cells has been made. xrs5 cells appeared more condensed than CHO cells and measurement of the lengths of chromosomes in xrs5 and CHO cells revealed a 2 fold difference in the length:width ratios (xrs5 cells, 2.9 and CHO cells, 6.2) which was more apparent in the absence of colcemid (xrs5, 3.5 and CHO, 9.6; Schwartz *et al* 1993, 1995). The over-condensed morphology of xrs5 chromosomes has been suggested to be the result of an overphosphorylation of those proteins involved in chromosome condensation. In addition, to the over-condensed appearance of xrs5 chromosomes, the inner and outer layers of the nuclear lamina were separated more in xrs5 cells than CHO cells, as shown by EM studies (Yasui *et al* 1991). Therefore, chromatin structure could be an important determinant in the translation of dsb into chromosome breaks. Also it has been suggested that depending on the cell cycle phase, as chromosome condensation or decondensation proceeds the chromosome structure may collapse at damaged sites yielding breaks and gaps (Pantelias 1986).

6.1.8: Cell cycle control and mitosis promoting factor

The cell cycle is controlled by cyclin dependent protein kinases and regulated by cyclins B, D and E (Goa and Zelenka 1997). Of particular interest is the sequence of events prior to mitosis that regulate the condensation of chromatin and produce mitotic chromosomes. Mitosis promoting factor (MPF) consists of the catalytic subunit $p34^{cdc2}$ and the regulatory protein cyclin B. MPF is necessary for the onset of mitosis and microinjection of $p34^{cdc2}$ into mammalian cells has been shown to induce chromatin condensation along with other the events associated with the early phases of mitosis (Riabowol *et al* 1989, Lohmann *et al* 1995). $p34^{cdc2}$ has been shown to play a central role in the protein phosphorylation cascade resulting in nuclear envelope disassembly, chromosomal condensation and construction of the mitotic spindle (Dunphy *et al* 1988). $p34^{cdc2}$ is the catalytic subunit of a serine threonine protein kinase complex that induces cyclin B as a regulatory subunit and whose kinase activity has been shown to vary as a function of cell cycle phase (Freeman and Donoghue 1991). MPF begins to rise in late S phase from very low levels to high levels at mitosis. Protein cyclin B is transcribed and translated at the beginning of late S phase and binds immediately to $p34^{cdc2}$ in the cytoplasm. The binding of $p34^{cdc2}$ to cyclin B targets the kinase to phosphorylate the tyrosine 15 and threonine 14 residues forming pre-MPF during G2 (Dunphy *et al* 1994). At the transition from G2 to mitosis the complex is activated and converted to MPF by the dephosphorylation of Thy 15 and Thr 14. Dephosphorylation is mediated through the phosphorylating tyrosine phosphatase cdc^{25}. cdc^{25} is activated by the serine/threonine phosphorylation of MPF probably by an autocatalytic feedback loop (Hoffman *et al* 1993). At the end of mitosis cyclin B is destroyed by the ubiquitin-mediated proteolytic pathway (Draetta *et al* 1989). Many studies have shown that the G2 delay in mammalian cells in response to IR is related to MPF levels (Lock and Ross 1990, Kharbada *et al* 1994, Barth *et al* 1996).

MPF activity may be involved in the transformation of radiation-induced DNA damage to chromosome breaks because a higher MPF activity has been associated with a rapid condensation of interphase chromatin and as a result an increase in PCC fragmentation for a given radiation dose (Cheng *et al* 1993). Therefore, the level and control of cell cycle MPF activity may influence the radiosensitivity of cells to killing and chromosome damage.

In the present study, the superhelical conformation in SCID and CB17 nucleoids were investigated in response to increasing concentrations of EB and NaCl to determine superhelical differences between the two cell lines. During the scoring of metaphase chromosomes in SCID and CB17 samples, it was noticed that SCID cells had a more condensed appearance of chromatids than CB17 chromatids, similar to that observed in xrs5 chromosomes. Therefore, the length of chromosome one in SCID and CB17 cells was measured from both *in vitro* and *in vivo* sources. Also the levels of MPF in SCID and CB17 cells were measured.

6.2: Materials and Methods

For cell culture, irradiation and chromosome preparation details see Chapter 2 section 2.2.

6.2.1: Fluorescent nucleoid assay

a) Cell preparation

CB17 and SCID fibroblast cell cultures were seeded at $2x10^6$ per flask overnight at 37°C. The following day the cells were trypsinised, resuspended in medium and centrifuged at 1200 rpm for 10 min. The cell pellets were resuspended at $1x10^6$ cells/ml in HBSS and the samples were kept on ice and taken to the FACScan (Becton Dickinson).

b) Preparation of cell samples for analysis

To each FACScan tube 1 ml of lysis solution (appendix 3), 100µl of cell suspension and the appropriate volume of EB (final concentrations between 5-50µg/ml) were added. The sample was mixed by gently pipetting prior to analysis. The cell cycle distribution of 5,000 cells in each sample was recorded and a mean forward scatter value calculated, reflecting the increase and decrease in nucleoid size in response to EB and NaCl. Lysis solutions containing various concentrations of salt were used ranging from 0.1M to 1M NaCl and varying concentrations of EB were used.

6.2.2: Fluorescent In Situ Hybridisation (FISH)

The length of chromosome one was measured in SCID and CB17 cells using FISH. Previously, whilst scoring chromatid breaks there appeared to be a difference in the size of the chromosomes from SCID and CB17 cells, suggesting a difference in chromatin structure between the two cell lines.

a) Preparation of metaphase chromosome slides

Metaphase preparations were made as described before (Chapter 2 section 2.2.6) for CB17 and SCID cells *in vitro* and bone marrow samples of metaphase chromosomes from SCID and CB17 mice *in vivo* were provided by Dr. Paul van Buul. The SCID mice were derived from CB17 mice having the spontaneous mutation present that gave rise to SCID. After preparation the slides were stored in the freezer until required. Prior to FISH detection the slides were heated to 54°C for 24 hours.

b) Hybridisation of probe to metaphase samples

The probe for mouse chromosome one was obtained from Cambio, Cambridge, UK and it was denatured at 65°C for 10 min and then incubated at 37°C for 60 min. Slides were dehydrated in an ethanol series, air dried and denatured at 65°C for 2 min (appendix 3) and immediately afterwards quenched in ice cold ethanol and dried. 15µl of the probe for chromosome one were placed onto the slides, covered with a coverslip and sealed. The slides were placed in a sealed humidified container overnight at 37°C.

c) Detection and measurement of chromosome one

The following day the coverslips were removed from the slides and the slides were washed twice in 50% formamide in 2xSSC for 5 min and once in 2xSSC for 10 min at 37°C. The slides were quickly rinsed in buffer (appendix 3) and overlaid with 100µl of blocking agent (non fat dried milk) and incubated at ambient temperature for 30 min. Afterwards the slides were washed three times in buffer (appendix 3) for 5 min, the undersides of the slides were dried and overlaid with 100µl of FITC-avidin (appendix 3), covered with parafilm and incubated in the dark for 30 min. Three 5 min washes in buffer were repeated,

the undersides of the slides were again dried and 100µl of B anti-avidin FITC were placed on each slide and incubated for a further 30 min. Three 5 min washes were repeated and the slides overlaid with 100µl of avidin-FITC and incubated for a further 30 min. The slides were washed as before, then in PBS and finally dehydrated in an ethanol series. Slides were stained with DAPI (4',6-di-amiodino-2-phenylindole) in antifadant solution (Vectashield; Vector laboratories).

d) Image analysis and scoring

Colour images were collected using a computer-controlled epifluorescence microscope equipped with a cooled charge-coupled device (CCD) camera (Photometrics) and Smart Capture software developed by Digital Scientific, Cambridge. Banding was obtained digitally. DAPI images (i.e. Q-banding patterns) were converted into monochrome images followed by changing the contrast. This procedure generates simultaneous G- and C-bands. G-bands were converted Q-bands and C-bands were generated by a hybridisation procedure (denaturing of chromosomes by a combination of heat and formamide). The images were transferred to Iplab which had an arbitrary scale enabling the measurement of chromosome one. Images were transferred to Adobe photoshop and printed on a Kodak colour laser printer.

6.2.3: Mitosis promoting factor assay

The MPF assay measures the phosphorylation of a single threonine residue on a $p34^{cdc2}$ kinase substrate peptide. The basic amino acid sequence of the peptide promotes attachment to phosphocellulose disks, so the phosphorylation of the peptide with radioactive ^{32}pATP can be measured.

a) Mitotic cell collection

Exponentially growing fibroblast cell cultures of SCID and CB17 cells were trypsinised and seeded at $2x10^7$ cells per roller bottle in Waymouth's medium containing hepes buffer (2%). Cells were incubated overnight at a speed of 2.5rpm at 37°C. The next day fresh medium was added and the cells were incubated for a further 24 hours. The following day the medium was replaced with medium containing Nocodazole (0.04µg/ml). Every hour the mitotic cells were collected by spinning the bottles at a high speed to collect the mitotic cells. The mitotic cell samples collected were counted and kept frozen until required (see appendix 3 for freezing media). Mitotic cell samples were used to measure MPF activity because the samples had been prepared and time did not permit the measurement of MPF in G2 cells.

b) Preparation of cells for Mitotic Promoting Factor (MPF) assay

Frozen mitotic cells were thawed, resuspended in hepes and centrifuged at 2000 rpm for 10 min. The supernatant was discarded and the cell pellet resuspended in lysis solution (appendix 3) and incubated on ice for 30 minutes with occasional agitation. Afterwards the samples were centrifuged at 13,000 for 45 min at 0°C. The supernatant was transferred to a small eppendorf tube and kept. A 30µl reaction volume was mixed (appendix 3) and incubated at 30°C for 20 min. The reaction was stopped by adding 20% TCA and storing on ice for 15 min, after which the samples were centrifuged at 6500 rpm for 15 min at 4°C. 10µl of each supernatant was spotted onto separate phosphocellulose disks. The disks were washed three times in 100mM phosphoric acid for 10 min and then in acetone for 10 min. The filters were placed in filter count to determine the amount of radioactive ATP incorporated onto each phosphocellulose disk. The experiment was carried out in triplicate and repeated twice.

c) Protein assay

A normal standard curve of varying BSA protein concentrations was made and used to determine the protein concentrations in the sample cell lysates. To 800µl of each cell lysate 200µl of the dye reagent (Bio-Rad, Lab. UK) were added. The solutions were mixed and incubated at room temperature for 30 min. The absorbance was measured at 595nm, using a spectrophotometer (Philips, PU 8620, UV/VIS/NIR).

6.3: Results

6.3.1: Response of SCID and CB17 nucleoids to ethidium bromide

Nucleoids were prepared from SCID and CB17 cells treated with 1M NaCl in lysis solution and changes in nucleoid size, as measured by the mean forward light scatter of 5,000 cells, in response to increasing concentrations of EB are shown in Figure 6.2 and Table 6.1. This was a single experiment because of time limitations. As the EB concentration increased the response of SCID and CB17 nucleoids differed markedly. Initially SCID cells showed an increase in nucleoid size due to a relaxation of the negative supercoils as EB was intercalated into the DNA duplex (Figure 6.2). However, as the concentration increased further the size of SCID nucleoids remained constant and EB concentrations greater than 15.0 μg/ml caused a sharp decrease in the size of SCID nucleoids, which may indicate a reversion to positive supercoiling. The supercoiling response of CB17 cells to increasing EB concentrations was unexpected as the intercalation of EB usually causes an unwinding of the negative supercoils followed by a rewinding to positive supercoils (Cook and Brazell 1975). However, the results in Figure 6.2 for CB17 cells suggest that initially there was a rewinding of the supercoils to the positive conformation followed by an immediate unwinding when EB concentration increased from 0.5 to 1.0μg/ml.

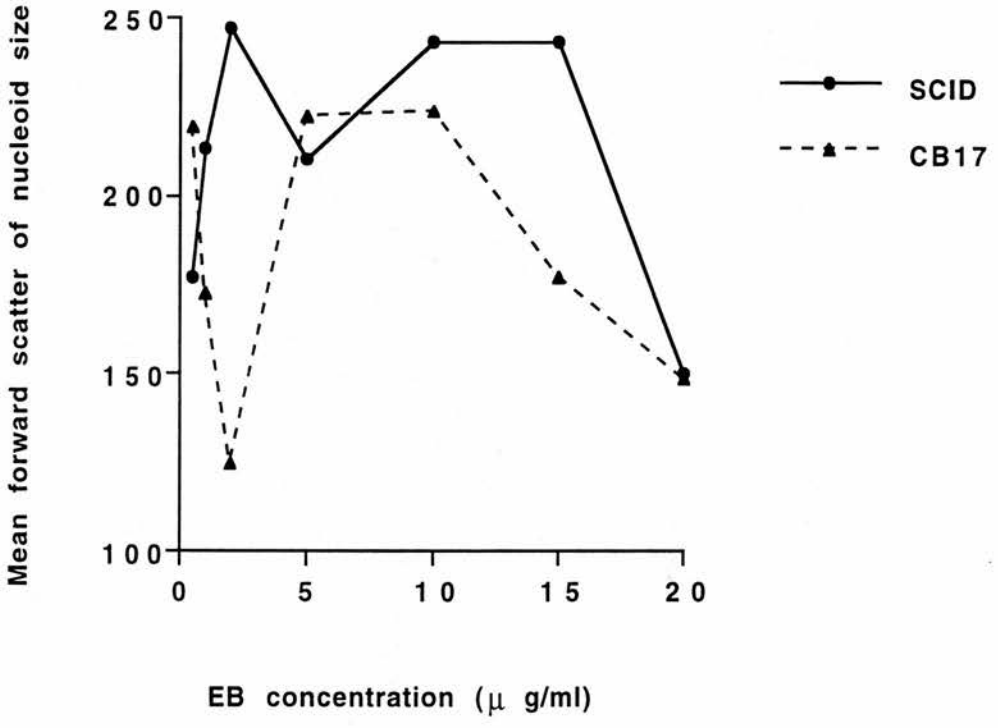

Figure 6.2: The supercoiling response of SCID and CB17 nucleoids treated with 1M NaCl and increasing concentrations of ethidium bromide. Results of a single experiment.

Table 6.1: Effect of increasing ethidium bromide concentrations on SCID and CB17 nucleoids.

Cell line	Treatment	Mean forward scatter*
SCID	0.5µg/ml ethidium bromide	177
CB17	0.5µg/ml ethidium bromide	219
SCID	1.0µg/ml ethidium bromide	213
CB17	1.0µg/ml ethidium bromide	173
SCID	2.0µg/ml ethidium bromide	247
CB17	2.0µg/ml ethidium bromide	125
SCID	5.0µg/ml ethidium bromide	210
CB17	5.0µg/ml ethidium bromide	222
SCID	10.0µg/ml ethidium bromide	243
CB17	10.0µg/ml ethidium bromide	224
SCID	15.0µg/ml ethidium bromide	243
CB17	15.0µg/ml ethidium bromide	177
SCID	20.0µg/ml ethidium bromide	150
CB17	20.0µg/ml ethidium bromide	149

* Data from a single experiment.

6.3.2: Response of SCID and CB17 nucleoids to increasing salt concentrations

SCID and CB17 nucleoids were treated with 5μg/ml EB and increasing concentrations of NaCl to determine the supercoiling changes in response to varying salt concentrations (Figure 6.3 and Table 6.2). A low EB concentration was used to minimise the affect on negative supercoils in the nucleoids. As the NaCl concentration increased from 0-1.5M the "halo effect" size was reduced, suggesting a more condensed structure due to the removal of the histones. Concentrations greater than 1.5M NaCl showed no significant changes in nucleoid size for both cell lines. Between 0-1M NaCl the nucleoid size was larger for CB17 cells showing a more condensed chromatin structure for SCID nucleoids. At 1.5M NaCl the forward mean scatter was the same for SCID and CB17 nucleoids showing similar values for minimum nucleoid size and maximum condensation configurations. A similar profile was obtained when the nucleoids were treated with 50μg/ml of EB and increasing salt concentrations (Figure 6.4). The minimum nucleoid size for SCID and CB17 cells treated with 50μg/ml was obtained with 1M NaCl. This result was lower than nucleoids treated with 5μg/ml EB and is likely due to the higher EB concentration. Similar to the results in Figure 6.3 the initial size of CB17 nucleoids was larger than SCID nucleoids. The baseline level in figure 6.2 appears to differ significantly from figures 6.3 and 6.4, since the experiment in figure 6.2 wasn't repeated it is not possible to do any statistical analysis. However, the differences may be explained by interexperimental and intraexperimental variability which is a significant problem when using the facscan. The cells may have been in different phases of the cell cycle when the samples were taken and the lysis conditions may have variable between samples. The results shown in Figure 6.2 were preliminary results and this experiment needs to be more thorougly investigated before any definite conclusions can be made.

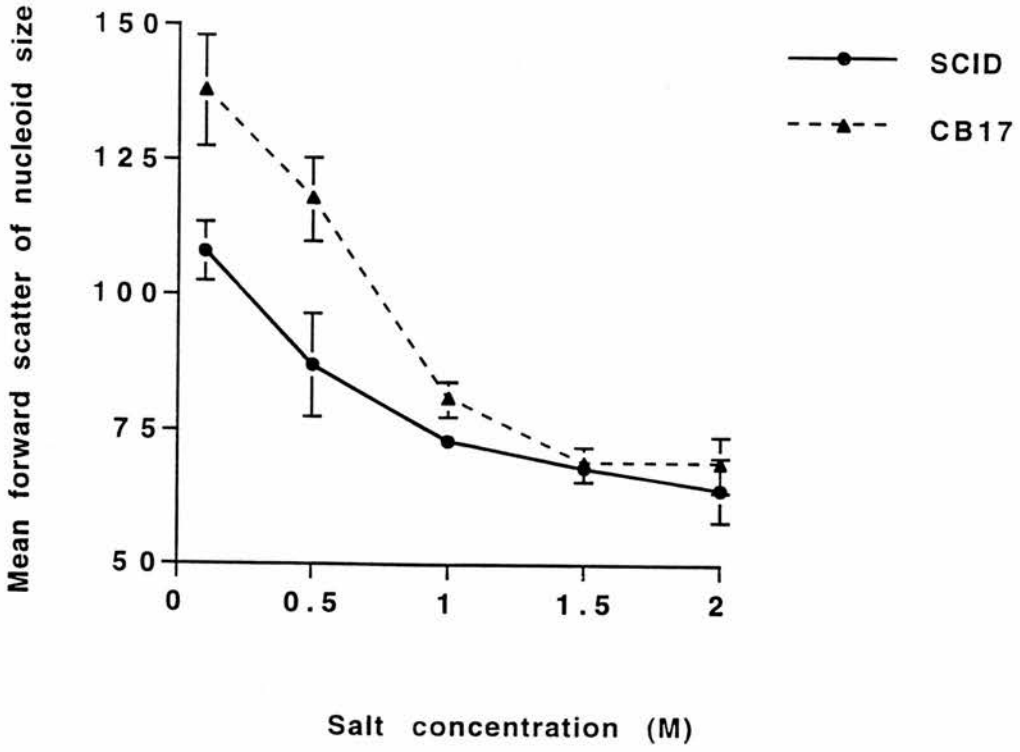

Figure 6.3: The response of SCID and CB17 nucleoids to increasing NaCl concentrations in the presence of 5 μg/ml ethidium bromide. The values plotted represent the means and standard errors from three independent experiments.

Table 6.2: Effect of increasing salt concentrations on SCID and CB17 nucleoids treated with 5μg/ml ethidium bromide.

Cell line	Treatment	Mean forward scatter*
SCID	0.1M NaCl	108 ± 5.5
CB17	0.1M NaCl	138 ± 10.3
SCID	0.5M NaCl	87 ± 9.5
CB17	0.5M NaCl	118 ± 7.7
SCID	1.0M NaCl	73 ± 0.6
CB17	1.0M NaCl	81 ± 3.4
SCID	1.5M NaCl	68 ± 1.5
CB17	1.5M NaCl	69 ± 3.3
SCID	2.0M NaCl	64 ± 6.0
CB17	2.0M NaCl	69 ± 5.1

*Data represent the mean and standard errors from two independent experiments.

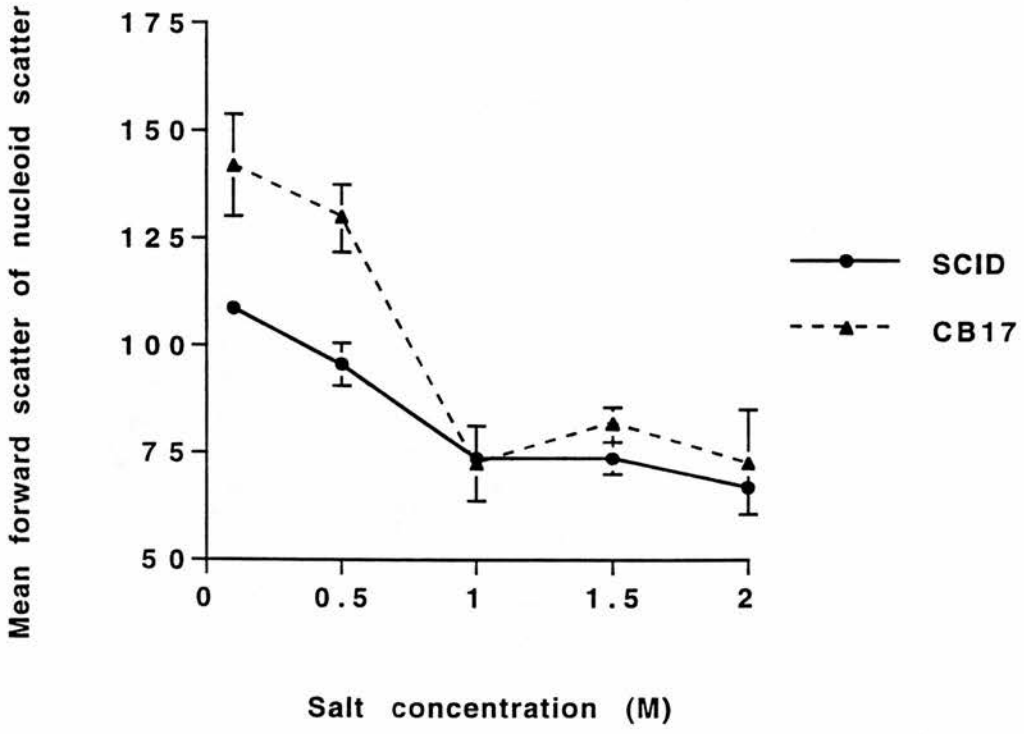

Figure 6.4: The response of SCID and CB17 nucleoids to increasing NaCl concentrations in the presence of 50 μg/ml ethidium bromide. The values plotted represent the means and standard errors from three independent experiments.

Table 6.3: Effect of increasing salt concentrations on SCID and CB17 nucleoids treated with 50μg/ml ethidium bromide.

Cell line	Treatment	Mean forward scatter*
SCID	0.1M NaCl	109 ± 1.7
CB17	0.1M NaCl	142 ± 12.0
SCID	0.5M NaCl	96 ± 4.8
CB17	0.5M NaCl	130 ± 8.0
SCID	1.0M NaCl	74 ± 2.1
CB17	1.0M NaCl	73 ± 8.8
SCID	1.5M NaCl	74 ± 3.5
CB17	1.5M NaCl	82 ± 4.2
SCID	2.0M NaCl	67 ± 2.4
CB17	2.0M NaCl	73 ± 12.3

*Data represent the mean and standard errors from two independent experiments.

6.3.3: Metaphase chromosome structure

The analysis of chromosomes from SCID and CB17 metaphase cells suggested a more condensed appearance for SCID chromosomes (Chapter 2). Therefore, it was decided to measure the length and width (both chromatids) of chromosome one in SCID and CB17 metaphase slides prepared from samples derived from *in vitro* and *in vivo* sources. Chromosome one was detected by using a probe specific for mouse chromosome one and labelling with FITC (Figure 6.5). Analysis was achieved using an image analysis system and the Iplab programme (e.g. FITC labelled chromosome one see Figure 6.5) had an arbitrary scale enabling the measurement of the length and width (both chromatids) of chromosome one, as shown in Table 6.4 a, b and c. The average length for chromosome one *in vitro* (established cell lines) was 27.93 $\pm$ 0.67 for SCID cells and 30.98 $\pm$ 0.49 for CB17 cells. SCID cells had a shorter chromosome length than CB17 cells which was statistically significantly different (t-test p=0.0004). Similarly, the length of chromosome one was measured in bone marrow cells extracted from SCID and CB17 mice to test whether the difference was apparent *in vivo* and not due to the established cell line in culture. The difference 17.55 $\pm$ 0.46 and 22.01 $\pm$ 0.82 for SCID and CB17 bone marrow cells respectively, *in vivo*, was also significantly different (t-test p=0.001). The average length of chromosome one from SCID and CB17 cells was much smaller *in vivo* than *in vitro* and there was also a statistical difference in the lengths of chromosome one for SCID and CB17 cells. The width of chromosome one was measured *in vitro* only (Table 6.4 b) because *in vivo* the chromatids were separated during spreading and accurate measurements could not be obtained. The widths of chromosome one were significantly different between SCID and CB17 cells *in vitro* (0.005) but the width:length ratios were not (Table 6.4 c).

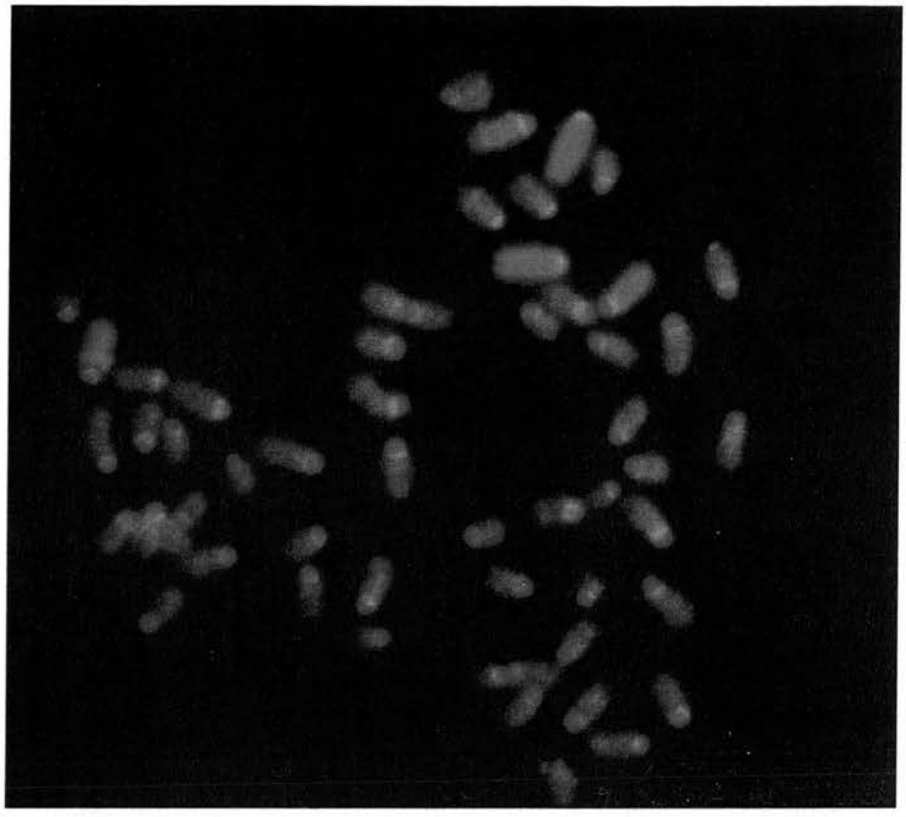

Figure 6.5: Murine SCID chromosomes above and CB17 chromosomes below hybridised with mouse chromosome one and stained with FITC. Chromosome one appears completely green.

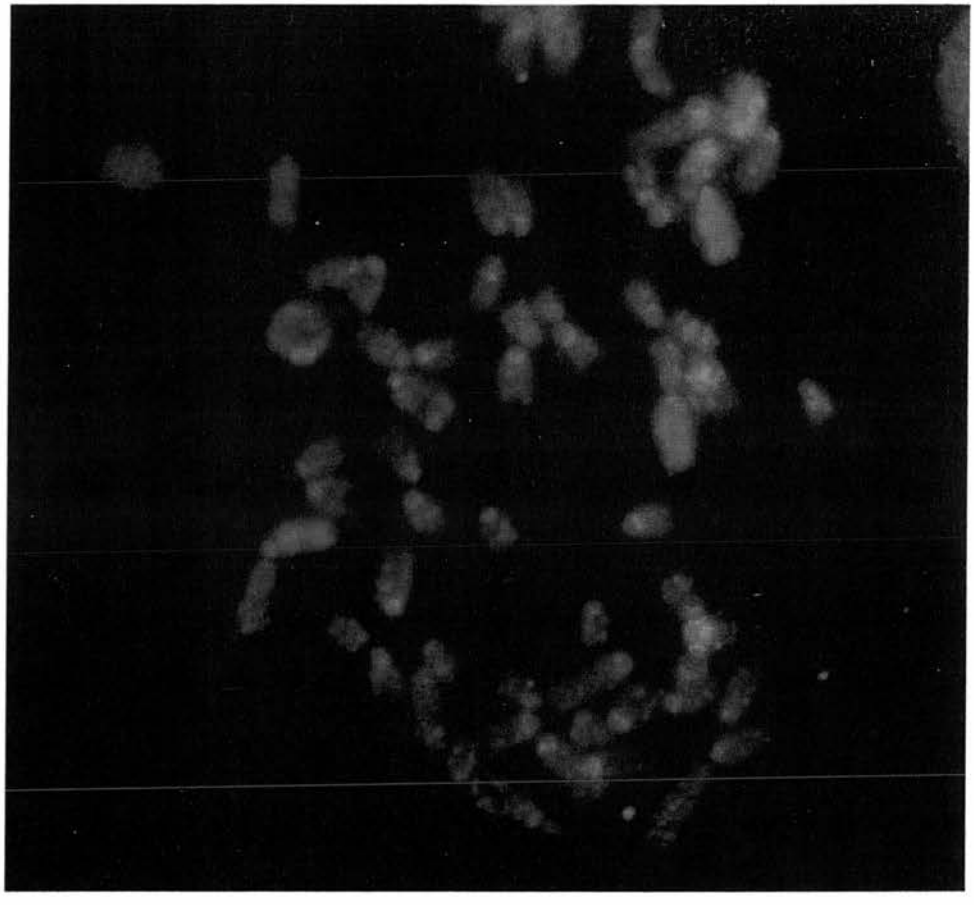

Table 6.4a: Length measurements of chromosome one from *in vitro* and *in vivo* preparations of SCID and CB17 cells.

Cell line	length*	T-test	P-value
SCID in vitro	27.91 ± 0.67	SCID +CB17 in vitro	0.0004
CB17 in vitro	30.98 ± 0.49		
SCID in vivo	17.55 ± 0.46	SCID + CB17 in vivo	0.001
CB17 in vivo	22.01 ± 0.82		

*Data represent the standard errors of the mean for the 50 metaphase cells scored.

Table 6.4b: Width measurements of chromosome one from *in vitro* preparations of SCID and CB17 cells.

Cell Line	width*	T-test	P-value
SCID in vitro	11.71 ± 0.27	SCID + CB17 in vitro	0.005
CB17 in vitro	12.50 ± 0.21		

*Data represent the standard errors of the mean for the 50 metaphase cells scored.

Table 6.4c: A comparison of the length/width ratios from *in vitro* preparations of SCID and CB17 cells.

Cell Line	width/ length ratio*	T-test	P-value
SCID in vitro	0.43 ± 0.020	SCID +CB17 in vitro	0.14
CB17 in vitro	0.41 ± 0.008		

*Data represent the standard errors of the mean for the 50 metaphase cells scored.

6.3.4: Measurement of MPF activity in SCID and CB17 cells

The phosphorylation of a $p34^{cdc2}$ kinase peptide by radiolabelled ATP was used to assay the MPF activity of mitotic cell lysates from SCID and CB17 cells. The average MPF activity from two experiments in SCID cells was 969.5 ± 131.2 and 465.5 ± 295.2 for CB17 cells, showing a difference of approximately 3-fold between the two cell lines (Table 6.5). In each experiment the samples were repeated three times (intra-experimental variability shown in Table 6.5) and the experiment was repeated twice. The first experiment showed a 1.3 fold increased MPF activity in SCID cells relative to CB17 cells and in the second experiment there was a 4.9 fold elevated MPF activity in SCID cells (Table 6.5). The MPF assay produced very variable results (an observation also made for Chinese hamster cells, Bryant personal comm.) and this may be explained by the use of different mitotic cell samples for each experiment.

Table 6.5: Levels of mitosis promoting factor (MPF) measured in mitotic SCID and CB17 cells by assaying the phosphorylation of a $p34^{cdc2}$ substrate peptide with 32pATP.

Cell line	32pATP dpm	Protein concentration in cell extracts	dpm per μg/ml protein
Experiment 1*			
SCID	12641.28 ± 535.4	11.25 μg/ml	1100.80
CB17	7102.50 ± 300.5	9.00 μg/ml	760.74
Control	256.75 ± 006.5		
Experiment 2*			
SCID	6943.96 ± 144.7	8.00 μg/ml	838.20
CB17	2746.34 ± 265.4	14.75 μg/ml	170.30
Control	238.36 ± 001.9		

Mean value of the two experiments dpm/μg/ml were 969.5±131.2 for SCID cells and 465.5±295.2 for CB17 cells.

* For each experiment there were three repeats of each sample. The errors represent the standard errors of the mean for the three repeats within an experiment (intra-experimental variability).

6.4 Discussion

6.4 Discussion

The supercoiling of mammalian DNA has been investigated previously, using intercalating dyes such as EB (Cook and Brazell 1975, Wilks *et al* 1996). In the present study the superhelical conformations of chromatin loops were investigated in SCID and CB17 cells treated with 1M NaCl and increasing EB concentrations (Figure 6.2). The response exhibited by SCID cells was similar to the biphasic response measured by nucleoid sedimentation and FACScan analysis for mammalian DNA (Cook and Brazell 1975, Wilks *et al* 1996). The initial increase in the size of the "SCID halo effect" reflected the relative superhelical density in SCID cells which reached a plateau and then sharply decreased due to the positive supercoiling of DNA. Unlike other mammalian DNA in which the negative supercoils are unwound followed by a flip over to a positive conformation, SCID cells demonstrated a constant nucleoid size without supercoils between 5-15 µg/ml EB. The reason for this conformation is unknown but it may be speculated that SCID cells require a higher concentration of EB to flip over to the positive conformation. The response of CB17 cells to increasing EB concentrations could not be explained according to previously published paradigms. Further experiments are required including detailed measurements of the response of SCID and CB17 nucleoids to EB. In addition, other factors such as cell growth phase, lysis buffer conditions, disaggregation conditions and temperature need to be studied to minimise experimental errors.

The treatment of nucleoids with increasing salt concentrations removes histones, revealing the negative supercoils (Cook and Brazell 1975). SCID and CB17 cells treated with increasing NaCl concentrations showed a decrease in nucleoid size, which is likely caused by the nucleoids becoming more condensed as histones H2A and H2B are removed, enabling histones H3 and H4 to induce more negative supercoils, thereby, decreasing the nucleoid size and explaining the more compact structure of chromatin in nucleoids

(Alberts *et al* 1989). At low salt concentrations there was a marked difference in nucleoid size for SCID and CB17 cells but removal of the histones at high salt concentrations produced nucleoids of similar size for both cell lines. This may be attributed to different superhelical structures in SCID and CB17 cells but removal of these structures show no difference between the naked DNA of SCID and CB17 nucleoids. During DNA repair chromatin structure is altered to allow the repair process to proceed. DNA-PK may maintain the chromatin in an "inactive" configuration during repair by controlling the phosphorylation of histone acetyltransferases and histone deacetylases (Featherstone and Jackson 1999). If this is true, it may explain the more compact structure of SCID cells because in the absence of DNA-PK histone stability may be altered resulting in a more compact structure.

The length of chromosome one was statistically smaller for SCID cells (Table 6.4) suggesting that SCID cells have a more condensed chromosome structure than CB17 cells. The condensed appearance of SCID chromosome one was investigated in bone marrow cells to confirm that this phenotype was present *in vivo* and was not an artefact of *in vitro* cell culture. A similar condensed appearance of chromosomes was present in radiosensitive xrs5 cells in comparison with control CHO cells and it was postulated that the condensed appearance was due to a hyper-phosphorylation of those proteins involved in chromosome condensation (Schwartz *et al* 1993). The hyper-phosphorylation of proteins involved in chromosome condensation may be the cause for SCID cells to have a more compact structure or there may be a chromatin structural difference between SCID cells and CB17 cells. However, the relationship of these differences to chromosomal radiosensitivity are as yet unclear.

The results from the MPF assay suggest a higher phosphorylation of $p34^{cdc2}$ in SCID cells. However, due to experimental variability within and between experiments, further

experiments are required to determine if SCID cells consistently show a higher phosphorylation of $p34^{cdc2}$ than CB17 cells. However, the higher MPF activity in SCID cells in these experiments may be responsible for the condensed appearance of SCID chromosomes but the relevance of this to the underlying radiosensitivity remains to be investigated. It has previously been proposed that MPF may be involved in radiosensitivity as CHO cells showed an increased frequency of PCC fragments due to increased MPF levels (Cheng *et al* 1993). The underlying mechanism for the increased frequency of chromatid breaks in SCID cells remains unknown. The variability between MPF assays with mitotic cell samples from the same cell line without concomitant variation in G2 chromatid break response suggests that the MPF level is not a critical determinant of chromatid break response.

In conclusion, the three experiments reported in this chapter have investigated chromatin structure and the MPF levels of mitotic cells in relation to radiosensitivity. Even though there were statistical differences between the lengths of chromosome one in SCID and CB17 cells it is unknown how relevant this is to the radiosensitivity of SCID cells. Previous studies have shown that xrs5 cells that had reverted back to the wildtype CHO phenotype had the same chromatin structure as mutant xrs5 cells but were not radiosensitive, suggesting that chromatin structure may not play a role in radiosensitivity (Schwartz *et al* 1995). The increased levels of MPF may explain the overcondensed appearance of SCID chromatids but further chromatin structural studies are required, such as isolating the proteins involved in determining chromatin structure in SCID and CB17 cells. 2-D gel electrophoresis may reveal differences in the proteins present in SCID cells compared with CB17 cells and these differences may relate to the radiosensitivity of SCID cells. Alternatively comparing the phosphorylation of factors thought to be involved in chromatin structure in both cell lines may reveal a reason for the observations in this study.

Chapter Seven

Detection of the ATM protein in mammalian cell extracts

7.1: Introduction

Chapter Seven

7.1: Introduction

The aim of the work described in this chapter was to determine the expression of the ATM protein in SCID cells, using western blotting, and to aid in the understanding of how SCID cells signal DNA damage in the absence of DNA-PK. A possible mechanism is the ATM protein takes over the function of DNA-PK in its absence. For this reason, the expression of the ATM protein was investigated in SCID cells before and after radiation exposure to confirm the presence of ATM protein and determine if the ATM protein levels were up-regulated in the absence of DNA-PK and in response to IR. Similarly, the levels of ATM protein expression were studied in CB17, $50D^-$, $100E^+$, irs2, V-79, CHO, xrs5 and xrs5 cells complemented with the human Ku80 gene.

7.1.1: DNA dependent protein kinase

DNA dependent protein kinase catalytic subunit (DNA-PK_{CS}) is a nuclear serine/threonine protein kinase that is only activated when bound to DNA (Anderson and Lees Miller 1992). DNA-PK_{CS} belongs to a group of proteins involved in non-homologous end joining (NHEJ) of dsb repair (Anderson 1993 and Jackson 1996). DNA-PK has many cellular targets including DNA binding and regulatory proteins, such as Jun, Fos and p53 (Jackson 1996, Jin *et al* 1997a). The possible functions of DNA-PK in dsb rejoining are: acting as a scaffold holding the DNA ends in place; inhibiting transcription so that is does not interfere with repair; or as a signalling protein recruiting other proteins to the damaged site, as shown diagrammatically in Figure 7.1 (Trolestra and Jaspers 1994, Gottlieb and Jackson 1994).

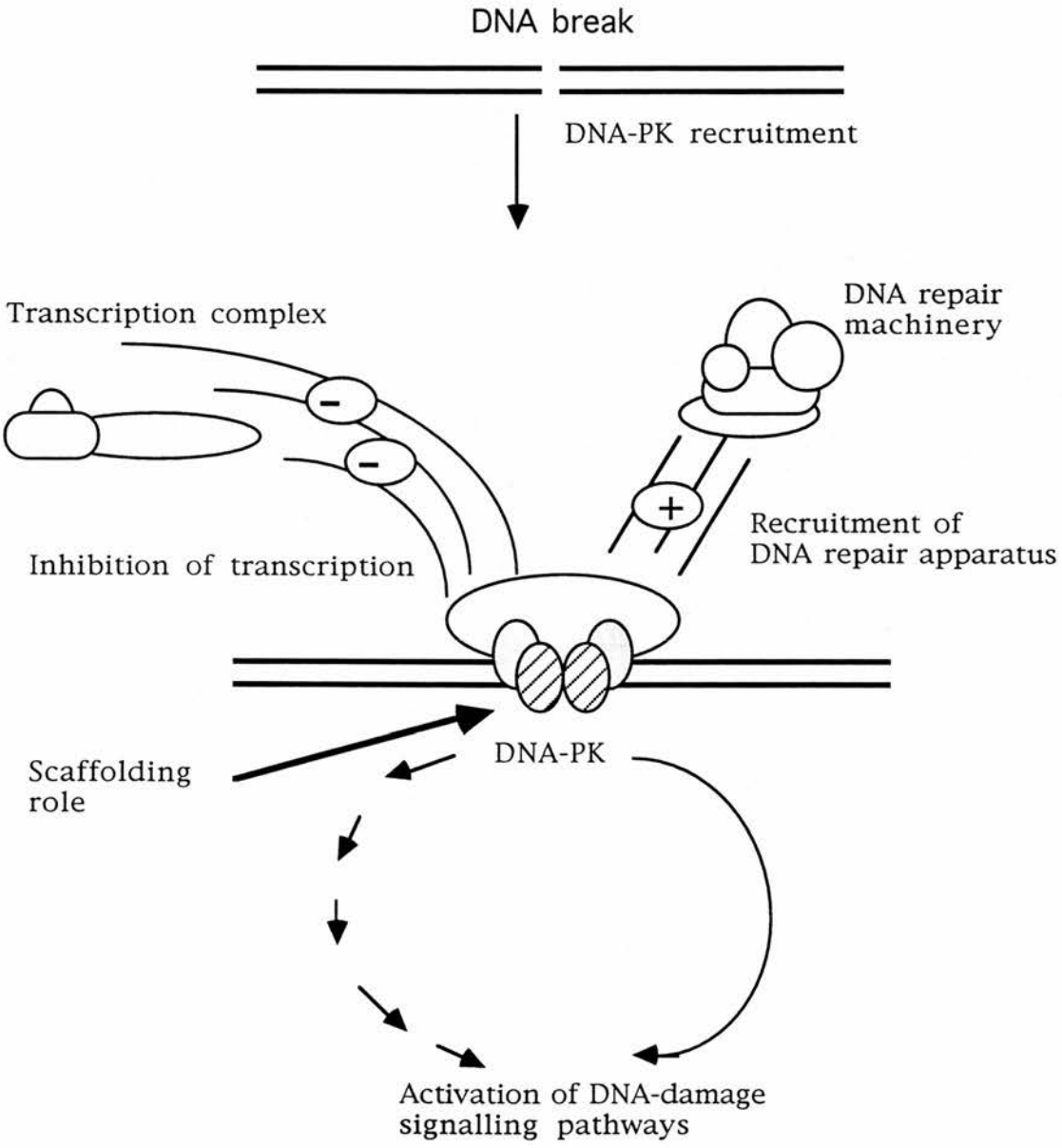

Figure 7.1: Model for DNA-PK functions (adapted from Gottlieb and Jackson 1994)

7.1.2: DNA-PK$_{CS}$ is a member of the PI3-K related kinases

Cloning of the *DNA-PK$_{CS}$* gene revealed an open reading frame which encodes for a 350 Kda protein (Araki *et al* 1997, Blunt *et al* 1996). The N-terminus of this protein has approximately 3500 amino acids that are not related to the other protein kinases in the PI-3K family. The N-terminus contains a leucine zipper motif thought to be the site for interaction with Ku (Jin *et al* 1997a). The C-terminus is of importance because it has 500 residues with sequence similarity to the catalytic domain of the phosphoinositol-3 kinase protein family (PI3-K, 110Kda, Keith and Schreiber 1995). The similarities between the sequences of *DNA-PK$_{CS}$* and PI-3K proteins form another subgroup of the PI-3 Kinase family known as PI-3K related kinases, of which DNA-PK$_{CS}$ is a member (Keith and Schreiber 1995, Poltorasky *et al* 1995). The PI-3K related kinases have different sequences surrounding the conserved catalytic residues of the ATP binding cleft and there are also differences in the amino and carboxy-terminal lobes but the distinct feature is the absence of lipid kinase activity. The PI-3 K related kinases have much larger molecular weights, above 250 Kda whereas, the PI-3K related proteins have a MW of 100Kda. In addition to DNA-PK$_{CS}$, the other members include TOR1, TOR2, FRAP, ATM, Tel1, Mei41, FRP and Mec1, all of these proteins have cellular functions involved with cell-cycle checkpoints, cell-cycle progression, DNA repair and DNA damage signalling pathways.

The ATM protein appears to be the most conserved sequence compared to other members of the PI3-K related kinases family. ATM, DNA-PK$_{CS}$, TOR1 and TOR2 are thought to be very similar in sequence specificity. DNA-PK$_{CS}$ has a single kinase domain located at the C-terminus which has 40% homology with other members. The kinase domain displays DNA-dependent protein kinase activity when combined with Ku and DNA-PK does not have lipid kinase activity (Poltorasky *et al* 1995). The C-terminus of DNA-PK$_{CS}$ has important implications in DNA repair because the murine SCID mutation has been

identified as a single point mutation in the C-terminus which results in the absence of the functional DNA-PK protein (Araki *et al* 1997, Blunt *et al* 1996). The equine SCID mutation causes a deletion of the PI-3K related domain and a more severe phenotype than murine SCID is observed. Murine SCID cells are only deficient in the formation of coding joints during V(D)J recombination, whereas the equine mutation causes no signal or coding joints to be formed in V(D)J recombination (Shin *et al* 1997). Therefore, the C-terminus of DNA-PK$_{CS}$ is important for DNA repair and V(D)J recombination pathways.

7.1.3: Similarities of DNA-PK$_{CS}$ protein and the ATM protein

The ATM protein is expressed ubiquitously and localised predominantly in the cell nucleus as is the DNA-PK protein (Lakin *et al* 1996). Similar to the DNA-PK holoenzyme, ATM protein binds to DNA and an associated protein kinase activity that is stimulated by DNA is triggered. p53 is a substrate for the ATM protein as is DNA-PK. The similarities of function and sequence of the ATM and DNA-PK proteins (Hartley *et al* 1995), suggests that in the absence of DNA-PK the ATM protein takes over its function, due to the similar biochemical pathways they appear to be involved in. A recent study, by Lakin *et al* (1996), investigated the expression levels of the ATM protein in xrs6 cells which are deficient in Ku80, a component of the DNA-PK holoenzyme, to determine whether in the absence of DNA-PK is there an up-regulation of the ATM protein. However, it was found that in the absence of the DNA-PK protein, in xrs6 cells, the ATM protein was not up-regulated.

Therefore, it was interesting to investigate whether the ATM protein was up-regulated in SCID cells as they are also defective for DNA-PK. Western blotting of total cell lysates extracted from SCID, CB17, 50D^{-}, 100E^{+}, CHO, xrs5, xrs5 complemented with the human Ku80 gene, V-79 and irs2 cells were used to determine the expression levels of the ATM protein before and after irradiation.

7.2: Materials and Methods

7.2.1: Preparation of cell lysate

Cells were seeded at $2x10^6$ per flask overnight at 37°C. The following day the cells were treated with 5 Gy of gamma radiation (^{137}Cs IBL437C γ-irradiator) at an ambient temperature and sampled immediately or left in culture for 2-3 hours. The medium was removed from the cell monolayer and the cells rinsed at room temperature with PBS. The following steps were carried out on ice. 1 ml of RIPA buffer (appendix 4) was added to the flask and the cells removed using a cell scraper. The cell suspension was transferred to a microfuge tube and the flask washed with another 1 ml of RIPA. The cell lysate was passed through a 21 gauge needle and 10 ml of 10μg/ml PMSF stock added and the samples held on ice for 30-60 min. Afterwards, the cell lysates were microfuged at 1000 rpm for 20 min at 4°C and the supernatant was kept, as it contained the total cell lysate, and stored at -70°C until required.

7.2.2: SDS polyacrylamide gel electrophoresis

Two 5% polyacrylamide gels (appendix 4) were poured into glass cassettes for use in a Protein II electrophoresis tank (Bio-Rad labs, UK). The separating gels (5%) were poured, overlaid with butanol and allowed to polymerase for 40 min. The butanol was poured off and rinsed with water. The stacker gel (1%) was added, the combs were fixed in place and the gel allowed to polymerase for 30 min. The electrophoresis tank was filled with running buffer (appendix 4) and the prepared total cell protein lysate samples (7.2.1) in sample buffer were heated to 95°C for 5 min, before being loaded onto the gel along with the standards. Electrophoresis was carried out at a current of 30 milliamps until the dye front was just at the bottom of the gel.

7.2.3: Western blotting

The materials to be used in western blotting were soaked in blotting buffer prior to use. The polyacrylamide gel was removed from the electrophoresis tank and allowed to equilibrate in blotting buffer for 30 min at room temperature after which the gel and the nitrocellulose paper were sandwiched between foam pads and filter paper and held in place by plastic pads. The plastic pads were inserted into the Bio-Rad transblot cell, filled with blotting buffer, and western blotting was carried out overnight at 300 milliamps.

7.2.4: Immunoreaction

The nitrocellulose paper to which the samples were transferred was removed. This was blocked for 45 min in BSA/TTBS to reduce the background staining. Afterwards the antibody specific for the ATM protein (2CI, monoclonal, Gene Tex, San Antonio Tex) was prepared and used at $2\mu gml^{-1}$ in 2.5% BSA/0.1% Tween 20/TBS. The nitrocellulose paper was incubated for 2 hours at room temperature with the ATM antibody. Afterwards the samples were washed three times in TTBS for 10 min. The samples were then incubated in anti-mouse alkaline phosphate conjugate (Sigma, Co. UK) (1/1000 in BSA/TTBS) for two hours at room temperature, washed for 10 min in TTBS and twice in TBS for 10 min and finally stained using BICP/NBT (Sigma). Once the bands had been stained clearly the nitrocellulose paper was rinsed in water and dried. The markers were prestained so they were outlined in pencil before the immunoreaction.

7.3 Results

7.3: Results

The expression of the ATM protein in SCID, CB17, 50D$^-$ and 100E$^+$ cells was studied by extracting total cell lysates from each cell line and detecting the presence of the ATM protein using an ATM antibody. Total cell lysates were taken from SCID and CB17 cells before and at 2 and 3 hours following 5 Gy of gamma radiation. The expression of the ATM antibody is shown in Figure 7.2a and b. A band with a molecular weight (MW) of 350 Kda was present in all samples for both SCID and CB17 cells, that is thought to be the ATM protein (Figure 7.2a well 2-7, 7.2b well 8-13). Interestingly, 3 hours after radiation there appeared to be a decrease in the amount of ATM expressed in CB17 cells (Figure 7.2.a. well 4), however, a repeat of this sample, as shown in 7.2b (well 8-10), did not show a difference in the amount of ATM expressed. The expression of the ATM protein in SCID cells did not change before or after IR, which is consistent with previously published results showing the ATM protein is not up-regulated in the absence of DNA-PK (Lakin *et al* 1996).

The ATM protein levels in 50D$^-$ and 100E$^+$ cells are shown in Figure 7.2.a wells 10 to 11. Similar to the responses exhibited by SCID and CB17 cells a band was present at 350 Kda which corresponds to the ATM protein and the levels did not fluctuate in response to gamma radiation, as there were no differences between the controls and irradiated samples. A similar band was also apparent in CHO, xrs5 and xrs5 cells complemented with the Ku80 gene suggesting that the ATM protein was present, but again there were no differences in the expression levels in any of the samples (Figure 7.2.a well 12-15 and Figure 7.2.b well 6-7).

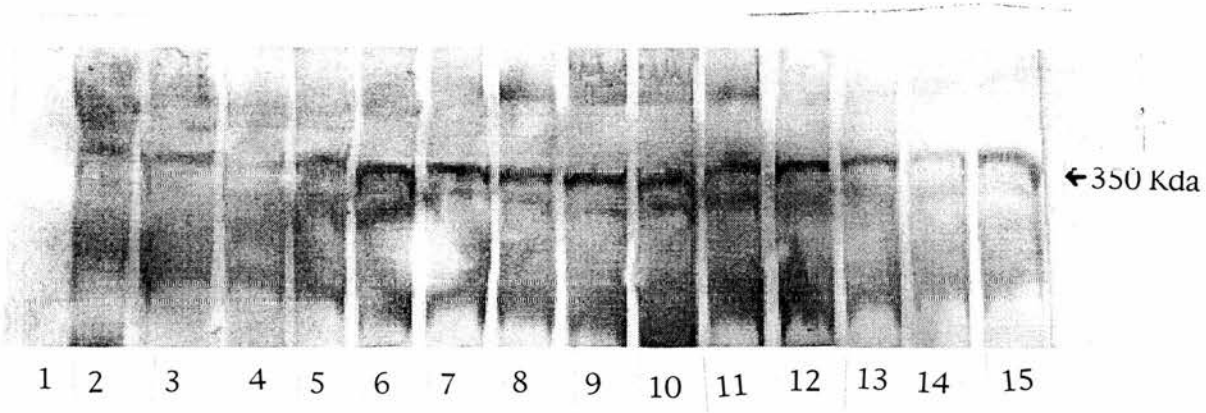

Figure 7.2.a: Western blot of mammalian cell extracts illustrating the presence of the ATM protein in control and samples at 2 or 3 h after 5 Gy gamma radiation

Well 1: Marker
Well 2-4: CB17 control, 2 and 3h after IR
Well 5-7: SCID control, 2 and 3h after IR
Well 8-9: 100E control, 2 after IR
Well 10-11: 50D control, 2 after IR
Well 12-13: CHO-K1 control, 2 after IR
Well 14-15: xrs-5 control, 2 after IR.

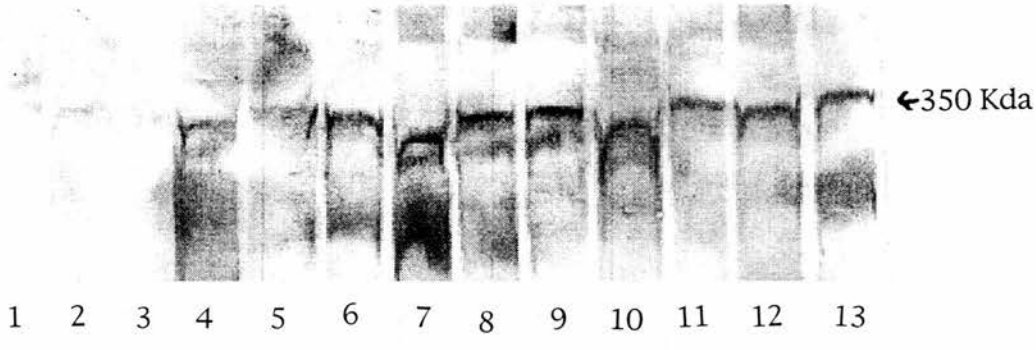

Figure 7.2.b: Western blot of mammalian cells illustrating the presence of the ATM protein in control cells and 2h after 5 Gy gamma radiation

Well 1: Marker
Well 2-3: irs-2 control, 2h after IR
Well 4-5: V-79 control, 2h after IR
Well 6-7: xrs-5 cells complemented with the Ku80 gene control and 2h after IR
Well 8-10: CB17 control, 2h and 3h after IR
Well 11-13: SCID control, 2 and 3h after IR.

Interestingly, no clear band was present at 350 Kda for the radiosensitive irs2 extract (Figure 7.2.b well 2-3) which suggests that the ATM protein is absent from irs2 cells. However, it is possible that the clarity of the gel is reduced so that a band is not clearly visible in the irs2 sample.

7.4 Discussion

7.4: Discussion

A clear band with a molecular weight of 350 Kda corresponding to the MW of the ATM protein was detected in all cell lines, except for irs2 cells. The ATM protein is assumed to be constitutively expressed in SCID, CB17, $100E^+$ and $50D^-$ cells. However, the ATM protein may not be functional in the absence of DNA-PK. Further analysis including an increased phosphorylation of ATM and its substrates may give a better insight into the functions of ATM in the absence of DNA-PK. Recently, the DNA-PK and ATM proteins have been proposed to be interdependent because of their similarities, including the phosphorylation of p53 and c-abl (Featherstone and Jackson 1999). Therefore, it may be speculated that in the absence of DNA-PK the ATM protein takes over the dsb signalling function of DNA-PK. Since the ATM protein is not the usual signalling protein for SCID cells, the overcompensating ATM signal may result in an elevated frequency of chromatid breaks in SCID and $50D^-$ cells. Therefore, ATM may simply be recruited at dsb sites following irradiation. A recent study showed the relocation of MRE11-RAD50-Nbs1 protein complex from a uniform distribution within the cell to form nuclear foci in response to IR, illustrating the importance of signalling DNA damage (Nelms *et al* 1998). In the absence of the Nbs1 protein these foci did not form (Nelms *et al* 1998, reviewed by Petrini 1999). Therefore, the formation of these foci in a knockout mutant of ATM or DNA-PK are likely to give an insight into the mechanisms of signalling DNA repair without these proteins.

The ATM protein was also present in xrs5 cells which are defective in dsb rejoining, due to the absence of Ku80 which activates the DNA-PK catalytic subunit. However, up-regulation of the ATM protein was similarly, not found in xrs5 cells compared with CHO cells confirming the response found previously in xrs6 cells (Lakin *et al* 1996).The apparent absence or very low expression of ATM protein in irs2 cells was interesting

because irs2 cells have a similar phenotype to AT cells, including an elevated chromosomal aberration frequency in response to IR but normal dsb rejoining. The results from this study suggest that XRCC8, which has not been cloned yet, may encode for the ATM protein. Complementation of the irs2 cell line with an ATM deficient cell line would test this hypothesis.

In conclusion, the radiosensitive cell lines (SCID, 50D$^-$ and xrs5) investigated all showed a clear band present at 350 Kda, by Western blotting, indicating the constitutive expression of the ATM protein in these cell lines. The ATM protein does not appear to be up-regulated in the absence of DNA-PK. This result is not suprising as most of the ATM proteins functions are mediated through phosphorylation (Canman and Lim 1999, Halazonetis and Shiloh 1999). Therefore, measuring changes in the phosphorylation of ATM substrates may be a more informative study. The results suggest that the ATM protein is not expressed or up-regulated in irs2 cells.

Chapter Eight

Overview

Chapter Eight:

8.1: Chromatid break induction in SCID, CB17, 50D$^-$ and 100E$^+$ cells treated with IR

The aim of the studies presented herein was to investigate the phenomenon of chromosomal radiosensitivity within the G2 phase of the cell cycle in murine SCID cells. SCID cells have previously been shown to have a deficiency in dsb rejoining, yet at the G2 chromosomal level the kinetics of the disappearance of chromatid breaks with time after irradiation were similar to wildtype CB17 cells (Chapter 2). However, even though there were parallel kinetics of chromatid break disappearance in SCID and CB17 cells, there was a 1.3-1.7 fold elevated chromatid break frequency in SCID cells. In addition, hybrid cells 50D$^-$ showed a two fold higher frequency of chromatid breaks than 100E$^+$ cells, illustrating that SCID and 50D$^-$ cells have an elevated radiosensitivity within G2. The elevated G2 radiosensitivity has been attributed to an elevated conversion of dsb into chromatid breaks in mammalian mutants, such as xrs5 and AT (Bryant 1998). However, this does not appear to be the case in SCID cells as there is a deficiency in G2 dsb repair in SCID cells (Chapter 5).

8.2: Dsb induction and repair in SCID and CB17 cells

Constant-field gel electrophoresis and Rotating field orthologonal gel electrophoresis both showed similar induction of dsb in exponential and G2/M SCID and CB17 cells. Further studies investigating the repair of dsb in G2/M SCID and CB17 cells were compatible with the interpretation that the elevated chromatid break frequency in SCID cells was related to the dsb rejoining deficiency. SCID cells showed a reduced dsb repair capacity from 10 min post-irradiation onwards, as measured by CFGE. This reflects the elevated frequency of chromatid breaks as measured by the G2 assay. Further analysis of the dsb rejoining at longer time intervals may have shown further convergence of dsb frequency in the two lines which is consistent with previously published results (Nevaldine *et al* 1997). The

hybrid cells $50D^-$ and $100E^+$ also showed a similar induction of dsb in exponential cells but due to time limitations the induction and repair of dsb were not measured in these hybrid cells.

8.3: Effects of AraA (a DNA synthesis inhibitor) on the G2 chromosomal response of SCID and CB17 cells to IR and the measurement of dsb repair

In the presence of the DNA synthesis inhibitor (araA) chromatid break frequency was potentiated in all 4 cell lines studied. However, 100μM araA did not have an effect on dsb induction and repair, as measured by CFGE, in SCID and CB17 lines (Chapter 5). It is suggested that although 100μM araA has no effect on dsb rejoining in these cell lines, it may be acting at the level of the chromatid recombinational rearrangements. Thus, araA is thought to inhibit the DNA synthesis associated with the semi-final step of a recombinational rearrangement within or between chromatids, leading to chromatid breaks as proposed by the signal model.

8.4: Treatment of SCID and CB17 cells with restriction endonucleases

The chromatid break response of SCID and CB17 cells to restriction endonucleases inducing dsb with different DNA ends was used as a possible way to assess the importance of DNA-PK as a DNA damage signalling molecule. The results revealed that blunt- and 3' cohesive-ended dsb cause an elevated chromatid break frequency in SCID cells relative to CB17 cells whereas 5'cohesive-ended dsb did not. This suggests that different repair pathways are required for 5' versus blunt or 3' ended dsb, and those pathways that repair 3' and blunt-ended dsb appear to be defective in SCID cells. The findings from this study suggest that NHEJ, defective in SCID cells, is a major pathway required to repair 3' and blunt-ended dsb explaining the elevated frequency of chromatid breaks. In conclusion,

DNA-PK appears to be an important signalling protein in response to 3' and blunt-ended dsb.

8.5: Chromatin structure of SCID and CB17 cells

Radiosensitivity may be influenced by an alteration in chromatin structure so differences between the chromatin structure of SCID and CB17 cells were investigated. Analysing the degree of supercoiling in SCID and CB17 nucleoids revealed a more compact structure in SCID cells and the measurement of chromosome one lengths in both lines revealed a shorter, more condensed structure in SCID cells. These results suggest that the chromatin structure of SCID cells is different to CB17 cells but how relevant this is to radiosensitivity is unknown. The MPF levels appear higher in SCID cells than CB17 cells. However, the variability between MPF assays with mitotics from the same cell line without concomitant variation in G2 chromatid break response suggests MPF level is not a critical determinant of chromatid break response.

8.6: ATM protein levels in mammalian mutant cells

In the absence of DNA-PK as a signalling molecule, as is the case in SCID cells, it may be speculated that the ATM protein may overcompensate for the loss of DNA-PK function. This hypothesis was investigated by measuring the expression levels of the ATM protein, by Western blotting, in SCID cells before and after radiation. The results did not show an up-regulation of the ATM protein in SCID and CB17 cells. This result is not suprising as most of the ATM protein functions are mediated through signalling by phosphorylation. Therefore, measuring the phosphorylation of ATM substrates may give a better evaluation of ATM's function in the absence of DNA-PK in SCID cells.

In conclusion, the dsb rejoining kinetics for SCID and CB17 cells can be interpreted as supporting a "breakage-first" model of chromatid breaks, i.e. kinetics of chromatid break disappearance with time was reflected in dsb rejoining in the two lines. However, the reported araA data for chromatid break kinetics and dsb rejoining show a striking lack of correlation between two end-points throwing serious doubt on a breakage-first interpretation. The araA data may be accounted for under the signal model in that araA, by affecting DNA synthesis could be inhibiting the semi-final step in the recombinational rearrangements within or between chromatids, thus leading to elevation of chromatid break frequency.

References

Adolph, K.W., Cheng, S.M., Paulson, J.R., *et al.* 1977. Isolation of a protein scaffold from mitotic HeLa cell chromosomes. Proc.Natl.Acad.Sci. **74**: 4937-4941.

Ager, D.D., Dewey, W.C., Gardiner, K., *et al.* 1990. Measurement of radiation-induced DNA double-strand breaks by pulsed field gel electrophoresis. Radiat.Res. **122**: 181-187.

Ager, D.D., Phillips, J.W., Columna, E.A., *et al.* 1991. Analysis of restriction enzyme-induced DNA double-strand breaks in Chinese hamster ovary cells by pulsed field gel electrophoresis: implications for chromosome damage. Radiat.Res. **128**: 150-156.

Alberts, B., Bray, D., Lewis, J., *et al.* 1989. The cells nucleus in Molecular Biology of the cell. 2ed Garland Inc.N.Y. p 481-551.

Anderson, C.W. and Lees-Miller, S.P. 1992. The nuclear serine/threonine protein kinase DNA-PK. Crit.Rev.Euk.Gene.Exp. **2**: 283-314.

Anderson, C.W. 1993 DNA damage and the DNA-activated protein kinase. TIBS. **18**:433-437

Anderson, C.W. 1992. The Nuclear Serine/Threonine Protein Kinase DNA-PK. Crit.Rev.Euk.Gene.Exp. **2**(4): 283-314.

Araki, R., Fujimori, A., Hamantani, K., *et al.* 1997. Nonsense mutation at Tyr-4046 in the DNA-dependent protein kinase catalytic subunit of severe combined immune deficiency mice. Proc.Natl.Acad.Sci.USA. **94**: 2438-2443.

Bannister, A.J., Gottlieb, T.M., Kouzarides, T., and Jackson, S.P. 1993. c-Jun is phosphorylated by the DNA- dependent protein kinase *in vitro*; definition of the minimal kinase recognition motif. Nucl.Acid.Res. **21:** 1289-1295.

Barford, D. 1996. Molecular mechanisms of the protein serine/threonine phosphatases. TIBS. **21**: 407-412.

Barth, H., Hoffman, I. and Kinzel, V. 1996. Radiation with 1 Gy Prevents the Activation of the Mitotic Inducers Mitosis-promoting factor (MPF) and cdc25-c in Hela Cells. Can.Res. **56**: 2268-2272.

Bender, M.A., Griggs, H.G. and Bedford, J.S. 1974. Mechanisms of chromosomal aberration production. III: Chemicals and ionizing radiation. Mutat.Res. **23**: 197-212.

Bhakdi, S., Tranum-Jensen, J. and Sziegoleit, A. 1985. Mechanism of Membrane Damage by Streptolysin-O. Infection and Immunity. **47**: 52-60.

Biedermann, K.A., Sun, J., Giaccia, A.J.,*et al.* 1991. Scid mutation in mice confers hypersensitivity to ionizing radiation and a deficiency in DNA double-strand break repair. Proc.Natl.Acad.Sci.USA. **88**: 1394-1397.

Blackwell, T.K. and Alt, F.W. 1989. Molecular characterisation of the lymphoid V(D)J recombination activity. J.Biol.Chem. **264**: 10327-10330.

Blier, P.R., Griffith, A.J., Craft, J. and Hardin, J.A. 1993. Binding of ku protein to DNA. Measurement of affinity for ends and demonstration of binding to nicks. J.Biol.Chem. **268**: 7594-7601.

Blöcher, D. 1982. DNA double strand breaks in Ehrlich ascites tumour cells at low doses of X-rays I. Determination of induced breaks by centrifugation at reduced speed. Int.J.Radiat.Biol. **42**:317-328.

Blöcher, D. 1990. In CHEF electrophoresis a linear induction of dsb corresponds to a nonlinear fraction of extracted DNA with dose. Int.J.Radiat.Biol. **57**: 7-12.

Blöcher, D., Einspeinner, M. and Zajackowski, J. 1989. CHEF electrophoresis, a sensitive technique for the determination of DNA double-strand breaks. Int.J.Radiat.Biol. **56**: 437-448.

Blöcher, D., Nusse, M. and Bryant, P.E. 1983. Kinetics of double strand break repair in the DNA of X-irradiated synchronised mammalian cells. Int.J.Radiat.Biol. **43**: 579-584.

Blöcher, D., Sigut, D. and Hannan, M.A. 1991. Fibroblasts from ataxia telangiectasia (AT) and AT heterozygous show an enhanced level of residual DNA double-strand breaks after low dose-rate γ-irradiation as assayed by pulsed field gel electrophoresis. Int.J.Radiat.Biol. **60**: 791-802.

Blunt, T., Finnie, N.J., Tacciol, G.E., *et al.* 1995. Defective DNA-Dependent Protein Kinase Activity is Linked to V(D)J Recombination and DNA Repair Defects Associated with the Murine Scid mutation. Cell. **80**: 813-823.

Blunt, T., Gell, D., Fox, M., *et al.* 1996. Identification of a nonsense mutation in the carboxy-terminal region of DNA-dependent protein kinase catalytic subunit in the *scid* mouse. Proc.Natl.Acad.Sci. **93**: 10285-10290.

Bogue, M. and Roth, D.B. 1996. Mechanism of V(D)J recombination. Curr.Opin.Immunol. **8**:175-180.

Bohr, V.A., Phillips, D.H. and Hanawalt, P.C. 1987. Heterogenous DNA damage and repair in the mammalian genome. Can.Res. **47**: 6426-6436.

Bosma, M.J. and Carroll, A.M. 1991. The SCID Mouse Mutant: Definition, Characterisation and Potential Uses. Ann.Rev.Immunol. **9**: 323-350.

Bosma, G.C., Custer, R.P. and Bosma, M.J. 1983. A severe combined immunodeficiency mutation in the mouse. Nature. **301**(10): 527-530.

Bosma, G.C., Davisson, M.T., Ruetsch, N.R., *et al.* 1989. The mouse mutation severe combined immune deficiency (SCID) is on chromosome 16. Immunogenetics. **29**: 54-57.

Boubnov, N.V. and Weaver, D.T. 1995. *Scid* Cells Are Deficient in Ku and Replication Protein A Phosphorylation by the DNA-Dependent Protein Kinase. Mol.Cell.Biol. **15**(10): 5700-5706.

Boulton, S.J and Jackson, S.P. 1996. Identification of a *Saccharomyces cerevisiae* ku80 homologue: roles in DNA double-strand break rejoining and telomeric maintenance. Nucl.Acid.Res. **24**:4639-4648.

Boulton, S.J. and Jackson, S.P. 1998. Components of the Ku-dependent non-homologous end-joining pathway are involved in telomeric length maintenance and telomeric silencing. EMBO.Journal. **17**: 1819-1828.

Bradley, M.O. and Kohn, K. 1979. X-ray induced double-strand break production and repair in mammalian cells as measured by neutral filter elution. Nucl.Acid.Res. **7**:793-804.

Brink, J.J. and LePage, G.A. 1965. 9-β-D-Arabinofuranosyladenine as an inhibitor of metabolism in normal and neoplastic cells. Canadian Journal of Biochemistry. **43**: 1-15.

Buckton, K.E. and Evans, H.J. 1973. Methods for the analysis of human chromosome aberrations. World Health Organisation. Genevea.

Bryant, P.E. 1983. 9-β-D-Arabinofuranosyladenine increases the frequency of X-ray induced chromosome abnormalities in mammalian cells. Int.J.Radiat.Biol.**43**: 459-464.

Bryant, P.E. 1984a. Effects of araA and fresh medium on chromosome damage and DNA double-strand break repair in X-irradiated stationary cells. Br.J.Can. **49** suppl.VI: 61-65.

Bryant, P.E. 1984b. Enzymatic restriction of mammalian cell DNA using PvuII and BamHI: evidence for the double-strand break origin of chromosomal aberrations. Int.J.Radiat.Biol. **46**: 57-65.

Bryant, P.E. 1985. Enzymatic restriction of mammalian cell DNA: evidence for double-strand breaks as potentially lethal lesions. Int.J.Radiat.Biol. **48**: 55-60.

Bryant, P.E. 1988. Use of restriction endonucleases to study relationships between DNA double-strand breaks, chromosomal aberrations and other end-points in mammalian cells. Int.J.Radiat.Biol. **54**: 869-890.

Bryant, P.E. 1989. Restriction endonuclease- and radiation-induced DNA double-strand breaks and chromosomal aberrations similarities and differences. In chromosome aberrations. Basic and applied aspects. Ed Obe, G and Natarajan, A.T. Springer-Verlag Berlin. p61-69.

Bryant, P.E. 1992a. Induction of chromosomal damage by restriction endonuclease in CHO cells porated with streptolysin O. Mutat.Res. **268**: 27-34.

Bryant, P.E. 1992b Mimicking radiation with restriction endonucleases. B.J.R.suppl. **24**: 35-38.

Bryant, P.E. 1993. Radiosensitive Chinese hamster irs2 cells show enhanced chromosomal sensitivity to ionizing radiation and restriction endonuclease induced blunt-ended double-strand breaks. Mutagenesis. **8**: 141-147.

Bryant, P.E. 1997. DNA damage, repair and chromosomal damage. Int.J.Radiat.Biol. **71**: 675-680.

Bryant, P.E. 1998. The signal model: a possible explanation for the conversion of DNA double-strand breaks into chromatid breaks. Int.J.Radiat.Biol. **73**: 243-251.

Bryant, P.E. and Blöcher, D. 1980. Measurement of the repair kinetics of DNA double-strand break repair in Ehrlich ascites tumour cells using the unwinding method. Int.J.Radiat.Biol. **38**: 335-347.

Bryant, P.E. and Blöcher, D. 1982. The effects of 9-β-D-arabinofuranosyladenine on the repair of DNA strand breaks in X-irradiated Ehrlich ascites tumour cells. Int.J.Radiat.Biol. **4**: 385-394.

Bryant, P.E., Birch, D.A. and Jeggo, P.A. 1987. High chromosomal sensitivity of Chinese hamster xrs5 cells to restriction endonuclease induced DNA double-strand breaks. Int.J.Radiat.Biol. **52**: 537-554.

Bryant, P.E. and Christie, A.C. 1989. Induction of chromosomal aberrations in CHO cells by restriction endonucleases: effects of blunt- and cohesive-ended double-strand breaks in cells treated by "pellet" methods. Mutat.Res. **213**: 233-241.

Bryant, P.E., Finnegan, C.E., Swaffield, L., *et al.* 1998. G2 chromatid breaks in murine SCID cells. Mutagenesis. **13**: 481-485.

Bryant, P.E., Jones, N.J. and Liu, N. 1993. Radiosensitive Chinese hamster irs2 cells show enhanced chromosomal sensitivity to ionizing radiation and restriction endonuclease induced blunt-ended double-strand breaks. Mutagenesis. **8**: 141-147.

Bryant, P.E. and Iliakis, G. 1984. Possible correlations between cell killing, chromosome damage and DNA repair after X-irradiation. In "DNA Repair and Its Inhibition". Eds A. Collins, R.T. Johnson and S.D. Downes. IRL Press Ltd. Oxford. Nucleic.Acid.Symp.Ser. **13** p291-308.

Bryant, P.E and Liu, N. 1994. Responses of radiosensitive repair-proficient cell lines to restriction endonucleases. Int.J.Radiat.Biol. **66**: 597-601.

Bryant, P.E. and Riches, A.C. 1989. Oncogenic transformation of murine C3H10T1/2 cells resulting from DNA double-strand breaks induced by a restriction endonuclease. Br.J.Cancer. **60**: 852-854.

Bryant, P.E. and Slijepcevic, P. 1993. G2 Chromatid Aberrations: kinetics and possible mechanisms. Environ.Mol.Mutag. **22**: 250-256.

Buckingham, L. and Duncan, J.L. 1983. Approximate dimensions of membrane lesions produced by streptolysin S and steptolysin O. Biochimica. Biophysica.Acta. **729**: 115-127.

Budach, W., Hatford, A., Gioioso. D., *et al.* 1992. Tumors Arising in SCID Mice share enhanced radiation sensitivity of SCID Normal tissues. Can.Res. **52**: 6292-6296.

Bühler, B., Kohler, G. and Nielsen, R.J., *et al.* 1995. Efficient nonhomologous and homologous recombination in scid cells. Immunogenetics. **42**: 181-187.

van Buul, P.P.W., Abramsson-Zetterberg, L., Zandman, I.M. *et al.* 1998. Further characterisation of the radiosensitivity of the *scid* mouse. Int.J.Radiat.Biol. **74**: 35-41.

van Buul, P.P.W., De Rooij, D.G., Zandman, I.M., *et al.* 1995. X-ray induced chromosomal aberrations and cell killing in somatic and germ cells of the scid mouse. Int.J.Radiat.Biol. **67**: 549-555.

Canman, C.E. and Lim, D.S. 1998. The role of ATM in DNA damage responses and cancer. Oncogene **24**: 3301-3308.

Carle, G.F., Frank, M. and Olsen, M.V., *et al.* 1986. Electrophoretic separation of large DNA molecules by periodic inversion of the electric field. Science. **232**: 65-68.

Carle, G.F. and Olsen, M.V. 1984. Separation of chromosomal DNA molecules from yeast by orthogonal-field-alternation gel electrophoresis. Nucl.Acid.Res. **12**; 5647-5664.

Carroll, A.M. and Bosma, M.J. 1991. T-lymphocyte development in scid mice is arrested shortly after the initiation of T-cell receptor δ gene recombination. Genes.Dev. **5**: 1357-1366.

Carroll, A.M., Hardy, R.R., Bosma, M.J., *et al.* 1989. Occurrence of mature B (IGM^+, $B220^+$) and T($CD3^+$) Lymphocytes in Scid mice. J.Immunol.**143**: 1087-1093.

Cary, R.B. 1997. DNA looping by Ku and the DNA-dependent protein kinase. Proc.Natl.Acad.Sci.USA. **94**: 4267-4272.

Chan, D.W. and Lees-Miller, S.P. 1996. The DNA-dependent protein kinase is inactivated by autophosphorylation of the catalytic subunit. J.Biol.Chem. **271**: 8963-8941.

Chang, C., Biedermann, K.A., Mezzina, M. *et al.* 1993. Characterisation of DNA double-strand break repair defect in Scid mice. Can.Res. **53**: 1244-1248.

Cheng, X., Pantelias, G.E., Okayasu, R., *et al.* 1993. Mitosis-promoting factor activity of inducer mitotic cells may affect radiation yield of interphase chromosome breaks in the premature chromosome condensation assay. Can.Res. **53**: 5592-5596.

Chu, G., Vollrath, D. and Davis, R.W. 1986. Separation of large DNA molecules by contour-clamped homogenous electric fields. Science. **234**: 1582-1585.

Chui, S-M, and Oleinick, N.L. 1982. The sensitivity of active and inactive chromatin to ionizing radiation-induced strand breakage. Int.J.Radiat.Biol. **41**: 71-77.

Chung, H.W., Phillips, J.W., Winegar, R.A., *et al.* 1991. Modulation of Restriction Enzyme-Induced Damage by Chemicals that Interfere with Cellular Responses to DNA Damage: A Cytogenetic and Pulsed-Field Gel Analysis. Radiat.Res. **125**: 107-113.

Cohen, S.S. and Plunkett, W. 1975. The utilization of nucleotides by animal cells. Ann.N.Y.Acad.Sci. **255**: 269-286.

Cook, P.R. and Brazell, I.A. 1975. Supercoils in human DNA. J.Cell.Sci. **19**: 261-279.

Cook, P.R. and Brazell, I.A. 1976. Conformational constraints in nuclear DNA. J.Cell.Sci. **22**: 287-302.

Cook, P.R. and Brazell, I.A. and Jost, E. 1976. Characterization of nuclear structures containing superhelical DNA. J.Cell.Sci. **22**: 303-324.

Cortès, F. and Ortiz, T. 1992. Chromosome damage induced by restriction endonucleases recognizing thymine-rich DNA sequences in electroporated CHO cells. Int.J.Radiat.Biol.**61**: 323-328.

Costa, N.D. and Bryant, P.E. 1988. Repair of DNA single-strand and double-strand breaks in the Chinese hamster xrs5 mutant cell line as determined by DNA unwinding. Mutat.Res. **194**: 93-99.

Costa, N.D. and Bryant, P.E. 1990a. The induction of DNA double-strand breaks in CHO cells by PvuII: kinetics using neutral filter elution (pH 9.6). Int.J.Radiat.Biol. **57**: 933-938.

Costa, N.D. and Bryant, P.E. 1990b. Neutral filter elution only limited inhibition of double-strand break repair by 9-β-D-arabinofuranosyladenine. Mutat.Res. **235**: 217-223.

Costa, N.D. and Bryant, P.E. 1991a. Elevated levels of DNA double-strand breaks (dsb) in restriction endonuclease treated xrs5 cells correlate with the reduced capacity to repair dsb. Mutat.Res. **255**:219-226.

Costa, N.D. and Bryant, P.E. 1991b. Differences in accumulation of blunt and cohesive ended double-strand breaks generated by restriction endonucleases in electroporated CHO cells. Mutat.Res. **254**: 239-246.

Countryman, P.I. and Heddle, J.A. 1976. The production of micronuclei from chromosome aberrations in irradiated cultures of human lymphocytes. Mutat.Res. **41**: 321-332.

Critchlow, S.E., Bowater, R.P., Jackson, S.P, *et al.* 1997. Mammalian DNA double-strand break repair protein XRCC4 interacts with DNA ligase IV. Curr.Biol. **7**: 588-598.

Custer, R.P., Gayle, M.D. and Bosma, M.J. 1985. Severe Combined Immunodeficiency(SCID) in the mouse : Pathology, reconstitution, neoplasm's. Amer.J.Path. **120**: 464-477.

Dahm-Daphi, J., Dikomey, E., Pyttlik, C. and Jeggo, P.A. 1993. Reparable and non-reparable DNA strand breaks induced by X-irradiation in CHO K1 cells and the radiosensitive mutants xrs1 and xrs5. Int.J.Radiat.Biol.**64**: 19-26.

Danska J.S., Holland, D.P., Mariathasan, S., *et al* . 1996. Biochemical and Genetic Defects in the DNA-dependent Protein Kinase in Murine scid lymphocytes. Mol.Cell.Biol. **16** (10): 5507-5517.

Darroudi, F. and Natarajan, A.T. 1989. Cytogenetical characterization of Chinese hamster ovary X-ray sensitive mutant cells, xrs5 and xrs6. IV. Study of chromosomal aberrations and sister-chromatid exchanges by restriction endonucleases and inhibitors of DNA topoisomerase II. Mutat.Res. **212**: 137-148.

Denekemp, J., Whitmore, G.F. and Jeggo, P. 1989. Biphasic survival curves for XRS radiosensitive cells: subpopulation or transient expression of repair competence? Int.J.Radiat.Biol. **55**: 605-617.

Disney, J.E., Barth, A.L. and Shultz, L.D. 1992. Defective repair of radiation-induced chromosomal damage in scid/scid mice. Cytogenet.Cell.Genet. **59**: 39-44.

Draetta, G., Lunca, F., Westendorf, J., *et al.* 1989. Cdc2 protein kinase is complexed with both cyclin A and B: evidence for a proteolytic inactivation of MPF. Cell. **56**: 829-838.

Duncan, J.L. and Schlegel, R. 1975. Effect of streptolysin O on Erythrocyte membranes, liposomes, and lipid dispersions. A Protein-cholesterol Interaction. J.Cell.Biol.**67**: 160-173.

Dunphy, W.G. and Newport, J.W. 1988. Unravelling of mitotic control mechanisms. Cell. **55**: 925-928.

Dunphy, W.G. and Newport, J.W. 1989. Fission yeast p13 blocks mitotic activation and tyrosine dephosphorylation of the *Xenopus* cdc2 protein kinase. **58**: 181-191.

Earnshaw, W.C. 1988. Mitotic chromosome structure. BioEssays. **9**: 147-150.

Eastman, Q.M., Leu, T.M. and Schatz, D.G., *et al.* 1996. Initiation of V(D)J recombination *in vitro* obeying the 12/23 rule. Nature. **380**: 85-88.

Elia, M.C. and Nichols, W.W. 1993. Technical report: Application of programmable autonomously controlled electrode (PACE) technology to the development of an improved pulsed-field gel electrophoresis assay for DNA double-strand breaks in mammalian cells. Int.J.Radiat.Biol. **63**: 7-11.

Evans, J.W., Liu, X.F., Kirchgessner, C.U. and Brown, J.M. 1996. Induction and Repair of Chromosome Aberrations in Scid cells measured by Premature Chromosome Condensation. Radiat.Res. **145**: 39-46.

Fangman, W.L. 1978. Separation of very large DNA molecules by gel electrophoresis. Nucl.Acid.Res. **5**: 653-665.

Featherstone, C. and Jackson, S.P. 1999. DNA-dependent protein kinase gets a break: its role in repairing DNA and maintaining genomic integrity. B.J.Cancer. **80**: 14-19.

Fenech, M. and Morley, A.A. 1985. Measurement of micronuclei in lymphocytes. Mutat.Res. **147**: 26-36.

Fenech, M. and Morley, A.A. 1986. Cytokinesis-block micronucleus method in human lymphocytes: an effect of in vivo ageing and low dose X-irradiation. Mutat.Res. **161**: 193-198.

Finnie, N.J., Gottlieb, T.M., Blunt, T., *et al.* 1995. DNA-dependent protein kinase activity in xrs-6 cells: Implications for site-specific recombination and DNA double-strand break repair. Proc.Natl.Acad.Sci.USA.**92**: 320-324.

Finnie N.J., Gottlieb T.M., Blunt, T., *et al.* 1996. DNA-Dependent protein kinase defects are linked to deficiencies in DNA repair and V(D)J recombination. Phil.Trans.R.Soc.Lond. B. **351**: 173-179.

Folle, G.A., Boccardo, E. and Obe, G. 1997. Localization of chromosome breakpoints induced by DNaseI in Chinese hamster ovary (CHO) cells. Chromosoma. **106**: 391-399.

Folle, G.A., Johannes, C., Mechoso, B.H., *et al.* 1992. The restriction endonuclease AluI induces sister chromatid exchanges in Chinese hamster ovary cells. Mutagenesis. **7**: 291-294.

Folle, G.A., Martinez-Lopez, W., Boccardo, E., *et al.* 1998. Localization of chromosome breakpoints: implications of the chromatin structure and nuclear architecture. Mutat.Res. **404**: 17-26.

Folle, G.A. and Obe, G. 1995. Localization of chromosome breakpoints induced by AluI and BamHI in Chinese hamster ovary cells treated in the G1 phase of the cell cycle. Int.J.Radiat.Biol. **68**: 437-445.

Folle, G.A., and Obe, G. 1996. Intrachromosomal localization of breakpoints induced by the restriction endonucleases AluI and BamHI in Chinese hamster ovary cells treated in S phase of the cell cycle. Int.J.Radiat.Biol. **69**: 447-457.

Foray, N., Arlett, C.F. and Malaise, E.P. 1995. Dose-rate effect on induction and repair rate of radiation-induced DNA double-strand breaks in a normal and an ataxia telangiectasia human fibroblast cell line. Biochimie. **77**: 900-905.

Frankenberg, D. 1969. A ferrous sulphate dosimeter independent of photon energy in the range from 25keV up to 50keV. Phy.Med.Biol. **14**: 597-605.

Frankenberg, D., Frankenberg-Schwager, M. 1981. Evidence for DNA double-strand breaks as critical lesions in yeast cells irradiated with sparsely or densely ionizing radiation under oxic or anoxic conditions. Radiat.Res. **88**: 524-532.

Freeman, R.S. and Donoghue, D.J. 1991. Protein kinases and protooncogene: biochemical regulation of the eukaryotic cell cycle. Biochemistry. **30**: 2293-2301.

Fried, L.M., Koumenis, C., Peterson, S.R., *et al.* 1996. The DNA damage response in DNA-dependent protein kinase-deficient SCID mouse cells: Replication protein A hyperphosphorylation and p53 induction. Proc.Natl.Acad.Sci.USA. **93**: 13825-13830.

Fukumura, R., Araki, R., Fujimora, A., *et al.* 1998. Murine cell line SX9 bearing a mutation in the *dna-pkcs* gene exhibits aberrant V(D)J recombination not only in the coding joint but also in the signal joint. J.Biol.Chem. **272**: 13058-13064.

Fulop, G.M. and Philips, R.A. 1990. The Scid mutation in mice causes a general defect in DNA repair. Nature.**347**: 479-482.

Furth, J.J. and Cohen, S.S. 1967. Inhibition of mammalian DNA polymerase by the 5'triphosphate of 9-β-D-arabinofuranosyladenine. Can.Res. **27**: 1528-1533.

Furth, J.J. and Cohen, S.S. 1968. Inhibition of mammalian DNA polymerase by the 5'-triphosphate of 1-β-D-arabinofuranosyladenine and the 5'triphosphate of 9-β-D-arabinofuranosyladenine. Can.Res. **28**: 2061-2067.

Goa, C.Y. and Zelenka, P.S. 1997. Cyclins, cyclin-dependent kinases and differentiation. BioEssays. **19**: 307-314.

Gardiner, K., Lass, W. and Patterson, D., *et al.* 1986. Fractionation of large mammalian DNA restriction fragments using vertical pulsed-field gradient gel electrophoresis. Som.Cell.Mol.Genet. **12**: 185-195.

Gellert, M. 1992. Molecular Analysis of V(D)J Recombination. Annu.Rev.Genet. **22**: 425-426.

Gellert, M. 1996. A new view of V(D)J recombination. Genes to Cells. **1**: 269-275.

Gerdes, M.G., Carter, K.C., Moen, P.T.Jr, *et al.* 1994. Dynamic changes in the higher-order chromatin organisation of specific sequences revealed by in situ hybridisation of nuclear halos. J.Cell.Biol. **126**: 289-304.

Gerstein, R.M. and Lieber, M.R. 1993a. Extent to which homology can constrain coding exon junctional diversity in V(D)J recombination. Nature. **363**: 625-627.

Gerstein, R.M. and Lieber, M.R. 1993b. Coding end sequence can markedly affect the initiation of V(D)J recombination. Genes.Dev. **7**: 1459-1469.

Getts, R.C. and Stamato, T.D. 1994. Absence of a ku-like DNA End Binding Activity in the xrs Double-strand Repair-deficient Mutant. J.Biol.Chem. **269**: 15981-15984.

Giaccia, A.J., Denko, N., MacLaren, R.A., *et al.* 1990. Human chromosome 5 complements the DNA double-strand break-repair deficiency and gamma-ray sensitivity of the XR-1 hamster variant. Am.J.Hum.Genet. **47**: 459-469.

Giaccia, A.J., MacLaren, R.A., Denko, N., *et al.* 1990. Increased sensitivity to killing by restriction endonucleases in the XR-1 DNA double-strand break repair-deficient mutant. Mutat.Res. **236**: 67-76.

Giaccia, A.J, Weinstein, R., Hu, J., *et al.* 1985. Cell Cycle Dependent Repair of Double-strand DNA Breaks in a γ-Ray-sensitive Chinese Hamster Cell. Som.Cell.Mol.Gen. **11**(5): 485-491.

Giffin, W., Kwast-Welfeid, J. and Rodda, D.J. 1997. Sequence-specific DNA binding and transcription factor phosphorylation by Ku autoantigen/DNA-dependent protein kinase. Phosphorylation of ser-527 of the rat glucocorticoid receptor. J.Biol.Chem. **272**: 5647-5658.

Goedecke, W., Eijpe, M., Offenberg, H.H. *et al.* 1999. Mre11 and Ku70 interact in somatic cells, but are differentially expressed in early meiosis. Nature Genetics. **23**:194-198.

Gottlieb, T.M. and Jackson, S.P. 1993. The DNA-Dependent Protein Kinase : Requirement for DNA Ends And Association with Ku Antigen. Cell. **72**: 131-142.

Gottlieb, T.M. and Jackson, S.P. 1994. Protein Kinases and DNA damage. TIBS. **19**: 500-503.

Grawunder, U. Zimmer, D., Kulesza, P., *et al.* 1998a. Requirement for an interaction of XRCC4 with DNA ligase IV for wildtype V(D)J recombination and DNA double-strand break repair *in vivo*. J.Biol.Chem. **18**: 24708-24714.

Grawunder, U., West, R.B. and Lieber, M.R. 1998b. Antigen receptor gene rearrangement. Curr.Opin.Immunol. **10**: 172-180.

Grigorova, M., Boei, J.J., van Duyn-Goedhart, A., *et al.* 1995. X-ray induced translocations in bone marrow cells of Scid and wild type mice detected by fluorescence in situ hybridisation using mouse chromosome specific DNA libraries. Mutat.Res. **331**: 39-45.

Gu, S., Jin, S., Gao. Y., *et al.* 1997. Ku-70 deficient embryonic stem cells have increased ionizing radiosensitivity, defective DNA end-binding activity, and inability to support V(D)J recombination. Proc.Natl.Acad.Sci. **94**: 8076-8081.

Gurley, K.E and Kemp, C.J. 1996. p53 induction, cell cycle checkpoints, and apoptosis in DNA-PK deficient scid mice. Carcinogenesis. **17**: 2537-2542.

Halazonetis, T.D. and Shiloh, Y. 1999. Many faces of ATM: eighth international workshop on Ataxia Telangiectasia. Biochem.Biophys.Acta. **29**: 1424 R45-55.

Hamantani, K., Matsuda, Y., Araki, R., *et al.* 1996. Cloning and chromosomal mapping of the mouse DNA-dependent protein kinase gene. Immunogenetics. **45**: 1-5.

Harrington, J., Hseih, C.L., Gerton, J., *et al.* 1992. Analysis of the defect in DNA End joining in the Murine Scid mutation. Mol.Cell.Biol.**12**: 4758-4768.

Hartley, K.O., Gell, D., Smith, G.C., *et al.* 1995. DNA-Dependent Protein Kinase Catalytic Subunit: A relative of Phosphatidyl-inositol-3-kinase and the Ataxia Telangiectasia Gene Product. Cell. **82**: 849-856.

Harvey, A.N. and Savage, J.R.K. 1997. Investigating the nature of chromatid breaks produced by restriction endonucleases. Int.J.Radiat.Biol. **71**: 21-28.

Heddle, J.A. and Bodycote, D.J. 1970. On the formation of chromosomal aberrations. Mutat.Res. **9**: 117-126.

Heine, D., Passmore, H.C., Patel, V., *et al.* 1996. Effect of the mouse *scid* mutation on meiotic recombination. Mammalian Genome. **7**: 497-500.

Helzlsouer, K.J., Harris, E.L., Parshad, R., *et al* . 1995. Familial clustering of breast cancer: possible interaction between DNA repair proficiency and radiation exposure in the development of breast cancer. Int.J.Can. **64**: 14-17.

Hendrickson, E.A., Qin, X.Q., Bump, E.A., *et al.* 1991. A link between double-strand break-related repair and V(D)J recombination: The Scid Mutation. Proc.Natl.Acad.Sci.USA. **88**: 4061-4065.

Hendrickson, E.A., Schatz, D.G. and Weaver, D.T. 1988. The Scid gene encodes a trans-acting factor that mediates the rejoining event of Ig gene rearrangement. Gen.Dev. **2**: 817-829.

Hensey, C., Gautier, J., *et al.* 1995. Regulation of cell cycle progression following DNA damage. Prog.Cell.Cycle.Res. **1**: 149-162.

Hesse, J.E., Lieber, M.R., Mizuuchi, K., *et al.* 1989. V(D)J recombination: a functional definition of the joining signals. Gene.Dev. **3**: 1053-1061.

Higurashi, M. and Cole, R.D. 1991. The combination of DNA methylation and H1 histone binding inhibits the action of a restriction nuclease on plasmid DNA. J.Biol.Chem. **266**: 8619-8625.

Hinton, D.M., and Bode, V.C. 1975. Purification of closed circular lambda deoxyribonucelic acid and its sedimentation properties as a function of sodium chloride concentration and ethidium binding. J.Biol.Chem. **250**: 1071-1079.

Hinton, D.M., and Bode, V.C. 1975. Ethidium bromide affinity of circular lambda deoxyribonucleic acid determined fluorometrically. The effect of NaCl concentration on supercoiling. J.Biol.Chem. **250**: 1061-1070

Ho, K.Y. 1975. Induction of DNA double-strand breaks by X-rays in a radiosensitive strain of the yeast *Saccharomyces cerevisiae*. Mutat.Res. **30**: 327-334.

Ho, K.Y. and Mortimer, R.K. 1975. Molecular mechanisms for repair of DNA, edited by P.C.Hanawalt, and R.B. Setlow (N.Y. Plenium) p: 545.

Hoffman, M. 1993. The cells nucleus shapes up. Science. **259**: 1257-1259.

Huang, L., Clarkin, K.C. and Wahl, G.M. 1996. p53-dependent cell cycle arrests are preserved in DNA-activated protein kinase-deficient mouse fibroblasts. Can.Res. **56**: 2940-2944.

Huang, P., Siciliano, M.J. and Plunkett, W. 1989. Gene deletion, a mechanism of induced mutation by arabinosyl nucleosides. Mutat.Res. **210**: 219-301.

Iborra, F.J., Pombo, A., Jackson, D.A., *et al.* 1996. Active RNA polymerases are localised within discrete transcription "factories" in human nuclei. J.Cell.Sci. **109**: 1427-1436.

Iliakis, G. 1980. Effects of β-arabinofuranoslyadenine on growth and repair of potentially lethal damage in Ehlrich ascites tumor cells. Radiat.Res. **83**: 537-552.

Iliakis, G., Metha, R. and Jackson, M. 1992. Level of DNA double-strand break rejoining in Chinese Hamster xrs-5 cells is dose dependent: implications for the mechanism of radiosensitivity. Int.J.Radiat.Biol. **61**: 315-321.

Iliakis, G.E. and Okayasu, R. 1990. Radiosensitivity throughout the cell cycle and repair of potentially lethal damage and DNA double-strand breaks in X-ray sensitive CHO mutants. Int.J.Radiat.Biol. **57**: 1195-1211.

Iliakis, G., Pantelias, G., Okayasu, R., *et al.* 1989. Comparative studies on repair inhibition by araA,araC and aphidicolin of radiation induced DNA and chromosome damage in rodent cells: comparison with fixation of PLD. Int.J.Radiat.Oncol.Biol.Phys. **16**: 1261-1265.

Itoh, M., Hamatani, K., Komatsu, K., *et al.* 1993. Human Chromosome 8 (p12-q22) Complements Radiosensitivity in the Severe Combined Immune Deficiency (SCID) Mouse. Radiat.Res. **134**: 364-368.

Jackson, D.A., Dickinson, P and Cook, P.R. 1990. Attachment of DNA to the nucleoskeleton of HeLa cells examined using physiological conditions. Nucl.Acid.Res. **18**: 4385-4393.
Jackson, S.P. 1996. DNA damage detection by DNA dependent protein kinase and related enzymes. Can.Surv. **28**: 261-279.

Jackson, S.P. 1997. Silencing and DNA repair connect. Nature. **388**: 829-830.

Jackson, S.P. and Jeggo, P.A. 1995. DNA double-strand break repair and V(D)J recombination: involvement of DNA-PK. TIBS. **20**: 412-415.

Jackson, S.P., MacDonald, J.J., Lees-Millar, S., *et al.* 1990. GC Box Binding Induces Phosphorylation of Sp1 by a DNA-Dependent Protein kinase. Cell. **63**: 155-165.

Jeggo, P.A. 1990. Studies on mammalian mutants defective in rejoining double-strand breaks in DNA. Mutat.Res. **239**: 1-16.

Jeggo, P.A. 1997. DNA-PK: at the cross-roads of biochemistry and genetics. Mutat.Res. **384**: 1-14.

Jeggo, P.A. and Kemp, L.M. 1983. X-ray sensitive mutants of Chinese hamster ovary cell line: Isolation and cross-sensitivity to other DNA damaging agents. Mutat.Res. **112**: 313-327.

Jeggo, P., Singleton, B., Beamish, H. and Priestley, A. 1999. Double strand break rejoining by the ku-dependent mechanism of non-homologous end-joining. CR.Acad.Sci. III. **322**: 107-12.

Jeggo, P.A., Taccioli, G.E. and Jackson, S.P. 1995. Menage à trois: double strand break repair ; V(D)J recombination and DNA-PK. Bioessays.**17**: 949-957.

Jin, S., Inoue, S. and Weaver, D.T. 1997a. Functions of the DNA dependent protein kinase. Can.Surv. **29**: 221-261.

Jin, S. and Weaver, D.T. 1997b. Double-strand break repair by Ku70 requires heterodimerization with Ku80 and DNA binding functions. EMBO.J. **16**: 6874-6885.

Johannes, C., Boes, R. and Obe, G. 1992. Uptake of the restriction endonuclease AluI by Chinese hamster ovary cells measured by frequencies of induced chromosomal aberrations: effect of hypertonic concentration of glycerol and sorbitol. Mutagenesis. **7**: 225-232.

Johannes, C. and Obe, G. 1991. Induction of chromosomal aberrations with the restriction endonuclease AluI in Chinese hamster ovary cells: comparison of different treatment methods. Int.J.Radiat.Biol. **59**; 1379-1393.

Johnston, P.J., MacPhail, S.H. , Stamato, T.D., *et al.* 1998. Higher-order chromatin structure- dependent repair of DNA double-strand breaks: involvement of the V(D)J recombination double strand break repair pathway. Radiat.Res. **149**: 455-462.

Joshi, G.P., Nelson, W.J., Revell, S.H., *et al.* 1982. X-ray induced chromosome damage in live mammalian cells and improved measurements of its effects on their colony forming ability. Int.J.Radiat.Biol.Chem.Med. S41-161-181.

Kapiszewaska, M., Wright, W.D., Lange, C.S., *et al.* 1989. DNA supercoiling changes in nucleoids from irradiated L5178Y-S and R cells. Radiat.Res. **119**: 569-575.

Keith, C.T. and Schreiber, S.L. 1995. PIK-related kinases: DNA repair, recombination, and cell cycle checkpoints. Science. **270**: 50-51

Kemp, L.M. and Jeggo, P.A. 1986. Radiation-induced chromosome damage in X-ray sensitive mutants (xrs) of the Chinese hamster ovary cell line. Mutat.Res. **166**: 255-263.

Kemp, L.M., Sedgwick, S. G., Jeggo, P.A., *et al.* 1984. X-ray sensitive mutants of Chinese hamster ovary cells defective in double-strand breaks rejoining. Mutat.Res. **132**: 189-196.

Kienker, L.J., Kuziel, W.A. and Tucker, P.W. 1991. T cell receptor γ and σ Gene junctional Sequences in SCID Mice: Excessive P nucleotide Insertion. J.Exp.Med. **174**: 769-773.

Kim, M-G., Schuler, W., Bosma, M.J., *et al.* 1988. Abnormal Recombination of IghD and J gene segments in Transformed pre-B cells of Scid Mice. J.Immunol. **141**: 1341-1347.

Kimura, H., Terado, T, Komatsu, K., *et al.* 1995. Cultured cells from a Severe Combined Immunodeficient Mouse Have a slower than Normal Rate of Repair of Potentially Lethal Damage Sensitive to Hypertonic Treatment. Radiat.Res. **142**: 176-180.

Kinashi, Y., Okayasu, R., Iliakis, G.E., *et al.* 1995. Induction of DNA double-strand breaks by restriction enzymes in X-ray sensitive mutant Chinese hamster ovary cells measured by pulsed field gel electrophoresis. **141**: 153-9.

King, J.S., Fairley, C.F., Morgan, W.F., *et al.* 1994. Bridging the Gap. Joining of nonhomologous ends by DNA polymerases. J.Biol.Chem. **269**: 13061-13064.

King, R.J.K. 1996. A balance of proliferation, death and differentiation in Cancer Biology. Addison Wesley Longman. p:123-137.

Kirchgessner, C.U., Patil, C.K., Evans, J.W., *et al.* 1995. DNA-Dependent kinase (p350) as a Candidate Gene for the Murine SCID Defect. Science. **267**: 1178-1183.

Kirchgessner, C.U., Tosto, L.M., Biedermann, K.A., *et al.* 1993. Complementation of the Radiosensitive Phenotype in Severe Combined Immunodeficient Mice by Human Chromosome 8. Can.Res. **53**: 6011-6016.

Knight, R.D., Parshad, R., Price, F.M., *et al.* 1993. X-ray induced chromatid damage in relation to DNA repair and cancer coincidence in family members. Int.J.Can. **54**: 589-593.

Kohn, K.W., Erickson, L.C., Ewig, R.A., *et al.* 1976. Fractionation of DNA from mammalian cells by alkaline elution. Biochem. **15**: 4629-4637.

Komatsu, K., Kubota, N., Gallo, M., *et al.* 1995. The Scid factor on Human Chromosome 11 Restores V(D)J recombination in addition to Double-strand break Repair. Can.Res. **55**: 1774-1779.

Komatsu, K., Yoshida, M. and Okymura, Y. 1993. Murine Scid cells complement ataxia-telangiectasia cells and show a normal post-irradiation response of DNA synthesis. Int.J.Radiat.Biol. **63**: 725-730.

Kufe, D.W., Major, P.P., Munroe, D., *et al.* 1983. Relationship between Incorporation of 9-β-D-Arabinofuranosyladenine in LIZ10 DNA and Cytoxicity. Can.Res. **43**: 2000-2004.

Kurimasa, A., Nagata, Y., Shimizu, M., *et al.* 1994. A human gene that restores DNA-repair defect in SCID mice is located on 8p11.1-q11.1 Hum.Gen. **93**: 21-26.

Lakin, N.D., Weber, P., Srankovic, T., *et al.* 1996. Analysis of the ATM protein in wild-type and ataxia telangiectasia. Oncogene. **13**: 2707-2716.

Lavin , M.F., Khanna, K.K., Beamish, H., *et al.* 1995. Relationship of the ataxia-telangiectasia protein ATM to phosphoinositide 3-kinase. TIBS. 382-383.

Leber, R., Wise, T.W., Mizuta, R., *et al.* 1998. The XRCC4 gene product is a target for and interacts with the DNA-dependent protein kinase. J.Biol.Chem. **273**: 1794-1801.

Lambert, H., Pankou, R., Gauthier, J., *et al.* 1990. Electroporation-mediated uptake of proteins into mammalian cells. Biochem.Cell.Biol. **68**: 729-734.

Lea, D.E. and Catcheside, D.G. 1942. The mechanism of the induction by radiation of chromosome aberrations in *Tradescentia*. J.Genet. **44**: 216-245.

Lee, W.W., *et al.* 1960. Potential anticancer agents.XL.Synthesis of β- anomer of 9(-D-arabinofuranosyl)-adenine. J.Am.Chem.Soc. **82**: 2648-2649.

Lee, S.E., Mitchell, R.A. and Cheng, A., *et al.* 1997. Evidence for DNA-PK dependent and -independent DNA double-strand break pathways in mammalian cells as a function of the cell cycle. Mol.Cell.Biol. **17**: 1425-1433.

Lees-Miller, S.P., Godbout, R., Chan, D.W., *et al.* 1995. Absence of p350 subunit of DNA-Activated Protein kinase from a radiosensitive Human Cell Line. Science. **267**: 1183-1185.

Lehmann, A.R. and Carr, A.M. 1994. DNA damage, repair and the cell cycle. Trend.Cell.Biol. **4**: 24-26.

Lehmann, A.R. and Stevens, S. 1977. The production and repair of double-strand breaks in cells from normal humans and from patients with ataxia telangiectasia. Biochemica et Biophysica Acta. **474**: 49-60.

LePage, G.A. 1970. Arabinosyladenine and arabinosylhypoxanthine metabolism in murine tumor cells. Can.J.Biochem. **48**: 75-78.

Lerman, L.S. and Firsch, H.L. 1982. Why does the electrophoretic mobility of DNA in gels vary with the length of the molecule? Biopolymers. **21**: 995-997.

Lewis, S.M. 1994. P nucleotide insertions and the resolution of hairpin DNA structures in mammalian cells. Proc.Natl.Acad.Sci.USA. **91**: 1332-1336.

Lewis, S.M. and Hesse, J.E. 1991. Cutting and closing without recombination in V(D)J joining. EMBO.J. **10**: 3631-3639.

Li, Z.,Otevrel, T., Gao, Y., *et al* .1995b. The XRCC4 Gene Encodes a Novel Protein Involved in DNA Double-strand Break Repair and V(D)J Recombination. Cell. **83**: 1079-1089.

Li, G.C., Yang, S.H., Kim, D., *et al.* 1995a. Suppression of heat-induced hsp70 expression by the 70Kda subunit of the human Ku autoantigen. Biochem. **92**: 4512-4516.

Lieber, M.R. 1991. Site-specific recombination in the immune system. FASEB. **5**: 2934-2944.

Lieber, M.R. 1992. The mechanism of V(D)J Recombination: A Balance of Diversity, Specificity, and Stability. Cell. **70**: 873-876.

Lieber, M.R. 1996. Immunoglobulin diversity: Rearranging by cutting and repairing. Current Biology. **6**: 134-136.

Lieber, M.R., Grawunder, U., Wu, X., *et al.* 1997. Tying loose ends: roles of Ku and DNA-dependent protein kinase in the repair of double-strand breaks. Current Biology. **7**: 99-104.

Lieber, M.R., Hesse, J.E., Lewis, S., *et al.* 1988. The defect in murine severe combined immune deficiency: Joining of signal sequences but not coding segments in V(D)J recombination. Cell. **55**: 7-16.

Lin, W-C. and Desidero, S. 1995. V(D)J recombination and the cell cycle. Immun.Today. **16**(6): 279-289.

Lin, J.Y., Multilmann-Diaz, M.I., Stackhouse, M.A., *et al.* 1997. An ionizing radiation-sensitive CHO mutant cell line: irs-20. IV. Genetic complementation, V(D)J recombination and the SCID phenotype. Radiat.Res. **147**: 166-171.

Liu, N. 1994. Hypersensitivity of ataxia telangiectasia cells to DNA double-strand breaks. Ph.D. Thesis, University of St. Andrews. Scotland.

Liu, N. and Bryant, P.E. 1993. Response of ataxia telangiectasis cells to restriction endonuclease induced DNA double-strand breaks: I. Cytogenetic characterization. Mutagenesis. **8**: 503-510.

Liu, N. and Bryant, P.E. 1994. Enhanced chromosomal response of ataxia-telangiectasia cells to specific types of DNA double-strand breaks. Int.J.Radiat.Biol. **66**: S115-S121.

Liu, N. and Bryant, P.E. 1997. Enhancement of frequencies of restriction endonuclease-induced chromatid breaks by arabinoside adenine in normal human and ataxia telangiectasia cells. Int.J.Radiat.Biol. **72**: 285-292.

Liu, N., Lamerdin, J.E., Tucker, J.D., *et al.* 1997. The human XRCC9 gene corrects chromosomal instability and mutagen sensitivities in CHO UV40 cells. Proc.Natl.Acad.Sci.USA. **94**: 9232-9237.

Liu, N., Lamerdin, J.E., Tebbs, R.S., *et al.* 1998. XRCC2 and XRCC3, new human Rad51-family members, promote chromosome stability and protect against DNA cross-links and other damage. Mol.Cell. **1**: 1-20.

Ljungman, M., Nyberg, S., Nygern, J., *et al.* 1991. DNA-bound Proteins Contribute Much More than Soluble Intracellular Compounds to the Intrinsic Protection against Radiation-Induced DNA strand Breaks in Human Cells. Radiat.Res. **127**: 171-176.

Lock, R.B., Ross, W.E., 1990. Inhibition of p34cdc2 kinase acting by eptoposide or irradiated as a mechanism of G2 arrest in Chinese hamster cells. Can.Res. **15**: 3761-3766.

Lohman, P.H.M., *et al.* 1995. Meeting report. Role of molecular biology in radiation biology. Int.J.Radiat.Res. **68**: 331-340.

Lumpkin, O.J., Dejardin, P., Zimm, B.H. 1985. Theory of gel electrophoresis of DNA. Biopolymers. **24**: 1573-1593.

Lustig, A.J. 1999. The kudos of non-homologous end-joining. Nature Genetics. **23**: 130-132.

Lutze, L.H., Cleaver, J.E., Morgan, W.F. and Winegar, R.A. 1993. Mechanisms involved in rejoining DNA double-strand breaks induced by ionizing radiation and restriction enzymes. Mutat.Res. **299**: 225-232.

MacLeod, R.A.F. and Bryant, P.E. 1990. Similar kinetics of X-ray induced chromatid aberrations in xrs5 and wildtype CHO cells. Mutagenesis. **5**: 407-410.

MacLeod, R.A.F. and Bryant, P.E. 1992. Effects of adenine aradinoside and coformycin on the kinetics of G2 chromatid aberrations in X-irradiated lymphocytes. Mutagenesis. **7**: 285-290.

McBlane, J.F., van Gent, D.C., Ramsden, D.A., *et al.* 1995. Cleavage at a V(D)J Recombination Signal requires Only RAG1 and RAG2 Proteins and Occurs in Two Steps. Cell. **83**: 387-395.

McMillan, T.J. and Cassoni, A.M. 1990. The relationship of DNA double-strand break induction to radiosensitivity in human tumour cell lines. Int.J.Radiat.Biol. **58**: 427-438.

Malyapa, R.S., Wright, W.D., and Roti Roti, J.L. 1994. Radiation Sensitivity Correlates with Changes in DNA supercoiling and Nucleoid Protein Content in Cells of three Chinese Hamster Cell lines. Radiat.Res. **140**: 312-320.

Malynn, B.A., Blackwell, T.K., Fulop, G.M., *et al.* 1988. The Scid Defect affects the final step of the immunoglobulin VDJ Recombinase Mechanism. Cell. **54**: 453 460.

Mateos, S., Slijepcevic, P., Macleod, R.A., *et al.* 1994. DNA double-strand break rejoining in xrs5 cells is more rapid in the G2 than in the G1 phase of the cell cycle. Mutat.Res. **315**: 181-187.

Melek, M. Gellert, M., van Gent, D.C. 1998. Rejoining of DNA by the RAG1 and RAG2 proteins. Science. **280**: 301-303

Miller, R.D., Hogg, J., Ozaki, J.H., *et al.* 1995. Gene for the catalytic subunit of mouse DNA-dependent protein kinase maps to the scid locus. Proc.Natl.Acad.Sci.USA. **92**: 10792-10795.

Mimori, T. and Hardin, J.A. 1986. Mechanism of interaction between ku Protein and DNA. J.Biol.Chem. **261**: 10375-10379.

Mirkovitch, J., Gasser, S.M., Lammeli, U.K., *et al.* 1987. Relation of chromosome structure and gene expression. Phil.Trans.R.Soc.Lond.B. **317**: 563-574.

Mombaerts, P., Lacomini, J., Johnson, R.S., *et al.* 1992. RAG-1-deficient mice have no mature B and T lymphocytes. Cell. **68**: 869-877.

Morgan, W.F., *et al.* 1990. The use of restriction endonucleases to mimic the cytogenetic damage induced by ionizing radiation. In ionizing radiation damage to DNA: Molecular Aspects. Edited by Wallace, S.S. and Painter, R.B. Wiley-Liss. New York. p191-199.

Morgan, W.F., Ager, D., Chung, H.W., *et al.* 1990. The cytogenetic effects of restriction endonucleases following their introduction into cells by electroporation. Prog.Clin.Biol.Res. **340B**: 355-61.

Morgan, W.F., Chung, H.W., Phillips, J.W., *et al.* 1989. Restriction endonucleases do not induce sister-chromatid exchanges in Chinese hamster ovary cells. Mutat.Res. **226**: 203-209.

Morgan, W.F., Corcoran, J., Hartmann, A., *et al.* 1998. DNA double-strand breaks, chromosomal rearrangements and genomic instability. Mutat.Res. **404**: 125-128.

Morgan, W.F., Day, J.P., Kaplan, M.I., *et al.* 1996. Genomic instability induced by ionising radiation. Radiat.Res. **146**: 247-258.

Morgan, W.F., Djordjevic, M.C., *et al* 1985. Delayed repair of DNA single-strand breaks does not increase cytogenetic damage. Int.J.Radiat.Biol.Relat.Stud.Phys.Chem.Med. **48**: 711-721.

Morgan, W.F., Fero, M.L., Land, M.C., *et al.* 1988. Inducible Expression and Cytogenetic Effects of the EcoRI Restriction Endonuclease in Chinese Hamster Ovary cells. Mol.Cell.Biol. **8**: 4204-4211.

Morgan, W.F., Valcarel, E.R., Columna, E., *et al.* 1991. Induction of Chromosome Damage by Restriction Enzymes during Mitosis. Radiat.Res. **127**: 101-106.

Moses, S.A.M., Christie, A.F., Bryant, P.E., *et al.* 1990. Clastogenecity of PvuII and EcoRI in electroporated CHO cells assayed by metaphase chromosomal aberrations and by micronuclei using the cytokinesis-block technique. Mutagenesis. **5**: 599-603.

Mozdarani, H. and Bryant, P.E. 1987. The effect of 9-β-D-arabinofuranosyladenine on the formation of X-ray induced chromatid aberrations in X-irradiated G2 human cells. Mutagenesis. **2**: 371-374.

Mozdarani, H. and Bryant, P.E. 1989a. Induction and rejoining of chromatid breaks in X-irradiated A-T and normal human G2 fibroblasts. Int.J.Radiat.Biol. **56**: 645-650.

Mozdarani, H. and Bryant, P.E. 1989b. Kinetics of chromatid aberrations in G2 ataxia-telangiectasia cells exposed to X-rays and araA. Int.J.Radiat.Biol. **55**: 71-84.

Müller, W.E., Maidhof, A., Zhan, R.K., *et al.* 1977, Effect of 9-β-D-Arabinofuransoyladanine on DNA synthesis In vivo. Can.Res. **37**: 2282-2290.

Müller, W.E., Rohde, H.J , Beyer, R., *et al.* 1975. Mode of action of 9-β-D-arabinofuranosyladenine on the synthesis of DNA, RNA and protein *in vivo* and *in vitro*. Can.Res. **33**: 2160-2168.

Müller, W.E. and Zhan, R.K. 1978. Biochemistry of antivirals mechanism of action and pharmacology. Res.Mol.Biol. **9**: 18-32.

Muller, C., Calsou, P., Frit, P., *et al.* 1998. UV sensitivity and impaired nucleotide excision repair in DNA-dependent protein kinase mutant cells. Nucl.Acid.Res. **26**: 1382-1389.

Nackerdien, Z., Michie, J., Bohm, L., 1989. Chromatin decondensation by acetlyation shows an elevated radiation response. Radiat.Res. **117**: 234-244.

Natarajan, A.T. and Obe, G. 1984. Molecular mechanisms involved in the production of chromosomal aberrations III. Restriction endonucleases. Chromosoma. **90**: 120-127.

Natarajan, A.T., Mullenders, L.H., Meijeis, M., *et al.* 1985. Induction of sister chromatid exchanges by restriction endonucleases. Mutat.Res. **144**: 33-39.

Nelms, B.E., Maser, R.S., MacKay, J.F., *et al.* 1998. In situ visualization of DNA double-strand break repair in human fibroblasts. Science. **280**: 590-592.

Nevaldine, B., Longo, J.A., Hahn, P.J., *et al.* 1997. The scid defect has a much slower repair of DNA double-strand breaks but not high levels of residual breaks. Radiat.Res. **147**: 535-540.

Nussenzweig, A., Chen, C., da Losta Soores, V., *et al.* 1996. Requirement for Ku80 in growth and immunoglobulin V(D)J recombination. Nature. **382**: 551-555.

Nussenzweig, A., Sokol, K., Burgman, P., *et al.* 1997. Hypersensitivity of Ku80-deficient cell lines and mice to DNA damage: The effects of ionizing radiation on growth, survival, and development. Proc.Natl.Acad.Sci.USA. **94**: 13588-13593.

Obe, G., Johannes, C., Schulte-Frohilde, D., *et al.* 1992. DNA double-strand breaks induced by sparsely ionising radiation and endonucleases as critical lesions for cell death, chromosomal aberrations, mutations and oncogenic transformation. Mutagenesis. **7**: 3-12.

Obe, G., Johannes, C., Weithmann, I., *et al.* 1993. Chromatid type aberrations induced by AluI in Chinese hamster ovary cells. Mutat.Res. **299**: 305-311.

Obe, G. and Kamra, OmP. 1986. Elevation of AluI induced frequencies of chromosomal aberrations in Chinese hamster ovary cells by neurospoara crasse endonuclease and by ammonium sulphate. Mutat.Res. **174**: 35-46.

Obe, G., Palihi, F., Tanzarella, C., *et al.* 1985. Chromosomal aberrations induced by restriction endonucleases. Mutat.Res. **150**: 359-368.

Obe, G., Van der Hude, W., Scheutwinkel-Reich, M., *et al.* 1986. The restriction endonuclease AluI induces chromosomal aberrations and mutations in the hypoxanthine phosphoryl transferase locus but not in the Na^+/K^+ ATPase locus in V79 hamster cells. Mutat.Res. **174**: 71-74.

Oettinger, M.A. 1996. Cutting apart V(D)J recombination. Curr.Opin.Genet.Dev. **6**: 141-145.

Oettinger, M.A., Schatz, Gorka, C., *et al.* 1990. RAG-1 and RAG-2, Adjacent Genes that Synergistically Activate V(D)J Recombination. Science. **248**: 1517-1523.

Ohno, Y., Spriggs, D., Matsukage, A., *et al.* 1989. Sequence-specific Inhibition of DNA strand Elongation by Incorporation of 9-β-D-Arabinofuranosyladenine. Can.Res. **49**: 2077-2081.

Okayasu, R., Bloecher, D. and Iliakis, G., *et al.* 1988. Variation through the cell cycle in the dose-response of DNA neutral filter elution in X-irradiated synchronous CHO cells. Int.J.Radiat.Biol. **53**: 729-747.

Okayasu, R. and Iliakis, G. 1993. Ionizing radiation induces two forms of interphase chromosome breaks in Chinese hamster ovary cells that rejoin with different kinetics and show different sensitivity to treatment in hypertonic medium or beta-araA. Radiat.Res. **136**: 262-270.

Okayasu, R. and Iliakis, G. 1994. Evidence that the product of the xrs gene is predominantly involved in the repair of a subset of radiation-induced interphase chromosome breaks rejoining with fast kinetics. Radiat.Res. **138**: 34-43.

Okazaki, K., Nishikawa, S.I. and Sakano, H. 1988. Aberrant Immunoglobulin gene rearrangement in SCID mouse bone marrow cells. J.Immun. **141**: 1348-1352.

Okura, A. and Yoshida, S. 1978. Differential Inhibition of DNA Polymerases of Calf Thymus by 9-β-D-Arabinofranosyladenine-5'-triphosphate. J.Biochem. **84**: 727-732.

Pang, D., Yuo, S., Dynan, W.S., *et al.* 1997. Ku proteins join DNA fragments as shown by atomic force microscopy. Can.Res. **57**: 1412-1415.

Pantelias, G.E. Radiation-induced cytogenetic damage in relation to changes in interphase chromosome conformation. Radiat.Res. **105**: 341-350.

Parker, W.B., Bapat, A.R., Shen, J.X., *et al.* 1988. Interaction of 2-halogenated dATP analogs (F, Cl and Br) with human DNA polymerases, DNA primase and ribonucleotide reductase. Mol.Pharma. **34**: 485-591.

Parshad, R., Gantt, R., Sanford, K.K., *et al.* 1982. Repair of chromosome damage induced by x-irradiation during G2 phase in a line of normal human fibroblasts and its malignant derivative. J.Natl.Can.Inst. **69**: 409-414.

Parshad, R., Sanford, K.K., Jones, G.M., *et al.* 1983. Chromatid damage after G2 phase X-irradiation of cells from cancer-prone individuals implicates deficiency in DNA repair. Proc.Natl.Acad.Sci.USA. **80**: 5612-5616.

Parshad, R., Gantt, R., Sanford, K.K., *et al.* 1984. Chromosomal radiosensitivity of human tumor cells during the G2 cell cycle period. Can.Res. **44**: 5577-5582.

Parshad, R., Sanford, K.K., Jones, G.M., *et al.* 1985a. G2 chromosomal radiosensitivity of ataxia-telangiectasia heterozygotes. Can.Genet.Cytogenet. **14**: 163-168.

Parshad, R., Sanford, K.K., Jones, G.M. 1985b. Chromosomal radiosensitivity during the G2 cell-cycle period of skin fibroblasts from individuals with familial cancer. Proc.Natl.Acad.Sci.USA. **82**: 5400-5403.

Parshad, R., Price, F.M., Pirollo, K.F., *et al.* 1993. Cytogenetic response to G2 phase X-irradiation in relation to DNA repair and radiosensitivity in a cancer-prone family with Li-fraumeni syndrome. Radiat.Res. **136**: 236-240.

Patil, M.S., Locher, S.E., Hariharan, P.V., *et al.* 1985. Radiation-induced thymine base damage and its excision repair in active and inactive chromosomes of Hela cells. Int.J.Radiat.Biol.Relat.Stud.Phys.Chem.Med. **48**: 691-700.

Pennycook, J., Marshall, A., Chang, Y., *et al.* 1996. High frequency of normal IgH rearrangement in scid mice. Ann.N.Y.Acad.Sci. **764**: 121-122.

Pergola, F., Zdzienicka, M.Z. and Lieber, M.R. 1993. V(D)J Recombination in Mammalian Cell Mutants Defective in DNA Double-Strand Break Repair. Mol.Cell.Biol. **13**(6): 3464-3471.

Peterson, S.R., Kurimasa, A., Oshimwa, M., *et al.* 1995. Loss of the catalytic subunit of the DNA-dependent protein kinase in DNA double-strand-break-repair mutant mammalian cells. Proc.Natl.Acad.SCi.USA. **92**: 3171-3174.

Peterson, S.R., Stackhouse, M., Waltman, M.J., *et al.* 1997. Characterization of two DNA double-stranded break repair-deficient cell lines that express inactive DNA-dependent protein kinase catalytic subunits. J.Biol.Chem. **272**: 10227-10231.

Petrini, J.H. 1999. The mammalian Mre11-Rad50-Nbs1 protein complex: integration of functions in the cellular DNA-damage response. Am.J.Hum.Genet. **64**: 1264-1269.

Phillips, J.W. and Morgan, W.F. 1994. Illegitimate recombination induced by DNA double strand breaks in a mammalian chromosome. Mol.Cell.Biol. **14**: 5794-5803.

Phillips, R.A. and Fulop, G.M. 1989. Pleiotropic effects of the Scid mutation: effects on lymphoid Differentiation and on repair of radiation damage. Curr.Top.Microbiol.Immunol. **152**: 10-17.

Plunkett, W. and Cohen, S.S. 1975. Two approaches that increase the activity of analogs of adenine nucleosides in animal cells. **35**: 1547-1554.

Plunkett, W., Lapi, L., Ortiz, P.J., *et al.* 1974. Penetration of mouse fibroblasts by the 5'-phosphate of 9-β-D-arabinofuranosyladenine and Incorporation of the nucleotide into DNA. Proc.Natl.Acad.Sci.USA. **71**: 73-77.

Poltoratsky, V.P., Shi, Y., York, J.D., *et al.* 1995. Human DNA-Activated Protein Kinase (DNA-PK) Is Homologous to Phosphatidylinositol kinases. J.Immunol. **155**: 4529-4533.

Priestley, A., Beamish, H.J., Gell, D., *et al.* 1998. Molecular and biochemical characterisation of DNA-dependent protein kinase-defective rodent mutant irs-20. Nucl.Acid.Res. **26**: 1965-1973.

Ramsden, D.A., McBlane, J.F., van Gent, D.C., *et al.* 1996. Distinct DNA sequence and structure requirements for the two steps of V(D)J recombination signal cleavage. EMBO.J. **15**(12): 3197-3206.

Ramsden, D.A., van Gent, D.C. and Gellert, M. 1997. Specificity in V(D)J recombination: new lessons from biochemistry and genetics. Curr.Opin.Immunol. **9**: 114-120.

Rathmell, W.K. and Chu, G. 1994a. A DNA End-Binding factor involved in Double-Strand Break Repair and VDJ Recombination. Mol.Cell.Biol. **14**: 4741-4748.

Rathmell, W.K. and Chu, G. 1994b. Involvement of the ku autoantigen in the cellular response to DNA double-strand breaks. Proc.Natl.Acad.Sci.USA. **91**: 7623-7627.

Reeves, W.H. and Sthoeger, Z.M. 1989b. Molecular Cloning of cDNA Encoding the p70 (ku) Lupus Autoantigen. J.Biol.Chem. **264**: 5047-5052.

Revell, S.H. 1955. A new hypothesis for "chromatid" exchanges in Z.M.bacq and P.Alexander (Eds.). Proc.Radiobiol.Symposium, *Lèige*, Butterworths, London. 1954. 243-253.

Revell, S.H. 1958. A new Hypothesis for the interpretation of chromatid aberrations and its relevance to theories for the mode of action of chemical agents. Ann.N.Y.Acad.Sci. **68**: 802-807.

Revell, S.H. 1966. Evidence for a dose-squared term in the dose response curve for real chromatid discontinuities induced by X-rays, and some theoretical consequences thereof. Mutat.Res. **3**: 34-53.

Revell, S.H. 1974. The breakage- and -reunion theory for chromosomal aberrations induced by ionizing radiation: a short history. Adv.Radiat.Biol. 4: 367-416.

Riabowol, K., Draetta, G., Brizuela, L., *et al.* 1989. The cdc^2 kinase is a nuclear protein that is essential for mitosis in mammalian cells. Cell. **57**: 393-401.

Roberts, S.A. 1999. Heritability of cellular radiosensitivity: a marker of low-penetrance predisposition genes in breast cancer. Am.J.Hum.Genet. **65**: 784-794.

Rosemann, M., Kanon, B., Konings, A.W., *et al.* 1993. An image analysis technique for the detection of radiation-induced DNA fragmentation after CHEF electrophoresis. Int.J.Radiat.Biol. **64**: 245-249.

Rosen, F.S., Max, M.D., *et al.* 1984. The Primary Immunodeficiencies. (second of two parts). New Eng.J.Med. **311**: 300-310.

Rosen, F.S., Max, M.D., *et al.* 1995. The Primary Immunodeficiencies. New Eng.J.Med. **333**: 431-440.

Ross, G.M., Eady, J.J., Mithal, N.P., *et al.* 1995. DNA Strand Break Rejoining Defect in xrs-6 Is Complemented by Transfection with the Human ku80 Gene. Can.Res. **55**: 1235-1238.

Roth, D.B., Lindahl, T. and Gellert, M. 1995. How to make ends meet. Curr.Biol. **5**: 496-499.

Roth, D.B., Menetski, J.P., Nakajima, P.B., *et al.* 1992. V(D)J recombination: broken DNA molecules with covalently sealed (hairpin) coding ends in SCID mouse thymocytes. Cell. **70**: 938-991.

Roth, D.B., Porter, T.N., Wilson, J.H., *et al.* 1985. Mechanisms of non-homologous recombination in mammalian cells. Mol.Cell.Biol. **5**: 2599-2607.

Roth, D.B. and Wilson, J.H. 1985. Relative rates of homologous and nonhomologous recombination in transfected DNA. **82**: 3355-3359.

Roth, D.B. and Wilson, J.H. 1986. Nonhomologous recombination in mammalian cells: role for short sequence homologies in the rejoining reaction. Mol.Cell.Biol. **6**: 4295-4304.

Roti-Roti, J.L and Wright, W.D. 1987. Visualization of DNA loops in nucleoids from HeLa cells: assays for DNA damage and repair. Cytometry. **8**: 461-467.

Sachs, R.K., van den Engh, G., Trask, B., *et al.* 1995. A random walk/giant-loop model for interphase chromosomes. Proc.Natl.Acad.Sci.USA. **92**: 2710-2714.

Sanford, K.K., Tarone, R.E., Parshad, R., *et al.* 1987. Hypersensitivity to G2 chromatid radiation damage in familial dysplastic naevus syndrome. Lancet. **2**: 1111-1116.

Sanford, K.K., Parshad, R., Ganh, R., *et al.* 1989. Factors affecting and significance of G2 chromatin radiosensitivity in predisposition to cancer. Int.J.Radiat.Biol. **55**(6): 963-981.

Sanford, K.K., Parshad, R., Price, F.M., *et al.* 1990. Enhanced chromatid damage in blood lymphocytes after G2 phase X-irradiation, a marker of the ataxia-telangiectasia gene. J.Natl.Cancer.Inst. **82**: 1050-1054.

Sanford, K.K., Parshad, R., Price, F.M., *et al.* 1993. X-ray induced chromatid damage in cells from Down syndrome and Alzheimer disease patients in relation to DNA repair and cancer proneness. Can.Genet.Cytogenet. **70**: 25-30.

Sanford, K.K., Parshad, R., Price, F.M., *et al.* 1996. Cytogenetic responses to G2 phase X-irradiation of cells from retinoblastoma patients. Can.Genet.Cytogenet. **88**: 43-48.

Sargent, R.G., Brenneman, M.A., and Wilson, J.H. 1997. Repair of site-specific double strand breaks in a mammalian chromosome by homologous and illegitimate recombination. Mol.Cell.Biol. **17**: 267-277.

Savage, J.R.K. *et al.* 1968. chromatid aberrations in *Tradescantia Bracteta* and a further test of Revell's hypothesis. Mutat.Res. 15: 47-56.

Savage, J.R.K. 1986. The "Revell loop" Clinical cytogenetics Bulletin. **1**: 192-196.

Sax, K. 1938. Chromosome aberrations induced by X-rays. Genetics. **23**: 494-516.

Sax, K. 1940. An analysis of X-ray induced chromosomal aberrations in *Tradescantia*. Genetics. **25**: 41-68.

Sax, K. 1941. Types and frequencies of chromosome aberrations induced by X-rays. Cold.Spring Harb.Symp.Quant.Biol. **9**: 93-103.

Schlissel, M., Constantinescu, A., Morrow, T., *et al.* 1993. Double-strand signal sequence breaks in V(D)J recombination are blunt, 5' phosphorylated, RAG-dependent, and cell cycle regulated. Gene.Dev. **7**: 2520-2532.

Schuler, W. 1990. The Scid Mouse Mutant: Biology and Nature of the Defect. Cytokines **3** : 132-153.

Schuler, W., Weiler, I.J., Schuler, A., *et al.* 1986. Rearrangement of Antigen Receptor Genes is Defective in Mice with Severe Combined Immune Deficiency. Cell. **46**: 963-972.

Schuler,W., Ruetsch, N.R., Amsler, M., *et al.* 1991. Coding joint formation of endogenous T cell receptor genes in lymphoid cells from Scid mice: unusual P-nucleotide additions in VJ-coding joints. Eur.J.Immunol. **21**: 589-596.

Schwartz, D.C. and Cantor, C.R. 1984. Separation of Yeast chromosome-sized DNAs by pulsed field gel electrophoresis. Cell. **37**: 67-75.

Schwartz, J.L., Cowen, J.M, Moan, E., *et al.* 1993. Metaphase chromosome and nucleoid differences between CHO-KI cells and its radiosensitive derivative xrs5. Mutagenesis. **8**: 105-108.

Schwartz, J.L., Brinkman, W.J., Kasten, L., *et al.* 1995. Altered metaphase chromosome structure in xrs-5 cells is not related to its radiation sensitivity or defective DNA break rejoining. Mutat.Res. **328**: 119-126.

Scott, D., Spreadborough, A.R., Levine, E., *et al.* 1994. Genetic Predisposition in breast cancer. Lancet **344**: 1444.

Scott, D., Spreadborough, A.R., Jones, L.A., *et al.* 1996. Chromosomal Radiosensitivity in G2-phase Lymphocytes as an Indicator of Cancer Predisposition. Radiat.Res. **145**: 3-16.

Shannon, W.M. 1975. Adenine arabinoside: Antiviral activity *in vitro.* In: Adenine Aradinoside; an antiviral agent. Pavan-lonston, D., Buchanan, R.A. and Alford, C.A. (Eds) Ravan press, N.Y. p 1-43.

Shin, E.K., Perryman, L.E. and Meek, K. 1997. A kinase-negative mutation of DNA-PK_{CS} in equine SCID results in defective coding and signal joint formation. J.Immunol. **158**: 3565-3569.

Shinkai, Y., Rathbun, G., Lam, K.P., *et al.* 1992. RAG-2-Deficient Mice Lack Mature Lymphocytes Owing to Inability to initiate VDJ Rearrangement. Cell. **68**: 855-867.

Sinclair, W.K. and Morton, R.A. 1966. X-ray sensitivity during the cell generation cycle of cultured Chinese hamster cells. Radiat.Res. **29**: 450-474.

Sinclair, W.K. 1968. Cyclic X-ray responses in mammalian cells in vitro. Radiat.Res. **33**: 620-643.

Singh, B. and Bryant, P.E. 1991. Induction of mutations at the thymidine kinase locus in CHO cells by restriction endonucleases. Mutagenesis. **6**: 219-223.

Singleton, B.K., Priestley, A., Steingrimsdottir, H., *et al.* 1997. Molecular and biochemical characterization of xrs mutants defective in Ku80. Mol.Cell.Biol. **17**: 1264-1273.

Smider, V., Rathmell, W.K., Lieber, M.R., *et al.* 1994. Restoration of X-ray resistance an V(D)J Recombination in Mutant Cells by ku cDNA. Science. **266**: 288-291.

Smith, C.L., Matsumoto, T., Niwa, O., *et al.* 1987. An electrophoretic karyotype for *Schizosaccharomyces pombe* by pulsed-field gel electrophoresis. Nucl.Acid.Res. **15**; 4481-4489.

Snell, R.G. and Wilkins, R.J. 1986. Separation of chromosomal DNA molecules from *C.albicans* by pulsed-field gel electrophoresis. Nucl.Acid.Res. **14**: 4401-4406.

Spanopoulou, E., Cortes, P., Shih, C., *et al.* 1995. Localization, Interaction, and RNA binding properties of the V(D)J recombination-activating proteins RAG1 and RAG2. Immunity. **3**: 715-726.

Stamato, T.D. and Denko, N. 1990. Asymmetric field inversion gel electrophoresis: A new method for detecting DNA double-strand breaks in mammalian cells. Radiat.Res. **121**: 196-205.

Stamato, T.D., Dipatri, A., and Giaccia, A. 1988. Cell-Cycle-Dependent Repair of Potentially Lethal Damage in the XR1 γ-ray sensitive Chinese Hamster Ovary cell. Radiat.Res. **115**: 325-333.

Stamato, T.D., Weinstein, R., Giaccia, A., *et al.* 1983. Isolation of cell cycle-dependent gamma ray-sensitive Chinese hamster ovary cell. Som.Cell.Genet. **9**: 165-173.

Staunton, J.E. and Weaver, D.T. 1994. scid cells efficiently integrate hairpin and linear substrates. Mol.Cell.Biol. **14**: 3876-3883.

Stoilvo, L., Mullenders, L.H.F. and Natarajan, A.T. 1986. Influence of bromodeoxyuridine substitution of the thymidine as sister-chromatid exchanges and chromosomal aberrations induced by restriction endonucleases. Mutat.Res. **174**: 295-301.

Surralles, J., Puerto, S., Ramirez, M.J., *et al.* 1998. Links between chromatin structure, DNA repair and chromosome fragility. Mutat.Res. **404**: 39-44.

Suwa, A., Hirakata, M., Takeda, Y., *et al.* 1994. DNA-dependent protein kinase (ku protein-p350 complex) assembles on double-stranded DNA. Proc.Natl.Acad.Sci.USA. **91**: 6904-6908.

Taccioli, G.E., Rathbun, G., Shinkai, Y., *et al.* 1992. Activities involved in V(D)J recombination. Curr.Top.Microbiol.Immunol. **182**: 107-114.

Taccioli, G.E., Rathburn, G., Oltz, E., *et al.* 1993. Impairment of V(D)J recombination in Double-Strand Break Repair Mutants. Science. **260**: 207-210.

Taccioli, G.E., Cheng, H.L., Varghese, A.J., *et al.* 1994a. A DNA Repair Defect in Chinese Hamster Ovary Cells Affects V(D)J Recombination Similarly to the Murine SCID mutation. J.Biol.Chem. **269**: 7439-7442.

Taccoili, G.E., Gottlieb, T.M., Blunt, T., *et al.* 1994b. Ku80: Product of the XRCC5 Gene and Its Role in DNA Repair and V(D)J Recombination. Science. **265**: 1442-1445.

Takiguchi, Y., Kurimasa, A., Chen, F., *et al.* 1996. Genomic structure and chromosomal assignment of mouse Ku70 gene. Genomics. **35**: 129-135.

Tanaka, T., Yamagami, T., Oka, Y., *et al.* 1993. The Scid mutation in mice causes defects in the repair system for both double-strand DNA breaks and DNA cross-links. Mutat.Res. **288**: 277-280.

Taniguchi, S., Hirabayashi, Y., Inoue, T., *et al.* 1993. Haemopoietic stem-cell compartment of the SCID mouse: Double-exponential survival curve after γ irradiation. Proc.Natl.Acad.Sci.USA. **90**: 4354-4358.

Taylor, Y.C., Duncan, P.G., Zhang, X., *et al.* 1991. Differences in the DNA supercoiling response of irradiated cell lines from ataxia-telangiectasia versus unaffected individuals. Int.J.Radiat.Biol. **59**: 359-373.

Tebbs, R.S., Zhao, Y., Tucker, J.D., *et al.* 1995. Correction of chromosomal instability and sensitivity to diverse mutagens by a cloned cDNA of the XRCC3 DNA repair gene. Proc.Natl.Acad.Sci.USA. **92**: 6354-6358.

Teo, S.H. and Jackson, S.P. 1997. Identification of *Saccharomyces cerevisiae* DNA ligase IV: involvement in DNA double-strand break repair. EMBO.J. **16**: 4788-4795.

Thode, S., Schäfer, A., Pfeiffer, P., *et al.* 1990. A novel pathway of DNA end-to-end joining. Cell. **60**: 921-928.

Thompson, L.H. and Jeggo, P.A. 1995. Nomenclature of human genes involved in ionizing radiation sensitivity. Mutat.Res. **337**: 131-134.

Troelstra, C. and Jaspers, N.G.. 1994. Recombination and repair: ku starts at the end. 4: 1149-1151.

TsangLee, M.Y.W., Byrnes, J.J., Downey, K.M., *et al.* 1980. Mechanism of inhibition of deoxyribonucleic acid synthesis by 1-β-D-arabinofuranosyladenine triphosphate and its potentiation by 6-mercaptocuprine ribonucleic 5'-monophosphate. Biochemistry. **19**: 215-219.

Tseng, W.C., Derse, D., Cheng, Y.C., *et al.* 1982. In vitro biological activity of 9-β-fluoradenine and the biochemical activity of its triphosphate on DNA polymerase and ribonucleotide reductase from Hela cells. Mol.Pharm. **21**: 474-477.

Tsukamoto, Y., Karo, J., Ikeda, H., *et al.* 1997. Silencing factors participate in DNA repair and recombination in *Saccharomyces cerevisiae*. Nature. **388**: 900-903.

Tubiana, M., Dutreix, J. and Wambersie, A. 1990. Effects of radiation on DNA molecules and chromosomes in Introduction to Radiobiology. Taylor and Francis. p: 34-78.

Tzung, T.Y. and Runger, T.M. 1998. Reduced joining of DNA double strand breaks with an abnormal mutation spectrum in rodent mutants of DNA-PKcs and Ku80. Int.J.Radiat.Biol. **73**: 469-474.

Ward, J.F. 1990. The yield of DNA double-strand breaks produced intracellularly by ionising radiation: A review. Int.J.Radiat.Biol. **57**: 1141-1150.

Weaver, D.T. 1995. What to do at an end: DNA double-strand-break repair. TIG. **11**: 388-392.

Weaver, D. 1996. Regulation and repair of double-strand DNA breaks. Crit.Rev.Euk.Gene.Exp. **6**: 345-375.

Weaver, D. and Hendrickson E. 1989. The Scid mutation disrupts gene rearrangement at the rejoining of coding strands. Curr.Top.Microbiol.Immunol. **152**: 77-84.

Weaver, D., Boubnov, N., Wills, Z., *et al.* 1996. V(D)J recombination: Double-strand break repair gene products used in the joining mechanism. Ann.N.Y.Acad.Sci. **764**: 99-111.

Weinert, T. 1998. DNA damage and checkpoint pathways: molecular anatomy and interaction with repair. Cell. **94**: 555-558.

Wiler, R., Leber, R., Moore, B.B., *et al.* 1995. Equine severe combined immunodeficiency a defect in V(D)J recombination and DNA-dependent protein kinase activity. Proc.Natl.Acad.Sci.USA. **42**: 11485-11489.

Wilks, D.P., Barry, J., Hughes, M.F., *et al.* 1996. Assessment of light scatter nucleoids as a rapid predictive assay of radiosensitivity. Radiat.Res. **146**: 628-635.

White, E.L. Shaddix, S.C., Brockman, R.W., *et al.* 1982. Comparison of the actions of 9-β-D-Arabinofuranosyl-2-fluoradenine and 9-β-D-Arabinofuranosyladenine on target enzymes from mouse tumour cells. Can.Res. **42**: 2260-2264.

Whitmore, G.F., Varghese, A.J., Gulyas, S., *et al.* 1989. Cell cycle responses of two X-ray sensitive mutants defective in DNA repair. Int.J.Radiat.Biol. **56**: 657-665.

Winegar, R.A. and Preston, J.R. 1988. The induction of chromosome aberrations by restriction endonucleases that produce blunt-end or cohesive-end double-strand breaks. Mutat.Res. **197**: 141-149.

Winegar, R.A., Phillips, J.W., Youngblom, J.H., *et al.* 1989. Cell electroporation is a highly efficient method for introducing restriction endonucleases into cells. Mutat.Res. **225**: 45-53.

Winegar, R.A., Lutze, L.H., Rufer, J.T., *et al.* 1992. Spectrum of mutations produced by specific types of restriction enzyme-induce double-strand break. Mutagenesis. **7**: 439-445.

Wlodek, D., Banath, J. and Olive, P.L. 1991. Comparison between pulsed field and constant-field gel electrophoresis for measurement of DNA double-strand breaks in irradiated Chinese hamster ovary cells. Int.J.Radiat.Biol. **60**: 779-790.

Wlodek, D. and Olive, P.L. 1990. Physical basis for detection of DNA double-strand breaks using neutral filter elution. Radiat.Res. **124**: 326-333.

Woo, R.A. McLure, K.G., Lees-Miller, S.P., *et al.* 1998. DNA-dependent protein kinase acts upstream of p53 in response to DNA damage. Nature. **394**: 700-704.
Wu, X. and Lieber, M.R. 1996. Protein-Protein and Protein-DNA Interaction Regions within the DNA End-binding Protein ku70-ku86. Mol.Cell.Biol. **16**(9): 5186-5193.

Yanagisawa, J., Ando, J., Nokayama, J., *et al.* 1996. A matrix attachment region (MAR) -binding activity due to a p 114 kilodalton protein is found only in human breast carcinomas and not in normal benign breast disease tissue. Can.Res. **56**: 457-462.

Yaneva, M., Kowalewski, T., Lieber, M.R., *et al.* 1997. Interaction of DNA-dependent protein kinase with DNA and with Ku: biochemical and atomic-force microscopy studies. EMBO.J. **16**: 5098-5112.

Yasui, L.S., Ling-Indeck, L., Johnson-Wint, B., *et al.* 1991. Changes in the nuclear structure in the radiation-sensitive CHO mutant cell, xrs-5. Radiat.Res. **127**: 269-277.

Yates, B.L. and Morgan, W.F. 1993. Non-homologous DNA end-joining in chromosomal aberration formation. Mutat.Res. **285**: 53-60.

Yokota, H., van den Engh, G., Hearst, J.E., *et al.* 1995. Evidence for the organization of chromatin in megabase pair-sized loops arranged along a random walk path in the human Go/G1 interphase nucleus. J.Cell.Biol. **130**: 1239-1249.

Zdzienicka, M.Z. 1995. Mammalian mutants defective in the response to ionizing radiation-induced DNA damage. Mutat.Res. **336**: 203-213.

Zdzienicka, M.Z., Jongmans, W., Oshimwa, M., *et al.* 1995. Complementation Analysis of the Murine Scid Cell line. Radiat.Res. **143**: 238-244.

Zdzienicka, M.Z., Tran, Q., van der Schans, G.P., *et al.* 1988. Characterisation of an X-ray hypersensitive mutant of V79 Chinese hamster cells. Mutat.Res. **194**: 239-249.

Zhang, S. and Dong, W. 1987. Chromosomal aberrations induced by the restriction endonucleases EcoRI, PstI, SalI and BamHI in CHO cells. Mutat.Res. **180**: 109-114.

Zhou, P.K., Hendry, J.H., Margisan, P., *et al.* 1997. Comparative measurements of radiation induced DNA double-strand breaks by graded voltage and pulsed-field gel electrophoresis. Int.J.Radiat.Biol. **71**: 95-100.

Zhu, C. and Roth, D.B. 1996. Mechanism of V(D)J recombination. Cancer.Surveys. **28**: 295-309.

Appendices

Appendix One

Giemsa stain

1g of BDH giemsa powder

66ml of glycerol

Mix both constituents and heat at 56-60^{o}C for 1.5-2 h with intermittent agitation.

Cool the mixture and add 66ml of absolute alcohol, shake vigorously.

Leave to mature for 2 weeks.

Final concentration of giemsa 0.76%.

Giemsa (4%) for chromosome staining

4ml giemsa solution (0.76%)

96ml of sorensens buffer.

Sorensens buffer.

Solution A

Potassium dihydrogen orthophosphate 1/15.

Solution B

Di-sodium hydrogen orthophosphate dihydrate.

Mix solution A and B to get a final solution with a pH of 6.8.

Appendix Two

Constant-Field Gel Electrophoresis

Lysis solution

0.4 mol/dm^3 EDTA
2% sodium-N-laurylsarcosine
1mg/ml Proteinase K.
adjust to pH 8.0

Pulsed-Field Gel Electrophoresis

Lysis solution

0.5mol EDTA
0.01 mol Tris
2% N-laurylsarcosine
0.1mg/ml Proteinase K
adjust to pH 8.0.

Appendix Three

Lysis solution for nucleoids

Base lysis solution

150mM NaCl
10mM Tris
10mM EDTA
0.025% v/v Triton X-100
adjust to pH 8.0

To the above solution the concentration of NaCl is adjusted to 0.1M, 1M, 1.5M and 2M.

FISH Buffer

100ml 20xSSC (final concentration 4xSSC)
400ml water
2.5ml Tween 20 10% solution

Denaturing solution

15ml of Formamide
35ml of 2xSSC
FITC and Texas red CAMBIO. UK
FITC 1µl in 500µl of blocking agent
Texas Red 2µl in 500µl of blocking agent

Freezing media

10% DMSO
in Foetal Calf serum (GIBCO-BRL)

Appendix Three continued

Mitotic promoting factor assay

Lysis solution

150mM NaCl
15mM $MgCl_2$
50mM b-Glycerolphosphate
1mM Ditheothreitol
20mM EGTA
25mM NaF
0.5% CHAPS
1mM PMSF

The following two reagents are added to the lysis solution as it is used

1mg/µl leupeptin
1mg/µl aprotinin

Reaction buffer

Make up in 50mM Hepes solution

50mM Tris-HCl
1mM Ditheothreitol
10mM $MgCl_2$
1mM EGTA

Reaction mixture (30µl)

3µl ATP (100mM)

3µ p34cdc2 kinase substrate peptide (365µM)

3.33µci g^{32}P

10µl cell lysate

Make the remainder up with reaction buffer.

Appendix Four

RIPA buffer

Make up in PBS

1% NP40

0.5% Sodium deoxycholate

0.1% SDS

PMSF in serpropanol (10ml ml^{-1}) 10 $ml/\mu l^{-1}$

Aprotinin (Sigma) 30 $ml/\mu l^{-1}$ added immediately prior to use.

Sodium orthoranodose (100mM) 10 $ml/\mu l^{-1}$

Twobin transfer buffer

15.12g Tris

72g Glycine

1 litre Methanol

5 litres H_2O

adjust pH 8.3-8.4

SDS PAGE Stacking gel buffer (x4)

12.11g Tris

SDS 10% solution 8ml (0.4%)

pH 6.8 adjust using conc. HCl

add H_2O to make up to 200ml

SDS PAGE Separating gel buffer (x4)

36.34g Tris (1.5M)

8mls of SDS 10% solution 0.4%

pH 8.8 adjust using conc. HCl

add H_2O to make up to 200ml

SDS PAGE Running buffer (x10)

30g Tris (3%)

144g Glycine (2M)

SDS 10% solution- 100ml (1%)

1 litre H_2O

TBS (x10)

1M Tris

pH 7.5

NaCl (0.9%)

H_20 500ml

Sample buffer (4x)

8g SDS

1M Tris pH 6.8

20g Glycerol

1mg Bromophenol Blue

10ml 2-mercaptoethanol

50 ml H_2O

Appendix five

$Nt = No\ e^{-\lambda t}$

$\ln (Nt/No) = -\lambda t$

For SCID:

$\ln (110/303) = -\lambda 2$

0.49 = rate constant (K)

$t_{1\backslash 2} = \ln (2)/K$

$t_{1\backslash 2} = 1.3$ h

For CB17

$\ln (77.6/ 238) = -\lambda 2$

0.58 = rate constant (K)

$t_{1\backslash 2} = \ln (2)/K$

$t_{1\backslash 2} = 1.2$ h

For $50D^{-}$

$\ln (53/140) = -\lambda 2$

0.48 = rate constant (K)

$t_{1\backslash 2} = \ln (2)/K$

$t_{1\backslash 2} = 1.4$ h

For $100E^{+}$

$\ln (38/94) = -\lambda 2$

0.45 = rate constant (K)

$t_{1\backslash 2} = \ln (2)/K$

$t_{1\backslash 2} = \ln 1.5$h

Appendix Six

Table 1:Percentage of SCID and CB17 cells in each phase of the cell cycle after araC treatment as measured by Facscan analysis using the "cell fit" programme.

Cell line	Time after araC treatment (h)	% cells in each cell cycle phase		
		G_0	G_1	G_2/M
SCID	0	4.2	64	25.5
CB17	0	2.4	68.9	28.6
SCID	4	1.5	28.6	69.9
CB17	4	1.2	43.4	55.4
SCID	6	1.3	28.6	65.2
CB17	6	3.45	36	60.5
SCID	8	0.8	28.6	68.9
CB17	8	4.3	24	71.9
SCID	10	60.2	30.0	8.2
CB17	10	42.5	56.2	1.4

From this initial experiment 8h, after araC treatment, was chosen as the time required to synchronise a maximum number of cells in G2. For every experiment after this a cell sample was taken and analysed using the facscan to determine the percentage of cells in G2 (examples of these results are shown overleaf).

Table 2: Examples of the percentages of SCID and CB17 cells in G2 after treating the cells with araC for 8h.

Cell line	% cells in phase of cell cycle		
	G_0	G_1	G_2/M*
SCID	2.3	24.3	73.4
CB17	1.1	27.0	68.9
SCID	1.87	23.13	75
CB17	2.8	18.0	77.0
SCID	1.56	28.6	69.9
CB17	2.3	28.0	67.2

* Note how reproducible the percentage of cells in G2/M were achieved from the individually collected samples of SCID and CB17 cells, indicating the reproducibility of the results.

Mutagenesis vol.13 no.5 pp.481–485, 1998

G2 chromatid breaks in murine SCID cells

Peter E. Bryant[1,3], Clodagh E. Finnegan[1], Lynda Swaffield[1] and Hossein Mozdarani[2]

[1]School of Biomedical Sciences, University of St Andrews, St Andrews KY16 9TS, UK and [2]School of Medical Sciences, Tarbiat Modaress University, PO Box 14155-4838, Tehran, Islamic Republic of Iran

The G2 chromosomal radiosensitivity of murine SCID (severe combined immunodeficient) and normal fibroblasts has been investigated. We have also investigated the G2 response of these cell lines to the restriction endonuclease *Pvu*II. We show that chromatid breaks are induced linearly with radiation dose in both cell lines and SCID cells are ~1.6 times as radiosensitive as normal murine fibroblasts when tested using a G2 assay with a 2 h sampling time. The disappearance of chromatid breaks with time after irradiation was first order with a half-time of ~1.5 h in both cell lines. Thus, although SCID cells are deficient in the rejoining of double-strand breaks (dsb), they show similar kinetics of disappearance of chromatid breaks with time as normal CB17 cells, indicating that the 'rejoining' of chromatid breaks does not reflect dsb repair. When CB17 and SCID cells were treated with *Pvu*II, which generates dsb in cellular DNA in the presence of streptolysin O (as a porating agent), ~3 times more chromatid breaks were observed in SCID than CB17 cells. We conclude that SCID cells convert a higher number of dsb into chromatid breaks than do CB17 cells. The conversion process is interpreted in terms of the recently proposed 'signal' model, whereby a signal, resulting from a single dsb, triggers the cell to make a recombinational exchange which, if incomplete, gives rise to a visible chromatid break. In terms of the signal model, elevated conversion of dsb into chromatid breaks results from altered signalling and the disappearance of chromatid breaks with time following irradiation represents the completion of recombinational exchanges rather than repair of dsb.

Introduction

Chromosomal radiosensitivity has been shown to vary significantly when measured in different individuals by the 'G2 assay' of human lymphocytes or fibroblasts and elevated radiosensitivity may be linked with a predisposition to cancer (Scott, 1994; Helzlsouer *et al.*, 1996). Forty per cent of a group of breast cancer patients showed elevated frequencies of chromatid breaks in the same range as that for a group of obligate ataxia telangiectasia heterozygotes, possibly indicating the presence of several cancer-predisposing genes with low penetrance (Scott, 1994). The reasons for elevated chromatid radiosensitivity are not understood, however, those genes which have been identified as strongly affecting G2 chromatid radiosensitivity, *ATM* (ataxia telangiectasia mutated, encoding for a p350 phosphatidylinositol 3-kinase) and *XRCC5* (X-ray repair cross-complementing, encoding for Ku80 protein), also have a role in the conversion of DNA double-strand breaks (dsb) into chromatid breaks (Kemp *et al.*, 1984; Bryant *et al.*, 1987; Liu and Bryant, 1994; Lakin *et al.*, 1996). It has thus become usual to link chromosomal and cellular radiosensitivity with DNA processing defects and, in particular, to altered rates of repair and residual levels of DNA dsb (see for example Taylor *et al.*, 1975; Kemp *et al.*, 1984; Foray *et al.*, 1995). However, as we have pointed out previously (see for example Bryant and Liu, 1994), this may not be an adequate explanation of high chromatid radiosensitivity of cells in the G2 phase of the cycle.

In examining the G2 chromatid break response of radiosensitive rodent (*irs 2*, VC4) and human AT fibroblastic and lymphoblastoid cell lines we and others showed that enhanced frequencies of chromatid breaks occur soon (within 1 h) after irradiation (Mozdarani and Bryant, 1989; Bryant *et al.*, 1993; Antoccia *et al.*, 1994; Bryant and Liu 1994; Liu and Bryant, 1994), although these cell lines are apparently proficient in dsb repair, at least over the first few hours following irradiation when assayed by available techniques, such as sucrose gradient centrifugation, filter elution and pulsed field gel electrophoresis (see for example Foray *et al.*, 1995). Moreover, irs2 and AT cell lines show no deficiency in V(D)J recombination. (Hsieh *et al.*, 1993; Kirsch, 1994; Thacker *et al.*, 1994).

A similar elevated frequency of chromatid breaks was observed soon after irradiation in (G2) AT cells using premature chromosome condensation (Pandita and Hittleman, 1992). We therefore suggested (Mozdarani and Bryant, 1989) that rather than invoking residual dsb as the cause of high chromatid radiosensitivity, higher frequencies of chromatid breaks were occurring as a result of enhanced 'conversion' of dsb into chromatid breaks. The same situation seems to apply in radiosensitive *xrs5* cells, which, like AT cells, already show elevated chromatid radiosensitivity at 1 h after irradiation (i.e. cells in G2 at the time of irradiation), although they show both a normal disappearance of chromatid breaks with time and normal dsb repair over the first few hours following irradiation, i.e. similar to wild-type CHO cells (MacLeod and Bryant; 1990, Bryant and Slijepcevic, 1993; Mateos *et al.*, 1994).

Murine SCID (severe combined immunodeficient) cells have, like *xrs* cells, been reported to show deficient overall dsb rejoining (Fulop and Phillips, 1990; Biedermann *et al.*, 1991; Hendrickson *et al.*, 1991; Chang *et al.*, 1993), defective V(D)J recombination (Schuler *et al.*, 1986; Lieber *et al.*, 1988, 1997; Weaver *et al.*, 1996), increased levels of chromosomal aberrations (Disney *et al.*, 1992; Kirchgessner *et al.*, 1993) and decreased rejoining of chromsome breaks as visualized by premature chromosome condensation and fluorescence *in situ* hybridization (Evans *et al.*, 1996). On the basis that the kinetics of disappearance of chromatid breaks with time reflect dsb rejoining, we sought to investigate whether deficient dsb

[3]To whom correspondence should be addressed. Tel: +44 1334 463510; Fax: +44 1334 463600; Email: peb@st.and.uk

rejoining would be reflected in comparative yields and kinetics of chromatid breaks in G2-exposed SCID compared with normal mouse cells.

The SCID mutation (*XRCC7*) has been mapped to mouse chromosome 16 (Bosma *et al.*, 1989). The gene encodes for the large (p450) catalytic subunit of the DNA-dependent protein kinase (DNAPKcs), which, together with the Ku70 and Ku80 proteins, forms the complex holoenzyme DNAPK, which has a putative dsb stabilizing or signalling role (Blunt *et al.*, 1995; Jeggo *et al.*, 1995; Finnie *et al.*, 1996).

The important difference between the sequence of the DNA *PKcs* gene in CB17 and SCID cells is a point mutation (T→A) resulting in an ochre stop codon (Blunt *et al.*, 1996; Danska *et al.*, 1996; Araki *et al.*, 1997). The mutation occurred in the C-terminal domain, which shows sequence similarity with the phosphatidylinositol 3-kinase superfamily, possibly suggesting a link between the SCID mutation and ATM.

Since Ku80 and p450 are thought to be linked as part of the same biochemical pathway, it might be predicted that the chromatid response of SCID cells to radiation would be similar to that of *xrs* mutants, which show elevated levels of chromatid breaks. We also examined the response of SCID and normal (CB17) murine cells to the restriction endonuclease *Pvu*II, since it was shown previously that *xrs5* cells were hypersensitive to the induction of chromatid breaks by restriction endonucleases (Bryant *et al.*, 1987).

In addition, we were interested to determine the dose–effect relationship for chromatid breaks at an early time following irradiation to test whether chromatid breaks were formed from single dsb (i.e. as a result of the action of single ionizing tracks) or whether they are the result of interaction between two dsb produced by two independent ionizing tracks.

Materials and methods

Cell culture

Murine fibroblast cells homozygous for the SCID (severe combined immunodeficient) mutation (SCID-st) and CB17 cell lines were obtained from Dr Martin Brown (Stanford University, CA). These were routinely passaged and maintained in exponential growth in Waymouth's medium containing 10% fetal calf serum. For experiments, cells were seeded at 1×10^6 cells/75 cm^2 flasks and incubated for 2 days at 37°C. Following irradiation, flasks were returned immediately to the incubator (total time out of the incubator was <2 min) and incubated for various times before sampling. Colcemid (0.04 μg/ml) was added for either 1.5 (in the case of dose–effect curves; Figure 1) or 1 h (in the case of break kinetics; Figure 2) before mitotic shake-off. Usually, 10 flasks were employed per dose or time point.

Irradiation

γ-Irradiation was carried out in a ^{137}Cs IBL437C γ-irradiator (CIS UK Bio-International, High Wycombe, UK). Doses were monitored by a modified ferrous sulphate method (Frankenberg, 1969). The dose rate was ~4 Gy/min.

Restriction endonuclease treatment

Flasks of exponentially growing cells were prepared as described above, medium removed and the cell monolayer rinsed in Hank's balanced salts solution (HBSS). The porating agent, streptolysin O (SLO; Murex Diagnostics, Dartford, UK) was added in 2 ml at a final concentration of 0.3 U/ml in HBSS with or without the restriction endonuclease *Pvu*II (Gibco BRL, Paisley, UK) at a concentration of 100 U/ml. Following a 5 min incubation at ambient temperature, the SLO was removed and the cells rinsed with growth medium. The cells were then incubated in fresh culture medium for 5 h before sampling by mitotic shake-off.

Metaphase chromosome preparations

Following mitotic shake-off, cells were pooled from 10 flasks, centrifuged at 2°C and resuspended in hypotonic solution (0.075 M KCl, 2°C) and held on ice for 10 min, centrifuged and the loosened pellets resuspended in 10 ml Carnoy's fixative (methanol:acetic acid 3:1). Cells were then washed three more times in fixative and spread from a dilute suspension of fixative on to angled slides in a strong cold air stream from a powerful hair drier. Slides were stained in 3% Giemsa and blotted dry.

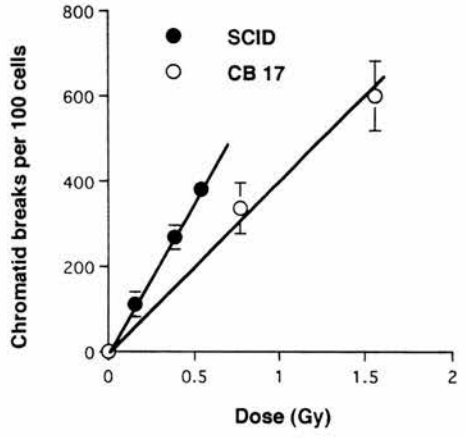

Fig. 1. Dose–effect relationship for chromatid breaks in SCID and CB17 cells. Chromatid breaks and gaps have been pooled from two independent experiments. Vertical bars represent standard errors. Linear regression analysis yielded a correlation coefficient $r = 0.997$ and 0.972 for SCID and CB17 cells respectively. The ratio of slopes is 1.58.

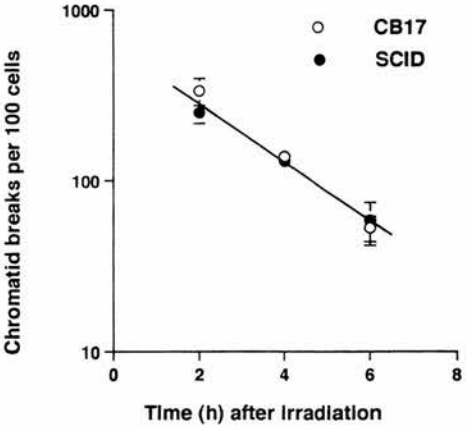

Fig. 2. Disappearance of chromatid breaks (pooled breaks and gaps) with time after irradiation for SCID and CB17 cells. SCID cells were given 0.385 and CB17 0.77 Gy. Results are pooled from five independent experiments. Vertical bars indicate standard errors.

Chromatid break analysis

Chromatid breaks and gaps (hereafter referred to simply as breaks) were scored in 100 metaphases per sample. Scoring was always carried out under code.

Frequency of labelled mitoses (FLM)

Monolayers of cells growing exponentially in Petri dishes were labelled with [^{3}H]TdR for various lengths of time, trypsinized, treated with hypotonic solution (0.075 M KCl) and fixed three times in methanol:acetic acid (3:1 v/v). Fixed cells were spread on slides and dipped in K2 autoradiographic emulsion (Ilford) and allowed to dry. Slides were stored in the dark for 4 days at 4°C. Following development (Kodak D19 for 3.5 min) and fixation (Kodak Unifix) for 5 min, slides were rinsed in cold water and stained with M$^-$D Diff-Quik (Merz and Dade).

Metaphases showing >10 grains were scored as labelled. In each of two independent experiments three slides were scored under code and a minimum of 30 metaphases were scored per slide.

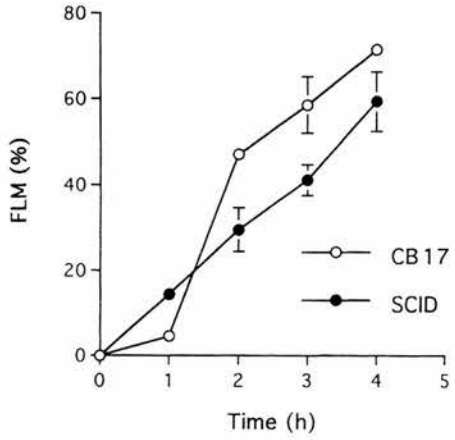

Fig. 3. FLM curves for SCID and CB17 cells. Vertical bars represent standard errors; where these are not visible, errors were smaller than the point size. Results are pooled from two independent experiments.

Results

Induction of chromatid breaks

The induction of chromatid breaks as a function of radiation dose is shown in Figure 1. Frequencies of chromatid breaks were determined at 2 h following irradiation, colcemid having been added at 30 min following irradiation. The induction of chromatid breaks in both cell lines was linear with dose for both cell lines (correlation coefficient r = 0.997 and 0.972 for SCID and CB17 respectively). The ratio between the slopes of the two lines was 1.58.

Kinetics of disappearance of breaks with time

Figure 2 shows the kinetics of disappearance of chromatid breaks with time following irradiation of CB17 and SCID cells. The data show an exponential (first order) decline in the number of chromatid breaks with time, with a half-time for the disappearance of breaks of ~1.5 h.

The doses (0.77 and 0.385 Gy for CB17 and SCID respectively) were chosen to deliver similar frequencies of chromatid breaks in the two cell lines. Since the yields of breaks at each time point were not significantly different, the ratio of yields at all three time points sampled was ~2, i.e. SCID cells were twice as radiosensitive as CB17 cells in this G2 assay. It is likely that at the last sampling time (6 h) a significant proportion of cells were in late S phase at the time of irradiation, since the length of G2 was found to be 2.3 h in CB17 and 3.5 h in SCID (Figure 3). However, as in previous studies with Chinese hamster cells, we find a monotonic exponential decline in chromatid break yield with time over the range 2–6 h.

Restriction endonuclease induced chromatid breaks

Table I shows the frequencies of chromatid breaks induced by *Pvu*II at 5 h after treatment. The sampling time of 5 h was chosen to allow the mitotic index to recover sufficiently following SLO treatment. Table I shows that *Pvu*II induced ~3 times as many chromatid breaks in the SCID cell line as in normal CB17 cells.

Discussion

The 3-fold increased G2 chromatid sensitivity of SCID cells compared with CB17 to the restriction endonuclease *Pvu*II

Table I. Frequencies of chromatid breaks in normal and SCID cells treated with the restriction endonuclease *Pvu*II (100 U/ml)

Cell line	Treatment	Mean breaks per 100 cells[a]	SE
CB 17 (normal)	None	5.0	1.15
	SLO	4.3	0.88
	*Pvu*II + SLO	42.7	6.33
SCID	None	7.7	2.40
	SLO	10.7	1.45
	*Pvu*II + SLO	128.3	4.10

[a]Pooled results of three independent experiments.

(Table I) shows that SCID cells convert higher numbers of dsb into chromatid breaks. The ratio of enhanced sensitivity of SCID to CB17 cells (~3) is higher than that found for γ-rays. This may reflect the difference in the end structures of *Pvu*II-induced dsb (3′-OH and 5′-PO_4 end groups with blunt ends) from those produced by γ-rays (dirty ends, many of which are likely to be cohesive). We are currently measuring the effects of a range of restriction endonucleases on SCID and CB17, which will be published elsewhere (Finnegan *et al.*, in preparation).

The difference in the G2 chromosomal radiosensitivity (Figure 1) using sampling times of 2 h between SCID and normal murine cells was found to be 1.58. This difference in yield is also seen in the kinetics of chromatid breaks as a function of time (Figure 2) constructed from chromatid break yields at various times following irradiation at either 0.77 (CB17) or 0.385 Gy (SCID). The ratio of yields for SCID and CB17 were thus ~2 in these experiments and are independent of the sampling time (e.g. mean yields at 2 h from Figure 2 were not significantly different: t value 0.025 for 7 degrees of freedom, $P > 0.1$), giving us confidence in the linear form of the dose–effect relationships in Figure 1. In the experiments shown in Figure 1 we limited the dose to 1.5 Gy since it was found to be very difficult to score samples after higher doses due to severe depression of the mitotic index.

Although we show that the length of G2 is different in SCID and CB17 cells (Figure 3), it is unlikely that the difference in chromatid radiosensitivity can be attributed to differential time for disappearance of breaks, since both the G1 and G2 arrest functions have been shown to be normal in SCID cells when tested with agents causing dsb (Gurley and Kemp, 1996).

The linearity of the dose–effect relationship for chromatid breaks suggests, in classical 'breakage-first' terms, that a 'one hit' process is involved in the formation of chromatid breaks. This result is surprising, given the large size of many of the breaks observed. Breaks representing loss of up to 10% of a chromatid are common. In molecular terms, these large deletions represent the loss of up to 40 Mbp in an average sized mouse cell chromosome and, therefore, might more reasonably be argued to result from interaction of two events (dsb) occurring at different points along the chromatid arm. However, the dose–effect relationship for chromatid breaks shows that only single events (presumably dsb) are involved. How could such a large 'deletion' result from a single dsb?

The 'signal' model, which is described in detail elsewhere (Bryant, 1998) explains the formation of a chromatid break as an incomplete recombinational exchange between DNA strands at the crossover point of looped chromatids, triggered by a

signal generated by a single dsb within the looped domain. The recombinational exchange essentially first requires the cell itself to make two breaks (dsb) at the point of exchange or crossover of chromatids at the 'neck' of a chromatin loop. These breaks are rejoined as the exchange process goes to completion. If the cell enters mitotic prophase while the cell-induced breaks are still open, chromosome condensation would prevent completion of the exchange, resulting in a visible chromatid break.

It was suggested that the loop domain may represent a large chromatin structure, such as that associated with the transcription 'factory' described by Iborra *et al.* (1997). These 'factories' are thought to contain looped chromatin domains of ~5 Mbp. One or more such domains might be involved in the formation of a chromatid break.

The signal model is based on Revell's exchange hypothesis (Revell, 1955), but with the important difference that the signal model proposes that only one dsb is required, whereas the Revell model proposes interaction of two chromatid 'lesions' (which were not defined) caused by two independent ionizing tracks. The interaction of two lesions would be reflected in a dose^2 relationship between chromatid breaks and dose, whereas we see from Figure 1 that the dose–effect relationship for chromatid breaks is linear. A similar linear dose–effect relationship for chromatid breaks is seen in human peripheral blood lymphocytes (Bryant, 1998). It should be noted that although the signal model differs from the Revell exchange model in proposing that only a single dsb is required to trigger an exchange, the types of chromatid breaks observed would be essentially the same (types 1–4) as those described by Revell.

If the DNA-dependent protein kinase (DNAPK) holoenzyme is the 'signal' which leads, via a phosphorylation step, to the cell making a recombinational exchange, then it might reasonably be asked why do we see more chromatid breaks when a major component of the holoenzyme (the p450 catalytic subunit of DNAPK) is mutated? The answer may lie in the use by the cell of an alternative biochemical pathway. In ataxia telangiectasia and *irs2* high chromatid break frequencies are seen, even though dsb repair is apparently normal over the first few hours when measured by available biochemical techniques. It is therefore possible that an alternative pathway takes over the signalling function from DNAPK and that the modified signal may alter the trigger for the exchange response, e.g. a delay in signalling could increase the probability of an incomplete recombinational exchange (i.e. failure to rejoin the cut ends) before the cell enters mitosis. The alternative signalling pathway may involve the ATM protein, which has a similar size (p350) and significant homology with DNAPK. Such a signalling function for the ATM gene product has recently been suggested (Lakin *et al.*, 1996).

Our results in Figure 2 show that although SCID cells are reportedly deficient in the rejoining of dsb (Biedermann *et al.*, 1991), the disappearance of chromatid breaks with time, which was previously interpreted in terms of the repair of the underlying causative dsb (Mozdarani and Bryant, 1989; Mateos *et al.*, 1994), is the same in SCID as in normal CB17 cells. Nevertheless, the chromatid break frequency is increased by a factor of ~2 in SCID cells as compared with normal controls. In terms of the signal model outlined above, chromatid breaks represent incomplete exchanges and the disappearance of chromatid breaks with time is therefore interpreted in terms of the sequential completion of recombinational exchanges and consequent closing of the incisions made by the cell during the exchange (Bryant, 1998). Thus, on the signal model the first order disappearance of chromatid breaks with time (Figure 2) is a property of the recombinational machinery (the genes for which have not been identified) and not of dsb repair (as mediated by the *XRCC4–7* genes). Hence, the same rate of disappearance of chromatid breaks may be seen in two different cell lines provided the genes for the recombinational exchange process are not mutated, and we could therefore envisage a situation (which presumably pertains in *xrs* and SCID cell lines) where the repair of primary (radiation-induced) dsb is altered as a result of mutations in *XRCC5* and *XRCC7* respectively, but chromatid break disappearance is not changed.

In summary, we suggest that the elevated frequencies of chromatid breaks seen in SCID cells result from an alteration in the mechanism signalling dsb, which leads to an increased level of recombinational exchange incompleteness.

Acknowledgements

The authors wish to thank John Macintyre and Angus Gleig for excellent technical assistance.

References

Antoccia,A., Palitti,F., Raggi,T., Catena,C. and Tanzarella,C. (1994) Lack of effect of inhibitors of DNA synthesis/repair on the ionising radiation-induced chromosomal damage in G2 stage of ataxia telangiectasia cells. *Int. J. Radiat. Biol.*, **66**, 309–317.

Araki,R., Fujimori,A., Hamantani,K., Mita,K., Saito,T., Mori,M., Fukumura,R., Morimyo,M., Muto,M., Itoh,M., Tatsumi,K. and Abe,M. (1997) Nonsense mutation at Tyr-4046 in the DNA-dependent protein kinase catalytic subunit of severe combined immune deficiency mice. *Proc. Natl Acad. Sci. USA*, **94**, 2438–2443.

Biedermann,K., Sun,J., Giaccia,A., Tasto,L. and Brown,J.M. (1991) The *scid* mutation in mice confers hypersensitivity to ionizing radiation and a deficiency in DNA double strand break repair. *Proc. Natl Acad. Sci. USA*, **88**, 1394–1397.

Blunt,T., Finnie,N.J., Taccioli,G.E., Smith,G.C., Demengeot,J., Gottlieb,T.M., Mizuta,R., Varghese,A.J., Alt,F.W., Jeggo,P.A. *et al.* (1995) Defective DNA-dependent protein kinase activity is linked to V(D)J recombination and DNA repair defects associated with the murine Scid mutation. *Cell*, **80**, 813–823.

Blunt,T., Gell,D., Fox,M., Taccioli,G.E., Lehmann,A.R., Jackson,S.P. and Jeggo,P.A. (1996) Identification of a nonsense mutation in the carboxyl-terminal refion of DNA-dependent protein kinase catalytic subunit in the scid mouse. *Proc. Natl Acad. Sci. USA*, **93**, 10285–10290.

Bosma,G.C., Davissan,M.T., Ruetsch,N.R., Sweet,H.O., Schultz,L.D. and Bosma,M.J. (1989) The mouse mutation severe combined immune deficiency (SCID) is on chromosome 16. *Immunogenetics*, **29**, 54–57.

Bryant,P.E. (1998) The signal model: a possible explanation for the conversion of DNA double-strand breaks into chromatid breaks. *Int. J. Radiat. Biol.*, **73**, 243–251.

Bryant,PE. and Liu,N. (1994) Responses of radiosensitive repair-proficient cell lines to restriction endonucleases. *Int. J. Radiat. Biol.*, **66**, 597–601.

Bryant,P.E. and Slijepcevic,P. (1993) G_2 chromatid aberrations: kinetics and possible mechanisms. *Environ. Mol. Mutagen.*, **22**, 250–256.

Bryant,P.E., Birch,P. and Jeggo,P.A. (1987) High chromosomal sensitivity of Chinese hamster *xrs* 5 cells to restriction endonuclease induced DNA double-strand breaks. *Int. J. Radiat. Biol.*, **52**, 537–554.

Bryant,P.E., Jones,N.J. and Liu,N. (1993) Radiosensitive Chinese hamster *irs2* cells show enhanced chromosomal sensitivity to ionizing radiation and restriction endonuclease induced blunt-ended double-strand breaks. *Mutagenesis*, **8**, 141–147.

Chang,C., Biedermann,A., Mezzina,K.M. and Brown,J.M. (1993) Characterization of the DNA double strand break repair defect in SCID mice. *Cancer Res.*, **53**, 1244–1248.

Danska,J.S., Holland,D.P., Mariathasan,S., Williams,K.M. and Guidos,C.J. (1996) Biochemical and genetic defects in the DNA-dependent protein kinase in murine scid lymphocytes. *Mol. Cell. Biol.*, **16**, 5507–17

Disney,J.E., Barth,A.L. and Shultz,L.D. (1992) Defective repair of radiation-induced chromosomal damage in SCID/SCID mice. *Cytogenet. Cell Genet.*, **59**, 39–44.

Evans,J.W., Liu,X.F., Kirchgessner,C.U. and Brown,J.M. (1996) Induction and repair of chromosome aberrations in SCID cells measured by premature chromosome condensation. *Radiat. Res.*, **145**, 39–46.

Finnie,N.J., Gottlieb,T.M., Blunt,T., Jeggo,P.A. and Jackson,S.P. (1996) DNA-dependent protein kinase defects are linked to deficiencies in DNA repair and V(D)J recombination. *Phil. Trans. R. Soc. Lond. B*, **351**, 173–179.

Foray,N., Arlett,C.F. and Malaise,E.P. (1995) Dose–rate effect on induction and repair of radiation-induced DNA double-strand breaks in a normal and an ataxia-telangiectasia human fibroblast cell line. *Biochemie*, **77**, 900–905.

Frankenberg,D. (1969) A ferrous sulphate dosemeter independent of photon energy in the range from 25 KeV up to 59 MeV. *Phys. Med. Biol.*, **14**, 597–605.

Fulop,G.M. and Phillips,R.A. (1990) The SCID mutation in mice causes a general defect in DNA repair. *Nature*, **347**, 479–482.

Gurley,K.E. and Kemp,C.J. (1996) p53 induction, cell cycle check-points, and apoptosis in DNAPK-deficient SCID mice. *Carcinogenesis*, **17**, 2537–2542.

Helzlsouer,K.J., Harris,E.L., Parshad,R., Perry,H.R., Price,F.M. and Sanford,K.K. (1996) DNA repair proficiency: potential susceptibility factor for breast cancer. *J. Natl Cancer Inst.*, **88**, 754.

Hendrickson,E.A., Qin,X., Bump,E., Schatz,D.G., Oettinger,M. and Weaver,D.T. (1991) A link between double strand break-related repair and V(D)J recombination: the *scid* mutation. *Proc. Natl Acad. Sci. USA*, **88**, 4061–4065.

Hsieh,C.L., Arlett,C.F. and Lieber,M.R. (1993) V(D)J recombination in ataxia telangiectasia, Bloom's syndrome, and a DNA ligase I-associated immunodeficiency disorder. *J. Biol. Chem.*, **268**, 20105–20109.

Iborra,F.J., Pombo,A., Jackson,D.A. and Cook,P.R. (1997) Active RNA polymerases are localized within discrete transcription 'factories' in human nuclei. *J. Cell Sci.*, **109**, 1427–1436.

Jeggo,P.A., Taccioli,G.E. and Jackson,S.P. (1995) Menage à trois: double strand break repair, V(D)J recombination and DNA-PK. *BioEssays*, **17**, 949–957.

Kemp,L.M., Sedgwick,S.G. and Jeggo,P.A. (1984) X-ray-sensitive mutants (*xrs*) of Chinese hamster ovary cells defective in double strand break rejoining. *Mutat. Res.*, **132**, 189–196.

Kirchgessner,C.U., Tosto,L.M., Biedermann,K.A., Kovacs,M., Araujo,D., Stanbridge,E.J. and Brown,J.M. (1993) Complementation of the radiosensitive phenotype in severe combined immunodeficient mice by human chromosome 8. *Cancer Res.*, **53**, 6011–6016.

Kirsch,I.R. (1994) V(D)J Recombination and ataxia-telangiectasia: a review. *Int. J. Radiat. Biol.*, **66**, S97–S108.

Lakin,N.D., Weber,P., Stankovic,T., Rottinghaus,S.T., Taylor,A.M.R. and Jackson,S.P. (1996) Analysis of the ATM protein in wild-type and ataxia telangiectasia cells. *Oncogene*, **13**, 2702–2716.

Lieber,M.R., Hesse,J.E., Lewis,S., Bosma,G.C., Rosenberg,N., Mizuuchi,K., Bosma,M.J. and Gellert,M. (1988) The defect in murine severe combined immune deficiency: joining of signal sequences but not coding segments in V(D)J recombination. *Cell*, **55**, 7–16.

Lieber,M., Grawunder,U., Wu,X. and Yaneva,M. (1997) Tying loose ends: roles of ku and DNA-dependent protein kinase in the repair of double-strand breaks. *Curr. Opin. Genet. Dev.*, **7**, 99–104.

Liu,N. and Bryant,P.E. (1994) Enhanced chromosomal response of ataxia-telangiectasia cells to specific types of DNA double-strand breaks. *Int. J. Radiat. Biol.*, **66**, S115–S121.

MacLeod,R.A.F. and Bryant,P.E. (1990) Similar kinetics of X-ray induced chromatid aberrations in *xrs*5 and wild type CHO cells. *Mutagenesis*, **5**, 407–410.

Mateos,S., Slijepcevic,P., MacLeod,R.A.F. and Bryant,P.E. (1994) DNA double-strand break rejoining in *xrs*5 cells is more rapid in the G2 than in the G1 phase of the cell cycle. *Mutat. Res. DNA Repair*, **315**, 181–187.

Mozdarani,H. and Bryant,P.E., (1989) Kinetics of chromatid aberrations in G2 ataxia telangiectasia cells exposed to X-rays and ara A. *Int. J. Radiat. Biol.*, **55**, 71–84.

Pandita,T.K. and Hittelman,W.N. (1992) Initial chromosome damage but not DNA damage is greater in ataxia telangiectasia cells. *Radiat. Res.*, **130**, 94–103.

Revell,S.H. (1955) A new hypothesis for 'chromatid' changes. In Bacq,S.H. and Alexander,P. (eds), *Radiobiology Symposium 1954*. Butterworth, London, UK, pp. 243–253.

Schuler,W., Weiler,I.J., Schuler,A., Phillips,R.A., Rosenberg,N., Mak,T.W., Kearney,J.F., Perry,R.P. and Bosma,M.J. (1986) Rearrangement of antigen receptor genes is defective in mice with severe combined immune deficiency. *Cell*, **46**, 963–972.

Scott,D. (1994) Genetic predisposition in breast cancer. *Lancet*, **344**, 1444.

Taylor,A.M.R., Harnden,D.G., Arlett,C.F., Harcourt,S.A., Stevens,S. and Bridges,B.A. (1975) Ataxia telangiectasia: a human mutation with abnormal radiation sensitivity. *Nature*, **258**, 427–429.

Thacker,J., Ganesh,A.N., Stretch,A., Benjamin,D.M., Zahalsky,A.J. and Hendrickson,E.A. (1994) Gene mutation and V(D)J recombination in the radiosensitive irs lines. *Mutagenesis*, **9**, 163–168.

Weaver,D., Boubnov,N., Wills,Z., Hall,K. and Staunton,J. (1996) V(D)J recombination: double-strand break repair gene products used in the joining mechanism. *Annls NY Acad. Sci.*, **764**, 99–111.

Received on September 3, 1997; accepted on June 3, 1998